



Cilt:7 Sayı:1 Volume:7 Number:1 ISSN:2602-3350

2023

DergiPark
AKADEMİK

Sayın Yazarlar;

Dergimize 4 dilde (Türkçe Tr, İngilizce En, Rusça Ru ve Ukraynaca Ua) yazı kabul etmekteyiz. Türkçe, Rusça ve Ukraynaca yazılarda İngilizce özet yazılması zorunludur.

ULUSLARARASI 3B YAZICI TEKNOLOJİLERİ VE DİJİTAL ENDÜSTRİ dergisi,

IJ3DPTDI, Endüstri 4.0 – dijital endüstri teknolojileri, 3B yazıcı teknolojileri, katmanlı-eklemeli imalat teknolojileri ve uygulamaları yani mühendislik, bilim, teknoloji gibi tüm disiplinlerle ilgili araştırmaların sonuçlarını yaymak için açık, hakemli, disiplinlerarası, uluslararası, bilimsel, akademik, online bir dergidir. ij3dptdi, Mühendislik, Teknoloji ve Bilimin Endüstri 4.0 daki uygulamaları, tüm araştırmaları, gözden geçirme makalelerini, kısa bilgi paylaşımlarını ve önemli ilerlemeleri sunan teknik notları online yayınlamak için yazarları davet eder.

Endüstri 4.0, Dijital Endüstri, 3B Yazıcılar üzerine tüm bilimsel mühendislik araştırma ve teknoloji alanı konuları;

3B baskı için tıbbi uygulamalar; dokuların ve organların biyografik baskıları, 3B vaskülarize organların oluşturulmasında karşılaşılan zorluklar, özelleştirilmiş implantlar ve protezler, düşük maliyetli protez parçaları, cerrahi hazırlık için anatomik modeller, sentetik cilt, kafatası değişimi, tıbbi donatımı, kemik, özel üretilen sensörler, kişiselleştirilmiş ilaç dozu, benzersiz dozaj şekilleri, kompleks ilaç salınım profilleri v.d.

3B yazıcı uygulama alanları; tıbbi ve diş hekimliği uygulamaları, diş hekimliği uygulamaları ve materyalleri, yumuşak robotik sistemleri, robot tutucu sistemler, bina uygulamaları, kalıp / kalıp uygulamaları, mimarlık uygulamaları, model uygulamaları, hızlı prototip uygulamaları, görsel sanat uygulamaları, tekstil uygulamaları, dijital fabrikalar, mimari model uygulamaları ve malzemeleri, endüstriyel uygulamalar ve malzemeler, gıda uygulamaları ve malzemeleri, sanatsal uygulamalar ve malzemeler, tarama yöntemleri ve modelleme v.d.

Endüstri 4.0 ve dijital sanayi; büyük veri, yapay zeka, dijital yaşam döngüsü, sensör motorları, artırılmış gerçeklik, görselleştirme, sistem simülasyonu, kablosuz iletişim, BİT güvenlik, dijital iş, blok zinciri, veri Güvenliği, özerk robotlar, sistem entegrasyonu, nesnelerin interneti (IoTs), siber güvenlik, bulut bilişim, dijital fabrika v.d.

3B yazıcı tasarım, modelleme ve analiz; 3D yazıcı tasarımı, ekstruder tasarımı, 3B baskı için ürün geliştirme, seramik sistemleri tasarımı, gıda sistemleri tasarımı, elektronik bileşenleri, mekanik parçalar, standart bileşenler v.d.

3B yazıcı malzeme ve mekanik özellikleri; polimer malzemeler, esnek malzemeler, biyo malzemeler, metalik malzemeler, toz malzeme üretim yöntemleri, ağaç malzemeler, kompozit malzemeler v.d.

3B yazıcı program kontrol teknolojileri; kontrol programları, tasarım programları, 3D tarama teknolojileri, DMLS teknolojileri, SLA teknolojileri, SLS teknolojileri, FDM teknolojileri, dijital üretim teknolojileri, diğer 3B yazıcı teknolojileri v.d.

ij3dptdi, online yayınlanan bir dergidir ve yılda 3 defa yayınlanır.

- 1.periyot Ocak-Nisan
- 2.periyot Mayıs-Ağustos
- 3.periyot Eylül-Aralık

ISSN 2602-3350

web-site : <http://dergipark.gov.tr/ij3dptdi>

e-mail : korayozsoy32@gmail.com

Dear author,

Our Journal accepts articles in 4 languages (Turkish Tr, English En, Russian Ru and Ukrainian Ua). Articles in Turkish, Russian and Ukrainian must have an abstract in English.

International Journal of 3D Printing Technologies and Digital Industry

ij3dptdi, is an open access peer-reviewed, interdisciplinary international platform for disseminating results of relevant research related to all the disciplines of engineering, science, technology etc on Industry 4.0 - digital industry technologies, 3D printer technologies, additive manufacturing technologies and applications . ij3dptdi, invites all research, review articles, short communications & technical notes that describe significant advances research in the areas of Engineering, Technology, Science on Industry 4.0, Digital Industry, 3D Printers, additive manufacturing;

All scientific engineering research & technology area on Industry 4.0, Digital Industry and 3D printers;

Medical applications for 3D printing; bioprinting tissues and organs, challenges in building 3D vascularized organs, customized implants and prostheses, low-cost prosthetic parts, anatomical models for surgical preparation, synthetic skin, cranium replacement, medical equipment, bone, tailor-made sensors, personalized drug dosing, unique dosage forms, complex drug-release profiles ect.

Application fields; medical and dental applications, dental practices and materials, soft robotics systems, robot gripper systems, building applications, die/mold applications, architecture applications, models applications, rapid prototype applications, visual arts applications, textile applications, digital factories, architectural-model applications and materials, industrial applications and materials, food applications and materials, artistic practices and materials, scanning methods and modeling ect.

Digital industry; big data, artificial intelligence, digital life cycles, sensors actuators, augmented reality, visualization, system simulation, wireless communication, ICT security, digital business, block chain, data safety, autonomous robots, system integration, internet of things (IT's), cyber security, cloud computing, digital factory ect.

Design, modelling and analysis; 3D printer design, extruder design, product development, ceramic systems design, food systems design, table system design, electronics components, mechanic components, standard components ect.

Mechanical properties of filaments; polymer materials, flexible materials, bio materials, metallic materials, wood materials, composite materials ect.

Program – control technologies; control programs, design programs, 3D scanning technologies, DMLS technologies, SLA technologies, SLS technologies, FDM technologies, Digital production technologies, other 3D printer technologies ect.

ij3dptdi, Its publication frequency is 3 issues per year.

- 1.Period January-April
- 2.period May-August
- 3.period September-December

ISSN 2602-3350
Web-site: <http://dergipark.gov.tr/ij3dptdi>
E-mail: korayozsoy32@gmail.com

Уважаемый автор,

наш журнал принимает статьи на 4-х языках (турецком, английском, русском и украинском). Статьи на турецком, русском и украинском языках должны сопровождаться аннотацией на английском языке.

Международный журнал технологий 3D-печати и цифровой индустрии

IJ3DPTDI – это рецензируемое издание с открытым доступом, междисциплинарная международная платформа для обмена результатами исследований по инженерно-конструкторским разработкам, теоретическим исследованиям, усовершенствованию технологий Индустрии 4.0, в том числе – технологий цифровой промышленности, 3D-печати, аддитивного производства и разработки приложений. **IJ3DPTDI** принимает исследовательские статьи, обзорные статьи, краткие сообщения и технические заметки, которые описывают значимые результаты исследований в области машиностроения, технологии, теоретической основы индустрии 4.0, цифровой промышленности, 3D печати, производства многокомпонентных материалов.

Тематика журнала включает все научно-технические исследования и обзор технологий Индустрии 4.0, цифровой промышленности и 3D печати.

Медицинские технологии 3D-печати: биопринтинг – воспроизведение объемных моделей тканей и органов, создание трехмерных васкуляризованных органов, индивидуализированных имплантатов и протезов, синтетической кожи, костей, замены частей черепа; удешевление технологии протезирования, разработка анатомических моделей для подготовки хирургов, тестовых хирургических операций, медицинского оборудования; изготовление датчиков с заданным набором характеристик, создание уникальных лекарственных препаратов с индивидуальными дозировками, сложных многокомпонентных лекарственных средств.

Области применения: материалы и оборудование для медицины и стоматологии, роботизированные системы на основе биологических прототипов, роботизированные захватные устройства, строительные материалы, пресс-формы, модели и прототипы в архитектуре, моделирование реальных объектов, прототипирование, сфера визуального искусства, текстильная промышленность, цифровые заводы, приложения и материалы для архитектурного моделирования, промышленные образцы и материалы, создание пищевых продуктов, технологии художественной обработки материалов, методы моделирования и сканирования и т.п.

Цифровая индустрия: большие данные, искусственный интеллект, жизненный цикл цифровых технологий, приводные механизмы датчиков, расширенная реальность, визуализация, моделирование систем, беспроводная связь, ИТ-безопасность, электронная коммерция, блокчейн технологии, безопасность данных, автономные роботы, системная интеграция, интернет вещей, кибербезопасность, облачные вычисления, цифровое производство.

Дизайн, моделирование и анализ: моделирование для 3D печати, экструдера; разработка разнообразных продуктов, проектирование систем керамического производства, усовершенствование технологии производства пищевых продуктов, проектирование предметов мебели, электронных компонентов, механических деталей, стандартных компонентов и т.п.

Механические свойства нитей: полимерные материалы, гибкие материалы, биоматериалы, изделия из металла и древесины, композиционные материалы.

Технологии управления приложениями: контрольные программы, проектные программы, технологии 3D-сканирования, технологии DMLS, SLA, SLS, FDM, цифровые технологии производства, другие технологии 3D-печати и т.п.

Периодичность выхода журнала – 3 раза в год:

1-й выпуск – январь-апрель;

2-й выпуск – май-август;

3-й выпуск – сентябрь-декабрь.

ISSN 2602-3350

Сайт журнала: <http://dergipark.gov.tr/ij3dptdi>

Электронная почта: korayozsoy32@gmail.com

Шановний авторе,

наш журнал приймає статті на 4-х мовах (турецькою, англійською, російською та українською). Статті турецькою, російською та українською мовою повинні супроводжуватися анотацією англійською мовою.

Міжнародний журнал технологій 3D-друку і цифрової індустрії

IJ3DPTDI – це рецензоване видання з відкритим доступом, міждисциплінарна міжнародна платформа для обміну результатами досліджень з інженерно-конструкторських розробок, теоретичних досліджень, удосконалення технологій Індустрії 4.0, в тому числі – технологій цифрової промисловості, 3D-друку, адитивного виробництва і розробки додатків. IJ3DPTDI приймає дослідні статті, оглядові статті, короткі повідомлення і технічні записки, які містять значущі результати досліджень в галузі машинобудування, технології, теоретичній основі індустрії 4.0, цифровій промисловості, 3D друку, виробництва багатокomпонентних матеріалів.

Тематика журналу охоплює всі науково-технічні дослідження та огляд технологій Індустрії 4.0, цифрової промисловості і 3D друку.

Медичні технології 3D-друку: біопрінтинг – відтворення об'ємних моделей тканин і органів, створення тривимірних васкуляризованих органів, індивідуалізованих імплантатів і протезів, синтетичної шкіри, кісток, заміни частин черепа; здешевлення технології протезування, розроблення анатомічних моделей для підготовки хірургів, тестових хірургічних операцій, медичного обладнання; виготовлення датчиків із заданим набором характеристик, створення унікальних лікарських препаратів із індивідуальними дозуваннями; складних багатокomпонентних лікарських засобів.

Сфери застосування: матеріали та обладнання для медицини і стоматології, роботизовані системи на основі біологічних прототипів, роботизовані захватні пристрої, будівельні матеріали, прес-форми, моделі і прототипи в архітектурі, моделювання реальних об'єктів, прототипування, сфера візуального мистецтва, текстильна промисловість, цифрові заводи, додатки та матеріали для архітектурного моделювання, промислові зразки і матеріали, створення харчових продуктів, технології художньої обробки матеріалів, методи моделювання та сканування і т.п.

Цифрова індустрія: великі дані, штучний інтелект, життєвий цикл цифрових технологій, приводні механізми датчиків, розширена реальність, візуалізація, моделювання систем, бездротовий зв'язок, IT-безпека, електронна комерція, блокчейн технології, безпека даних, автономні роботи, системна інтеграція, інтернет речей, кібербезпека, хмарні обчислення, цифрове виробництво.

Дизайн, моделювання і аналіз: моделювання для 3D друку, екструдера; розробка різноманітних продуктів, проектування систем керамічного виробництва, удосконалення технології виробництва харчових продуктів, проектування предметів меблів, електронних компонентів, механічних деталей, стандартних компонентів і т.п.

Механічні властивості ниток: полімерні матеріали, гнучкі матеріали, біоматеріали, вироби з металу і деревини, композиційні матеріали.

Технології управління додатками: контрольні програми, проектні програми, технології 3D-сканування, технології DMLS, SLA, SLS, FDM, цифрові технології виробництва, інші технології 3D-друку і т.п.

Періодичність виходу журналу – 3 рази на рік:

1-й випуск – січень-квітень;

2-й випуск – травень-серпень;

3-й випуск – вересень-грудень.

ISSN 2602-3350
Web-site: <http://dergipark.gov.tr/ij3dptdi>
E-mail: korayozsoy32@gmail.com

ULUSLARARASI 3B YAZICI TEKNOLOJİLERİ VE DİJİTAL ENDÜSTRİ DERGİSİ

Cilt:7 Sayı: 1 Yıl: 2023

INTERNATIONAL JOURNAL OF 3D PRINTING TECHNOLOGIES AND DIGITAL INDUSTRY

Volume:7 Number: 1 Year: 2023

ISSN: 2602-3350

Yazıların tüm bilimsel sorumluluğu yazar(lar)a aittir. Editör, yardımcı editör ve yayıncı dergide yayımlanan yazılar için herhangi bir sorumluluk kabul etmez. Bu dergi, aşağıda listelenen veri tabanları tarafından taranmaktadır. All the scientific responsibilities of the manuscripts belong to the authors (s). The editor, assistant editor and publisher accept no responsibility for the articles published in the journal. The Journal is indexed by the following abstracting and indexing databases.

TR Dizin, Google Scholar, ResearchBib, Index Copernicus, Asos indeks



<http://dergipark.gov.tr/ij3dptdi>

Uluslararası 3B Yazıcı Teknolojileri ve Dijital Endüstri Dergisi / International Journal of 3D Printing Technologies and Digital Industry

Vol: 7, No:1 (2023)

Cilt: 7, Sayı:1 (2023)

Editörler ve Kurullar / Editors and Boards

Yayın Kurulu Başkanı / Publication Board Manager

Dr. Kerim ÇETİNKAYA, Antalya BELEK Üniversitesi, Sanat ve Tasarım Fakültesi, TÜRKİYE

Baş Editör / Editor-in-Chief

Dr. Kerim ÇETİNKAYA, Antalya BELEK Üniversitesi, Sanat ve Tasarım Fakültesi, TÜRKİYE

Editörler Kurulu / Editorial Board

Dr. Koray ÖZSOY, Isparta Uygulamalı Bilimler Üniversitesi, Isparta OSB MYO, Makine ve Metal Teknolojileri Bölümü, TÜRKİYE

Dr. Burhan DUMAN, Isparta Uygulamalı Bilimler Üniversitesi, Teknoloji Fakültesi, Bilgisayar Mühendisliği Bölümü, TÜRKİYE

Dr. Ahu ÇELEBİ, Celal Bayar Üniversitesi, Mühendislik Fakültesi, Malzeme Mühendisliği Bölümü, TÜRKİYE

Dr. Hatice EVLEN, Karabük Üniversitesi, Teknoloji Fakültesi, Endüstriyel Tasarım Mühendisliği Bölümü, TÜRKİYE

Dr. Murat Aydın, Karabük Üniversitesi, Teknoloji Fakültesi, Endüstriyel Tasarım Mühendisliği Bölümü, TÜRKİYE

Dr. Emaka AMALU, Teesside Üniversitesi, Doğa ve Bilim Bölümü, Middlesbrough, İNGİLTERE

Dr. Hanane ZERMANE, Batna 2 Üniversitesi, Endüstri Mühendisliği Bölümü, CEZAYİR

Dr. Serhii Yevseiev, Simon Kuznets Kharkiv Ulusal Ekonomi Üniversitesi, Siber Güvenlik ve Bilgi Teknolojileri Bölümü, UKRAYNA

Dr. Pınar DEMİRCİOĞLU, Aydın Adnan Menderes Üniversitesi, Mühendislik Fakültesi, Makine Mühendisliği Bölümü, TÜRKİYE

Dr. Bekir AKSOY, Isparta Uygulamalı Bilimler Üniversitesi, Teknoloji Fakültesi, Mekatronik Mühendisliği Bölümü, TÜRKİYE

Dr. İshak ERTUĞRUL, Muş Alparslan Üniversitesi, Teknik Bilimler MYO, Mekatronik Programı, TÜRKİYE

Dr. Levent AYDIN, Kocaeli Üniversitesi, Sağlık Hizmetleri MYO, Sağlık Bakım Hizmetleri Bölümü, TÜRKİYE

Dr. Kıyas KAYAALP, Isparta Uygulamalı Bilimler Üniversitesi, Teknoloji Fakültesi, Bilgisayar Mühendisliği Bölümü, TÜRKİYE

Dr. Senai YALÇINKAYA, Marmara Üniversitesi, Teknoloji Fakültesi, Makine Mühendisliği Bölümü, TÜRKİYE

Dr. İbrahim KARAAĞAÇ, İmalat Mühendisliği, Teknoloji Fakültesi, Gazi Üniversitesi, TÜRKİYE

Dr. Yasin HAMARAT, Biyoteknoloji, Kaunas University Of Technology, LİTVANYA

Mizanpaj Editörü/ Layout Editor

Mehmet YÜCEL, Isparta Uygulamalı Bilimler Üniversitesi, Teknoloji Fakültesi, Mekatronik Mühendisliği Bölümü, TÜRKİYE

Danışma Kurulu / Advisory Board

Dr. M. Cengiz KAYACAN, SÜLEYMAN DEMİREL ÜNİVERSİTESİ, TR

Dr. N. Nnamdi EKERE, WOLVERHAMPTON UNIVERSITY, UK

Dr. Hüseyin Rıza BÖRKLÜ, GAZİ ÜNİVERSİTESİ, TR

Dr. Cem SİNANOĞLU, ERCİYES ÜNİVERSİTESİ, TR

Dr. Mustafa BOZDEMİR KIRIKKALE ÜNİVERSİTESİ, TR

Dr. Savaş DİLİBAL, İSTANBUL GEDİK ÜNİVERSİTESİ, TR

Dr. Cem Bülent ÜSTÜNDAĞ, YILDIZ TEKNİK ÜNİVERSİTESİ, TR

Dr. Ahmet CAN, NECMETTİN ERBAKAN ÜNİVERSİTESİ, TR

Dr. Fuat KARTAL, KASTAMONU ÜNİVERSİTESİ, TR

Dr. İhsan TOKTAŞ, YILDIRIM BEYAZIT ÜNİVERSİTESİ, TR

Dr. Okan ORAL, AKDENİZ ÜNİVERSİTESİ, TR

Dr. Barış Berat BULDUM, MERSİN ÜNİVERSİTESİ, TR

Dr. Serap ÇELEN, EGE ÜNİVERSİTESİ, TR

Dr. Mustafa Aydın, KÜTAHYA DUMLUPINAR ÜNİVERSİTESİ, TR

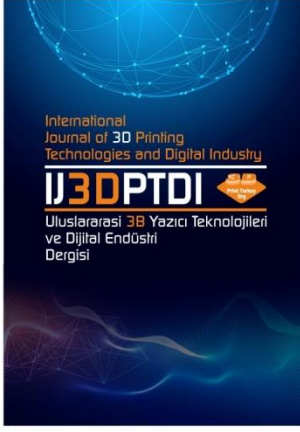
Dr. Serkan BÜRKEN, OSTİM TEKNİK ÜNİVERSİTESİ, TR

Dr. Samsun M. BAŞARICI, AYDIN ADNAN MENDERES ÜNİVERSİTESİ, TR

Dr. İsmail BÖĞREKÇİ, AYDIN ADNAN MENDERES ÜNİVERSİTESİ, TR

ISSN 2602-3350

İçindekiler /Table of Contents	Sayfa /Pages
Araştırma Makaleleri/Research Articles	
1. FAN KANATLARINDAKİ DENGESİZLİĞİN VE YUVARLANMALI YATAK ARIZASININ TİTREŞİME ETKİSİ Menderes KAM Serkan GÜLLE	1-8
2. 1420 MHZ RADYO TELESKOP UYGULAMALARI İÇİN MİKROŞERİT BASAMAK EMPEDANS REZONATÖRLÜ BANT GEÇİREN FİLTRE TASARIMI Bilge ŞENEL	9-17
3. DESIGN AND MANUFACTURING OF A TWO-STAGE REDUCTION GEARBOX WITH 3D PRINTERS Serpil KARAKUŞ	18-28
4. FROM DESIGN CONCEPT TO PRODUCTION: USING GENERATIVE DESIGN OUTPUT AS DESIGN INSPIRATION Utku KOCAMAN Abdullah TOĞAY	29-37
5. OPTIMIZATION OF 3D PRINTING PARAMETERS TO MECHANICAL STRENGTH IMPROVEMENT OF SUSTAINABLE PRINTING MATERIAL USING RSM Erman ZURNACI	38-46
6. NATURE-INSPIRED DESIGN IDEA GENERATION WITH GENERATIVE ADVERSARIAL NETWORKS Nurullah YÜKSEL Hüseyin Rıza BÖRKLÜ	47-54
7. CYBER ATTACKS FOR DATA BREACH AND POSSIBLE DEFENSE STRATEGIES IN INTERNET OF HEALTHCARE THINGS ECOSYSTEM Ahmet Ali SÜZEN	55-63
8. 3B YAZICILAR İÇİN CAM FİBER KATKILI KOMPOZİT FİLAMENT ÜRETİMİ VE MEKANİK ÖZELLİKLERİ Suat ALTUN Buğra SEKBAN	64-77
9. AN EVALUATION OF STUDENTS' CYBERSECURITY AWARENESS IN THE MARITIME INDUSTRY İsmail KARACA Ömer SÖNER	78-89
10. CSS ÇATILARININ KULLANIMINDA KARŞILAŞILAN SORUNLAR VE ÇÖZÜM ÖNERİLERİ Anar MUSAYEV Zülfikar SAYIN	90-104
11. THE EFFECT OF NOZZLE DIAMETER AND LAYER THICKNESS ON MECHANICAL BEHAVIOUR OF 3D PRINTED PLA LATTICE STRUCTURES UNDER QUASI-STATIC LOADING Emre DEMİRCİ Safa ŞENAYSOY Salih Emre TUĞCU	105-113
12. A COMPARATIVE STUDY ON PRECISION METROLOGY SYSTEMS FOR ADDITIVE MANUFACTURING Binnur SAĞBAŞ Özgür POYRAZ Numan DURAKBASA	114-123
13. PRODUCTION OF WASTE JUTE DOPED PLA (POLYLACTIC ACID) FILAMENT FOR FFF: EFFECT OF PULVERIZATION Ayberk SÖZEN Alperen DOĞRU Murat DEMİR Havva Nur ÖZDEMİR Yasemin SEKİ	124-128
14. USING CFD TO ANALYZE WIND VELOCITY AROUND BUILDINGS TO DETERMINE THE APPROPRIATE WIND VELOCITY Mehmet BAKIRCI Noor MOHAMMED	129-141



ULUSLARARASI 3B YAZICI TEKNOLOJİLERİ
VE DİJİTAL ENDÜSTRİ DERGİSİ

INTERNATIONAL JOURNAL OF 3D PRINTING
TECHNOLOGIES AND DIGITAL INDUSTRY

ISSN:2602-3350 (Online)

URL: <https://dergipark.org.tr/ij3dptdi>

FAN KANATLARINDAKİ DENGESİZLİĞİN VE YUVARLANMALI YATAK ARIZASININ TİTREŞİME ETKİSİ

THE EFFECT OF FAN BLADE UNBALANCE AND
ROLLING ELEMENT BEARING FAULT ON VIBRATION

Yazarlar (Authors): Menderes Kam^{ID*}, Serkan Gülle^{ID}

Bu makaleye şu şekilde atıfta bulunabilirsiniz (To cite to this article): Kam M., Gülle S., “Fan Kanatlarındaki Dengesizliğin ve Yuvarlanmalı Yatak Arızasının Titreşime Etkisi” *Int. J. of 3D Printing Tech. Dig. Ind.*, 7(1): 1-8, (2023).

DOI: 10.46519/ij3dptdi.1129705

Araştırma Makale/ Research Article

Erişim Linki: (To link to this article): <https://dergipark.org.tr/en/pub/ij3dptdi/archive>

FAN KANATLARINDAKİ DENGESİZLİĞİN VE YUVARLANMALI YATAK ARIZASININ TİTREŞİME ETKİSİ

Menderes Kam^a , Serkan Glle^b 

^aDzce niversitesi, Dr. Engin PAK Cumayeri MYO, Makine ve Metal Teknolojileri Blm, TRKİYE

^bDzce niversitesi, Fen Bilimleri Enstits, TRKİYE

* Sorumlu Yazar: mendereskam@duzce.edu.tr

(Received: 13.06.2022; Revised: 09.08.2022; Accepted: 03.04.2023)

Z

Dnen makine sistemlerinde, arızanın erken belirlenebilmesi sadece makine elemanlarını korumak iin deęil, aynı zamanda byk bir arızadan nce mevcut arızanın tespit edilebilmesi iin de gereklidir. Bu alıřmada, fan kanatlarında oluřan dengesizlięin ve yuvarlanmalı yatak (rulman) arızasının titreřime etkisi incelenmiřtir. Bu baęlamda, bir yuvarlanmalı yatakta oluřan i bilezik hatasının ve fan kanatlarında oluřan dengesizlięin rulmandan ve fan motorundan alınan lm sonuları ile belirlenebilmesi amacıyla kullanım yerinde alıřma gerekleřtirilmiřtir. Titreřim lmleri ve analizi iin VSE150 titreřim analizr ile VSA001 kodlu ivmeler kullanılmıřtır. Elde edilen bulgular analiz edilmiř ve sonu olarak, titreřim analizinin titreřime sebep olan etkenlerin tespit edilmesinde etkin olarak kullanılabileceęi grlmřtir. Sonular, titreřim analizi ile rulman arıza tespitinin bařarılı bir Őekilde yapılabileceęini ortaya koymaktadır.

Anahtar Kelimeler: Titreřim, Rulman Arızası, Arıza Tespiti, Dengesizlik, Fan Kanadı.

THE EFFECT OF FAN BLADE UNBALANCE AND ROLLING ELEMENT BEARING FAULT ON VIBRATION

ABSTRACT

In rotating machinery systems, early detection of the failure is not only necessary to ensure the health of the machinery elements but also to detect the current fault before catastrophic failure. In this study, the determination of the unbalance in the fan blades and the rolling element bearing fault by vibration analysis were investigated. In this context, in order to determine the inner ring defect in a rolling element bearing and the unbalance caused in the fan blades with the measurement results taken from the fan motor and rolling element bearing, an experimental study was conducted. In the study, VSE150 vibration analyzer and VSA001 code accelerometer were used for vibration measurements and their analysis. Obtained findings were analyzed. As a result, it has been seen that vibration analysis can be effectively used in detecting the factors that cause vibration. The results reveal that the fault detection in the bearing can be successfully performed by vibration analysis.

Keywords: Vibration, Bearing Fault, Fault Detection, Unbalance, Fan Blade.

1. GİRİŐ

Titreřim, bir cismin denge konumunda yaptıęı yer deęiřimi hareketi olarak tanımlanır. Hareketli bileřenlere sahip dnen makine sistemlerinde ve makinelere baęlı bileřenlerde oluřan dinamik kuvvetlerin etkisi neticesinde titreřimler meydana gelir. Mekanik olarak iyi

dengelenmiř bir makede oluřan titreřim ok azdır. Dięer yandan yk altında alıřması sonucu makine paraları ařınır, bazı paralarda kkte olsa Őekil deęiřimleri ve dinamik zelliklerinde deęiřiklikler meydana gelir. Bu deęiřimlere baęlı olarak paralar arasında bořluklar oluřur, eksen kaıklıkları ve

dengelesizlik gibi problemler ortaya çıkabilir. Bütün bu oluşan problemler makine sistemlerinin titreşimlerinde bir artış meydana getirir [1-3].

Endüstride kullanılan makine sistemlerinin büyük bir çoğunluğu dönme hareketine bağlı olarak iş yapmaktadır. Bu makine sistemlerinde oluşabilecek arızaların başlangıç aşamasında tespit edilmesi ve tespit edilen arızaların giderilmesi üretimin verimliliği bakımından büyük önem taşır. Bu mekanik arızaların tespiti için kullanılabilir yöntemler arasında titreşim analizi ilk sıralarda yer alır ve dönen elemanların kestirimci bakım uygulaması endüstride yaygın olarak kullanılmaktadır [1, 4]. Döner makine sistemlerine etki eden iç ve dış kuvvetler nedeni ile çalışma esnasında titreşimin oluşmaması mümkün değildir. Önemli olan bu titreşimlerin belirlenen limitlerde tutulmasıyla makinenin çalışma ömrünün ve verimliliğinin artırılmasıdır [1, 2]. Ayrıca, bu sistemlerde en sık karşılaşılan problemler; dengelesizlik, mekanik gevşeklik, eksen kaçıklığı ve yuvarlanmalı yatak arızalarıdır. Bu problemlerin neden olduğu titreşimler hareketli parçalar aracılığı ile mekanik gövdeye veya yataklara aktarılır. Bu noktalardan bir titreşim algılayıcısı ile yapılan ölçümler sayesinde makinenin içyapısında meydana gelen sorunlar rahatlıkla belirlenebilir. Ölçülen titreşim değerleri Fast Fourier Transform (FFT) metodu ile zaman ekseninden frekans eksenine dönüştürülür. Farklı mekanik sebeplerden kaynaklanan arızalar, farklı frekanslarda titreşim sinyalleri ürettiği için frekans analizi ile makine sistemlerinde oluşan arızalar belirlenebilir. Titreşim analiziyle kestirimci bakım, makine sistemlerinde üretimi durdurmadan kullanılan bakım yöntemi olarak bilinmektedir. Bu yöntemde makine sistemlerinde periyodik olarak gerçekleştirilen ölçümlerle elde edilen veriler titreşim analizi ile incelenir, tespit edilen arızanın nedeni ve seviyesi makinelere zarar vermeden belirlenebilir [1-5].

Literatürde, döner bir makinenin eksen kaçıklığı veya dengelesizliği sonucu oluşan titreşimler deneysel olarak analiz edilmiş ve titreşim değerlerinin tahammül edilebilir sınırlar içinde olduğu sonucu elde edilmiştir [1]. Yapılan bir çalışmada endüstriyel tesislerin bakımında titreşim analiziyle kestirimci bakım yöntemi incelenmiştir [5]. Diğer bir çalışmada,

rulmanlarla desteklenmiş döner makinelerde titreşim analizi ile kestirimci bakım yöntemi ele alınmıştır [6]. Literatür çalışmalarında; döner makinelerde en sık karşılaşılan gevşeklik, dengelesizlik, eksen kaçıklığı, yuvarlanmalı yatak arızaları ve farklı işlem uygulanmış millerin dinamik davranışları analiz edilmiştir [7-10]. Ayrıca literatür çalışmalarında, makine sistemlerinin titreşim davranışları, yuvarlanmalı yataklar, motor devir ve yükünün titreşime etkisi gibi birçok çalışma yapılmış ve ayrıntılı olarak incelenmiştir [12-14].

Kestirimci bakıma en uygun yaklaşım olarak sürekli izlemeyi benimsemiş bir çimento fabrikasında gerçekleştirilen çalışmada; bir mekanizmayı etkileyebilecek arızaları tespit etmek, bozulmaları öngörmek ve bu arızaların muhtemel nedenlerini belirlemek için hız ve ivme seviyelerinin analizi ve spektral analizi kullanılmıştır. Bu bağlamda, gerçek ölçümler, makinede arızaya neden olan zayıf noktaların tespit edilmesine yol açan titreşim ile analiz edilmiş, bu nedenle çevrimiçi kontrol sistemi aracılığıyla bozulmanın izlenmesi ile bakımın optimizasyonu gerçekleştirilmiştir. Titreşim analizi, titreşim seviyesinin sabit düzeltme eşiği sınırına ulaştıktan sonra arızalı bileşenleri tespit etme olanağı sağlamıştır [16]. Uysal, çalışmasında; makinelerde titreşim analizi ile kestirimci bakım yöntemi gerçekleştirmiş ve periyodik olarak titreşim verileri almış, bu verileri frekans analizi ile değerlendirerek arızaları tespit etmeye çalışmıştır. Rulman arızaları, mekanik gevşeklik ve fan kanat geçiş frekansı tespit etmiştir [17]. McFadden ve Smith çalışmalarında, sabit yük altındaki bir yuvarlanmalı yatak iç bileziğinde oluşan hasarların nedeni olduğu titreşimi belirlemek amacıyla bir matematiksel model oluşturmuş ve hesaplanan sonuçlar ile deneysel sonuçların birbiri ile örtüştüğünü gözlemlemişlerdir [18, 19]. Döner makinelerdeki dengelesizlik arızası için bir rotor düzeneğinde yapılan deneysel çalışmada; beş farklı devirde rotoru çalıştırıp titreşim hız ölçümleri yapılmış, spektrum ve faz analizi gerçekleştirilmiştir. Farklı kuvvetlerde ve hızlarda elde edilen veriler kıyaslanmıştır [20]. Diğer bir çalışmada, rulmanların dış bilezik, iç bilezik ve yuvarlanma elemanları üzerindeki hasarları titreşim analizi ile belirlemişlerdir. Arızaların yeri FFT spektrumu ile gösterilmiş ve her iki yataktaki motor ve fanda yatay yönde gösterilmiştir. Titreşim hızını azaltmak için ağırlık eklenerek yerinde

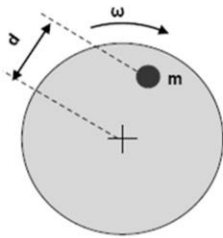
dinamik denge sağlanmıştır [21]. Milind çalışmasında, erken arıza tespiti ve acil bakım maliyetinde tasarruf sağlayabileceğinden dolayı FFT analizi kullanarak yuvarlanmalı yatak arızalarını tespit etmiştir [22]. Titreşim analizi ile makine ve ekipmanlarında oluşabilecek arızalar önceden tespit edilerek daha büyük arızaların oluşması önlenmektedir. Literatür çalışmalarının genelinde olduğu gibi üretim esnasında oluşabilecek arızaların önceden tespit edilmesi hayati önem taşımaktadır. Bu nedenle büyük bir arıza oluşmadan önce tespit edebilmek amacıyla bu çalışmada, fan kanatlarında oluşan balans bozukluğu ve yuvarlanmalı yataklarda oluşan arızanın titreşime etkisi incelenmiştir.

2. DÖNEN MAKİNELERDE OLUŞAN ARIZALAR

Dengesizlik, mekanik gevşeklik, eksen kaçıklığı ve rulman aşınmaları dönme hareketi ile iş yapan makinelerde en çok karşılaşılan arızalar olarak bilinmektedir [1].

2.1. Dengesizlik

Balans ifadesi dönme hareketi ile iş yapan makinelerde dönen bileşenler ile oluşturulan bütün kuvvetlerin dengede olması durumu olarak ifade edilebilir. Bu denge halinin bozulmaya uğraması dengesizliğe sebep olur. Dengesizlik, makinelerde oluşan titreşimlere sebep olan mekanik problemlerin en başında gelir. Teorik olarak, mükemmel dengelenmiş bir makinede titreşim oluşması beklenmez. Ancak, çalışma esnasında tüm makineler azda olsa dengesizdirler. Bunun nedenleri olarak, elemanların geometrik olarak simetrik olmaması, elemanlarda kullanılan malzemelerin homojen olmaması, çalışma şartlarında oluşan değişimler ve montaj hatalarından kaynaklanabilir [1, 2, 9, 12, 13, 17]. Dengesizlik kütlelerinin şematik gösterimi Şekil 1’de gösterilmiştir. Denklem (1) ile açısal hız ve Denklem (2) ile dengesizlik kuvveti hesaplanabilir.



Şekil 1. Dengesizlik kütle şematik gösterimi [7, 8].

$$\omega = \frac{2\pi \cdot N}{60} \quad (1)$$

$$F_{\text{deng}} = m \cdot d \cdot \omega^2 \quad (2)$$

F_{deng} = Dengesizlik kuvveti (N)

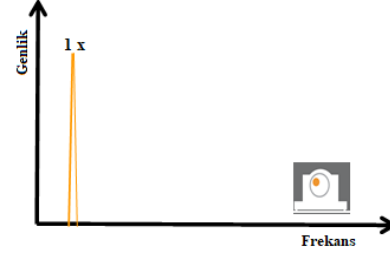
m = Dengesizlik kütlesi (kg)

d = Dengesizlik kütlesi ile dönme eksenini arasındaki uzaklık (m)

ω = Açısal hız (rad/s)

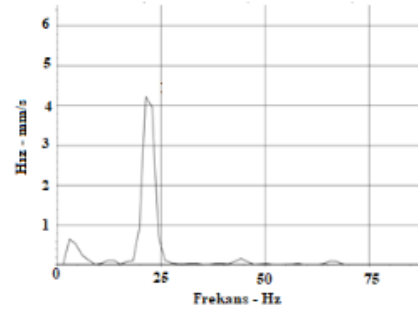
N = Devir sayısı (dev/dak)

Dengesizlik spektrum grafiği mil dönme frekansında (1x) bir tepe oluşturur (Şekil 2).



Şekil 2. Dengesizliğin frekans analizi grafiğinde gösterimi.

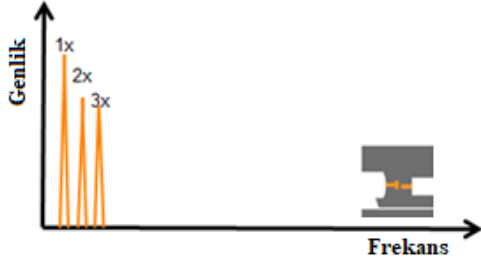
1282 devir/dakika (21,36 Hz) ile çalışmakta olan bir fan motoru üzerinden yapılan titreşim ölçümü sonucu elde edilen değerler incelendiğinde mil dönme frekansının 1. katında tepe oluşması (Şekil 3), dengesizliği göstermektedir.



Şekil 3. Fan motorunda oluşan dengesizliğin frekans analizinde yeri.

2.2. Eksen Kaçıklığı

Bir kaplin bağlantısı aracılığı ile millerin aynı eksende olmaması durumunda eksen kaçıklığı oluşur. Genellikle dönen makinelerin mekanik olarak yanlış hizalanması sonucu oluşmaktadır [1, 6-8, 17]. Eksen kaçıklığı sonucu oluşan titreşimler spektrum grafiğinde (Şekil 4) mil dönme frekansının 1, 2 ve 3. katında görülür.



Şekil 4. Eksen kaçıklığının frekans analizi grafiğindeki yeri.

2.3. Mekanik Gevşeklik

Mekanik gevşeklik, hem dönen hem de dönmeyen makinelerde titreşimlere neden olabilir. Genellikle aşırı yatak boşlukları, gevşek montaj cıvataları, uyumsuz parçalar,

2.4. Rulman Arızaları

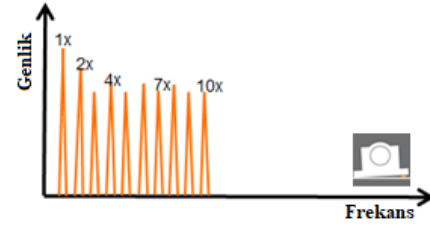
Rulman arızası kaynaklı problemler dönen makine elemanlarındaki arızaların sebep olduğu duruşların ve verimsizliğin temel nedenidir. Yapılan araştırmalar sonucunda; meydana gelen arızaların yaklaşık olarak % 50'lik kısmının rulman kaynaklı problemler sonucu oluştuğu bildirilmiştir [1, 2, 7].

Rulmanlar dönme hareketi ile iş yapan makinelerin yataklanması için kullanılan elemanların başında gelir. Sürekli hareket halinde olmaları ve yüke maruz kalmaları nedeni ile bozulma olasılıkları oldukça yüksektir. Problemsiz çalışmaları, makinenin verimliliği ve çalışma ömrü açısından büyük önem taşımaktadır. Rulmanlar, sürekli hareket halinde olduğu için oluşan sürtünmelerin doğal bir etkisi olarak aşındığında veya üzerinde bir çatlak ya da çizik oluştuğunda çeşitli frekanslarda titreşim üretir. Geometrik yapısına bağlı olarak rulmanın mekanik bileşenleri olan dış bilezik, iç bilezik ve yuvarlanma elemanı (bilya) üzerinde birbirinden bağımsız frekans bileşenleri oluşur. Bu bileşenler sayesinde rulmanda meydana gelen hata ve hatanın gelişimi ile ilgili kritik bilgiler elde edilir. Frekans spektrumu incelendiğinde titreşimin frekansı hatanın türünü ve genliği ise problemin büyüklüğünü gösterir. Arıza frekansları ile motorun devir sayısı arasında doğrusal olarak bir ilişki vardır. Motor devir sayısı değiştiğinde bilya hatalı kısımdan geçiş sıklıkları değişir ve bu nedenle hata frekansları da yer değiştirir [6-8, 23-32].

Rulman arızaları, Şekil 6'da görülen yuvarlanmalı yatak geometrisi ve mil dönme

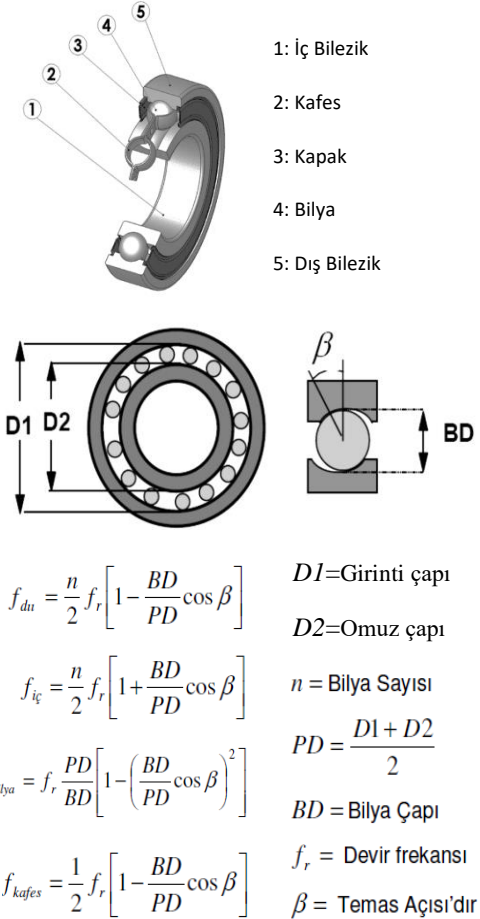
yapıdaki korozyon ve çatlaklardan kaynaklanır [1, 6-8].

Gevşeklik türüne bağlı olarak, titreşimler, makinenin dönüş hızının 10 katına kadar kendisini belli eder. (Şekil 5)



Şekil 5. Mekanik gevşekliğin frekans analizi grafiğindeki yeri.

hızına bağlı olarak formüller ile bulunan arıza frekansları ile belirlenir. Spektrum analizi ile rulman bileşenlerinden hangisinde bir arıza meydana gelmiş ise bu bileşenin arıza frekanslarında, bunun katlarında ve bazı durumlarda dönen mil devir sayısı ile oluşturduğu yan bant frekanslarında problemler görülür [6-8, 12, 17, 23, 29].

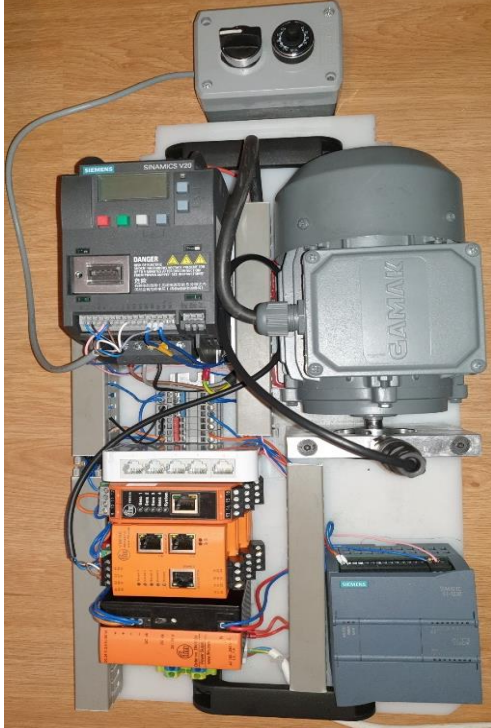


Şekil 6. Yuvarlanmalı yatak geometrisi ve arıza frekanslarının hesaplanması [2, 12, 23, 29].

3. MATERYAL VE METOT

Fan kanatlarında oluşan dengesizliğin titreşim analizi ile belirlenebilmesi amacıyla kullanım yerinde çalışma yapılmış ve fan motorundan ivmeölçer ile veriler alınmıştır.

İç bileziği arızalı olduğu bilinen SKF6205 kodlu rulmanın frekans analizi ile arıza tespitinin yapılabilmesi amacıyla Şekil 7’de görülen deney düzeneği oluşturulmuştur.

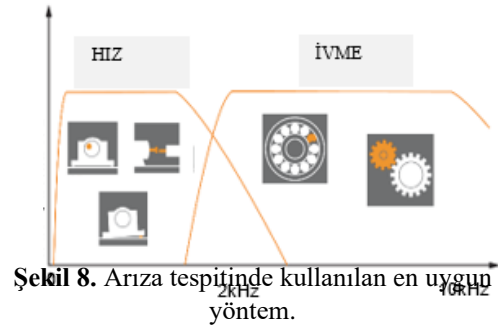


Şekil 7. Deney düzeneği ve şematik gösterimi: (1) Motor; (2) İvmeölçer; (3) Yuvarlanmalı yatak yuvası ve yuvarlanmalı yatak (Rulman); (4) Hız kontrol; (5) Bilgisayar ve titreşim yazılım programı.

Çalışmada rulman yatağına SKF6205 kodlu rulman takılmış, VES004 yazılımı ile ISO 10816’ya göre titreşim ölçümü ve spektrum analizi yapılmıştır. Vibrasyon ölçer, ISO 10816’e göre bir ölçüm yapılmasına izin veren bir mod ile donatılmıştır.

3.1. Titreşim Ölçümünde Hız ve İvme Çalışan mekanik bir sistemde oluşan titreşimleri tespit etmek için kontrol edilecek sistemin dönme frekansına bağlı olarak, hız veya ivme birimleri cinsinden ölçüm kullanılabilir. Arıza tespitinde en uygun yöntem (Hız-İvme) Şekil 8’de gösterilmiştir. Hangisinin en uygun olduğu, arızanın ortaya çıkma sıklığına bağlıdır. Belirli bir problemi tespit etmek için kullanılacak yöntem arızanın hangi frekansta oluştuğuna bağlıdır. Sanayide kullanılan sensörler genellikle hız cinsinden ölçüm yapan ve 10-1000 Hz aralığındaki titreşimlerin Root Mean Square (RMS) ortalamasını alan sensörlerdir.

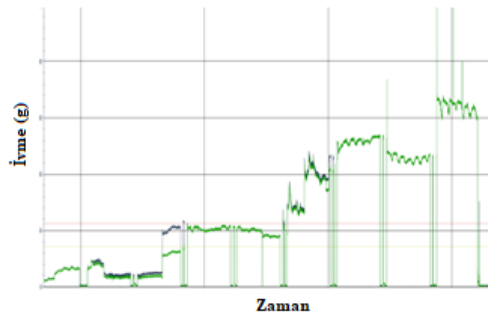
Dengesizlik, eksen kaçıklığı, gevşeklik vb. gibi arızaları tespit etmek için hız birimi cinsinden ölçüm kullanılabilir. İvme ile çok daha yüksek frekanslar izlenebilir. Yatak hasarının başlangıcında meydana gelen küçük şoklar ve darbeler, dişli kutusu arızaları vb. gibi arızaları tespit etmek için ivme ölçümleri kullanmak daha iyi sonuç verir [1, 6-8, 11, 12, 24-29].



Şekil 8. Arıza tespitinde kullanılan en uygun yöntem.

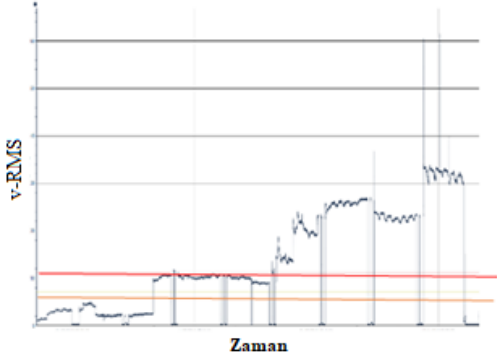
4. BULGULAR VE TARTIŞMA

Şekil 9’da görülen 1282 rpm (revolution per minute - devir/dak) hızla çalışan bir boyahane fan motorundan elde edilen ivme değerleri incelendiğinde; yaklaşık 4 aylık bir süreçte ivme değerlerinin değişimi görülmüş ve bu değişime sebep olan etkenin fan kanatlarındaki kirlenmeden dolayı oluşan balans bozukluğu olduğu gözlemlenmiştir.



Şekil 9. Fan motoru titreşim ölçümü.

Şekil 10'da hız cinsinden (v-RMS) titreşimin zamana bağlı değişimi grafik olarak verilmiş ve bu grafik incelendiğinde titreşimin zamana bağlı olarak artış eğiliminde olduğu görülmektedir.



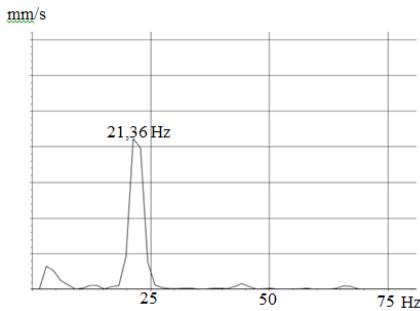
Şekil 10. Hız cinsinden (v-RMS) titreşimin zamana bağlı değişimi.

Şekil 11'de titreşimi ölçen algılayıcıdan verilerin alınması ve analiz sonucu gösterilmiştir. Frekans analizi (FFT) incelendiğinde (Şekil 11-b) titreşime neden olan ana etmenin dengesizlik olduğu görülmektedir. Literatür çalışmaları ile karşılaştırıldığında, dengesizlik probleminin FFT analizi ile belirlenmesine yönelik çalışmaların yapıldığı ve benzer sonuçlar elde edildiği gözlenmiştir [1, 9, 12, 20, 24-29].

Verilerin alınması



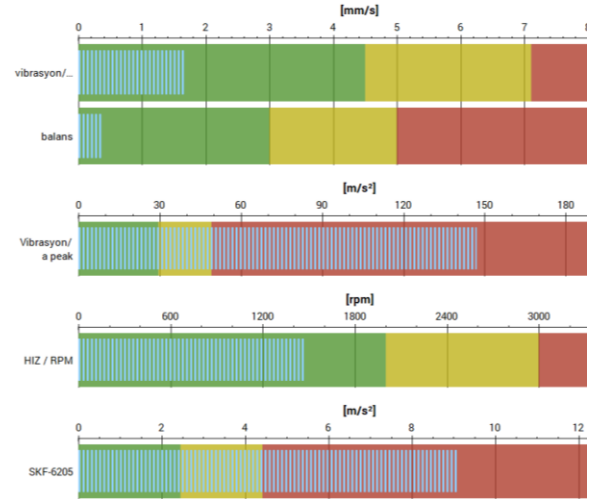
a)



Şekil 11. İvmeölçer ile verilerin alınması ve analiz sonucu; a) Verilerin alınması, b) FFT analiz sonucu.

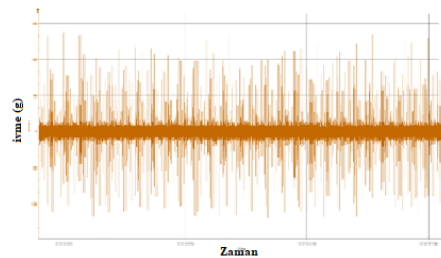
Şekil 11-b titreşimin balans probleminden kaynaklandığını açıkça göstermektedir. Burada 21,36 Hz ile dönen bir fan motoru üzerinden yapılan titreşim ölçümü sonucu mil dönme frekansının 1. katında tepe oluşması dengesizliği göstermektedir.

Titreşim analizinde kullanılan Hız (v-RMS) ve ivme (a-peak) ölçüm birimlerinin farklılığını daha iyi açıklayabilmek için Şekil 6-a'da oluşturulan deney düzeneğinde arızalı bir rulmandan gelen titreşimler incelenmiştir. Bunun için iç bileziği önceden hatalı olan SKF6205 kodlu rulman, rulman yatağına bağlanmış ve Şekil 12'deki ölçüm sonuçları elde edilmiştir.

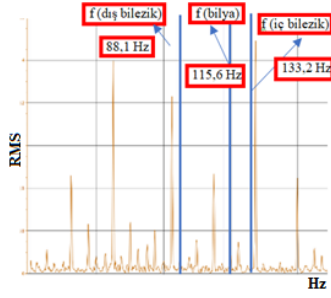


Şekil 12. Hız (v-RMS) ve ivme cinsinden ölçüm sonuçları.

Görüldüğü gibi motor 1476 rpm hız ile dönerken ölçülen titreşim değeri v-RMS cinsinden 1,6 mm/s değerinde ve ISO10816 ya göre arıza limitlerinin altındadır. Buna karşın ivme cinsinden alınan ölçümlerde ise a-peak değeri ve SKF6205 için arıza frekanslarında oluşan titreşim seviyesi belirlenen limitleri aşmış ve kırmızı alarm seviyesindedir. Bu farklılıkların sebeplerini daha iyi anlayabilmek için spektrum analizi yapılmış, Şekil 13 ve Şekil 14'de görülen grafikler elde edilmiştir.



Şekil 13. İvmeölçer ile zamana bağlı titreşim değerleri.



Şekil 14. SKF6205 için hesaplanmış arıza frekanslarındaki problemlerin analizi.

Şekil 14’te 1476 devirle dönmekte olan SKF6205 kodlu rulman için hesaplanmış arıza frekanslarında oluşan hataların büyüklükleri görülmektedir. Rulman geometrisine (Şekil 6) bağlı arıza frekansları hesabına göre SKF6205 kodlu rulman için hesaplanan frekanslar dış bilezik, bilya ve iç bilezik için sırası ile 88,1 Hz, 115,6 Hz ve 133,2 Hz’dir.

Şekil 14’te yaklaşık 134,8 Hz de bir problem görülmüş olup problemin rulman iç bileziğinden kaynaklandığı saptanmıştır.

5. SONUÇLAR

Bu çalışmada, bir rulmanda oluşan arızanın titreşime etkisinin belirlenebilmesi amacıyla çalışma yapılmıştır. Çalışmada SKF6205 kodlu rulman kullanılmış ve iç bileziğinde oluşturulan hasarın frekans analizi yöntemi ile tespit edilebileceği görülmüştür. Gerçek bir çalışma ortamında ise fan motorundan alınan titreşim ölçüm sonuçları ile fan kanatlarında kirlenme etkisi ile meydana gelen dengesizliğin titreşime olan etkisi gözlemlenmiştir. Titreşim analizi ile izleme yapmanın ekipman sağlığı için olumlu sonuçlar verdiği saptanmıştır. Ayrıca, titreşim ölçümü için kullanılacak yöntem ve ölçüm birimlerinin titreşim analizindeki önemi gözlemlenmiştir. Yuvarlanmalı yatak arıza analizi uygulamasında hız cinsinden v-RMS alınan ölçümde vibrasyonun ISO10816’ya göre belirlenmiş sınırlar içerisinde olduğu halde ivme cinsinden ölçümlerde ise problemin açıkça fark edildiği görülmüştür.

Sonuç olarak, dönen makinelerde titreşim analizinin rulman arızasının belirlenmesinde ve titreşime sebep olan etmenlerin tespit edilmesinde etkin olarak kullanılabileceği görülmüştür. Sonuçlar, titreşim analizi ile yataktaki arıza tespitinin başarılı bir şekilde yapılabileceğini ortaya koymaktadır.

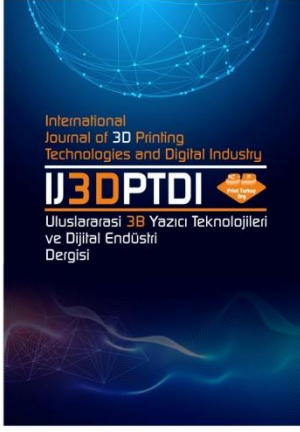
TEŞEKKÜR

Bu bilimsel çalışmaya destekleri için IFM Elektronik firmasına teşekkür ederiz.

KAYNAKLAR

- Alçelik, N., Kam, M., “Dönen makinelerde aksel kaçıklık ve dengesizliğin titreşim analizi”. Bilecik Şeyh Edebali Üniversitesi Fen Bilimleri Dergisi, Cilt 7, Sayı 100. Yıl Özel, Sayfa 256-269, 2020.
- Kam, M., “Kriyojenik işlem görmüş millerin dinamik davranışlarının deneysel analizi”, Doktora Tezi, [Experimental analysis of cryogenic treated shafts dynamic behaviors] [Thesis in Turkish], Düzce Üniversitesi Fen Bilimleri Enstitüsü, Makine Mühendisliği Anabilim Dalı, Düzce, 2016.
- Kam, M., Saruhan, H., İpekçi, A., “FDM yöntemi ile üretilen kovan yatakların titreşimi sönümlenme kabiliyetlerinin deneysel analizi”, Politeknik Dergisi, Cilt 25, Sayı 1, Sayfa 137-143, 2021.
- Kam, M., Saruhan, H., İpekçi, A., “Experimental investigation of vibration damping capabilities of 3D printed metal/polymer composite sleeve bearings”. Journal of Thermoplastic Composite Materials, 08927057221094984, 2022.
- Belek, T., “Endüstriyel tesislerin bakımında modern yaklaşım: dinamik erken uyarıcı bakım yöntemleri”, Mühendis ve Makina, Cilt 29, Sayfa 29-36, 1988.
- Orhan, S.. “Rulmanlarla yataklanmış dinamik sistemlerin titreşim analiziyle kestirimci bakımı”, Doktora Tezi, Kırıkkale Üniversitesi Fen Bilimleri Enstitüsü Makine Anabilim Dalı, Kırıkkale, 2002.
- Orhan, S., “Dönen makinelerde oluşan arızalar ve titreşim ilişkisi”. Teknoloji, Cilt 6, Sayı 3-4, Sayfa 41-48, 2003.
- Orhan, S., Arslan, H., Aktürk, N., “Titreşim analiziyle rulman arızalarının belirlenmesi”. Gazi Üniversitesi Mühendislik Mimarlık Fakültesi Dergisi, Cilt 18, Sayı 2, Sayfa 39-48, 2003.
- Uysal, V., Morgül, Ö., “Dönen makinelerdeki dengesizlik (balanssızlık) arızasının titreşim analizi ve faz açısı yardımıyla teşhisi”. Sakarya Üniversitesi Fen Bilimleri Enstitüsü Dergisi, Cilt 19, Sayı 3, Sayfa 245-256, 2015.
- Kam, M., Saruhan, H., “Kriyojenik işlem uygulanmış millerin yuvarlanmalı ve kaymalı yataklarda deneysel titreşim analizi”, Politeknik Dergisi, Cilt 22, Sayı 1, Sayfa 129-134, 2019.

11. Saruhan H., Kam M., “Experimental spectral analysis of split sleeve bearing clearance effect on a rotating shaft system”. *Makine Teknolojileri Elektronik Dergisi*, Cilt 13, Sayı 4, Sayfa 1-8, 2016.
12. Karahan, F., “Titreşim analizi ile makinalarda arıza teşhisi”, Yüksek Lisans Tezi, Celal Bayar Üniversitesi Fen Bilimleri Enstitüsü Makine Mühendisliği Ana Bilim Dalı, Manisa, 2005.
13. Açık, S., “Sürekli form baskı makinasının titreşim sinyali yardımıyla kestirimci bakımının yapılması”, Yüksek Lisans Tezi, Gazi Üniversitesi Fen Bilimleri Enstitüsü, İleri Teknolojiler Anabilim Dalı, Ankara, 2008.
14. Gözüoğlu, S. G., Doğan, Z.. “Durum izleme ve istatistiksel süreç kontrolü kullanarak şebeke kalkışlı daimi mıknatıslı senkron motorda rulman arızası tespiti”. *El-Cezeri Journal of Science and Engineering*, Cilt 7, Sayı 2, Sayfa 781-794, 2020.
15. Jagtap, H. P., Bewoor, A. K., Kumar, R., “Failure analysis of induced draft fan used in a thermal power plant using coordinated condition monitoring approach: A case study”. *Engineering Failure Analysis*, Vol. 111, 104442, 2020.
16. Taleb, M., & Chaib, R., “Vibration analysis of rotating machines for an optimal preventive maintenance. *Mining Science*”, Vol. 23, Pages 191-202, 2016.
17. Uysal, V., “Enerji santrallerinde titreşim analizi ile kestirimci bakım”, Yüksek Lisans Tezi, Sakarya Üniversitesi, Fen Bilimleri Enstitüsü, Makine Mühendisliği Anabilim Dalı, Sakarya, 2019.
18. Mcfadden, P. D., Smith, J. D., “Model for the vibration produced by a single point defect in a rolling element bearing”, *Journal of Sound and Vibration*, Vol. 96, Issue 1a, Pages 69-82, 1984.
19. Mcfadden, P. D., Smith, J. D., “The vibration produced by a multiple point defect in a rolling element bearing”, *Journal of Sound and Vibration*, 98(2), 263-273, 1985.
20. Kumar, K. B., Diwakar, G., Satynaryana, M. R. S., “Determination of unbalance in rotating machine using vibration signature analysis”, *International Journal of Modern Engineering Research (IJMER)* Vol.2, Issue.5, pp-3415-3421, Sep-Oct. 2012.
21. Prasad, P. V. V., & Kumar, V. R., Detection of bearing fault using vibration analysis and controlling the vibrations. *International Journal of Engineering Sciences & Research*, Vol. 4, Issue 10, Pages 539-550, 2015.
22. Milind N., “Bearing fault analysis using frequency analysis and wavelet analysis”, *International Journal of Innovation, Management and Technology*, Vol. 4, No. 1, February 2013.
23. Saruhan, H., Saridemir, S., Çicek, A., Uygur, I., “Vibration analysis of rolling element bearings defects”. *Journal of applied research and technology*, Vol. 12, Issue 3, Pages 384-395, 2014.
24. Yiğit, A., “Rulmanlı yatak arızalarının titreşim analizi ile belirlenmesi”. Yüksek Lisans Tezi, Dokuz Eylül Üniversitesi, Fen Bilimleri Enstitüsü, Makine Mühendisliği Ana Bilim Dalı, İzmir, 2008.
25. Geramitchioski, T., Trajcevski, I., “Case study: vibration analysis of a vertical pump of cooling system in fero-nickel industry”. In 8th International Symposium, Pages 1-6, June 2014.
26. Kumar, A., Kumar, R., “Role of signal processing, modeling and decision making in the diagnosis of rolling element bearing defect: a review”. *Journal of Nondestructive Evaluation*, Vol 38, Issue 1, Pages 1-29, 2019.
27. Ayan, Ö. A., “Döner makine elemanların titreşim analizi ile kestirimci bakımı”. Yüksek Lisans Tezi, Trakya Üniversitesi, Fen Bilimleri Enstitüsü, Makine Mühendisliği Anabilim Dalı, 2019.
28. AlShorman, O., Irfan, M., Saad, N., Zhen, D., Haider, N., Glowacz, A., & AlShorman, A., “A review of artificial intelligence methods for condition monitoring and fault diagnosis of rolling element bearings for induction motor”. *Shock and vibration*, 2020.
29. Yıldırım, E., Karahan, M. F., “Titreşim analizi ile rulmanlarda kestirimci bakım”. *Celal Bayar Üniversitesi Fen Bilimleri Dergisi*, Cilt, 11, Sayı 1, Sayfa 17-23, 2015.
30. Girit, O., Atakok, G., Ersoy, S., “Data analysis for predictive maintenance of Servo Motors”. *Shock and Vibration*, 2020.
31. Adin, H., Adin, M. Ş., Akgül, S. “Araçlarda kullanılan fren diskinin sonlu elemanlar yöntemiyle hasar analizi”. *International Symposium on Engineering, Natural and Social Sciences (ISENS-21)*, Sayfa 25-28 November 2021, Batman, Türkiye, 2021.
32. Adin, H., Adin, M. Ş., “Numerical Analysis of Damaged Helical Gear Wheel”. *Batman Üniversitesi Yaşam Bilimleri Dergisi*, Vol. 11, Issue 1, Pages 43-56, 2021.



ULUSLARARASI 3B YAZICI TEKNOLOJİLERİ
VE DİJİTAL ENDÜSTRİ DERGİSİ

INTERNATIONAL JOURNAL OF 3D PRINTING
TECHNOLOGIES AND DIGITAL INDUSTRY

ISSN:2602-3350 (Online)

URL: <https://dergipark.org.tr/ij3dptdi>

1420 MHZ RADYO TELESKOP UYGULAMALARI İÇİN MİKROŞERİT BASAMAK EMPEDANS REZONATÖRLÜ BANT GEÇİREN FİLTRE TASARIMI

SIR MICROSTRIP BAND-PASS FILTER DESIGN FOR
1420 MHZ RADIO TELESCOPE APPLICATIONS

Yazarlar (Authors): Bilge Şenel 

Bu makaleye şu şekilde atıfta bulunabilirsiniz (To cite to this article): Şenel B., “ 1420 Mhz Radyo Teleskop Uygulamaları İçin Mikroşerit Basamak Empedans Rezonatörlü Bant Geçiren Filtre Tasarımı” *Int. J. of 3D Printing Tech. Dig. Ind.*, 7(1): 9-17, (2023).

DOI: 10.46519/ij3dptdi.1137571

Araştırma Makale/ Research Article

Erişim Linki: (To link to this article): <https://dergipark.org.tr/en/pub/ij3dptdi/archive>

1420 MHZ RADYO TELESKOP UYGULAMALARI İÇİN MİKROŞERİT BASAMAK EMPEDANS REZONATÖRLÜ BANT GEÇİREN FİLTRE TASARIMI

Bilge Şenel^a 

^aSüleyman Demirel Üniversitesi, Mühendislik Fakültesi, Elektrik-Elektronik Mühendisliği Bölümü, TÜRKİYE

* Sorumlu Yazar: bilgeturkel@sdu.edu.tr

(Received: 29.06.2022; Revised: 18.10.2022; Accepted: 04.04.2023)

ÖZ

Radyo teleskoplar, gökbilimcilere, görsel veya optik bölgenin çok ötesine uzanan erişilebilir elektromanyetik spektrumun tamamında gözlem yapma imkânı sunarlar. Her frekans aralığı kendi içgörülerini sağlar ve genellikle kendi teleskop ve dedektör çeşitlerini gerektirir. Radyo astronomlar, 13 MHz ile 2000 GHz aralığında frekanslarda enerji yayan veya emen nesnelere incelerler ve atmosferin şeffaf olduğu her frekans değerinde çalışmalar yapılır. 1420 MHz radyo astronomik ölçümlerin yapıldığı frekans değerlerinden birisidir. Yaklaşık 1420 MHz'de 21 cm'lik bir dalga boyuna sahip olan nötr hidrojen (HI) emisyonları, galaksideki uzak yerlerden ve yönlerden kaynaklanır, yıldızlararası bulutlardan geçer ve Doppler kaydırılmış frekanslarda yer tabanlı radyo teleskop gözlemlerinde ortaya çıkar. HI emisyonlarından yapılan haritalar, Samanyolu Galaksisi'nin sarmal yapısını ortaya çıkarır. Ölçümler radyo teleskop sistemlerinin RF bloğu ile gerçekleştirilir. Bant geçiren filtreler bu RF bloğun çok önemli bileşenlerindedir. Bu çalışmada 1420 MHz radyo teleskop uygulamaları için Basamak Empedans Rezonatör yapısı kullanılarak mikroşerit bant geçiren filtre tasarımı yapılmıştır. Tasarımda basamak empedans rezonatörü ile paralel kuplajlı hat yapısı beraber kullanılmıştır. Filtre Keysight ADS simülatörü ile tasarlanmış ve istenen tasarım kriterlerine ulaşmak için paralel kuplajlı hat uzunlukları optimize edilmiştir. Yapılan simülasyonlar neticesinde tasarlanan filtrenin 3dB bant genişliği 130 MHz, ekleme kaybı (S_{21}) -0.152 dB, giriş yansıma katsayısı (S_{11}) -38.018 dB olarak bulunmuştur. Çalışmada tasarlanan filtre 1420 MHz radyo teleskoplarının RF alıcı bloğunda kullanılacak kriterlere sahiptir. Ayrıca filtre eğitim ve deney amaçlı radyo teleskop sistemlerinde kullanılabilir.

Anahtar Kelimeler: Radyo Teleskop, 1420 MHz Nötr Hidrojen (HI) Emisyonu, Mikroşerit Bant Geçiren Filtre, Basamak Empedans Rezonatör.

SIR MICROSTRIP BAND-PASS FILTER DESIGN FOR 1420 MHZ RADIO TELESCOPE APPLICATIONS

ABSTRACT

Radio telescopes allow astronomers to observe across the entire accessible electromagnetic spectrum that extends far beyond the visual or "optical" region. Each frequency range provides its own insights and often requires its own variety of telescopes and detectors. Radio astronomers research objects which emit or absorb energy from 13 MHz to 2000 GHz and studies are carried out at every frequency where the atmosphere is transparent. 1420 MHz is one of the frequency values where radio astronomical measurements are carried out. Neutral hydrogen (HI) emissions, with a wavelength of 21 cm at about 1420 MHz, originate from distant places and directions in the galaxy, pass through interstellar clouds and occur in ground-based radio telescope observations at Doppler shifted frequencies. Maps made from HI emissions reveal the spiral structure of the Milky Way Galaxy. Measurements are carried out with the RF block of radio telescope systems. Bandpass filters are one of the most important components of this RF block. In this study, a microstrip bandpass filter was designed for 1420 MHz radio telescopes using the Stepped Impedance Resonator (SIR). In the design, parallel coupled lines are used together

with the stepped impedance resonator. The filter was designed with the Keysight ADS and lengths of parallel coupled lines were optimized to achieve the desired design criteria. As a result of the simulations, the 3dB bandwidth of the designed filter was found to be 130 MHz, the insertion loss (S_{21}) was -0.152 dB, and the input reflection coefficient (S_{11}) was -38.018 dB. The designed filter has the criteria to be used in the RF receiver block of 1420 MHz radio telescopes. The filter designed in the study can be used in radio telescope systems for educational and experimental purposes

Keywords: Radio Telescope, 1420 MHz Neutral Hydrogen (HI) Emission, Microstrip Bandpass Filter, Stepped Impedance Resonator.

1. GİRİŞ

Güneşin de içinde bulunduğu Samanyolu Galaksisi 100.000 ışık yılı çapa sahiptir. Çubuklu sarmal bir yapıda olup, içerisinde zayıf bir şekilde her yana dağılmış yaklaşık 200 milyar yıldız kümesi bulunduğu tahmin edilmektedir. Yıldızlararası ortam denilen toz ve gaz bulutları yıldızların doğumları ve ölümleri ile meydana gelmektedir. Yıldızlararası ortamı oluşturan maddenin %99'u gazlardan %1'i ise tozlardan oluşur. Gazlar atom, molekül, iyon ve elektronlardan; tozlar ise gezegen, asteroit, kuyruklu yıldız, manyetik alanlar ve kozmik ışıklardan meydana gelmektedir. Yıldızlararası ortamda gazların %90'nını hidrojen, %10'nunu ise helyum oluşturmaktadır. Hidrojen, atomik yapıda-nötr hidrojen H(I), iyonik yapıda H(III) ve moleküler yapıda (H_2) şeklinde bulunur. Gözlemler, yıldızlararası ortamı oluşturan maddeye bakılarak yapıldığından gök bilimciler açısından yıldızlararası ortamın önemi çok büyüktür. Atomik hidrojenin yarısı, moleküler hidrojenin ise tamamı yıldızlararası ortamdaki bulut adı verilen yüksek yoğunluklu, düşük sıcaklıklı bölgede yer almaktadır. Atomik yapıdaki hidrojen (H(I)-nötr hidrojen) bulutlarının özellikleri radyo gözlemleriyle 1420 MHz'de ($\lambda = 21cm$ -bu ışın 21cm dalga boyuna sahiptir) saptanmaktadır. Yıldızlararası bölgenin radyo dalgaları ile gözlemlenmesi ile gökadamdaki atomik hidrojenin sütun yoğunluğu hesaplanmaktadır. Ayrıca 1420 MHz'de emisyon (yayımlama) ve soğurma çizgisine bakılarak HI bulutlarının sıcaklığı ve yoğunluğu hakkında bilgiler elde edilmektedir. 21 cm dalga boyuna sahip 1420 MHz'deki bu emisyon radyo teleskoplar vasıtasıyla gözlemlenmektedir. Radyo teleskoplarda, yansıtıcı 'çanak' tarafından alınan sinyal daha sonra alt reflektöre yansıtılır ve sonrasında odak noktasına gider. Antenden sonra, verilerin monitör ekranında görüntülenebilmesi için sinyali elektronik bir sinyale dönüştüren bir

işleme cihazı vardır. Özet olarak, radyo teleskopların RF bloğu anten, yükselteç, bant geçiren filtre, mikser, detektörler ve yazılım biriminden meydana gelmektedir [1]. Blok elemanları tasarıma göre değişiklik gösterebilmektedir. Bu çalışmada 1420 MHz radyo teleskop sistemleri RF bloğunda istihdam edilmek üzere mikroşerit formda bant geçiren filtre tasarımı yapılmıştır. Filtre tasarımında Basamak Empedans Rezonatör (BER-Stepped Impedance Rezonator-SIR) yapısı ile paralel kuplajlı hat yapısı kullanılmıştır. Filtre Keysight ADS simülatörü kullanılarak pasif devre tasarım rehberi yardımıyla tasarlanmıştır. Pasif devre tasarım rehberi yardımıyla, istenilen merkez frekansı (f_c), Bant Genişliği (BG), geçiş bandı dalgalanması, durdurma bandı zayıflatması gibi optimizasyon hedeflerine göre paralel kuplajlı hat uzunlukları optimize edilmiştir. Tasarımda istenen sonuçlar elde edilmiştir ve tasarlanan filtre 1420 MHz radyo teleskop uygulamaları için gerekli isteri sağlamaktadır.

Literatürde, radyo teleskop uygulamaları için mikroşerit yapıda filtre tasarımları mevcuttur [2–7]. Rajendran ve arkadaşları çalışmalarında yazılım tabanlı radyo teleskoplar için 1.42 GHz merkez frekansında, paralel kuplajlı mikroşerit bant geçiren filtre tasarımı yapmışlardır. Filtre Chebyshev genlik tepkisine göre tasarlanmıştır [4]. Pandian ve arkadaşları ise eğitim amaçlı kullanmak üzere düşük maliyetli 1420 MHz (21cm) radyo teleskop tasarımı yapmışlardır. Sistemin RF bloğunun bir parçası olarak ise 1420 MHz merkez frekansında, 110MHz bant genişliğine sahip bir mikroşerit filtre tasarımı yapmışlardır. Çalışmada tasarlanan filtre Chebyshev genlik tepkisine sahiptir [3]. Zhang ve arkadaşları çalışmalarında C-bant alıcılar için (6 GHz merkez frekansında) radyo astronomi uygulamalarında kullanılmak üzere geniş bant mikroşerit bant geçiren filtre tasarımı yapmışlardır [2]. Liu ve arkadaşları

çalışmalarında radyo astronomi uygulamaları için paralel hatlı basamak empedans rezonatörlü yüksek dereceli dengeli süper iletken bant geçiren filtre tasarımı çalışmışlardır. Filtreyi S-bandı radyo astronomi uygulamaları için Chebyshev genlik tepkisine göre tasarlamışlardır [5]. Mundia ve Stander ise çalışmalarında 18- 45 GHz arasında çalışan bir radyo astronomi alıcısı tasarımı yapmışlardır. Analog yan bant kalibrasyonu ile RF laminat üzerinde çoklu çip modülü (MCM) olarak gerçekleştirilmiştir. Üzerinde LNA, mikser, dörtlü hibrit yapı, güç bölücü, dijital zayıflatıcı, balun gibi yapılar bulunmaktadır. Bunlara ek olarak çalışmada 4-11GHz bandında çalışan orta frekans bant geçiren filtre tasarımı da yapılmıştır. Filtre mikroşerit formda tasarlanmıştır. Basamak empedans rezonatörlü alçak geçiren bir filtre ile kısa devre çeyrek dalga saplamalı yüksek geçiren filtre kaskad bağlanarak bant geçiren formu elde edilmiştir [7].

Radyo teleskop ve radyo astronomi uygulamaları haricinde mikroşerit filtreler literatürde çok yaygın ve güncel kullanım alanlarına sahiptir [8].

Bu çalışmadaki filtre eğitim amaçlı kullanılabilir yazılım tabanlı radyo teleskopların RF bloğunda kullanılmak üzere tasarlanmıştır. Filtre üretildikten sonra, karasal radyo parazitini filtrelemek için yazılım tabanlı radyo teleskobunun radyo alıcısında kullanılabilir. Dünyanın birçok ülkesinde var olan devasa boyutlardaki radyo teleskoplar ile rutin olarak 21cm'lik gözlemler yapılmaktadır [9,10]. Bu devasa boyutlu radyo teleskoplar çok hassas ve karmaşık gözlem görevlerini yerine getirme yeteneğine sahipken, literatürde eğitim ve deney amaçlı basit radyo teleskop çalışmalarına da rastlamak mümkündür [2-4]. Eğitim ve deney amaçlı bu tür teleskopları inşa etmek, evrenin sırlarına perde aralarken aynı zamanda elektronik, antenler, sinyal işleme, programlama ve astronomi gibi çeşitli disiplinler arası alanlarda eğitim fırsatları sağlar.

Makalenin geri kalanı ise şu şekilde organize edilmiştir. 2.bölümde radyo teleskoplardan, hidrojen emisyon ölçümlerinin öneminden, radyo teleskopların RF bloğundan bahsedilmiştir. 2.bölümde aynı zamanda çalışmada seçilen mikroşerit BER filtre tasarımı ve performans parametrelerinden de bahsedilmiştir. 3.bölümde ise deneysel

bulgulara yer verilmiştir. Makale 4. Bölüm olan Sonuçlar bölümü ile sonlandırılmıştır.

2. MATERYAL VE METOT

Çalışmada radyo teleskopları RF bloğunun önemli bileşenlerinden olan bant geçiren filtre tasarımı yapılmıştır. Çalışma frekansı olarak 1420 MHz olarak tercih edilmiştir. Atomik yapıdaki hidrojen 1420 MHz frekansında radyo dalgaları yaymaktadır. Hidrojen emisyon ölçümleri radyo astronomide yıldızlararası ortam hakkında bilgi verdiği için büyük öneme sahiptir. Çalışmanın bu bölümünde radyo astronomi, radyo teleskoplar, 1420 MHz ve radyo astronomide nötr hidrojen emisyonunun önemi başlıkları detaylı bir şekilde anlatılmıştır. Tasarlanan filtre mikroşerit Basamak Empedans Dönüştürücü (BER-SIR) yapısı kullanılarak tasarlanmıştır. Çalışmanın bu bölümünde ayrıca yazılım tabanlı radyo teleskopların RF bloğu, BER (SIR) filtreler hakkında teorik bilgilere de yer verilmiştir.

2.1. Radyo astronomi ve Radyo Teleskoplar

1931'den önce astronomi çalışmak, gece gökyüzünde görünen nesnelere incelemek anlamına geliyordu. O zamanlar evreni atmosferimizin ötesinde gözlemlemenin başka bir yolu olduğuna dair hiçbir fikrimiz yoktu. Görünür ışığın yalnızca küçük bir dalga boyu aralığı ve enerji frekansları içerdiği biliniyordu. Ayrıca elektromanyetik spektrumda görünür ışıktan başka radyo dalgaları, kızılötesi, X ışınları ve Gama ışınlarının da yer aldığı bilinen bir gerçektir. Ancak 1931'de hiç kimse RF radyasyonunun milyarlarca dünya dışı kaynaktan da yayıldığını ve bu frekansların bazılarının Dünya atmosferinden doğrudan yerdeki alanımıza geçtiğini bilmiyordu. Bu radyasyonu saptamak için ihtiyacımız olan tek şey yeni bir tür "göz"dü. Aynı yıl Bell Laboratuvarında radyo mühendisi olarak çalışan Karl G. Jansky okyanus boyunca radyo-telefon sinyalleri gönderilirken (özellikle gök gürültüsü ve fırtınalı havalarda) statığı en aza indirecek bir anten tasarlamakla görevlendirildi. Gözlemediği statığın bir kısmını yakınındaki gök gürültüsü ve fırtınalara bir kısmını ise uzağındaki gök gürültüsü ve fırtınalara bağladı. Ancak kaynağını bulamadığı statiklerde vardı. Statığın kaynağının öncelikle güneş olduğunu düşündü. Bununla birlikte, radyasyonun her gün yaklaşık 4 dakika önce zirveye ulaştığını gözlemledi. Dünya'nın yıldızlara göre dönüş süresi (astronomlar tarafından yıldız günü

olarak bilinir) bir güneş gününden (Dünya'nın güneşe göre dönüş süresi) yaklaşık 4 dakika daha kısadır. Jansky bu nedenle bu radyasyonun kaynağının güneşten çok daha uzakta olması gerektiği sonucuna vardı. Daha fazla araştırma ile bu ışımanın kaynağını Samanyolu Galaksisi olarak belirledi ve 1933'te bulgularını yayınladı. İlk yıllarda Jansky'nin çalışmaları çok dikkat çekmedi. Fakat 1937 yılında Grote Reber, Jansky'nin çalışmalarını da dikkate alarak evinin bahçesinde ilk modern radyo teleskop prototipini oluşturdu. Reber, 40'lı yılların başında araştırmalarına devam etti ve 1944'te ilk radyo frekansı gökyüzü haritalarını yayınladı. Reber, II. Dünya Savaşı'nın sonuna kadar dünyadaki tek radyo astronomdu. Bu arada, savaş sırasında İngiliz radar operatörleri, Güneş'ten gelen radyo emisyonlarını tespit etmişti. Savaştan sonra radyo astronomi hızla gelişti ve evreni gözlemlememizde ve incelememizde hayati bir önem kazandı. Dünya atmosferine nüfuz edebilen RF dalgaları, birkaç milimetrelilik dalga boylarından yaklaşık 100 metreye kadar değişir. Bu dalga boylarının insan gözü veya fotoğraf plakaları üzerinde fark edilebilir bir etkisi olmamasına rağmen, anten gibi bir iletkende çok zayıf bir elektrik akımı indüklerler. Çoğu radyo teleskop anteni, gökyüzünün herhangi bir yerine doğru yönlendirilebilen parabolik (çanak şeklinde) yansıtıcılarıdır. Radyasyonu toplarlar ve radyasyonun yoğunlaştığı merkezi bir odağa yansıtırlar. Odadaki zayıf akım daha sonra bir radyo alıcısı tarafından yükseltilebilir, böylece ölçmek ve kaydetmek için yeterince güçlü hale gelirler. Alıcıdaki elektronik filtreler, bir seferde bir frekans aralığını (veya "bant") yükseltmek için ayarlanabilir veya karmaşık veri işleme teknikleri kullanılarak binlerce ayrı dar frekans bandı tespit edilebilir. Böylece, RF radyasyonunda hangi frekansların bulunduğunu ve bunların göreceli güçlerinin ne olduğunu öğrenebiliriz. Elde edilen RF radyasyonunun frekans ve polarizasyonu incelendiği zaman RF kaynakları hakkında bize birçok ipucu vermektedir. Dünya'ya ulaşan RF enerjisinin yoğunluğu (veya gücü), görünür aralıkta alınan radyasyonla karşılaştırıldığında küçüktür. Bu nedenle, bir radyo teleskopunun kullanışlı olması için geniş bir "toplama alanı" veya anteni olmalıdır [11]. Bilinen devasa boyutlu radyo teleskoplarla sürekli olarak gözlem yapılmakta ve Evrenin bilinmeyen yönleri keşfedilmeye çalışılmaktadır. Bunun yanında daha küçük boyutlarla ve küçük ölçekli, eğitim

amaçlı inşa edilen radyo teleskoplar da mevcuttur [2-4]. Bu çalışmada eğitim amaçlı kullanılacak yazılım tabanlı radyo teleskopların RF bloğunda kullanılmak üzere mikroşerit bant geçiren filtre tasarımı yapılmıştır.

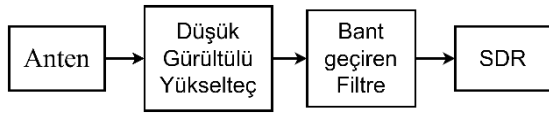
2.2. 1420 MHz ve Radyo Astronomide Nötr Hidrojen (neutral hydrogen-HI) Emisyonunun Önemi

Evrenin bazı bileşenleri yalnızca radyo frekansı imzaları aracılığıyla incelenebilir. Bu durum özellikle, yalnızca 1420 MHz (21cm) spektral hattı aracılığıyla tespit edilen, en bol malzeme bileşeni olan nötr hidrojen (*neutral hydrogen – HI*) için geçerlidir. Yaklaşık 1420 MHz'de 21 cm'lik bir dalga boyuna sahip olan *HI* emisyonları, bir galaksideki uzak yerlerden ve yönlerden kaynaklanır, yıldızlar arası bulutlar arasında seyahat eder ve Doppler kaydırmalı frekanslarda yer tabanlı radyo teleskop gözlemler ile ortaya çıkar [12]. Bu frekans kaymasına ilişkin araştırmalar, emisyon bölgesinin düzeninin ve bağlı hızlarının ayrıntılarını verir. Bu *HI* emisyonlarından yapılan haritalar, Samanyolu'nun sarmal yapısını ortaya çıkarmıştır. Bugün Hindistan'daki Pune yakınlarındaki "*Giant Metrewave*" Radyo Teleskobu, Avustralya'daki "*Parkes*" Radyo Teleskobu, ABD'deki "*Greenbank*" teleskobu ve İngiltere'deki "*Jodrellbank*" teleskobu gibi birçok radyo teleskopu rutin olarak 21cm'lik gözlemler yapmaktadır. Bu dev teleskoplar çok hassas ve karmaşık gözlem görevlerini yerine getirme yeteneğine sahipken, insanlar eğitim ve deney amaçlı basit radyo teleskoplar da inşa etmektedirler. Bu tür teleskopları inşa etmek, elektronik, antenler, sinyal işleme, programlama ve astronomi gibi çeşitli disiplinler arası alanlarda eğitim fırsatları sağlar [9,10]. Bu çalışmada eğitim amaçlı inşa edilmesi planlanan radyo teleskopların alıcı bloğunda kullanılmak üzere mikroşerit bant geçiren filtre tasarımı yapılmıştır.

2.3. Radyo teleskopların RF bloğu ve Bant Geçiren Filtrelerin Radyo Teleskoplar Açısından Önemi

Yıldızlar, galaksiler, kuasarlar ve diğer astronomik nesnelerin tümü kozmik radyo kaynaklarıdır. Bu kozmik sinyalleri incelemek için radyo teleskoplar kullanılır. Yazılım tabanlı basit bir radyo teleskop sistemi bir radyo anteni,

bir düşük gürültülü yükselteç, bir bant geçiren filtre ve bir yazılım biriminden (yazılım tabanlı radyo) oluşur. Eğitim ve deneysel amaçlı da kullanılabilir basit bir radyo teleskop RF alıcı bloğu Şekil 1’de gösterilmiştir. Alınan kozmik sinyaller zayıftır ve karasal radyo parazitleri tarafından bozulmaya açıktır. Yazılım tanımlı radyo teleskop, düşük maliyetli bir teleskoptur ve eğitim amaçlı kullanılabilir [4]. Kozmik sinyaller farklı bozulmalara da maruz kalabilir. Bu sebeple radyo alıcısındaki gürültünün ve istenmeyen diğer sinyallerin bir Bant Geçiren Filtre (BGF) kullanılarak filtrelenmesi gerekir.



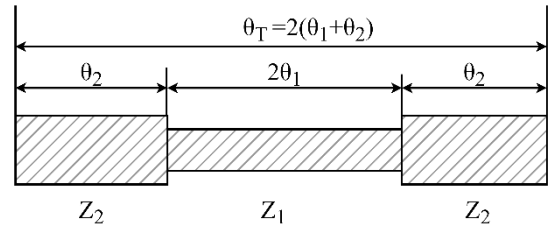
Şekil 1. Radyo teleskop RF alıcı bloğu.

Bu çalışmada yazılım tabanlı radyo teleskopların RF bloğunda kullanılmak üzere mikroşerit BGF tasarımı yapılmıştır. Şekil 1’de de gösterildiği gibi radyo teleskopların alıcı bloğunda anten, düşük gürültülü yükselteç, BGF ve sinyal işlemci bloğu yer almaktadır. Kozmik sinyaller çok zayıftır ve bu sinyaller karasal radyo parazitleri tarafından da bozulurlar. Radyo alıcısındaki gürültünün BGF kullanılarak filtrelenmesi gerekir. Radyo teleskopların RF bloğundaki her bir eleman ayrı ayrı tasarlanabileceği gibi ticari olarak da satın alınabilirler.

Filtreler frekans tepkisine göre alçak geçiren, yüksek geçiren, bant geçiren, bant durduran olmak üzere 4’e ayrılırlar. Genlik tepkisine göre filtreler ise binomial (Butterworth), Chebyshev, elliptic (Cauer) ve Bessel olarak 4’e ayrılır. Alçak geçiren filtre, temel filtre türüdür. Alçak geçiren filtrenin frekans dönüşümü ile yüksek geçiren, bant geçiren ve bant durduran filtreler tasarlanabilirler. Chebyshev filtresinin zayıflaması, makul dalgalanma sınırları içerisinde, genlik-frekans eğrisinde daha diktir ve dolayısıyla talep edilen aynı zayıflama için diğer filtre türlerine göre daha az aşama gerektirir [13]. Gereksinimlere ve kullanım yerlerine bağlı olarak, RF/mikrodalga filtreler, toplu elemanlı veya dağılmış elemanlı devre yapılarında tasarlanabilir; dalga kılavuzu, koaksiyel hat ve mikroşerit gibi çeşitli iletim hattı yapılarında gerçekleştirilebilirler [14]. Toplu elemanlar kullanmanın avantajı küçük

boyutlarındadır, ancak Q-faktörleri, dağılmış elemanlardan daha düşüktür, bu da filtre uygulamaları için daha yüksek ekleme kaybına neden olur. Dağılmış elemanların dezavantajı ise devre içerisinde daha fazla yer kaplamasıdır.

Mikroşerit yapılar, dielektrik bir alt tabaka üzerinde metalik iletim hatlarından meydana gelir. Basitlikleri ve düzlemsel yapıları nedeniyle katı-hal radyo sistemlerinde sıklıkla kullanılan mikrodalga ve milimetre dalga hibrit entegre devreler için çok kullanışlıdır [15]. Geleneksel mikroşerit alçak geçiren veya bant geçiren formlarda tasarlanabilen basamak empedans rezonatörlü filtreler çok yaygın kullanım alanlarına sahiptir. Basamak empedans rezonatörleri, farklı karakteristik empedanslara sahip iki iletim hattından oluşur ve kompakt bant geçiren filtrelerin tasarımı için oldukça kullanışlıdır. Genel bir BER yapısı Şekil 2’de gösterilmiştir [16]. BER yapısında Z_1 ve Z_2 empedansları iletim hattı genişliklerine (W_1 ve W_2) bağlıdır [17]. $W_1 > W_2$ olabileceği gibi $W_1 < W_2$ ’de olabilir. BER yapısı simetriktr. Z_1 ve Z_2 değerlerinde iki karakteristik empedansa ve Y_1 ve Y_2 değerlerinde karakteristik admitansa sahiptir.



Şekil 2. Basamak Empedans Rezonatör yapısı.

$$Y_i = jY_2 * \frac{2(K \tan \theta_1 + \tan \theta_2) * (K - \tan \theta_1 * \tan \theta_2)}{K(1 - \tan^2 \theta_2) - 2(1 + K^2) * \tan \theta_1 * \tan \theta_2} \quad (1)$$

Burada K empedans oranıdır ve şu formülle ifade edilir;

$$K = \text{empedans oranı} = Z_2 / Z_1 \quad (2)$$

$Y_i = 0$ ise rezonans durumu elde edilir. Şekil 2’deki BER yapısı için (3) ve (4) eşitlikleri geçerlidir [18].

$$K = Z_2 / Z_1 < 1 \quad (3)$$

$$\theta_T < \pi \quad (4)$$

Filtre tasarımında çeşitli ödünleşimler vardır. Fakat tasarımda genel olarak sayacağımız parametreler önemli rol oynamaktadır; Ekleme Kaybı (EK), dalgalanma (*ripple*), bant genişliği (BG), kesirsel bant genişliği (KBG) bunlardan bazılarıdır.

Ekleme Kaybı ($EK-S_{21}$): Bir RF devre yoluna eklenen ideal bir filtre, geçiş bandında hiçbir kayba sebep olmaz. Fakat pratikte mutlaka filtre kaynaklı bir zayıflama meydana gelecektir. Filtrenin eklendiği sistemde meydana getirdiği zayıflama ekleme kaybı olarak adlandırılır.

$$EK = 10 \log \frac{P_{giris}}{P_{yük}} \quad (5)$$

$$EK = -10 \log (1 - |\Gamma_{giris}|^2) \quad (6)$$

Denklem (1) ve Denklem (2) ile tanımlanan EK formülünde; $P_{yük}$, yüke aktarılan gücü, P_{giris} ise kaynaktan girişe gelen gücü tanımlar. $|\Gamma_{giris}|$ ise filtre girişindeki yansıma katsayısıdır.

Dalgalanma: Geçirme bandındaki sinyalin düzlüğü dalgalanmayı tanımlamak için sayısallaştırılabilir. Dalgalanma maksimum ve minimum genlik tepkisi arasındaki dB olarak dalgalanmayı ifade eder. Chebyshev filtreleri tasarımcıya dalgalanmayı kontrol imkânı sağlarlar.

Bant genişliği (BG^{3dB}): Denklem 3'te gösterildiği gibi Geçiş bandında $3dB$ zayıflama noktalarındaki alt kesim ve üst kesim frekans farkı ile tanımlanır.

$$BG^{3dB} = f_{üst}^{3dB} - f_{alt}^{3dB} \quad (7)$$

Kesirsel Bant Genişliği (KBG): $3dB$ bant genişliğinin, filtrenin merkez frekansına oranı olarak tanımlanır. Matematiksel olarak Denklem 4 ile ifade edilir.

$$KBG = \frac{BG^{3dB}}{f_0} \quad (8)$$

3. DENEYSEL BULGULAR

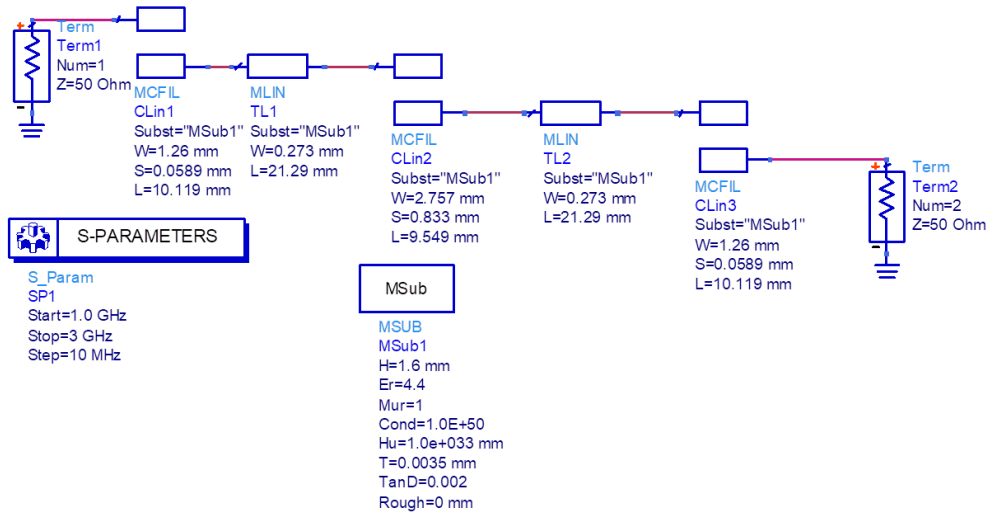
3.1. Mikroşerit BER Bant Geçiren Filtre Tasarımı

Çalışmada radyo teleskop uygulamalarında kullanılmak üzere 1420 MHz merkez frekanslı mikroşerit BER filtre tasarımı yapılmıştır. Filtre ADS Pasif Devre Simülasyon Asistanı

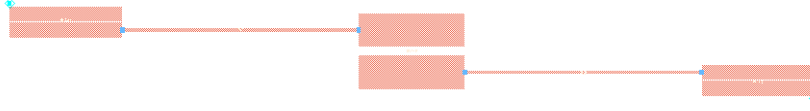
kullanılarak tasarlanmıştır. Pasif devre tasarım rehberi yardımıyla, istenilen merkez frekansı (f_c), bant genişliği (BG), geçiş bandı dalgalanması, durdurma bandı zayıflatması gibi optimizasyon hedeflerine göre paralel kuplajlı hat uzunlukları optimize edilmiştir. Optimizasyon ile tasarım hedeflerine ulaşılmış ve istenen sonuçlar elde edilmiştir. Filtre 1420 MHz radyo teleskop uygulamaları için gerekli kriterleri sağlamaktadır. Çalışmada tasarlanan filtre BER mikroşerit yapıdadır. Ucuz ve kolay bulunabilir olduğu için taban malzeme olarak FR_4 ($\epsilon_r = 4.4$, $\tan\delta = 0.002$, $h = 1.6mm$, $T = 0.0035mm$) tercih edilmiştir. Filtre ADS modeli ve baskı devre modelleri sırasıyla Şekil 3 ve Şekil 4'te gösterilmiştir.

Filtre $72mm \times 7.5mm$ boyutlarındadır. Filtre gerçekleştirilebilir uzunluktadır. Tasarımı yapılan filtrenin S_{21} ve S_{11} grafikleri Şekil 5 ve Şekil 6'da gösterilmiştir. 1420 MHz frekansında S_{21} ve S_{11} sırasıyla $-0.152dB$ ve $-38dB$ bulunmuştur. Şekil 6'da gösterildiği gibi Filtre BG^{3dB} değeri yaklaşık 130 MHz'dir. Şekil 5'te genişletilmiş frekans ekseninde gösterildiği gibi filtre empedans bant genişliği ise yaklaşık 90 MHz'dir. Filtre faz cevabı ise Şekil 7'de gösterilmiştir. Filtre lineer bir faz cevabına sahiptir. Çalışmada tasarlanan filtrenin genel özellikleri ve simülasyon sonuçları Çizelge 1'de özetlenmiştir. Çizelgede de özetlendiği gibi filtre Chebyshev genlik tepkisine ve yaklaşık %6 KBG 'ye sahiptir.

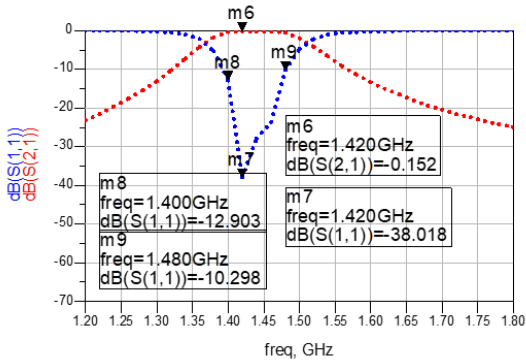
Çalışmada tasarlanan filtre literatürde bulunan radyo teleskop uygulamaları için tasarlanmış diğer bazı filtrelerle Çizelge 2'de karşılaştırılmıştır. Çalışmada tasarlanan filtre literatürde radyo teleskop uygulamaları için tasarlanmış diğer filtrelerle mukayese edildiğinde; merkez frekansında ekleme kaybı (S_{21}) ve giriş yansıma katsayısının (S_{11}) diğer tasarımlara göre en iyi değerlere sahip olduğu görülmüştür. Filtre $3dB$ ve $10dB$ bant genişlikleri de uygulama için yeterli seviyelerdedir.



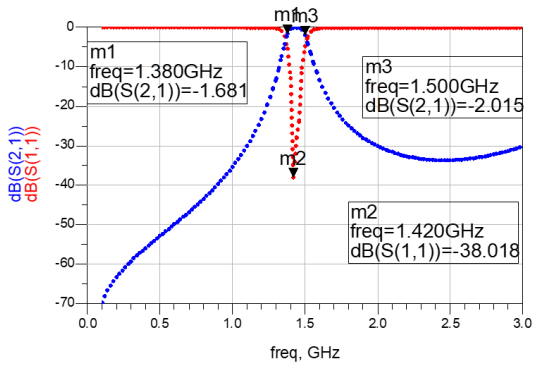
Şekil 3. Filtre ADS Modeli.



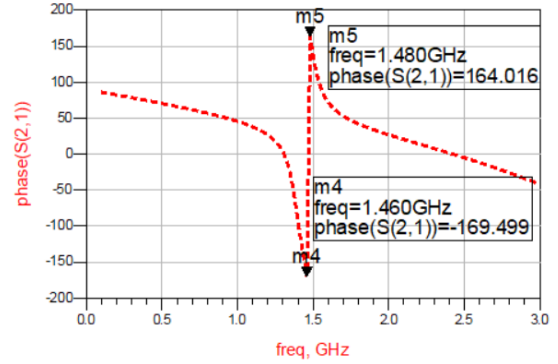
Şekil 4. Filtre baskı devre modeli.



Şekil 5. S_{21} ve S_{11} sonuçları.



Şekil 6. S_{21} ve S_{11} sonuçları.



Şekil 7. Filtrenin faz cevabı.

Çizelge 1. Tasarlanan filtrenin özellikleri

Filtre Türü	Microstrip BER
f_0	1420 MHz
$S_{21} (@f_0)$	-0.152 dB
$S_{11} (@f_0)$	-38.018 dB
BG^{3dB}	~130MHz
KBG	% 5.63
Filtre genlik tepkisi	Chebyshev

Çizelge 2. Çalışmada tasarlanan filtrenin literatürdeki diğer filtrelerle karşılaştırması.

	Filtre Teknolojisi	Uygulama	Filtre Türü	f_0 (GHz)	Dalgalanma (dB)	EK (dB)	S_{11} (dB)	BG^{3dB} (MHz)
[2]	Mikroşerit Interdigital	Radyo Teleskop	NA	6	NA	>-0.6	<-20	3960
[3]	Mikroşerit Interdigital	Radyo Teleskop	Chebyshev	1.42	0.01	>-3	<-10	110
[4]	Mikroşerit kuplajlı hat	Radyo Teleskop	Chebyshev	1.42	0.5	-2.806	<-10	300
Bu çalışma	Mikroşerit BER	Radyo Teleskop	Chebyshev	1.42	<0.1	-0.152	-38	130

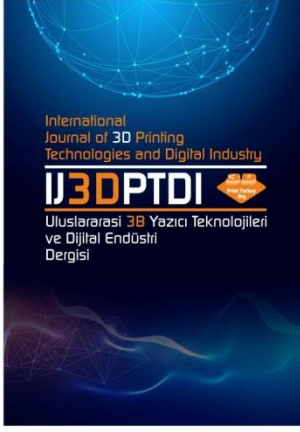
4. SONUÇLAR

Çalışmada 1420 MHz radyo teleskop uygulamaları için mikroşerit BGF tasarımı yapılmıştır. 1420 MHz atomik yapıdaki nötr hidrojen emisyon ölçümleri yıldızlararası ortam hakkında bilgi verdiği için oldukça önemlidir. Çalışmada radyo teleskopların RF bloğunda istihdam edilmek üzere paralel kuplajlı hatlar kullanılarak BER yapısında mikroşerit bant geçiren filtre tasarımı yapılmıştır. Filtre Chebyshev genlik tepkisine göre tasarlanmıştır. Tasarlanan filtrenin ekleme kaybı (S_{21}) -0.152 dB, yansıma katsayısı (S_{11}) -38 dB, 3dB bant genişliği (BG_{3dB}) 130 MHz, empedans bant genişliği (BG_{10dB}) ise yaklaşık 90 MHz değerlerindedir. Filtre kesirsel bant genişliği (KBG) ise %5.63 olarak hesaplanmıştır. Düşük yansıma katsayısı ve ekleme katsayısı değerleri ile çalışmada tasarlanan filtre radyo teleskop RF bloğu için gerekli şartları sağlamaktadır. Ayrıca elde edilen diğer sonuçlar filtrenin 1420 MHz radyo teleskopların RF bloğu için gerekli şartları sağladığını göstermektedir. Filtre baskı devre haline getirildikten sonra geçirme bandı dışında istemeyen sinyalleri filtreleyecektir. İlerleyen çalışmalarda hidrojen emisyon ölçümleri için eğitim amaçlı bir radyo teleskop inşa edilmesi planlanmaktadır. Bu çalışmada tasarlanan bant geçiren filtre gerçekleştirilerek bu sisteme entegre edilecektir.

KAYNAKLAR

- Sobirin FF, Nugraha S, Haz F, Sitompul P. "Study of Cassegrain-type antenna for radio telescope", Journal of Physics: Conference Series, Vol. 2214, Pages 1–9, 2022.
- Zhang G, Lancaster MJ, Huang F, Pan Y, Roddis N. "Wideband microstrip bandpass filters for radio astronomy applications", 2006 European Microwave Conference, Pages 661–663, 2006.
- Pandian BA, Ganesh L, Inbanathan SSR, Ragavendra KB, Somashekar R, Prabu T. "Galaxy rotation curve measurements with low cost 21 cm radio telescope", Sādhanā, Vol. 47, Pages 1–13, 2022.
- Rajendran J, Peter R, Soman KP. "Design and Optimization of Band Pass Filter for SoftwareDefined Radio Telescope", International Journal of Information and Electronics Engineering, Vol. 2, Pages 649–651, 2012.
- Liu H, Xu Y, Liu F, Wang Y, Song Y. "High-Order Balanced Superconducting Filter with High Selectivity, Low Insertion Loss, and Wide Stopband Range for Radio Astronomy", IEEE Transactions on Microwave Theory and Techniques, Vol. 67, Pages 2720–2729, 2019.
- Tang J, Liu H, Yang Y. "Balanced Dual-Band Superconducting Filter Using Stepped-Impedance Resonators with High Band-to-Band Isolation and Wide Stopband", IEEE Transactions on Circuits and Systems II: Express Briefs, Vol. 68, Pages 131–135, 2021.
- Mundia S, Stander T. "Detailed Design of an 18-45 GHz Multi-Purpose Radio Astronomy Receiver", 2022 International Conference on Electromagnetics in Advanced Applications (ICEAA), Pages 220–224, 2022.
- Şenel B, Şenel FA. "Bandpass Filter Design Using Deep Neural Network and Differential Evolution Algorithm", Arabian Journal for Science and Engineering, Pages 1–12, 2022.
- Johnson D, Rogers AE. "Developing a New Generation Small Radio Telescope", American Astronomical Society Meeting Abstracts 221, Vol. 221, Pages 210–255, 2013.

10. Patel NA, Patel RN, Kimberk RS, Test JH, Krolewski A, Ryan J, et al. "A low-cost 21 cm horn-antenna radio telescope for education and outreach", American Astronomical Society Meeting Abstracts 224, Vol. 224, Pages 401–415, 2014.
11. Valley G-A, Telescope R. "Basics of Radio Astronomy", 1998.
12. Kulkarni SR, Heiles C. "Neutral hydrogen and the diffuse interstellar medium", Galactic and extragalactic radio astronomy, Springer, Pages 95–153, 1988.
13. Li RC-H. "RF circuit design", Wiley; 2009.
14. Hong J-S, Lancaster MJ. "Microstrip Filters for RF/Microwave Applications", John Wiley & Sons, 2001.
15. Schneider M V. "Microstrip lines for microwave integrated circuits", Bell System Technical Journal, Vol. 48, Pages 1421–1444, 1969
16. Makimoto M, Yamashita S. "Compact bandpass filters using stepped impedance resonators", Proceedings of the IEEE, Vol. 67, Pages 16–19, 1979
17. Gonzalez G. "Microwave transistor amplifiers analysis and design", Prentice-Hall, Inc.; 1996.
18. Makimoto M, Yamashita S. "Bandpass Filters Using Parallel Coupled Stripline Stepped Impedance Resonators", IEEE Transactions on Microwave Theory and Techniques, Vol. 28, Pages 1413–1417, 1980




ULUSLARARASI 3B YAZICI TEKNOLOJİLERİ
VE DİJİTAL ENDÜSTRİ DERGİSİ

INTERNATIONAL JOURNAL OF 3D PRINTING
TECHNOLOGIES AND DIGITAL INDUSTRY

ISSN:2602-3350 (Online)

URL: <https://dergipark.org.tr/ij3dptdi>

DESIGN AND MANUFACTURING OF A TWO-STAGE REDUCTION GEARBOX WITH 3D PRINTERS

Yazarlar (Authors): Serpil Karakuş 

Bu makaleye şu şekilde atıfta bulunabilirsiniz (To cite to this article): Karakuş S., “Design and Manufacturing of A Two-Stage Reduction Gearbox With 3D Printers” *Int. J. of 3D Printing Tech. Dig. Ind.*, 7(1): 18-28, (2023).

DOI: 10.46519/ij3dptdi.1206809

Araştırma Makale/ Research Article

Erişim Linki: (To link to this article): <https://dergipark.org.tr/en/pub/ij3dptdi/archive>

DESIGN AND MANUFACTURING OF A TWO-STAGE REDUCTION GEARBOX WITH 3D PRINTERS

Serpil Karakuş^a 

^aZonguldak Bülent Ecevit University, Zonguldak and 67100, Turkey

* Corresponding Author: serpilkarakus@yahoo.com

(Received: 18.11.2022; Revised: 12.01.2023; Accepted: 24.04.2023)

ABSTRACT

3D printers, which have been used in recent years, enable the conversion of a digital model into a physical 3D object by placing the filament material layer by layer and can help a wide variety of industries. Digital models can be created using software such as Solidworks and Catia or data created by a 3D scanner. This study designed all parts of a two-stage reducer gearbox consisting of spur and helical gear pairs. The torques are calculated according to the input power. Shafts that can transmit torques are designed. Gear wheels were calculated according to the total reduction ratio and were designed to transmit torques. CAD software (Solidworks) designed the gearbox parts, assembled them, and simulated them. Thus a digital model has been created. CAD models were transferred to the 3D printer. The slicing was done precisely using Cura software. On the other hand, the Marlin software reads the G codes created with Cura software sent from the computer. PLA (Polylactic Acid) was used as the filament material. The digital model, in other words, the CAD assembly, has been checked with Solidworks simulation. It has been seen that the gears work in harmony with each other, and the shafts turn smoothly. On the other hand, the model produced with a 3D printer was checked by applying torque to the input shaft on a small lathe spindle. The tachometer was used to measure rotational revolutions. It was seen that the gears and shafts worked smoothly. Gearboxes made of PLA work silently, do not require lubrication with industrial machine oil, and are clean. PLA material is a plant-based plastic that is not harmful to human health.

Keywords: Gearbox, PLA Material, 3D printing, CAD, Additive Manufacturing.

1. INTRODUCTION

Gear systems used to reduce the input rotation speed to the desired output rotation speed in places where the rotational movement taken from the motor is higher than the need is called reducer. Gearboxes are independent elements added to the needed system.

Gearboxes can be used wherever there is force and movement. Walking grates, pumps, machine tools, elevators, cranes, textile machinery, sheet bending machines, rams, rotary drums, conveyors, etc. They are used where there are many rotational movements. Various designs are available, manufactured in different torque and sizes.

It is crucial to create a hygienic environment in the food, beverage, food industry, chemical, and

pharmaceutical industries and sensitive product areas. In most cases, the climate should be completely free of bacteria. Machine lubricating oils are also harmful to human health. This problem has been solved with hygienic type special gear motors and gearboxes.

Previous studies investigated the effects of nozzle temperature and filler density on the mechanical properties of structures produced with polylactic acid (PLA), one of the commonly used 3D Printer materials. These studies evaluated three-dimensional printer product structures regarding mechanical properties, production time, and cost [1]. The gearbox of a belt conveyor carrying coal and operating in dusty environments in a thermal power plant has been investigated. The causes and solutions of

significant faults in such gearboxes are explained [2]. Another study created a bolt and nut model using Solidworks software. Precise slicing was done using Cura software on the three-dimensional printer and directed to the print. PLA and ABS were used as printing materials [3]. The mechanical properties of the samples produced as layers from PLA and TPU materials were investigated. Tensile and compression tests were applied to the samples prepared with 20%, 60%, and 100% filling percentages.

1.1. Nomenclature

List of symbols.		
P_1	(kW)	Input power
P_2	(kW)	Output power
n_1	(rpm)	Input speed
n_4	(rpm)	Output speed
i_T	(-)	Total reduction ratio
i_{12}	(-)	Reduction ratio between first and second gears
i_{34}	(-)	Reduction ratio between third and fourth gears
z	(-)	Number of teeth
η_t	(-)	The efficiency of the system
d_0	(mm)	Section circle diameter
m	(mm)	Module
m_n	(mm)	Normal module for helical gears
m_t	(mm)	Transverse module
M_t	(Nm)	Torque
s	(-)	Safety factor
d	(mm)	Shaft diameter

List of abbreviations	
CAD	Computer-Aided Design
3D Printing	Three-Dimensional Printing
STL	Stereolithography
SD Card	Secure Digital Memory Card

It was observed that sample sizes and filler percentage significantly affect mechanical performance. Filling percentages are essential for designers using mechanical loading applications [4]. A single-stage reduction gearbox has been outlined. The gears, shafts, and gearbox casing have been optimized [5]. In this study, several simple CAD systems are examined. Thus, technical and economic criteria were evaluated. It has been shown how the designed models can be used in 3D printing. This work illustrates the possibilities and limitations that can be expected when using simple CAD systems. [6]. This study gives general information about 3D printing techniques,

classification, materials used, and applications in various industries [7]. This article examines the wide variety of materials applied in 3D printing. The article also describes the applications of 3D printed products made of different materials and the different processes of 3D techniques. Advice has been given to people who will work on 3D printing. A study has emerged that will be useful to people who are interested in 3D printing [8]. This article is an experimental study of a Ganesh idol demonstrating its critical benefits such as additive manufacturing or 3D printing, rapid prototyping, flexible design, and waste minimization. Therefore, this article provides an overview of 3D printing and a survey. There are applications and information about how fast 3D printing technology is developing and globally focused research results [9]. Here the author reviews several standard simple CAD systems. Thus, he examined the technical and economic criteria. It also showed how models designed in this way could be used in 3D printing. This is a case study. It shows the possibilities and limitations of using basic CAD systems [10]. The author; First, three geometric models of rectangular, oblong, and ellipse are used at different nozzle distances and scan speeds. Then, using these geometric models, it created three new G-code programs for manufacturing. The difference between the CAD model and the oblong model showed that the oblong model is a better choice for controlled 3D printing of microchannels [11]. This article presents four new sabotage attacks for fused filament fabrication (FFF) based 3D printing: (1) spacing via filament kinetics, (2) density variation via filament state, (3) density variation via filament velocity, and (4) dynamic thermal manipulations were examined. In this study, small attacks that are difficult to detect are examined [12].

In this study, the top cover design and prototype production of a carpet washing machine was made. It aims to make a design change on the upper part of the device to increase export sales and produce a new model product at a low cost. For this purpose, three different designs were made. A design was selected by applying concept tracking/scoring matrices to the designs. A prototype of the selected design has been produced, aiming to make controls on the prototypes [18]. In this study, autonomous underwater vehicle design and application were carried out using 3D printing technology. The shell design of the autonomous underwater robot

was carried out by observing creatures with high maneuverability underwater, and Computational Fluid Dynamics analyzes were carried out. After the shell design and manufacturing were completed, the propulsion system and electronic equipment were completed, and the physical structure of the autonomous underwater vehicle was completed [19]. In this study, high flame appearances of firearms, especially in night use, were investigated. The model to be developed was designed with SolidWorks, and internal airflow analyses were made with Solidflow. The prototype of a previously produced model was reproduced with a three-dimensional printer. The new design aims to increase night vision and conceal the wearer's position by minimizing the appearance of flame after a muzzle blast [20]. These studies aim to reduce the noise caused by gears in automobile transmissions. The geometric design parameters of the gearbox were optimized [21], [22]. The Real Coded Genetic Algorithm (RCGA) has been applied to obtain the optimum helical gear design. In this study, the volume of a helical gear pair is minimized by including the module, face width, and the number of teeth, as well as the profile shift coefficients as design variables using RCGA [23]. It is a review article and aims to provide an overview of the studies on gear optimization, as well as to summarize the results obtained by other researchers and to formalize the gear optimization process [24]. In this study, the author made multi-objective Optimization of the gear train design to improve efficiency and transmission error. It has realized the multi-purpose Optimization of the gear unit with a multi-scale approach from the gear main idea to the complete transmission. A genetic algorithm technique called Non-Dominant Sequence Genetic Algorithm II (NSGA-II) was used in the Optimization [25]. This study evaluated the effects of gear addendum and dedendum on the optimization results for gear macro geometry design. Gear mass, efficiency, and transmission errors were considered objective functions for Optimization. Optimization results were normalized to min-max, and mean values of total scores were compared [26]. This study presents a method for calculating root and contact stresses for metal, spur, and helical gears. The results are verified by finite element calculations [27]. In this study, the macro geometry of a helical gear pair is optimized for low weight, high efficacy, and low noise; Furthermore, optimal solution trends were analyzed for five combinations of

the three goals [28]. This study investigated the effects of helix angle, mechanical errors, and coefficient of friction on the time-varying tooth-root stress of helical gears [29]. This work is a platform for 3D printers, additive manufacturing, and 3D printed structures of the future [30]. This study developed a new composite filament that can be used in low-cost 3D printers to produce complex ceramic shapes [31]. In this article, a study was carried out on optimizing effective design parameters for a five-speed automotive gearbox. During the Optimization, the tooth-bending stress was taken as the objective function [32].

2. GEAR DESIGN

2.1. Material Selection

PLA filament is a 3D printer material. PLA (Polylactic Acid) is a plant-based and biodegradable plastic. PLA is plastic produced from products such as corn starch and sugar cane. Since PLA is produced from organic materials, PLA filament is not harmful to human health.

In Figure 1, stress-strain curves of PLA material according to different filling densities. Table 1 shows the attributes and values of PLA filament.

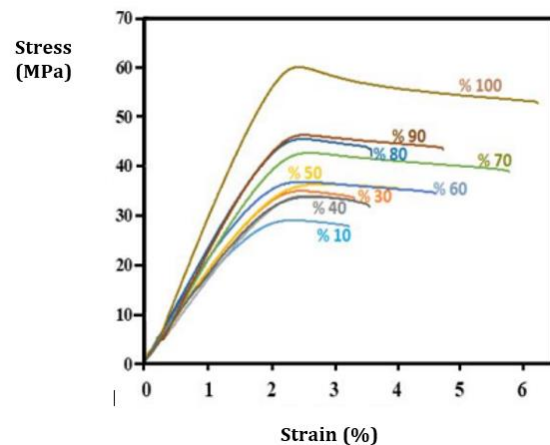


Figure 1. PLA material stress-strain values according to different filling densities [1]

Table 1. PLA material mechanical properties

Parameter	Attributes and values
Density	1.3 g/cm ³
Young's modulus	3.5 GPa
Elongation limit	6.0 %
Specific strength	38 kN-m/kg
Ultimate tensile strength	50 MPa
Shear modulus	2.4 GPa

2.2. Filament Consumption During Printing

Low filling density can be preferred in applications that require fast production and lightweight. On the other hand, high filler density could be preferred in cases where high-impact strength and flexibility are significant. (Table 2).

Table 2. PLA material filling ratios tensile stress.

Parts	PLA filling density %	PLA tensile stress MPa	Filling pattern
1 st gear	60	36	grid
2 nd gear	60	36	grid
3 rd gear	60	36	grid
4 th gear	60	36	grid
1 st shaft	80	45	grid
2 nd shaft	80	45	grid
3 rd shaft	80	45	grid
Lower case	20	30	line
Upper case	20	30	grid

2.3. Gear Calculations

The design data was determined according to the stress values of the PLA material.

Input power P_1 is 0.3 kW, and the input revolution speed $n_1=800$ rpm. The total reduction ratio is $i_T=20$.

The total reduction ratio,

$$i_T = \frac{n_1}{n_4} \quad (1)$$

$$i_T = i_{12} \cdot i_{34} \quad (2)$$

Reduction ratio between first and second gears,

$$i_{12} \cong 1.2 \cdot \sqrt{i_T} \quad (3)$$

$$i_{12} = \frac{n_1}{n_2} = \frac{z_2}{z_1} \quad (4)$$

Reduction ratio between third and fourth gears,

$$i_{34} = \frac{n_2}{n_3} = \frac{z_4}{z_3} \quad (5)$$

Output power and total efficiency,

$$P_2 = P_1 \cdot \eta_t \quad (6)$$

Pitch circle diameter of spur gears,

$$d_0 = m z \quad (7)$$

Transverse module,

$$m_t = \frac{m_n}{\cos\beta} \quad (8)$$

Pitch circle diameter of helical gears,

$$d_0 = m_t z \quad (9)$$

Torque,

$$M_t = 9550 \frac{P_1}{n_1} \quad (10)$$

In this gearbox, the input speed is the speed of the first shaft and the output speed is the speed of the third shaft. The pressure angle between cooperating gears is taken as $\alpha=20^\circ$, and the helix angle in helical gears is taken as $\beta=15^\circ$. The calculated values of the gears are given in Table (3).

Table 3. Gear calculations.

Gear number	Type	Number of teeth, z	Module m, mt (mm)	Pitch circle d ₀ , (mm)	Face width, b (mm)
1	spur	15	1.25	18.75	10
2	spur	81	1.25	101.25	10
3	helical	18	1.75	31.50	15
4	helical	67	1.75	117.25	15

2.4. Shaft Calculations

Shafts are machine elements used in power and motion transmission. The shafts in this study are rod elements of circular cross section and enable the gears on them to rotate. They are forced by torsional and bending stresses due to the gear forces that occur depending on the input speed and torque.

$$\tau_{te} = \frac{M_t}{W_t} \quad (11)$$

τ_{te} is the torsion stress as (N/mm²), M_t is the torsion moment as (Nmm), and W_t is the bending strength moment as (mm³).

$$M_t = 9.55 \cdot 10^6 \frac{P}{n} \quad (12)$$

P is the power as (kW), and n is the number of shaft revolutions as (rpm).

$$W_t = \frac{\pi d^3}{16} \quad (13)$$

The maximum bending stress (σ_{max}) took as 45 MPa.

$$\sigma_e = \frac{\sigma_{max}}{s} \tag{14}$$

σ_e is the safe stress, s is the safety factor, and $s=1.2$ is chosen. The shaft diameter calculates as follows.

$$d = \sqrt[3]{\frac{32 M_t}{\pi \sigma_e}} \tag{15}$$

Table 4. Calculated values of shafts

Shaft number	Number of revolutions, n (rpm)	Torques, M_t (Nm)	Shaft diameters, d mm
1	800	3.581	11
2	149	19.228	18
3	40	74.645	28

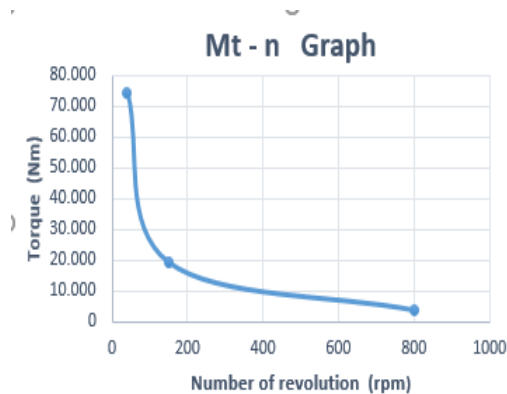


Figure 2. Torque-number of revolution diagram

The number of revolutions in Table 3 is calculated from equations (1), (4), (5), torques are calculated from equation (10), and shaft diameters are calculated from equation (15). During operation, radial and tangential forces occur in the gears. These forces are usually calculated in the 2D plane. These are transmitted to the rolling shaft bearings as a reaction force. In this way, bending moments occur in the shafts. This study calculated bending moments for each of the three shafts. The sections dangerous against breakage were depicted. The locations and diameters of the steps on the shafts were determined. At all stages of calculations, tooth bending stresses and tooth contact stresses are considered.

In order to make gear strength calculations, basic calculations, and geometric measurements must be made and known. If these values are changed due to strength calculations, the calculations are made again with new values. Strength

calculations are iteration on the one hand and vicious circle calculations on the other. The processes continue until the calculations and measurements match each other. This study is used in the ISO 6336 standard for strength and dynamic calculations. Especially in the calculations of bending stresses and gear contact stresses. Although we take ISO 6336 as a guide in this study, it has always been considered that the material we use is Poly Lactic Acid. In order to prevent tooth root fractures filling ratio of PLA material is kept high, and the tightest fill pattern is used.

3. CAD MODELLING

Solidworks, a CAD software, is used in various industries for product designs. It provides a fast, economic and efficient study. In this study according to the calculated measurements, shafts, keys, and upper and lower casings were drawn with Solidworks software. Spur and helical gears, ball bearings, bolts, screws, and nuts were created according to ANSI metric standards in the design library in Solidworks software.

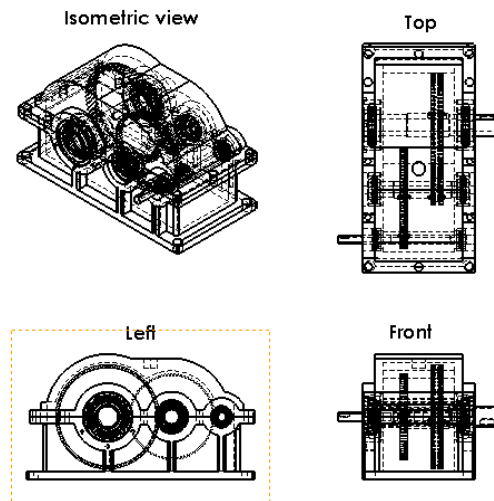


Figure 3. Reducer gearbox assembly modelling

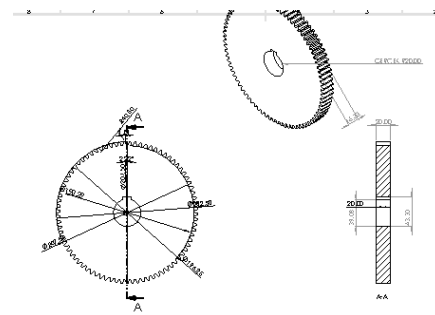


Figure 4. An example of a dimensional part.

4. PRINTING

Cura software is a three-dimensional slicing program. In this study, the STL file format was used in Cura software. On the other hand, the Marlin software reads the G codes created with Cura software sent from the computer and provides the printer's control.

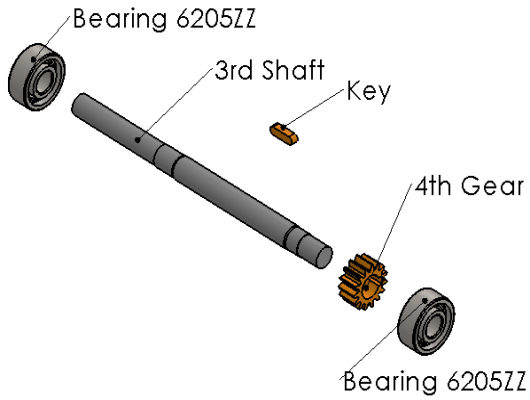


Figure 5. CAD modelling of the first shaft

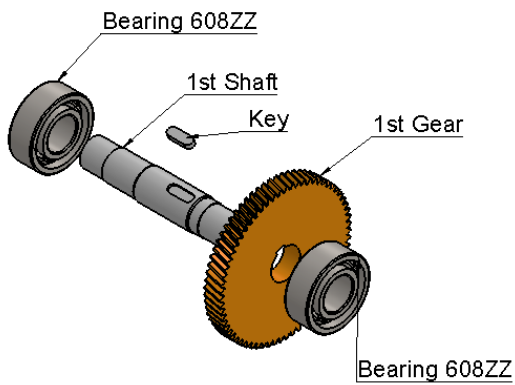


Figure 6. CAD modeling of the intermediate shaft.

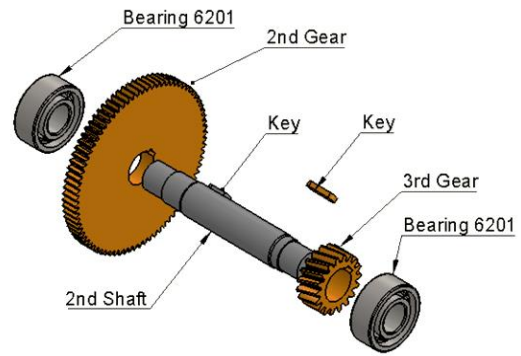
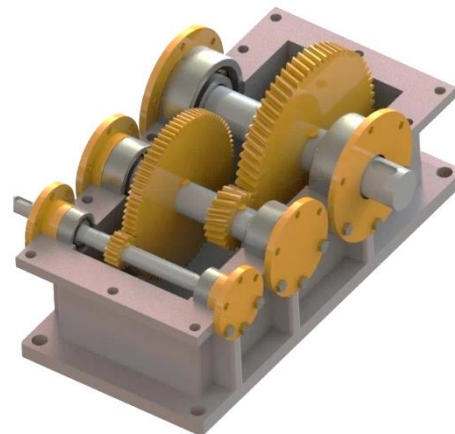
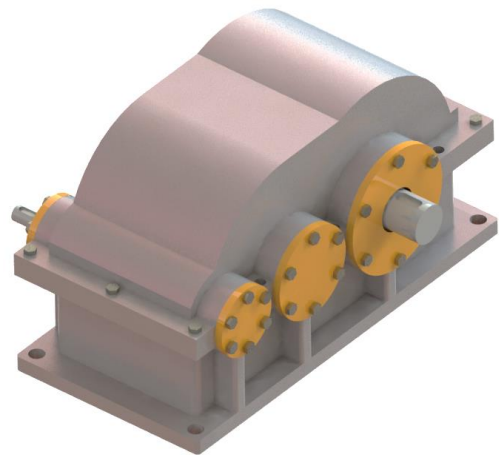


Figure 7. CAD modeling of the output shaft.



(a)



(b)

Figure 8. (a), (b) CAD modeling of the gearbox.

This study converts each part drawn with CAD software to STL format. The part to be produced was extruded along the z-axis. The printing parameters in Table 6. were entered for this study. After the printing parameters, the slicing software was started. The slicer software converted the STL file and printing parameters into G-codes and sent them to the printer control software.

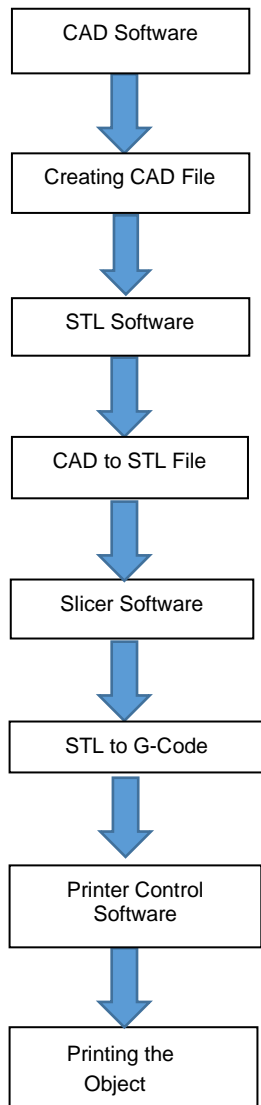
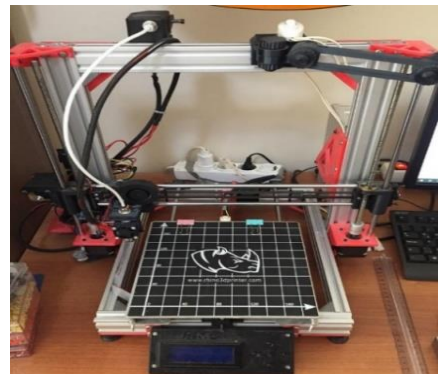


Figure 9. 3D printing process flow chart.

Figure 9 shows the flowchart for the 3D printer. Solidworks software was used as CAD software. In this study. Four different tooth wheels, three different shafts, four different keys, six different covers, and two different gearbox case solid models were drawn for this reducer gearbox, and CAD files were created. Each file was imported into the slicer software as an STL file. Ultimaker

Cura was applied as the slicer software. G-codes were generated by entering operating voltage, extruder structure, nozzle temperature, table temperature, nozzle diameter, layer thickness, and filament diameter. G code files SD card was loaded printer separately. The parts produced with 3D printers were assembled. Moreover, the assembly used six different bearings, many screws, and nuts. In this study, the PLA material filling rate was 60% for gears and 80% for shafts, and 20% for the lower and upper boxes. A 1.2 mm diameter nozzle was used for the upper and lower boxes. The lower box was printed in one go, the upper box piecemeal. The printing time for the boxes was in the range of 14-20 hours. A 0.6 mm diameter nozzle was used for gears and shafts. Due to the high number of walls in the gears, much filling was not required. The printing time for the gears was in the range of 4-8 hours. Printing time for shafts was in the range of 2-4 hours. There are hundreds of setting options in Cura software, and changing even one of these options changes the printing time, weight, and amount of filament. The printing time can be significantly reduced by using the appropriate options.



(a)



(b)

Figure 10. (a), (b) Printers used in production.

Table 5. Features of printer 1.

Parameter	Printer 1
Print volume	200x200x190
Model	(mm)
Software	Anet A8
Operating voltage	(current)
Extruder structure	Marlyn
Maximum nozzle temperature	24 V DC, 20A
Maximum table temperature	Bowden
	Extruder
	275°
	130°

Table 6. Features of printer 2.

Parameter	Printer 2
Print volume	300x300x400
Model	(mm)
Software	Tronxy X5SA
Operating voltage	Default
Extruder structure	software
Maximum nozzle temperature	24 V DC,
	30A
Maximum table temperature	Bowden
	Extruder
	265°
	90°

Table 7. Print parameters.

Parameter	Attributes and values
Nozzle diameter	0.6 mm
Layer thickness	0.4 mm
Wall number	2
Print temperature	210°C
Table temperature	60°C

Table 8. Filament properties.

Parameter	Attributes and values
Amount of filament	1000 gr.
Filament type	PLA+
Filament diameter	1.75 mm

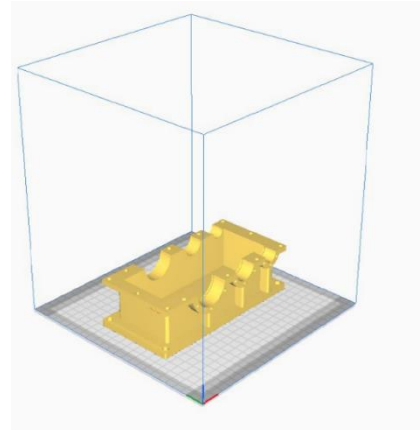


Figure 11. Gearbox case in Cura slicer software.

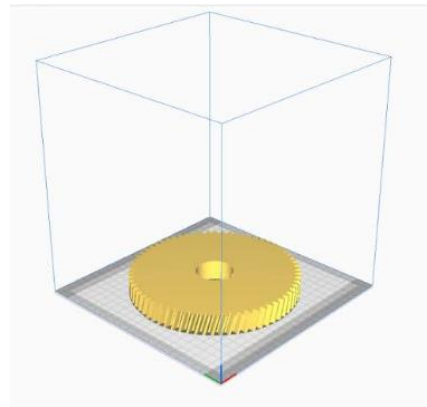


Figure 12. Helical gear wheel in Cura slicer software.

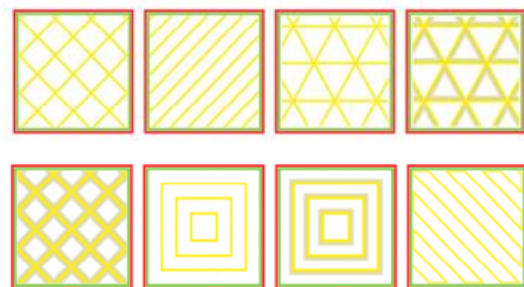


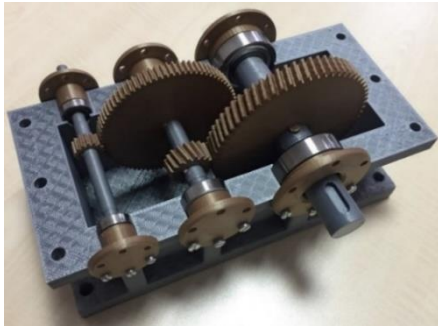
Figure 13. Cura 3D fill pattern [17].

If this model is used for mechanical purposes, the best option is to choose a 2D pattern such as Grid, Lines, or Triangles. The grid pattern consumes more material but is more rigid. The printing time of the grid pattern is also longer. The line pattern prints quickly and consumes less material. The triangular pattern provides good wall strength in thin structures. This study mainly used the grid pattern as a filled form. A small amount of line pattern was also used.

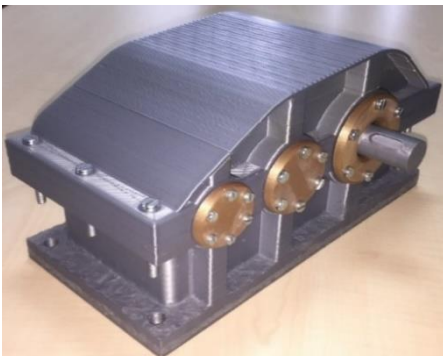
5. RESULTS

Figure 14 shows the gearbox prototypes, the parts of which were 3D printed and then hand-assembled. Bearings, screws, and nuts are purchased as standard parts. The outer dimensions of the gearbox are $280 \times 135 \times 160$ cubic millimeters. The total reduction ratio of the system is $1/20$. The reduction ratio has been reduced from $n_1 = 800$ rpm to $n_3 = 40$ rpm (Figure 2). For example, this reducer can be attached to the belt conveyor motor to transport lightweight and hygienic goods. In the food industry, chemical and pharmaceutical industries, and sensitive products areas.

However, the box casing can be redesigned in Solidworks software according to the geometric situation of the place where it will work and can be printed on a 3D printer. Similarly, gears can be redesigned and printed according to the desired speed and torque value. So everyone can make their design.



(a)



(b)

Figure 14. (a), (b) Prototypes of the gearbox manufactured with a 3D printer.

In this study, a 100% filling rate of PLA material was not preferred to shorten the long printing times of solid parts. This preference negatively affected the strength of the elements. In particular, the small cross-section of the input shaft means that it is subject to rapid breakage.

Therefore, we intend to manufacture this reducer as in figure 15.



Figure 15. A new design to work on [33].

In the new study, the shafts will be steel. This time, we will use a helical gear pair in the 1st stage because the first drive comes to the first-stage gears via the input shaft. However, helical teeth grasp each other more strongly. Gears and box cases will be made of PLA material using a 100% fill rate. Shafts and box cases will have a long life. Lifetime calculations of gears will be made, and their spare parts will be produced. For gears, colors in white and light gray tones will be preferred. For the box case, light pink and yellow colors will be preferred. In this way, reducers will have a clean appearance. After these experiences, gearboxes with different planes of input and output shafts can also be produced.

6. CONCLUSIONS

Our main goal is to convert a digital model (CAD drawings) into a 3D physical object. Since the density of PLA material is low, the weight of the produced parts is lightweight. It is economical and easier to manufacture. However, it is not resistant to high temperatures and abrasions. The reducer-gearbox made of PLA can be used at low temperatures (less than 60 degrees Celsius).

REFERENCES

1. Kaygusuz, B., Özerinç, S., “3 Boyutlu Yazıcı ile Üretilen PLA Bazlı Yapıların Mekanik özelliklerinin İncelenmesi”, Makine Tasarım ve İmalat dergisi, Vol.16, Issue 1, Pages 1-6, 2018.
2. Prabhu, R., Devaraju, A., “Failure analysis and restructuring model of transfer feeder gearbox in thermal powerplant”, Materials Today: Proceedings, Vol. 39, Pages 633–638, 2021.
3. Haghbin, N., Bone, D., Young, K., ‘Controlled extrusion-based 3D printing of micro-channels with the geometric modelling of deposited roads’, Journal of Manufacturing Processes, Vol. 67, Pages 406-417, 2021.
4. Elmrabet, N., Sieges, P., “Dimensional onsiderations on the mechanical properties of 3D printed polymer parts”, Polymer Testing, Vol. 90, Issue 106656, 2020.
5. Kishore, S.N., Reddy, A.V.V., Rao, L.B., “Design and optimization of spur gears in a single-stage reduction gearbox”, Materials Today: Proceedings Article in Press, 2022.
6. Jadhav, A., Jadhav, V.S., “A review on 3Dprinting: An additive manufacturing technology”, Materials Today: Proceedings, Article in press, 2022.
7. Mikolajczyk, T., Malinowski, T., Moldowan, L., Fuvén, H., “CAD-CAM system for manufacturing innovative hybrid design using 3D printing”, Procedia Manufacturing, Vol. 32, Pages 22-28, 2019.
8. Ranjan, R., Kumar, D., Kundu, M., Moi, S.C., “A critical review on Classification of materials used in 3D printing Process”, Materials Today: Proceedings”, Vol. 61, Pages 43-49. 2022.
9. Kumar, D., Manohar, G.A., Teja, R.S., “The state of art 3D printing: A case study of Ganesh Idol”, Materials Today: Proceedings, Vol. 56, Pages 455-461, 2022.
10. Junk, S., Kuen, C., “Review of Open Source and Freeware CAD Systems for Use with 3D-Printing”, 26th CIRP Design Conference, Pages 430-435, 2016.
11. Haghbin,N., Bone, D., Young, K., “Controlled extrusion-based 3D printing of micro-channels with the geometric modelling of deposited roads”, Journal of Manufacturing Processes”, Vol. 67, Pages 406-417, 2021.
12. Rais, M.H., Li, Y., Ahmed, I., “Dynamic-thermal and localized filament-kinetic attacks on fused filament fabrication based 3D printing process”, Additive Manufacturing, Vol. 46, Issue 102200, 2021.
13. Sharma, A., Rai, A., “Fused deposition modelling (FDM) based 3D & 4D Printing: A state of art review”, Materials Today: Proceedings, Article in press, 2022.
14. ISO 6336-5, Calculation of spur and helical gears load capacity, 2016.
15. Solidworks Software 2020-2021.
16. Shigley, J.E., Mischke, C.R., Budynas, R.G., "Mechanical Engineering Design", 7th edition, McGraw-Hill publishers, 2004.
17. <https://3detay.com/cura-egitimi-cura-3d-dilimleme/>
18. Maden H., Kamber Ö.Ş., Kamber B.R. “QVAC Halı Yıkama Makinesinin Üst Kapak Tasarımı Geliştirilmesi ve Prototip Üretimi”, Int. J. of 3D Printing Tech. Dig. Ind., 5(2): 109-119, 2021.
19. Karaçor M., Delioğlu B., Şahin C. “3b Baskı Teknolojisi Kullanılarak Otonom Sualtı Aracı Tasarımı Ve Prototip Üretimi”, Int. J. of 3D Printing Tech. Dig. Ind., 5(3): 663-675, 2021.
20. Özaslan H., Bozdemir M., “Alev Gizleyen Tasarımı ve Prototip İmalatı”, Int. J. of 3D Printing Tech. Dig. Ind., 6(1): 176-185, 2022.
21. Bozca, M., Fietkau, P., “Empirical model based optimization of gearbox geometric design parameters to reduce rattle noise in an automotive transmission”, Mechanism and Machine Theory Vol. 45, Pages 1599-1612, 2010.
22. Bozca, M., “Transmission error model-based optimisation of the geometric design parameters of an automotive transmission gearbox to reduce gear-rattle noise”, Applied Acoustics Vol. 130, Pages 247-259, 2018.
23. Raia, P., Agrawala, A., Sainia, M.L., Jodderb, C., Gopal Barman, A., “Volume optimization of helical gear with profile shift using real coded genetic algorithm”, Procedia Computer Science Vol. 133, Pages 718-724, 2018.
24. Miler, D., Hoi, M., “Optimization of cylindrical gear pairs: A review”, Mechanism and Machine Theory, Vol. 156, Issue 104156, 2021.
25. Younes, E.B., Changenet, C., Bruyere, J., Rigaud, E., Liaudet, J.P., “Multi-objective optimization of gear unit design to improve efficiency

and transmission error”, Mechanism and Machine Theory, Vol. 167, Issue 104499, 2022.

26. Choi, C., Ahn, H., Park, Y.J., Lee, G.H., Kim, S.C., “Influence of gear tooth addendum and dedendum on the helical gear optimization considering mass, efficiency, and transmission error”, Mechanism and Machine Theory, Vol. 166, Issue 104476, 2021.

27. Jabbour, T., Asmar, G., “Tooth stress calculation of metal spur and helical gears”, Mechanism and Machine Theory, Vol. 92, Pages 375–390, 2015.

28. Kim, S.C., Moon, S.G., Sohn, J.H., Park, Y.J., Choi, C.H., Lee, G.H., ”Macro geometry optimization of a helical gear pair for mass, efficiency, and transmission error”, Mechanism and Machine Theory, Vol. 144, Issue 103634, 2020.

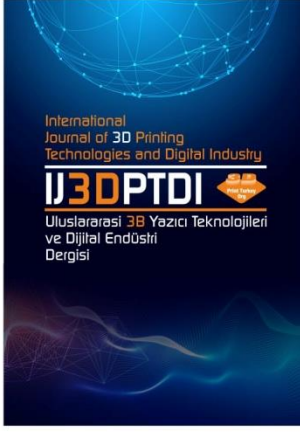
29. Zhang, J., Fard, M., ”Effects of helix angle, mechanical errors, and coefficient of friction on the time-varying tooth-root stress of helical gears”, Measurement, Vol. 118, Pages 135–146, 2018.

30. Roach, D.J., Hamel, C.M., Dunn, C.K., Johnson, M.V., Kuang, X., Qi, H.J., “The m⁴ 3D printer: A multi-material multi-method additive manufacturing platform for future 3D printed structures”, Additive Manufacturing, Vol. 29, Issue 100819, 2019.

31. Veteška, P., Hajdúchová, Z., Feranc, J., Tomanová, K., Milde, J., Kritikos, M., L ubošBa ěca, Janek, M., “Novel composite filament usable in low-cost 3D printers for fabrication of complex ceramic shapes”, Applied Materials Today Vol. 22, Issue 100949, 2021.

32. Bozca, M., “Optimisation of Effective Design Parameters for an Automotive Transmission Gearbox to Reduce Tooth Bending Stress”, Modern Mechanical Engineering, Vol. 7, Pages 35-56, 2017.

33. Yılmaz Redüktör, www.yr.com.tr Erişim Tarihi: 26 April, 2023



ULUSLARARASI 3B YAZICI TEKNOLOJİLERİ
VE DİJİTAL ENDÜSTRİ DERGİSİ

INTERNATIONAL JOURNAL OF 3D PRINTING
TECHNOLOGIES AND DIGITAL INDUSTRY

ISSN:2602-3350 (Online)

URL: <https://dergipark.org.tr/ij3dptdi>

FROM DESIGN CONCEPT TO PRODUCTION: USING GENERATIVE DESIGN OUTPUT AS DESIGN INSPIRATION

Yazarlar (Authors): Utku Kocaman *, Abdullah Toğay 

Bu makaleye şu şekilde atıfta bulunabilirsiniz (To cite to this article): Kocaman U., Toğay A., “From Design Concept to Production: Using Generative Design Output as Design Inspiration” *Int. J. of 3D Printing Tech. Dig. Ind.*, 7(1): 29-37, (2023).

DOI: 10.46519/ij3dptdi.1220263

Araştırma Makale/ Research Article

Erişim Linki: (To link to this article): <https://dergipark.org.tr/en/pub/ij3dptdi/archive>

FROM DESIGN CONCEPT TO PRODUCTION: USING GENERATIVE DESIGN OUTPUT AS DESIGN INSPIRATION

Utku Kocaman^a , Abdullah Toğay^a 

^a Gazi University, Faculty of Architecture, Department of Industrial Design, TURKEY

* Corresponding Author: utkukocaman@gmail.com

(Received: 16.12.2022; Revised: 27.12.2022; Accepted: 24.04.2023)

ABSTRACT

With the rapid development of information technologies, the generative design has started to rethink the future roles of industrial designers. The simulation integrated into generative design helps designers to create manufacturable products. Therefore, this study examines how generative design can progress with conventional production processes and how this progress can help designers in the future. The potential of generatively obtained form-seeking processes to create optimal results is discussed within the scope of this study. For this purpose, a generative design triggered design process was conducted with a firm in the real sector about re-designing a bicycle frame. Generative design outputs have been optimized in terms of manufacturability. The effects of generative design-based inputs on the final product have been discussed through material usage and the sustainability. Based on the outcomes of the study, suggestions have been developed on how generative design can be transformed into results that can be a source of innovation.

Keywords: Generative Design, Designer Role, Design Processes.

1. INTRODUCTION

1.1. Design Processes

The digital revolution, which started with the production of the first transistor, reached its climax with the spread of personal computers. With the use of digital technologies in the industry, production processes have become more efficient. With digital automation, processes have started to take place faster and more smoothly. Thus, it enabled production to be made in a shorter time and with higher productivity. In addition, thanks to digital technologies, production processes have become more accessible and understandable [1].

It is undeniable that the digital revolution, accelerated by the spread of personal computers, affects every aspect of life. Designers use one or more design tools throughout the act of designing [2, 3]. The digital age, which started with the transition from analogue computers to digital computers, also enabled the evolution of the tools used by the designer [4]. Electronic pens and screens have replaced the paper and pen used by the

designer; the mathematical formulas entered on the black screen during production have been replaced by Computer-Aided Design (CAD) software with modern interfaces controlled by peripherals called mouse [5]. Actions such as prototyping and optimization, which take a long time to perform with conventional methods, have become faster and more effective thanks to CAD software. Thus, the design processes have also changed with the changing industrial production processes.

The act of the designer seeking a solution to a problem forms the basis of the design process [6]. Although there are many interpretations of this process in the literature, the common process definition includes problem analysis, concept design, evaluation, enlightenment, and validation steps [7]. When viewed from a broader perspective, it is seen that the design process has a much more complex structure. In the process, a much more comprehensive structure emerges, including technical information on basic and applied sciences, economics, social and geopolitical issues, and the definition of needs [8]. The experiences

gained at each step of the design process form the basis of the next step.

When descending from the main steps to the intermediate steps, prototyping and optimization can be seen among these steps [9]. Prototyping and optimization are cyclical, multidisciplinary efforts for finding a better solution [10]. In markets where new designs are constantly sought, speed and diversity gain importance in the new product development process. For this reason, it is necessary to select multiple alternatives from among potential solution proposals quickly. It is also essential for companies to produce many prototypes and perform optimization on these prototypes.

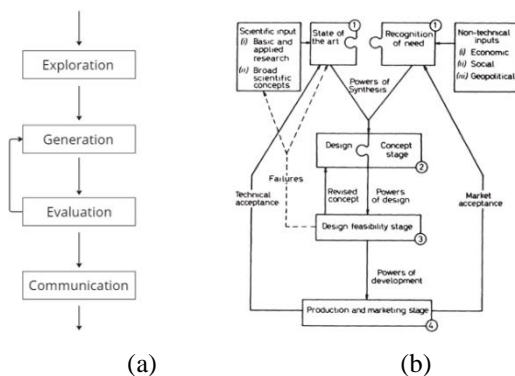


Figure 1. Cross's simple four-stage design process model (a) and Gregory's definition of the design process (b).

The CAD software used by the designers in the design process is as essential as the steps of the process. The designers, who tried to prevent error by simulating the prototypes and analyses in digital environments before they were produced, started to produce more complex designs using CAD tools. As designs evolve into more complex structures with this software, there is a need for utility programs that will reveal the work done more effectively. One of these needs was to make it easier for designers to produce forms based on specific algorithms and within defined limits. The designers using algorithms and boundaries were looking for a CAD tool that would minimize the margin of error, effectively reveal form alternatives, and allow random occurrences in alternatives. [11]. For this reason, specialized CAD helpers emerged that would make iterations or changes in the textures of designs easier and faster. Although these assistants emerged as a software add-on at first, they have become stand-alone software over time. The design model made by

producing forms with software which have these algorithms is called generative design (GD), and its history dates to the early 1900s. [12].

1.2. Generative Design

GD is a CAD technique that allows the quickly developing of design alternatives [13]. The GD, whose processes (See Figure 2) are cyclical and based on iterations [14], emerged with the effects of the digital age and showed itself first in the field of informatics and then in architecture [11]. The biggest reason why it is seen in the field of architecture was the fact that innovative architects and thinkers questioned the architectural designs of their periods at the end of the 19th century and the necessity of establishing the design on universal principles and keeping it away from individual tastes was realized [14]. During this period, the focus of attention of many architects and designers turned to nature. The book *Art Forms in Nature*, published by biologist E. Haeckel in 1904, attracted the attention of designers who shared the same idea, and the traces of nature can be seen in many designs made after this date.

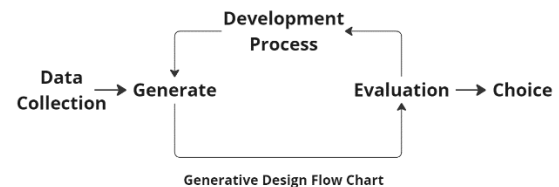


Figure 2. GD processes [15].

This software, which architects use when making decisions on buildings, has turned into a tool that includes simulation and optimization in its infrastructure with the advancement of information technologies (See Figure 3). This simulation transforms the form to be produced into optimal design solutions according to the specified materials and the forces given. While the previously created forms were defined only through aesthetic perceptions and textures, it has now made it questionable how well they will fulfil the functionality.

GD work is primarily done in the fields of architecture and engineering. In the literature research, it has been seen that architects mostly use GD to produce forms [16-18], and engineers use it to search for more economical solutions for the designs to be made [19-21]. In one, all variations of the desired design forms are observed, and in the other, the search for the

best possible solution from all variations within the desired limits is discussed [22]. GD adopts a design approach that imitates the evolutionary formation of nature. With this approach, computer sciences involved in the GD process create difficulties for designers who have little expertise in these subjects [23]. With the spread of additive manufacturing in the industry the issue of GD comes to the fore more and gets closer to industrial design. Despite the convergence of GD with industrial design, there needs to be more work done in the field of industrial design literature.



Figure 3. GD-1 [24] (Designer: Kiarash Kiany)
GD-2 [25] (Designer: Lightning motorcycle).

Although the design processes have survived almost unchanged throughout history, they have changed rapidly since the Industrial Revolution and have kept up with technology. The most significant technological changes were undoubtedly the internet age, which became widespread with the digital revolution [26]. The limited native processing power of personal computers allowed designers to work with a limited number of forms while using GD. We can easily see the Internet's and internet-connected technologies' effects in the industry on GD [27]. Thanks to the cloud technology that emerged after the internet, GD work has become much faster and much more form study can be done on a remote server, independent of personal computers [28].

Since the production patterns of the GD outputs are determined in the problem definition process, the results are formed in accordance with these production processes. In this context,

manufacturers need to have these production processes in their production lines for GD to be a valuable tool. However, for a designer, the output of this tool not always be the final product. If the outputs are considered as form suggestions, a design approach that can be progressed with different production processes can be put forward. Thus, the outputs of the GD tool during the production process will be carried over to the design process.

In their study, Singh and Merrick state that GD can become a helpful tool for designers when examined within a framework specific to industrial design [29]. The limited technical knowledge infrastructure of industrial designers, such as force, statics, and resistance, makes it difficult for them to use this tool. However, if this technical information is given to them, they can quickly adapt and include it in the design processes. This study aims to research how GD affects the role of industrial designers in the industry and how it can change it.

2. METHOD

A firm from the real sector was selected in the study, in which the potential of GD to be a resource for design and innovation in the processes leading up to production was investigated. In this context, interviews were held with jewellery design, furniture, and steel companies. The potential of working on a product that meets the criteria of having a function and a form that can be produced with GD has been questioned. In the study, it is aimed that the product to be designed with a GD will be under the effects of a structural force, that the designed product will not be hidden under another shell, and that the end user can easily observe it. The method of the study is a six-step process, and each step will be explained in this section. In this research, “Autodesk Fusion 360” CAD software was used for GD studies.

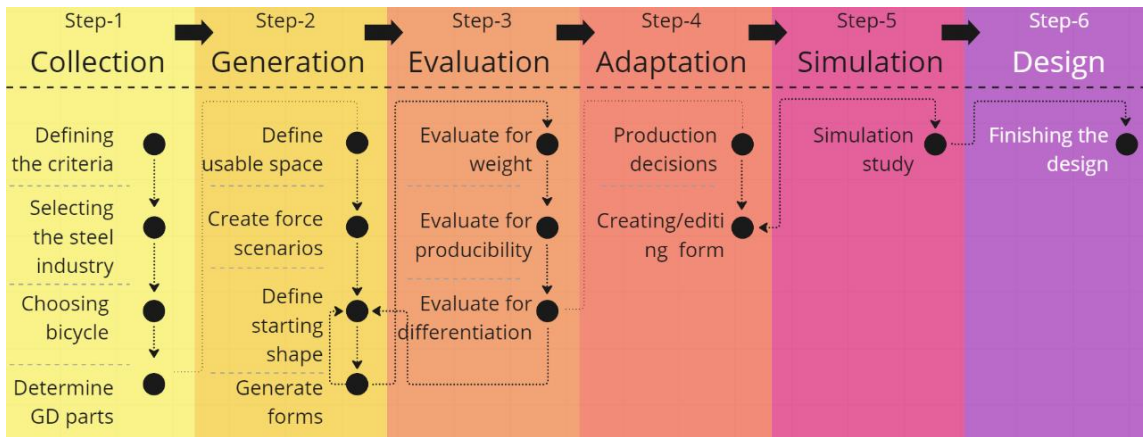


Figure 4. Research method.

2.1. Step 1

Within the scope of the study, the criteria for the product to be produced with GD were established. These criteria are that the product to be designed must be under the influence of a particular force, it should not require special conditions to be produced, and it is not covered with shell or other parts, making it difficult to see. In this context, because of the interviews, it was decided to collaborate with a firm from the steel industry about a bicycle, which is a product in which both function and form gain importance, and the bicycle frame was chosen as the product. Within the scope of the study, an example of a conventional product with defined functional limits was emphasized, a conventional bicycle was chosen, and it was considered a control example (See Figure 5).



Figure 5. The bicycle that has a conventional frame.

It was decided which parts would be included in the GD with the study on the bicycle. Accordingly, basic behaviour models were analysed by preserving the connection points in the product. Based on the decisions made, it was evaluated which parts would be included in the study and compared. In this context, those shown in green in Figure 6, and denoted by the

letter “a” shows the parts that are planned to be included in the GD.

2.2 Step 2

After the bicycle frame parts to be included in the GD were decided, the areas that could be used by the GD were determined. As seen in Figure 6, those marked with the letter “b” on the bicycle form and shown in red indicate the areas where the GD tool is prohibited, that is, the areas closed to GD, and those that are indicated with “c” and shown in blue indicate the parts that will not be included in the design process. After the parts of the conventional bicycle are separated, the bare frame weighs 3.6 kg.

To be able to distribute the load in the GD tool, it is necessary to define the load scenario first. Figure 6 shows that the front wheel boundary is defined as a spherical obstacle so that the front wheel can turn left and right in the bicycle frame example. To define the space better where the GD tool will work, the moving or screwed parts of the green areas to be included in the design are marked with red barriers to prevent errors. After the boundaries on the forms are determined, the loads are defined. The forces that will physically affect the bicycle frame were investigated, and a multi-scenario study was arranged in which all loads were affected. In the determined scenarios, a series of force inputs, including the buckling and rotational moments that the cyclist will exert the bike at the highest level, is created.

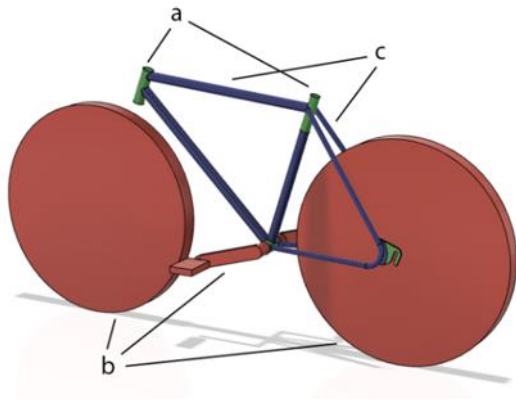


Figure 6. Boundaries of the bike frame

The definition of loads on the design is shaped according to the design outputs expected from the GD tool. This study is designed for an urban

bike with users weighing a maximum of 130kg. As can be seen in Figure 7, the distributions are prepared to simulate various events such as statics (where the bike is not going and the user is stationary on it), rotation (individually resisting axial rotational force of the handlebar and middle section) and buckling (the stress caused by the sudden impact of the bike while it is in motion) as scenario-based inputs.

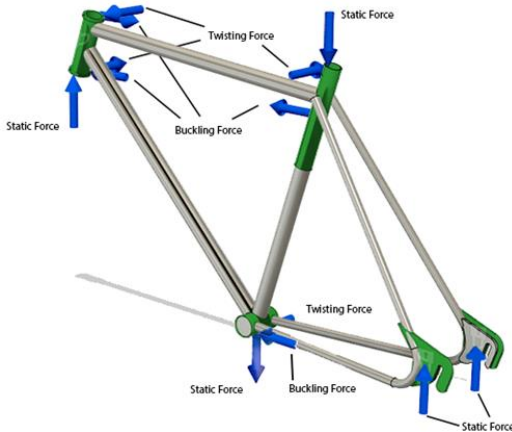


Figure 7. Load distribution.

2.3. Step 3

As a result of operating the GD processes, ninety-four GD studies and ninety-four load distribution scenarios were made. Each study was conducted with at least twenty-five iterations and four different materials. The total number of iterations was more than 9400. As a result of the study, the process continued a form deemed appropriate.

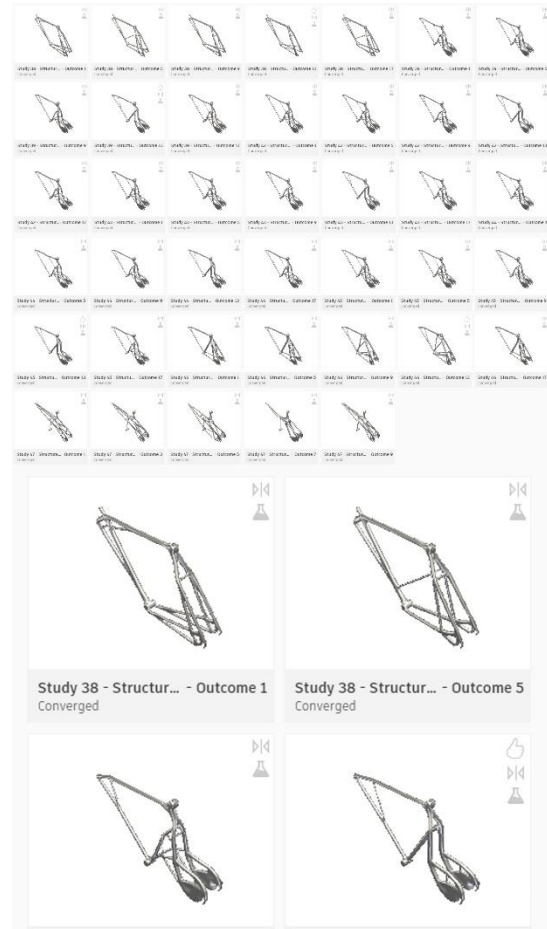


Figure 8. Thirty-nine out of ninety-four GD printouts and detailed sample images.

2.4. Step 4

A study was conducted to make the form obtained with iterations producible with the firm's production processes. In terms of being suitable for conventional production processes, it was decided to produce the resulting form by using conventional profile pipes. It has been reconstructed with basic forms so that the organic form can be produced more easily with conventional methods (See Figure 9). The lattice structure was defined on the edges of the new form, and the bearer system solution was created over this structure.

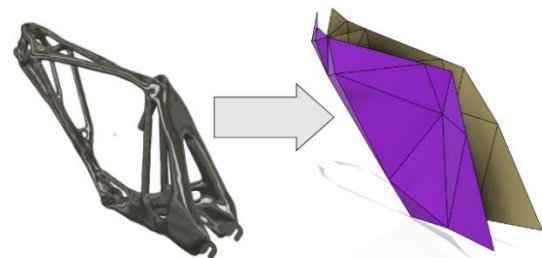


Figure 9. Organic shape to Basic Shape.

2.5. Step5

The simulation of the implemented form of the bearer system solution has been performed (See Figure 10). In this context, a new study has been initiated for the simulation, and the forces entered in the GD process have been repeated in this step. It has been investigated whether the new design relies on the given forces, like the GD output.

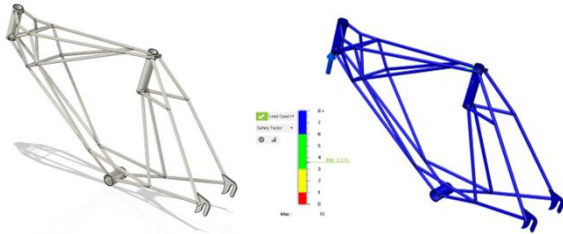


Figure 10. Design solution and its simulation result.

2.6. Step 6

After observing that the design idea works in the simulation, the other elements that can be included in the design are emphasized. The necessary parts are added to create the solution, the final changes are made to the design, and the final product is reached.

3. RESULTS

The GD tool, by its nature, aims to reach the optimized final form from a certain space by using the iterative space-freeing technique. For this reason, the form outputs produced by the tool are always solid structures, and it is entirely up to the designer's choice whether to use these outputs as they are. At this point, the first results that emerged in this study, in terms of form structure, are close to the structures available in the market, although partially different form outputs can be seen (See Figure 8). However, when the results are compared with the form structures in the market, it is seen that the GD tool cannot produce a lighter form in terms of weight. The first stage of the study was created using different materials to compare the material and design outputs. On the weight/safety table, steel-derived materials are clustered in heavy-weighted region; titanium is concentrated in the medium-weight region, while aluminium is concentrated in the lightest region.

After observing that the GD outputs reached similar results with each other, the form formation processes of each of the outputs were

examined starting from the first iteration step. Looking at the common denominator of these outputs, it is seen that the initial iterations are the same. From this point of view, the subsequent iterations will not have hugely different form outputs. For this reason, it is aimed to obtain different results by creating a wider area that the GD tool can use.

It has been observed that the GD outputs with the initial form defined are more different and functional than the previously produced forms (See Figure 11). However, the fact that these forms are even heavier than the previous forms make them a design that cannot be produced. For this reason, a new process has been designed, inspired by the GD outputs.

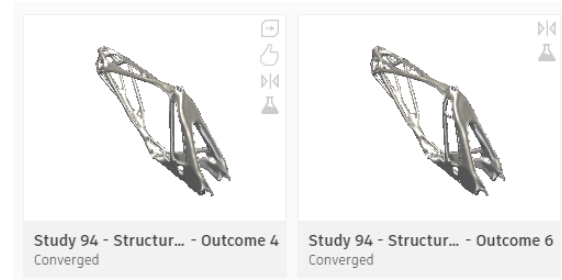


Figure 11. Output whose form has changed by giving the initial form.

In the process, it has been observed that although the path followed by the GD tool in creating the desired designs is different, the results are always the same. Since the frame to be designed cannot be produced in a hollow structure like conventional bodies, the structures are composed of completely solid materials, and therefore the frame designs are heavy. Since more than the GD tool is needed to create hollow forms, the created forms need to be reconsidered by the designer. It will be easier to produce if the physical strength of the output in an organic structure can be solved with a simpler structure. For this reason, the output was reconstructed using surfaces modelled with basic forms to transform highly detailed organic structures into simpler ones (See Figure 9).

The first study on the form in the basic structure (See Figure 12) shows that the lattice structure created by the GD tool can reach a positive result. The design's behaviour against the load is close to the area indicated by the green area numbered 3-6 and defined as favourable conditions. When the design is examined, it has been observed that the right and left sides of the

hull diverge from each other in some areas and converge in some areas, and its structural integrity is disrupted. When viewed from the GD output (See Figure 9), it has been observed that those regions are thicker than the other sides.

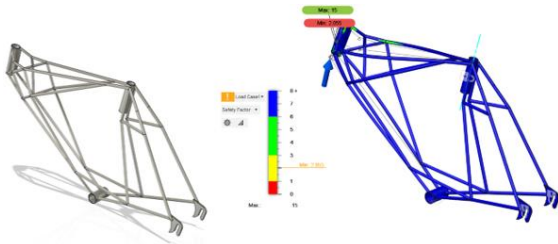


Figure 12. First model after basic form and its simulation result.

After the observation, an iterative design process was conducted on the design. This process created support points in the regions where bending was observed after the simulation. The static simulation of the new design was performed again, and progress was made to use the least material. In the process, not only additions were made, but also unnecessary parts were removed. When the final design (See Figure 10) is reached, a structure with a weight of 2.3 kg and a strength of up to 3.5 times the 130 kg force given is obtained.

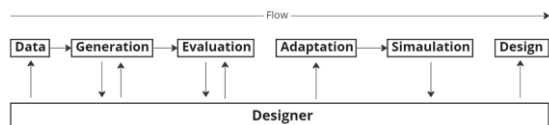


Figure 13. The GD process diagram in the study.

In the design process of the research (See Figure 13), the designer was assigned to evaluate, synthesize and re-flow multiple disciplines by taking tasks such as data identifier, output determinant, design idea selector, adaptor, simulation evaluator and designer. Considering the design processes, the process used in this research is shorter than French's ten-stage design process [30]. The main reason for this is that algorithms analyse the given data. There is no single right way in the design processes used in this research. If lighter structural integrity is expected from the design, it is known that this can be achieved faster with the GD tool.



Figure 14. Production process and the final product.

At the end of the process, frame manufacturing was conducted on the defined production line and evaluated from an innovative perspective. A more functional design has been created with a different approach to the frame structure, which looks different from the products on the market. The study, which has been manufactured, was analysed, and it was observed that up to 33% reduction was achieved when compared to conventional bicycle frames. In addition, with this lightning, it has become a bicycle that users can carry more easily and ride with less effort.

4. CONCLUSION

This research aimed to reveal the potential of GD for conventional manufacturing techniques and examined the role of the industrial designer by questioning the place of the GD tool in the industry. While the article focuses on the form creation skills of the GD tool developed with simulation analysis, it also examined the results of the designs that will emerge by using the GD outputs as a source of inspiration in the design processes of industrial designers.

The study started with a literature search. The design processes with the developing technology and the role of the designer in the industry are discussed through GD. A special 6-step GD method was developed for this research, and product design was made with this method. With this method, which has steps such as data collection, production, evaluation, adaptation, simulation and design, GD is examined from a different perspective. GD outputs were evaluated as a source of inspiration, and it was ensured that the design ideas that could be put forward were based on the data.

In this study, the designer had roles that interfered with both design, production, and the safety of the design. The fact that GD is gradually taking place in the industry and is a sought-after tool in high-tech designs shows

that the designer will also assume different roles in the future. It is foreseen that industrial designers can unleash this tool's potential, especially in the design of parts and products that will perform the same job by using lesser materials. This study proves that designers can realize extraordinary designs by incorporating GD tools into their production processes at a time when products are not only designed as a shell.

It is seen that the generative design process carried out in this article also contributes to the sustainability development goals of the United Nations. A transportation vehicle, which has great advantages about using clean energy, such as bicycle, is produced with less material than conventional vehicles, resulting in less carbon footprint. With less carbon-footprint it ensures the production is sustainable. Lighter bicycle means it can be used by a wider range of users, so that means it can reach more people and use more clean energy on transport. Also, when the materials lessened, manufacturing costs will reduce.

Lighter products create less carbon while manufacturing, shipping, repairing, and in usage. From this point of view, this research has an innovative approach to using generative design in the scope of sustainability.

Although creating a form with a GD tool may seem simple to an outside observer, it cannot be easy to find a suitable form, considering the production conditions. Forms created with iterations within limits set by the designer with specific algorithms often do not carry the desired aesthetic concern. For this reason, GD studies appear as a chain of work based on constantly getting different results with new parameters.

As a result, the emergence of a design can sometimes be hidden in the designer's mind and sometimes on the surfaces of a dice put forward. The designer designs by being open to all surprises, sometimes knowing where he will go and sometimes not knowing what will come out. At this point, the designer looking for inspiration often looks at other products and related works around him. These inspirations rarely lead the design to a vastly different point from other manufactured products. Although being different does not always mean being distinctive, it is always the first goal to create

easily distinguishable differences in the products made by designers. The first feature that the GD tool provides to the designer is to provide optimized form outputs that will fulfil the function. The second feature is to inspire the designer with these outputs and create a space for reflection.

While it is difficult to generalize based on a single case, this study has shown that designers can look outside the box, find more innovative approaches in GD tools, and capture different approaches in design and manufacturing processes with these tools.

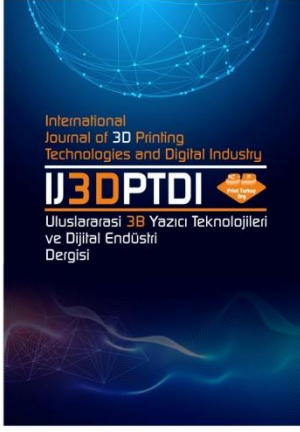
ACKNOWLEDGES

Authors can refer to companies, businesses, public institutions, or projects that contributed to the study in this section.

REFERENCES

1. Schwab, K., "The fourth industrial revolution", Crown Business, New York, 2017.
2. Do, E.Y.-L., Gross, M.D., "Drawing as a means to design reasoning", *AI in Design*, June, 1996.
3. Ekströmer, P., Wever, R., "“Ah, I see what you didn't mean” exploring Computer Aided Design tools for design ideation", *The Design Journal*, Vol. 22, Issue 1, Pages 1883-1897, 2019.
4. Şeker, T.B., "Bilgi teknolojilerindeki gelişmeler çerçevesinde bilgiye erişimin yeni boyutları", *Selçuk Üniversitesi Sosyal Bilimler Enstitüsü Dergisi*, Vol. 13, Issue 1, Pages 377-391, 2005.
5. Woodbury, R., "Elements of parametric design", Routledge, New York, 2010.
6. Brown, T., "Design thinking", *Harvard Business Review*, Vol.86, Issue 6, Pages 84, 2008.
7. Lawson, B., "How designers think", Architectural Press, Oxford, 2005.
8. Gregory, S.A., "The design method", Springer, Birmingham, 1966.
9. Brown, T., "Change by design", Harper Business, New York, 2009.
10. Gomes, S., Antoine, V., Sagot, J.-C., "Functional design and optimisation of parametric CAD models in a knowledge-based PLM environment", *International Journal of Product Development*, Vol. 9, Issue 1-3, 2009.

11. Lobos, A., "Finding balance in generative product design", Norddesign 2018, Sweden, 2018.
12. Proctor, R., "Architecture from the cell-soul: René Binet and Ernst Haeckel", *The Journal of Architecture*, Vol. 11, Issue 4, Pages 407-424, 2006.
13. Khan, S., Awan, M.J., "A generative design technique for exploring shape variations", *Advanced Engineering Informatics*, Vol. 38, Issue 1, Pages 712-724, 2018.
14. Agkathidis, A., "Generative design: form-finding techniques in architecture", Laurence King Publishing, London, 2016.
15. Walmsley, K., "Getting started with generative design for AEC", <https://www.autodesk.com/autodesk-university/class/Getting-Started-Generative-Design-AEC-2018>, March 22, 2021.
16. Huang, Y., "Generative forms of historical architectural arts—the example of caisson in historical temple", *International Journal of Culture and History*, Vol. 3, Issue 3, 2017.
17. Schumacher, P., "Parametricism: a new global style for architecture and urban design", *Journal of Architectural Design*, Vol. 79, Issue, 4 Pages 14-23, 2009.
18. Janssen, P., R. Stouffs, "Types of parametric modelling", 20th International Conference of the Association for Computer-Aided Architectural Design Research in Asia, Pages 157-166, 2015.
19. Fryer, T., "The end of the engineer?", *Engineering & Technology*, Vol. 12, Issue 9, Pages 26-29, 2017.
20. Gunpinar, E., Coskun, U.C., Ozsipahi, M., Gunpinar, S., "A generative design and drag coefficient prediction system for sedan car side silhouettes based on computational fluid dynamics", *Computer-Aided Design*, Vol. 111, Pages 65-79, 2019.
21. Renner, G., Ekárt, A., "Genetic algorithms in computer aided design", *Computer-Aided Design*, Vol. 35, Issue 8, Pages 709-726, 2003.
22. Chen, X.A., Tao, Y., Wang, G., Kang, R., Grossman, T., Coros, S., Hudson, S.E., "Forte: User-driven generative design", 2018 Conference on Human Factors in Computing Systems, Paper 496, Pages 1-12, 2018.
23. Curralo, A., "Generative Design and Information Visualization", 7th International Conference on Digital Arts, Pages 99-104, 2015.
24. Kiany, K., "Parametric Roof", <https://parametrichouse.com/serpentine-sackler-gallery/>, November 5, 2022.
25. Association of Equipment Manufacturers, "Generative design: solving design challenges with artificial intelligence", <https://www.aem.org/news/generative-design-solving-design-challenges-with-artificial-intelligence>, August 21, 2019.
26. Togay, A., Çetinkaya, K., "Üretken tasarım ve üretken tasarım etkisinde tasarımcı", 4th International Congress on 3d Printing (Additive Manufacturing) Technologies and Digital Industry. 2019. Antalya, TURKEY.
27. McDonagh, D., Hekkert, P., Erp, J.V., Gyi, D., "Design and emotion", Taylor & Francis, London, 2004.
28. Buonamici, F., Carfagni, M., Furferi, R., Governi, L., "Generative design: an explorative study", *Computer-Aided Design and Applications*, Vol. 8, Issue 1, Pages 144-155, 2020.
29. Gu, N., Singh, V., Merrick, K., "A framework to integrate generative design techniques for enhancing design automation", 15th International Conference of the Association for Computer-Aided Architectural Design Research in Asia, Pages 127-136, 2010.
30. Cross, N., "Engineering design methods: strategies for product design", John Wiley & Sons, West Sussex, 2001.




ULUSLARARASI 3B YAZICI TEKNOLOJİLERİ
VE DİJİTAL ENDÜSTRİ DERGİSİ

INTERNATIONAL JOURNAL OF 3D PRINTING
TECHNOLOGIES AND DIGITAL INDUSTRY

ISSN:2602-3350 (Online)

URL: <https://dergipark.org.tr/ij3dptdi>

OPTIMIZATION OF 3D PRINTING PARAMETERS TO MECHANICAL STRENGTH IMPROVEMENT OF SUSTAINABLE PRINTING MATERIAL USING RSM

Yazarlar (Authors): Erman Zurnacı *


Bu makaleye şu şekilde atıfta bulunabilirsiniz (To cite to this article): Zurnacı E., “Optimization of 3D Printing Parameters to Mechanical Strength Improvement of Sustainable Printing Material Using Rsm” *Int. J. of 3D Printing Tech. Dig. Ind.*, 7(1): 38-46, (2023).

DOI: 10.46519/ij3dptdi.1231076

Araştırma Makale/ Research Article

Erişim Linki: (To link to this article): <https://dergipark.org.tr/en/pub/ij3dptdi/archive>

OPTIMIZATION OF 3D PRINTING PARAMETERS TO MECHANICAL STRENGTH IMPROVEMENT OF SUSTAINABLE PRINTING MATERIAL USING RSM

Erman Zurnaci 

Kastamonu University, Engineering and Architecture Faculty, Mechanical Engineering Department, TURKEY

*Corresponding Author: ermanzurnaci@kastamonu.edu.tr

(Received: 08.01.2023; Revised: 02.02.2023; Accepted: 24.04.2023)

ABSTRACT

Fused Deposition Modelling (FDM), one of the most widely used methods of Additive Manufacturing Technique known as 3D Printing, is a popular technique used to produce different engineering components using common engineering polymers. PLA filament, a synthetic polymer derived from corn starch, is generally used in production with the FDM. Although PLA material is recyclable and biodegradable, its carbon emission is not zero. One of the filament types developed to produce more sustainable products is Wood PLA filament materials. This study presents an experimental study examining the effect of printing parameters on the mechanical properties of components produced with Wood PLA filaments. The effects of the printing parameters determined as infill pattern, infill density and nozzle temperature on the mechanical strength parameter determined as tensile strength and flexural strength of PLA Wood samples produced in standard sizes were investigated experimentally. The experimental design was carried out in accordance with the Taguchi L9 orthogonal array, and the relationship between the printing parameters and the mechanical strength parameters was modelled mathematically. The predicted strength values calculated using mathematical models were compared with the experimental test results. The results showed that the tensile strength and flexural strength values were directly proportional to the infill density. Experiments have shown that the most effective 3D printing parameter on the mechanical strength parameters is the infill density parameter with a contribution ratio of 63.09% for tensile strength and 73.83% for flexural strength. As a result of the RSM optimization, it was determined that the infill density 60%, the nozzle temperature value 202.62 C° and the infill pattern type lines to maximize the flexural strength and tensile strength values.

Keywords: Sustainable material, 3D printing parameters, Mechanical strength optimization, Response Surface Methodology.

1. INTRODUCTION

Three-dimensional production technique has become increasingly popular due to its advantages such as ease of use, economic accessibility and fast production process. One of the most important factors in the spread of this technique is the easy accessibility of this technology. In addition, researchers can produce prototypes of the designs they have developed with this technique without the need for complex and experience-requiring production techniques and they can make design changes when necessary. The production of products with complex geometry has also become possible with this method [1]. The interest in 3D production techniques has led to

the development of 3D printers, and it has become possible to use different materials in production from polymers to metals, from glass to concrete.

The Fused Deposition Technique (FDM) is the most common production technique known in additive manufacturing technology. A printer working with the FDM technique heats the filament material until it becomes semi-molten using a heater extruder and follows the tool path created by the software, stacking the layers on top of each other from the bottom up to form a three-dimensional object. In the FDM technique, printing parameters can be easily changed and optimized [2, 3].

Different filament materials have been developed by considering factors such as the melting point and extrudability of the material to be used in the FDM technique [4]. The most commonly used ones are acrylonitrile butadiene styrene (ABS), polyethylene terephthalate glycol (Pet-G) and polylactic acid (PLA) thermoplastic filaments with low melting temperatures. PLA filaments are the most commonly used filament material due to their low melting temperature, low cost and positive environmental effects [5, 6]. PLA is one of the biodegradable polymers produced from corn starch. PLA is environmentally friendly, unlike materials such as polypropylene, polyethylene and acrylonitrile butadiene styrene [7]. In addition, it does not pose any health risk to humans in areas where ventilation is provided under appropriate conditions, and it is biodegradable [8].

Although PLA material is an environmentally friendly material, it emits ~1.3 kg of CO² equivalent/kg of synthesized plastic [9]. Considering the advantages of PLA filament material, the idea of producing more sustainable materials by mixing these thermoplastic filaments with different biological materials has come to the fore to reduce the effects of intensive material use.

Wood-filled polylactic acid filaments are one of the highly sustainable renewable materials used in production with the FDM technique. Wood is a lignocellulosic material and is carbon negative [10]. By using biological materials, the carbon emissions from printing materials can be reduced. The wood raw material is turned into flour and combined with PLA material by foaming technique, and wood-based PLA filaments can be produced [11]. Wood flour imparts good workability, low density, thermal resistance and corrosion resistance to PLA filament, while also facilitating interlayer adhesion [12].

Academic studies carried out in recent years have focused on examining the effect of printing parameters on different mechanical properties. Optimization of printing parameters for ideal properties determined by different application areas is an important issue for the final use of the product. There is still a deficiency in the literature examining the mechanical properties of filaments developed

with different filling materials. Optimization of the mechanical properties of biomaterials is important in terms of increasing the use of sustainable materials.

In this study, the effect of 3D printing parameters on the mechanical properties of samples produced using Wood PLA filament was investigated. The effects of the production parameters determined as infill type, infill density and nozzle temperature on the tensile strength and flexural strength of the samples produced according to the Taguchi L9 experimental design were investigated. Response Surface Methodology was used to determine the effect of each printing parameter on the output values and to determine the optimum printing parameters.

2. MATERIAL AND METHODS

2.1. Printing Material and Parameters

In this study, the effect of the 3D printing parameters of the samples produced with biomaterial (Wood) based filament material on the mechanical properties of the samples was investigated experimentally, and the results were evaluated using statistical methods. ESUN brand Wood PLA filament with wood additive was used in the production of the samples. The filament diameter is 1.75 mm and the same filament was used from a single package throughout the production. The vendor supplied material properties of the filament used are given in Table 1.

Table 1. Wood PLA filament properties.

Parameters	Value
Density	1.1 g/cm ³
Melt index	190 C°/2.16 Kg
Tensile strength	40.74 MPa
Izod notched impact strength	10.55 kJ/m ²
Elongation at break	76.85 %
Flexural strength	61.62 MPa
Flexural modulus	2570.75 MPa
Heat distortion temperature	50.4 C°

For experimental tests, tensile test specimens were designed in accordance with ASTM D638-IV and three-point bending test specimens ASTM D790 test standards. Three-dimensional models of the samples were created with Solidworks solid modeling software and then converted to STL format with Ultimaker Cura software.

2.2. Experimental Design

The printing parameters are an effective factor on the mechanical strength criteria of the samples produced with the FDM technique [13]. Three different printing parameters were used in the production of the samples produced with Wood PLA filaments: infill pattern, infill density and nozzle temperature. Taguchi optimization technique is a frequently used method in the literature to determine optimum mechanical parameters by reducing product development costs [14]. Experimental design was carried out in accordance with the Taguchi L9 orthogonal array with the printing parameters and levels given in Table 2. The

cross-sectional views of the tensile specimens converted to STL format for different printing parameters are given in Figure 1.

Table 2. Taguchi design factors and levels.

Factors	Units	Level 1	Level 2	Level 3
Infill Pattern	-	Lines	Triangles	Cubic
Infill Density	%	20	40	60
Nozzle Temp	C°	190	205	215

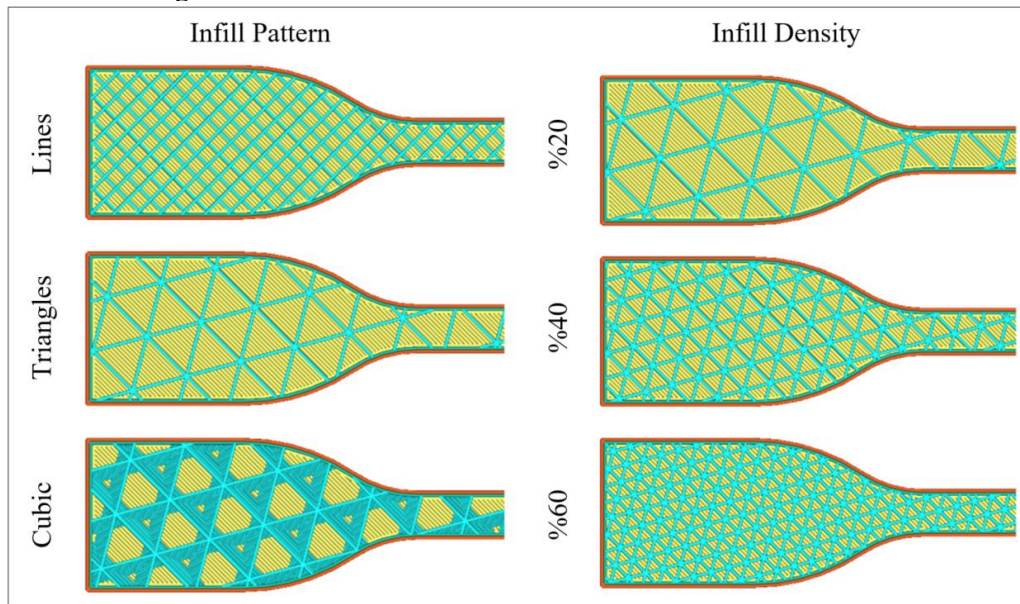


Figure 1. Infill pattern and infill density cross section views.

2.3. Production of Experimental specimens

Experimental test samples based on Wood PLA were produced at room temperature in a commercially available Creality Ender 3 S1 printer, which produces with FDM technique. In the mechanical tests, the number of upper and lower layers was limited to three layers in order to make the effect of the printing parameters on the mechanical properties more evident. Thus, it is aimed to increase the effect of infill pattern and infill density parameters on mechanical properties. In order not to deteriorate the dimensional stability of PLA Wood filaments by being affected by thermal changes, support was created for the samples in the production of the first layer. The printing parameters used in the production of experimental test samples are given in Table 3. In order to ensure the experimental measurement accuracy, a total of

27 samples, three from each sample, were produced.

Table 3. FDM printing parameters.

Parameters	Values
Filament colour	Grey
Filament diameter	1.75 mm
Nozzle size	0.4 mm
Build plate temperature	65 C°
Printing speed	50 mm/s
Density	1.1 g/cm ³
Layer height	0.2 mm
Wall thickness	0.8 mm
Wall line count	2
Top/bottom thickness	0.8 mm
Layer number	3
Build plate adhesion type	Brim
Brim width	4 mm

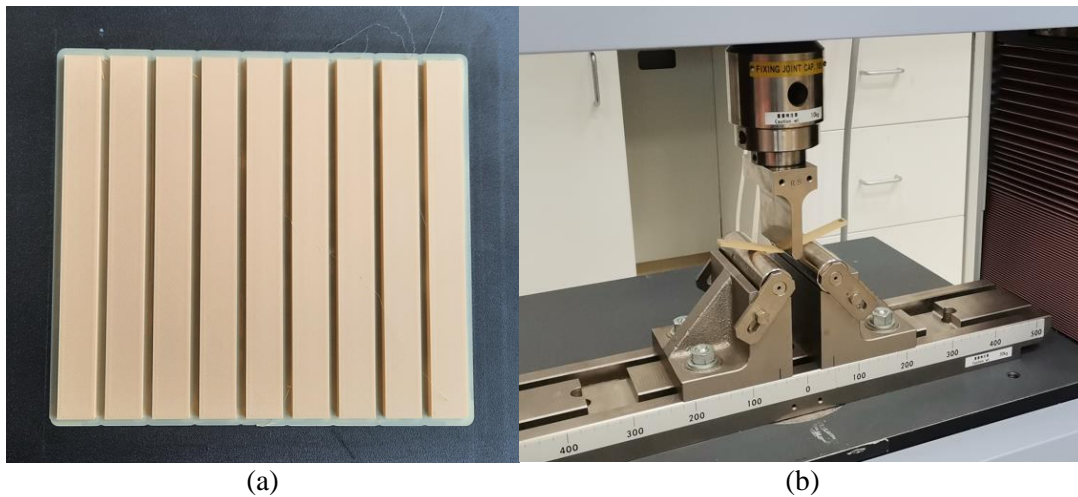
3. EXPERIMENTAL STUDY

3.1. Tensile Test Setup

Tensile test specimens were produced in accordance with ASTM D638-IV test standard. The tests were carried out in the 100 kN capacity Shimadzu Autograph AGS-X tensile testing device in Kastamonu University Central Research Laboratory. Tensile tests were carried out with reference to the literature at a speed of 5 mm/min and the tests were continued until the specimens fractured. Tests for each sample were performed at room temperature in triplicate. As a result of the experiments, the tensile strength values of the samples were determined.

3.2. Flexural Test Setup

The flexural test specimens were produced in accordance with the ASTM D790 test standard (Figure 2a) and the specimens were tested using a three-point bending test apparatus in the device used for the tensile test (Figure 2b). Tests for each sample were carried out at a speed of 1.365 mm/min with reference to the literature, and the test was terminated after 5% deflection occurred in the samples. Three point bending test apparatus loading span diameter of 10 mm and a support roller with a diameter of 30 mm with supporting span length of 51.2 mm were used for the flexural tests. Bending load-displacement curves were recorded from the experimental tests. Experimental specimens and test setup is shown in Figure 2.



(a) (b)
Figure 2. a) Flexural test specimens and b) test setup.

4. RESULTS AND OPTIMIZATION

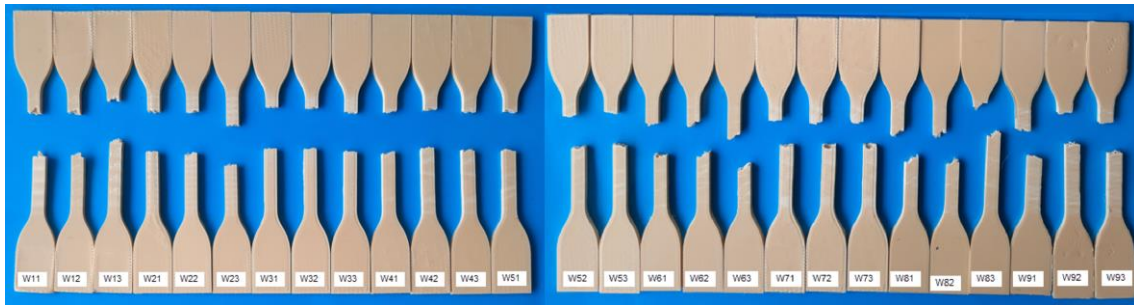
4.1. Experimental Results

In this study, the effect of 3D printing parameters on the mechanical properties of Wood PLA material samples was investigated. As a result of the experiments carried out with 27 samples, the tensile strength and flexural

strength values of the samples were obtained. The arithmetic means of the test results performed three times for each sample was calculated. Experimental test results are given in Table 4. The post-test images of the tensile test specimens are shown in Figure 3.

Table 4. L₉ Taguchi orthogonal array and experimental results.

	Infill Pattern	Infill Density (%)	Nozzle Temp (C°)	Tensile Strength (MPa)	Flexural Strength (MPa)
1	Lines	20	190	13.53	36.67
2	Lines	40	205	14.30	43.94
3	Lines	60	215	16.76	49.30
4	Triangles	20	205	12.35	34.98
5	Triangles	40	215	12.78	39.34
6	Triangles	60	190	14.56	40.68
7	Cubic	20	215	13.24	33.98
8	Cubic	40	190	14.64	39.14
9	Cubic	60	205	17.98	47.56

**Figure 3.** Image of tensile test specimens after testing.

4.2. Response Surface Methodology

In order to produce Wood PLA samples with the best mechanical strength properties, optimization of 3D printer printing parameters is required. Response Surface Methodology (RSM) is a method that optimizes output parameters according to the determined objective function by calculating the statistical relationship between input parameters and output parameters [15]. In this study, RSM was used to determine the relationship between 3D printing parameters and tensile strength and flexural strength output parameters. Optimization calculations were performed using Minitab 21.2 software. The "maximize" objective function was determined for both output variables as the optimization criterion (Figure 4).

Response	Goal	Lower	Target	Upper
Flexural Strength	Maximize	33.98	49.3	49.3
Tensile Strength	Maximize	12.35	17.98	17.98

Figure 4. RSM optimization parameters.

Analysis of variance (ANOVA) at the 95% confidence interval was applied on experimental test results to determine the contribution of 3D printing parameters on output parameters. When the results of the ANOVA analysis were examined, it was determined that the most effective 3D printing parameter on tensile strength was infill density

with an additive ratio of 63.09%. The infill pattern parameter, on the other hand, was calculated as the second most effective parameter on tensile strength with a contribution rate of 25.85% (Table 5). The R² value of the ANOVA analysis for the tensile strength parameter was calculated as 0.89. This value shows that the regression equations are highly successful in explaining the predicted tensile strength [16].

When the results of the ANOVA analysis performed for the flexural strength parameter are examined; it was determined that the most effective 3D printing parameter on flexural strength was the infill density parameter with an additive rate of 73.83%. The infill pattern parameter, on the other hand, was calculated as the second most effective parameter on flexural strength with a 16.42% contribution rate (Table 6). The R² value of the ANOVA analysis for flexural strength was calculated as 93.81. This value shows that the regression equations are highly successful in explaining the predicted flexural strength value.

Regression equations to be used to optimize the output variables were created in accordance with the objective function determined by RSM. The regression equations for the factors are presented in Equations 1-6, respectively, to predict the responses of tensile strength and

flexural strength. Since the infill pattern is a categorical variable, the constant coefficients of the regression equations change for different infill patterns. For this reason, the regression equations for the infill pattern were given separately. Using these regression equations, the predicted output parameters for the

experimental design parameters were calculated (Table 7). In addition, a graph showing the relationship between the predicted output values and the experimental test results is given in Figure 5.

Table 5. Results of ANOVA for tensile strength.

Source	DF	Seq SS	Contribution	Adj SS	Adj MS	F-Value	P-Value
Regression	4	24.3637	89.00%	24.3637	6.0909	8.09	0.034
Infill Density	1	17.2721	63.09%	17.2721	17.2721	22.93	0.009
Nozzle Temp	1	0.0148	0.05%	0.0148	0.0148	0.02	0.895
Infill Pattern	2	7.0769	25.85%	7.0769	3.5384	4.70	0.089
Error	4	3.0125	11.00%	3.0125	0.7531		
Total	8	27.3762	100.00%				
R²			89.00%				

Table 6. Results of ANOVA for flexural strength.

Source	DF	Seq SS	Contribution	Adj SS	Adj MS	F-Value	P-Value
Regression	4	215.642	93.81%	215.642	53.910	15.16	0.011
Infill Density	1	169.708	73.83%	169.708	169.708	47.74	0.002
Nozzle Temp	1	8.182	3.56%	8.182	8.182	2.30	0.204
Infill Pattern	2	37.751	16.42%	37.751	18.876	5.31	0.075
Error	4	14.220	6.19%	14.220	3.555		
Total	8	229.862	100.00%				
R²			93.81				

Infill Pattern	Regression Equations
Cubic	$11.09 + 0.0848 \text{ Infill Density} + 0.0039 \text{ Nozzle Temp}$ (1)
Lines	$Tensile\ Strength\ (MPa) = 10.67 + 0.0848 \text{ Infill Density} + 0.0039 \text{ Nozzle Temp}$ (2)
Triangles	$9.03 + 0.0848 \text{ Infill Density} + 0.0039 \text{ Nozzle Temp}$ (3)
Cubic	$10.7 + 0.2659 \text{ Infill Density} + 0.0928 \text{ Nozzle Temp}$ (4)
Lines	$Flexural\ Strength\ (MPa) = 13.8 + 0.2659 \text{ Infill Density} + 0.0928 \text{ Nozzle Temp}$ (5)
Triangles	$8.8 + 0.2659 \text{ Infill Density} + 0.0928 \text{ Nozzle Temp}$ (6)

Table 7. Experimental test results and predicted output values in accordance with the experimental design parameters.

	Infill Pattern	Infill Density	Nozzle Temp	Tensile Strength (MPa)	Predicted Tensile Strength (MPa)	Difference ratio (%)	Flexural Strength (MPa)	Predicted Flexural Strength (MPa)	Difference ratio (%)
1	Lines	20	190	13.53	13.22	-2.29	36.67	36.10	-1.55
2	Lines	40	205	14.30	14.72	2.94	43.94	45.02	2.46
3	Lines	60	215	16.76	16.63	-0.78	49.30	48.78	-1.05
4	Triangles	20	205	12.35	12.22	-1.05	34.98	34.46	-1.49
5	Triangles	40	215	12.78	12.47	-2.43	39.34	38.77	-1.45
6	Triangles	60	190	14.56	14.98	2.88	40.68	41.76	2.65
7	Cubic	20	215	13.24	13.66	3.17	33.98	35.06	3.18
8	Cubic	40	190	14.64	14.51	-0.89	39.14	38.62	-1.33
9	Cubic	60	205	17.98	17.67	-1.72	47.56	46.99	-1.20

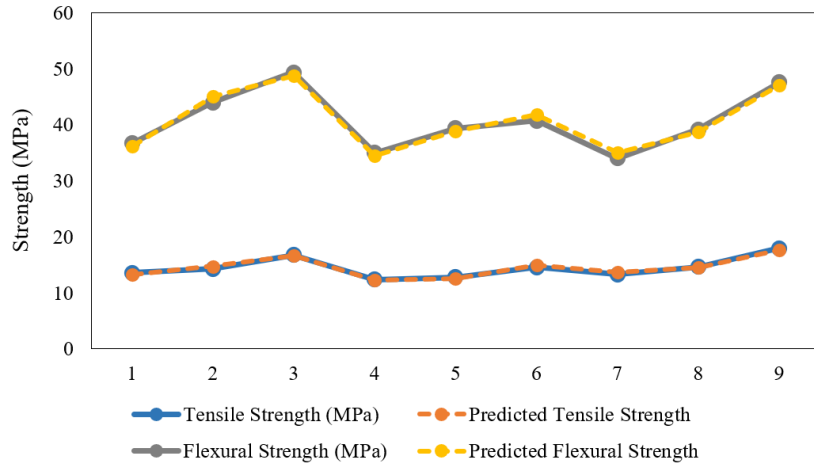


Figure 5. Comparison of experimental and predicted mechanical strength results.

Contour plots graphs are very useful for examining the relationship between a response variable and two factors. In a contour plot graph, the factor values that affect the response variable are shown on the x and y axes, and the values of the response variable are represented by shaded regions called contours [17]. A contour plots graphs is similar to a topographic map, using coordinates instead of longitude, latitude, and elevation. Contour plot graphs

obtained as a result of the optimization performed with the RSM method show the relationship between 3D printing parameters and output parameters. In the contour plot graphs were given in Figure 6, the relationship between two different 3D printing parameters and output variables is shown for the factor levels of the categorical 3D printing parameter infill pattern.

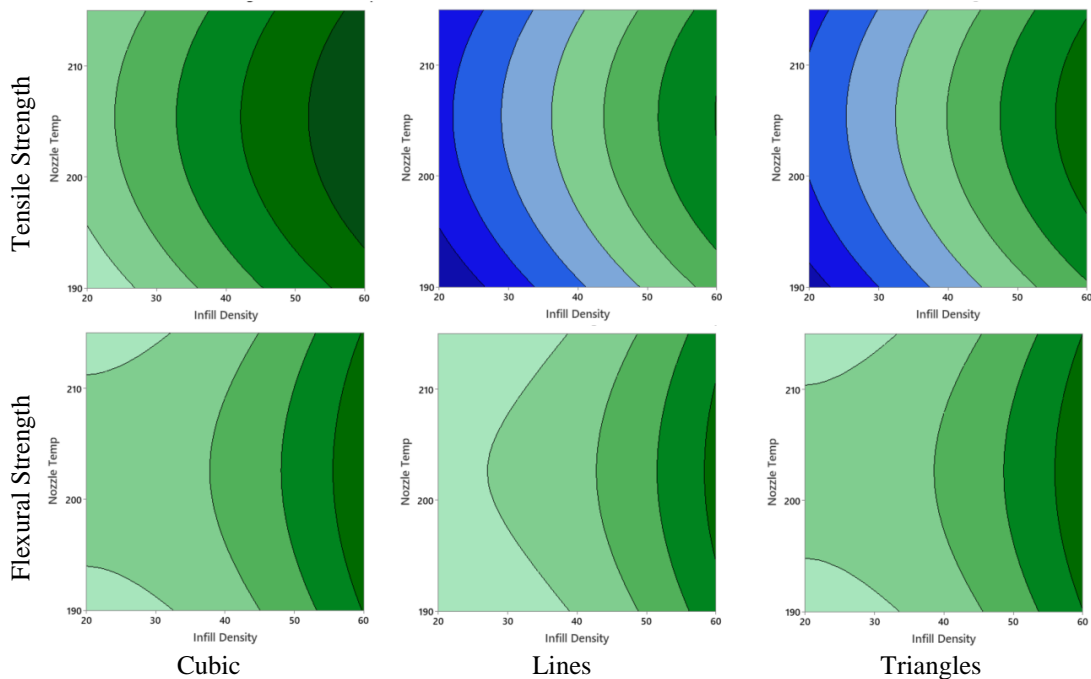


Figure 6. Contour Plot graphs of the relationship between printing parameters and mechanical strength criteria.

As a result of RSM optimization, necessary factor levels were calculated to maximize flexural strength and tensile strength values. The response optimizer graph shown in Figure 7 gives 3D printing parameters that can

optimize flexural strength and tensile strength values together. When the results were interpreted, it was determined that in order to maximize flexural strength and tensile strength values, infill density value should be 60%,

nozzle temperature value should be 202.62 C° and infill pattern type should be lines categorical parameters. The predicted flexural strength value to be obtained as a result of the selection of these parameters was calculated as 49.96 MPa and the predicted tensile strength value was calculated as 17.27 MPa.

The response optimizer graph also calculates the composite desirability. This value

represents the value of countervailing the objective function of the optimization and varies between 0 and 1 [18]. The composite desirability value calculated for this optimization is 0.93. This shows that the determined factor values are 93% successful in countervailing the objective function.

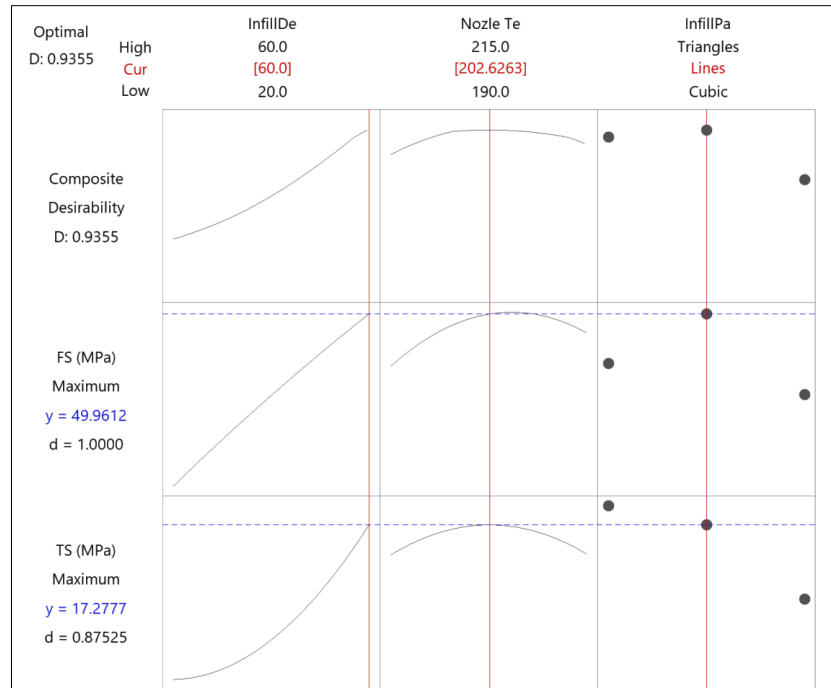


Figure 7. Response optimizer graph.

5. CONCLUSIONS

In this study, statistical analysis and optimization of 3D printing parameters affecting the mechanical properties of samples produced from Wood PLA material were performed using Response Surface Methodology. Regarding experimental tests and statistical analysis, the following conclusions can be drawn:

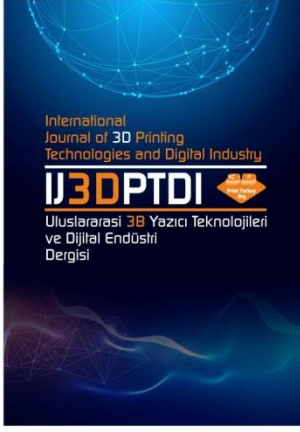
- Changes in 3D printing parameters are effective on the mechanical properties of the samples, and the mechanical properties can be improved by parameter optimization.
- ANOVA analysis results show that the most effective parameter among the tested parameter values in improving the mechanical properties of the samples produced from Wood PLA material is the infill density parameter. The second most effective parameter is the infill

pattern, and the effect of nozzle temperature on mechanical properties is too low to be considered.

- The low difference (less than 4%) between the experimental test results and the predicted test results confirms the accuracy and precision of the optimization procedure to determine the optimized combination of input variables.
- The optimal values of the input variables were determined so that the samples produced from Wood PLA material could provide maximum tensile strength and flexural strength.

REFERENCES

1. Dawood, A., Marti, B.M., Sauret-Jackson, V., Darwood, A.. "3D printing in dentistry", *British Dental Journal*, Vol. 219, Issue 11, Pages 521-529, 2015.
2. Atakok, G., Kam, M., Koc, H.B., "Tensile, three-point bending and impact strength of 3D printed parts using PLA and recycled PLA filaments: A statistical investigation", *Journal of Materials Research and Technology*, Vol. 18, Pages 1542-1554, 2022.
3. Bilgin, M., "Optimization of 3D Processing Parameters used FDM Method in the Production of ABS Based Samples", *International Journal of 3D Printing Technologies and Digital Industry*, Vol. 6, Issue 2, Pages 236-249, 2022.
4. Dey, A., Eagle, I.N.R., Yodo, N., "A review on filament materials for fused filament fabrication", *Journal of Manufacturing and Materials Processing*, Vol. 5, Issue 3, Pages 5-3, 2021.
5. Frunzaverde, D., Cojocar, V., Ciubotariu, C.R., Miclosina, C.O., Ardeljan, D.D., Ignat, E.F. Marginean, G., "The Influence of the Printing Temperature and the Filament Color on the Dimensional Accuracy, Tensile Strength, and Friction Performance of FFF-Printed PLA Specimens", *Polymers*, Vol. 14, Issue 10, Pages 1-23, 2022.
6. Günay, M., "Modeling of Tensile and Bending Strength for PLA Parts Produced By FDM", *International Journal of 3D Printing Technologies and Digital Industry*, Vol. 3, Issue 3, 204-211, 2019.
7. Vassallo, C., Rochman, A. and Refalo, P., "The impact of polymer selection and recycling on the sustainability of injection moulded parts", *Procedia CIRP*, Vol. 90, Pages 504-509, 2020.
8. Pakkanen, J., Manfredi, D., Minetola, P., Luliano, L., "About the use of recycled or biodegradable filaments for sustainability of 3D printing: State of the art and research opportunities", *Sustainable Design and Manufacturing*, Vol. 68, Pages 776-785, 2017.
9. Vink, E.T.H, Davies, S., "Kolstad JJ. The eco-profile for current Ingeo polylactide production" *Industrial Biotechnology*, Vol. 6, Issue 4, Pages 212-224, 2010.
10. Venendaal, R., Jørgensen, U., Foster, C.A., "European energy crops: A synthesis" *Biomass and Bioenergy*, Vol. 13, Issue 4, Pages 147-185, 1997.
11. Ayırlmış, N., Kariz, M., Kwon, J.H., Kitek, Kuzman, M., "Effect of printing layer thickness on water absorption and mechanical properties of 3D-printed wood/PLA composite materials" *International Journal of Advanced Manufacturing Technology*, Vol. 102, Issue 5-8, Pages 2195-2200, 2019.
12. Faludi, G., Dora, G., Renner, K., Móczó, J. Pukánszky, B. "Improving interfacial adhesion in pla/wood biocomposites" *Composites Science and Technology*, Vol. 89, Pages 77-82, 2013.
13. Cojocar, V., Frunzaverde, D., Miclosina, C.O., Marginean, G., "The Influence of the Process Parameters on the Mechanical Properties of PLA Specimens Produced by Fused Filament Fabrication—A Review" *Polymers*, Vol. 14, Issue 5, Pages 1-23, 2022.
14. Nalbant, M., Gökkaya, H., Sur, G., "Application of Taguchi method in the optimization of cutting parameters for surface roughness in turning", *Materials & Design*, Vol. 28, Issue 4, Pages 1379-1385, 2007.
15. Dean, A., Voss, D., Draguljić, D., "Response Surface Methodology", *Design and Analysis of Experiments*, Pages 565-614, Springer, Cham, New York City, 2017.
16. Akıncıoğlu, S., Gökkaya, H., Uygur, İ., "The effects of cryogenic-treated carbide tools on tool wear and surface roughness of turning of Hastelloy C22 based on Taguchi method" *The International Journal of Advanced Manufacturing Technology*, Vol. 82, Pages 303-314, 2016.
17. Minitab Ltd. Overview for Contour Plot. Minitab Ltd., <https://support.minitab.com/en-us/minitab/20/help-and-how-to/graphs/contour-plot/overview/>, December 20, 2022.
18. Myers, R.H., Montgomery, D.C., Anderson-Cook, C.M. "Response surface methodology: process and product optimization using designed experiments", Pages 369-375, John Wiley & Sons, Inc., New Jersey, 2016.



ULUSLARARASI 3B YAZICI TEKNOLOJİLERİ
VE DİJİTAL ENDÜSTRİ DERGİSİ

INTERNATIONAL JOURNAL OF 3D PRINTING
TECHNOLOGIES AND DIGITAL INDUSTRY

ISSN:2602-3350 (Online)

URL: <https://dergipark.org.tr/ij3dptdi>

NATURE-INSPIRED DESIGN IDEA GENERATION WITH GENERATIVE ADVERSARIAL NETWORKS

Yazarlar (Authors): Nurullah Yüksel , Hüseyin Rıza Börklü 



Bu makaleye şu şekilde atıfta bulunabilirsiniz (To cite to this article): Yüksel N., Börklü H. R., “Nature-Inspired Design Idea Generation With Generative Adversarial Networks” *Int. J. of 3D Printing Tech. Dig. Ind.*, 7(1): 47-54, (2023).

DOI: 10.46519/ij3dptdi.1239487

Araştırma Makale/ Research Article

Erişim Linki: (To link to this article): <https://dergipark.org.tr/en/pub/ij3dptdi/archive>

NATURE-INSPIRED DESIGN IDEA GENERATION WITH GENERATIVE ADVERSARIAL NETWORKS

Nurullah Yüksel^a , Hüseyin Rıza Börklü^a 

^aGazi University, Technology Faculty, Industrial Design Engineering Department, TURKEY

* Corresponding Author: nurullahyuksel@gazi.edu.tr

(Received: 19.01.2023; Revised: 21.03.2023; Accepted: 24.04.2023)

ABSTRACT

Generating new, creative, and innovative ideas in the early stages of the design process is crucial for developing better and original products. Human designers may become too attached to specific design ideas, preventing them from generating new concepts and achieving ideal designs. To come up with original design ideas, a designer needs to have a creative mind, as well as knowledge, experience, and talent. Verbal, written, and visual sources of inspiration can also be valuable for generating ideas and concepts. This study presents a visual integration model that uses a data-supported Artificial Intelligence (AI) method to generate creative design ideas. The proposed model is based on a generative adversarial network (GAN) that combines target object and biological object images to produce new creative product images inspired by nature. The model was successfully applied to an aircraft design problem and the resulting sketches inspired designers to generate new and creative design ideas and variants in a case study. It was seen that this approach improved the quality of the ideas produced and simplified the idea and concept generation process.

Keywords: Generative Adversarial Network, Biomimicry, Idea Generation.

1. INTRODUCTION

The design process involves several stages, including task clarification, conceptual design, embodiment design, and detailed design [1]. Conceptual design is a crucial stage in which the problem definition and functions, solution principles search, various design options creation, and evaluation and selection take place. Traditional and modern techniques can be used in this stage to arrive at the ideal concept. Traditional product and engineering design utilize scientific, intuitive, experiential, and creative knowledge and methods, while modern methods employ information technologies and Artificial Intelligence (AI) to shorten processes, increase creativity, obtain sensitive results, and reduce costs [2].

The term "Artificial Intelligence" (AI) refers to computer programs that simulate specific mental functions and behaviors observed in living beings. These programs are used in various disciplines for learning, understanding, prediction, problem-solving, suggestion, and decision-making [3]. Although the term AI was

first used in 1956, recent developments in computer technology, such as increased processing speed and memory, and easier access to data have led to significant advancements in AI over the last 15 years. AI techniques have also become increasingly prevalent in engineering and product design processes, allowing software to compare, evaluate, and estimate design options, generate innovative and creative ideas, and enhance creativity capabilities when integrated into various methods.

With the development of machine learning and deep learning methods, intelligent software can now support creative design activities such as ideation, concept creation, and inspiration [15, 17]. One such model is the use of generative adversarial networks (GANs) to generate original design ideas. GANs can combine biological and target objects to enhance designer creativity in idea generation [18]. The visual concept assembly method is a powerful tool that allows designers to create visually appealing designs and communicate

information effectively. The integration of data-driven artificial intelligence and visual concepts provides an advantage over previous studies as it has the potential to simplify complex information, create compelling designs, and emotionally connect with audiences. By combining visual and textual elements, designers can create catchy and effective designs that engage the audience emotionally.

2. RELATED STUDIES

Creating creative and original ideas is very important in the product design process. However, because of psychological inertia, it could only sometimes be feasible to develop original and unique ideas [4]. This situation can be an obstacle in the conceptual design process to focus on an idea and reach the ideal/perfect design [5, 6]. Employing verbal, textual, and visual sources of inspiration might help to get beyond this conceptual production roadblock. [7-9]. Recently, AI-powered software has also been used to create inspiration for designers. For example, Wang et al. [10] created a data-dependent idea network employing resources from the web and scientific publications. They, therefore, sought to lessen the workload associated with the literature review during the early design phase. Designers developed them as a source of inspiration by recognizing vitally significant conceptual words. This machine learning-based approach measures similarity (proximity) between concepts. Thus, creativity levels can be measured by detecting close-far relationships. A program named "The Combinator" was created by Han et al. [4] to combine concepts without obvious relationships. Semantic networks connect the data that web browsers collect and evaluate using tools for natural language processing. It is possible to develop inventive product ideas by combining many comparable ideas in new ways [11, 12]. "The Combinator" sparks creativity by merging text and visual data in various ways. It makes it easier for designers to explore the design space for solutions. Jin and Dong [13] analyzed the RedDot award-winning 998 products with the help of QSR NVivo data analysis software and created ten new design heuristics cards [14]. With text mining, machine learning, and natural language processing software, ontology-based approaches may identify links between concepts. Shi et al. Developed a design and engineering-oriented

unsupervised ontology network called WordNet [15, 17].

Bell and Bala [16] aimed to inspire designers by using Siamese CNN trained with real product photos. Chen et al. [18] tried to create inspiration for designers with two different models. The initial model is A semantic network developed using data mining and NLP approaches. Semantic networks are a useful tool for locating and displaying related concepts, Close and distant concept interactions facilitate the rapid and effortless generation of creative ideas. The visual concept combination model is another instrument for inspiration generation. The GANs model creates new pictures combining these two items after being trained using photos of a biological thing and a target object. Both biological object and target object attributes are present in the new photos. Thus, the designer's imagination might generate fresh thoughts and associations. The quantity and variety of training data are key factors in model performance.

Inspiration studies generally include machine learning, deep learning, and natural language processing algorithms. As these methods become widespread and access to data/information becomes easier may also shorten the market research and literature review process for new product design. In addition, semantic networks can be created with natural language processing algorithms. These networks can also generate new and creative ideas by revealing the relationship between design concepts. With various combinations of visual data, new connections of concepts can be discovered. In this study, designers were stimulated using the deep learning model GAN at the conceptual design stage. GAN by fusing with images of the goal and natural object, it seeks to generate new shapes in the designer's head. The validity of the method is demonstrated in an aircraft design problem.

2.1. Deep Learning

Machine learning is the general name of statistical AI methods that can make predictions and inferences based on data [19-21]. Unlike traditional programming, it does not need an exact algorithm to learn [22]. Instead, it detects patterns in the data set and uses these patterns to interpret future data. Just like the human learning mechanism, the ability to interpret

improves as the number of data increases. The increase in the amount of data, ease of access to big data, and increase in computer performance increase the success of machine learning prediction and identification. On the other hand, deep learning is a machine learning method with multi-layered neural networks. Some of these models are Autoencoder (AE), Convolutional Neural Networks (CNNs), Recurrent Neural Networks (RNNs), and Generative Adversarial Networks (GANs) [23]. Deep learning algorithms are very successful in image classification, object recognition, voice recognition, face recognition, and language translation. In the design field, topology optimization, generating design concepts, computational design, computer-aided engineering, and simulation tasks can be done with deep learning methods [24]. CNNs are used in 2D and 3D image recognition and classification tasks [22, 25]. On the other hand, GANs have provided a new perspective on deep learning. A single architecture contains two distinct networks known as the generator and discriminator [26]. Operations like producing previously unimagined pictures, boosting the resolution of already existent images, and text-to-image translation are all possible using generative contention networks [27]. In addition, operations such as converting sketches to colour images, coloring black and white photographs can be done with GANs [28].

Machine learning algorithms also have some downsides. For example, huge amounts of data are required to increase learning success. As the number of data increases, processing times may also increase [29]. Creating labeled datasets is cumbersome. It needs to be fully explained how machine learning algorithms achieve results. Although they have a high success rate, there is always the possibility of error [30].

3. VISUAL CONCEPT INTEGRATION

The cognitive process that provides the ability to develop new, original and useful ideas is called creativity. Creative ideas and concepts produced during the conceptual design phase significantly contribute to the final product's success [31, 32]. Although the conceptual design is a cognitive process, verbal, written, and visual sources of inspiration are generally used to produce creative ideas and concepts [7-9]. One of them is Arthur Koestler's "bisociation" model, which will create

inspiration in the designer's mind by bringing together different concepts [33]. A data-driven visual concept unification model was created to facilitate the creative thinking process based on this model. Two images that are not closely related can be combined to create a new image. This new image must carry both conceptual features in a certain proportion.

GAN, one of the current and promising deep learning methods, can contribute to the solution to this design problem. GAN; It is a new deep learning algorithm used to generate and edit data such as images, audio, video, and 3D models. A standard GANs architecture includes two deep neural networks: a generator and a discriminator. The generating network is trained with images made up of random pixels and creates new (fake) images. The discriminatory network tries to separate the produced images from the real ones. These two networks' educational purposes are to develop generation and discrimination skills, respectively [34]. Thus, new and realistic visuals can be produced. In the design process, computer-aided engineering/design tasks such as inspiration generation, idea/concept generation, and computational (computational) design topology optimization can be easily done with the help of GAN [35, 36, 37].

A dataset is created to develop a visual combination model by collecting biological and target object images. The normalization of the resulting images follows a series of data pre-processing. Finally, a noise distribution is used to generate new images. This study uses the Deep Convolutional Generative Adversarial Network (DCGAN) model to train generator and discriminator networks.

The overall approach for training a DCGAN model involves updating the discriminator and generator models in an alternating manner using their respective loss functions and optimizers. The loss functions determine how well the models are able to differentiate between real and fake data, while the optimizers modify the weights of the models to minimize the loss. The ultimate objective is to achieve an equilibrium where the generator produces realistic images that deceive the discriminator [38,39]. To begin training a DCGAN model, we first initialize the generator and discriminator models with random weights. Next, we define loss functions

to measure the performance of each model and optimizers to update the network weights based on the loss functions. Finally, we create a loop that iterates until convergence or a maximum number of iterations is reached [40]. The specific steps for training the DCGAN are shown in the following pseudo-code.

- Initialize generator G and discriminator D with random weights
 - $G = \text{Generator}()$
 - $D = \text{Discriminator}()$
- Define loss functions L_G and L_D for G and D respectively
 - $L_G = \dots$
 - $L_D = \dots$
- Define optimizers O_G and O_D for G and D respectively
 - $O_G = \dots$
 - $O_D = \dots$
- Loop until convergence or maximum number of iterations N for i in range(N):
 - Generate a batch of fake data x_{fake} using G
 - $x_{\text{fake}} = G.\text{generate}(\text{batch_size})$
 - Get a batch of real data x_{real} from training set X_{train}
 - $x_{\text{real}} = X_{\text{train}}.\text{sample}(\text{batch_size})$
 - Calculate discriminator outputs y_{fake} and y_{real} for x_{fake} and x_{real} respectively
 - $y_{\text{fake}} = D.\text{predict}(x_{\text{fake}})$
 - $y_{\text{real}} = D.\text{predict}(x_{\text{real}})$
 - Calculate discriminator loss $L_D(y_{\text{fake}}, y_{\text{real}})$
 - $d_{\text{loss}} = L_D(y_{\text{fake}}, y_{\text{real}})$
 - Update discriminator weights w_D using $O_D(d_{\text{loss}}, w_D)$
 - $w_D = O_D(d_{\text{loss}}, w_D)$
 - Generate another batch of fake data x_{fake} using G
 - $x_{\text{fake}} = G.\text{generate}(\text{batch_size})$
 - Calculate generator output y_{gen} using D
 - $y_{\text{gen}} = D.\text{predict}(x_{\text{fake}})$
 - Calculate generator loss $L_G(y_{\text{gen}})$
 - $g_{\text{loss}} = L_G(y_{\text{gen}})$
 - Update generator weights w_G using $O_G(g_{\text{loss}}, w_G)$
 - $w_G = O_G(g_{\text{loss}}, w_G)$
- Save or display the final generator model
 - $\text{save_or_display}(\text{generator})$

4. RESULTS

The proposed DCGAN architecture consists of a discriminator and a generator, as shown in Figure 1. Here, the generating network learns to generate new data using the Gaussian point distribution. First, a tensor of $n \times n \times m$ size is created by reshaping a Z-dimensional random pixel set. Then, a new $n \times n \times 1$ -dimensional tensor (fake image) is obtained with deconvolution layers. While the LeakyReLU activation functions transfer information from one de-convolution layer to the other, the tanh

activation function is used in the last layer. The number of layers, kernels (m), and tensor dimensions specified here are determined intuitively based on experience [18].

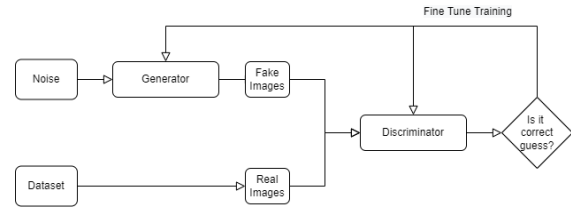


Figure 1. A schematic representation of the GAN model

On the other hand, the discriminative network, which includes a classical CNN architecture, is tried to distinguish between the images from the training set and the fake images. The $n \times n \times 1$ -dimensional image is converted into an $n \times n \times 64$ -dimensional tensor with convolution layers. Then, this tensor is flattened into a one-dimensional matrix. A fully connected neural network performs the classification (real/fake) process in the final stage. To increase the performance of these two networks, the DCGAN model is trained with the classical loss function shown in equation 1 [38]. Min and max mean minimizing Generator (G) loss and maximizing Discriminator (D) loss. Here x denotes the real images, and z denotes the noise input [27]. Adam optimization approach was used for model training. A learning rate of 0,0001 was preferred for training batch size 128. The training process is stopped after 1.000 cycles.

$$\min \max(D, G) = E_x [\log(D(x))] + E_z [\log(1 - D(G(z)))] \quad (1)$$

A case study was conducted to demonstrate the success of this deep learning model in generating design concepts. A visual combination model inspired designers in an aircraft form design problem. In this context, the great solutions in nature can be a source of inspiration in design. It is aimed to adapt the form features of sharks, which move quickly and can maneuver underwater, to the aircraft form design.

Initially, 2,964 aircraft (target object) and 3,013 sharks (biological object) images were combined into a dataset. These images, which have different image sizes, were converted to 128 x 128 x 3 sizes for model training. Some of

the normalized airplane and shark images collected are shown in Figure 2. The generative deep learning model was trained using these images with 1.000 cycles. This proposed model can automatically generate an unlimited number of biologically inspired images after training [24]. Although these images produced by the generative model do not have a clean/clear image, they include features such as color, shape, and texture of sharks and planes (Figure 3).



Figure 2. Some of example images taken from the dataset



Figure 3. Bio-inspired visuals generated by the generative model

The success of creating a new concept from the biologically inspired visuals created with the deep learning-supported visual combination model has been examined with an experimental study. In other words, it was examined to what extent these biologically inspired visuals, which include a combination of airplanes and sharks, would inspire designers during the design Process [17]. For this purpose, 2 final year students of the Department of Industrial Design Engineering were given these new images and asked to use them in creating new design concepts. Students were asked to first examine the images and choose the ones that evoked the design concept. Then, inspired by these selected images, they created new aircraft form variants. Thus, it was tried to develop new, original and creative ideas with the first images that were automatically created with the help of AI and the associations (inspirational sparks) created in the mind of the designer. The images generated by the generative model can offer unique potential ideas for different shark and airplane combinations. Some of the images produced by

this model and the concepts inspired by these images are shown in Figure 4.

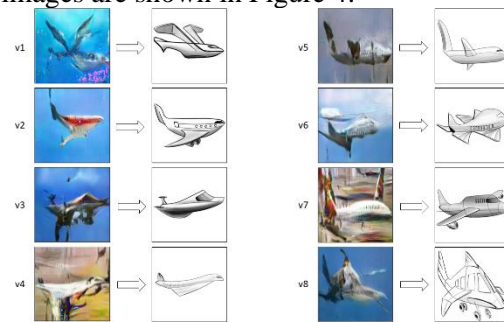


Figure 4. Visuals generated by the visual combination model (on the left side), and concept variants created by the designer (on the right side).

5. DISCUSSION

This study demonstrates the potential of DCGAN architecture to create nature-inspired design concepts [18]. By leveraging a dataset of aircraft and shark images, the generative deep learning model successfully generated a diverse range of visuals that combined the features of both entities. While not completely clean or clear, these images contain key features such as the color, shape and texture of sharks and planes [17].

An experimental study to evaluate the effect of these nature-inspired images on the design process has yielded promising results. When provided with the generated images, industrial design engineering students could select those that resonated with their design concepts and subsequently create novel aircraft form variants inspired by the visuals. This demonstrates the efficacy of the generative model in sparking creative associations in designers' minds and fostering innovative ideas' development [42].

Despite the generative model's success in producing bio-inspired images, the rendered images need improvement. Future research could focus on refining the DCGAN architecture or exploring alternative generative models to enhance the resolution and detail of the generated visuals. Additionally, expanding the dataset to include a wider variety of biological entities or exploring other design domains could further enrich the creative possibilities offered by the model. Furthermore, the experimental study in this research was limited to a small sample of design students. Future investigations could involve a more extensive and diverse group of participants to assess the generalizability of the findings and

better understand the impact of AI-generated visuals on various stages of the design process. This could lead to the development of more sophisticated generative models that cater to the specific needs of designers across different disciplines and design challenges.

6. CONCLUSION

This study presents a deep learning-based visual concept merging model to produce new and creative design concepts [41]. The GAN-based algorithm synthesized “airplane” and “shark” visuals to generate ideas for a design task. Since a clear relationship cannot be established between the concepts in the classical idea generation process, the concepts produced are limited in number and have similar features. This algorithm, on the other hand, can easily generate visual stimuli to generate ideas and increase the innovation level and quality of the ideas generated. Therefore, it can increase the designer’s potential to create new and creative design concepts. This model; outperforms the classical idea generation process in terms of innovation, number, and variety. However, more data is needed to comment on the functional properties of the generated concepts. The effect of the proposed model on function and aesthetics can be revealed by detailed evaluation. Therefore, more than this may be required for complex engineering design problems.

ACKNOWLEDGES

This article was presented orally at the 6th International Congress on 3D Printing (Additive Manufacturing) Technologies and Digital Industry 2022. Additionally, This study is supported by TUBITAK-1001 project (122E411).

REFERENCES

1. Börklü, H. R., Yüksel, N., Çavdar, K. and Sezer, H. K. “A practical application for machine design education”, *Journal of Advanced Mechanical Design, Systems, and Manufacturing*, Vol. 12, Issue 2, 2018.
2. Yüksel N. and Börklü, H. R., “Yapay Zekâ Destekli Kavramsal Tasarım: Tekerlekli Sandalye Tasarım Seçenekleri Değerlendirmede Bulanık Mantık Kullanımı,” *Gazi Journal of Engineering Sciences*, Vol. 7, Pages 309-316, 2021.
3. Huang, Y., Li, J. and Fu, J., "Review on Application of Artificial Intelligence in Civil

Engineering", *Computer Modeling in Engineering & Sciences*, Vol. 121, Issue 3, Pages 845-875, 2019. [Online]. Available: <http://www.techscience.com/CMES/v121n3/38073>

4. Han, J., Shi, F., Chen, L. and Childs, P. R. N. "The Combinator – a computer-based tool for creative idea generation based on a simulation approach", *Design Science*, Vol. 4, Pages e11, 2018.
5. Vasconcelos L. A. and Crilly, N., "Inspiration and fixation: Questions, methods, findings, and challenges," *Design Studies*, Vol. 42, Pages 1-32, 2016/01/01/ 2016.
6. Jansson, D. G. and Smith, S. M., "Design fixation", *Design Studies*, Vol. 12, Issue. 1, Pages 3-11, 1991.
7. Goldschmidt, G. and Smolkov, M., "Variances in the impact of visual stimuli on design problem solving performance", *Design Studies*, Vol. 27, Issue 5, Pages 549-569, 2006.
8. Goldschmidt, G. and Sever, A. L., "Inspiring design ideas with texts", *Design Studies*, Vol. 32, Issue 2, Pages 139-155, 2011.
9. Jiang, S. Luo, J., Ruiz-Pava, G., Hu, J. and Magee, C. L., "Deriving Design Feature Vectors for Patent Images Using Convolutional Neural Networks", *Journal of Mechanical Design*, Vol. 143, Issue 6, 2021.
10. Liu, Q., Wang, K., Li, Y. and Liu, Y., "Data-Driven Concept Network for Inspiring Designers' Idea Generation", *Journal of Computing and Information Science in Engineering*, Vol. 20, Issue 3, 2020.
11. Boden, M. A., “The Creative Mind: Myths and Mechanisms”, London, UK: Routledge, 2004.
12. Ward, T. B., and Kolomyts, Y., "Cognition and Creativity," in *The Cambridge Handbook of Creativity*, J. C. Kaufman and R. J. Sternberg Eds., Cambridge Handbooks in Psychology. Cambridge: Cambridge University Press, Pages 93-112, 2010.
13. Jin, X., and Dong, H., "New design heuristics in the digital era," *Proceedings of the Design Society: DESIGN Conference*, Vol. 1, Pages 607-616, 2020.
14. Yilmaz, S., Daly, S. R. Seifert, C. M. and Gonzalez, R., "Evidence-based design heuristics for idea generation", *Design Studies*, Vol. 46, Pages 95-124, 2016.
15. Shi, F., Chen, L., Han, J. and Childs, P. C., "A Data-Driven Text Mining and Semantic Network

- Analysis for Design Information Retrieval", *Journal of Mechanical Design*, Vol. 139, Issue 11, 2017.
16. Bell, S. and Bala, K., "Learning visual similarity for product design with convolutional neural networks", *ACM Transactions on Graphics*, Vol. 34, Pages 98:1-98:10, 2015.
 17. Yu, S., Dong, H., Wang, P., Wu, C., and Guo, Y., "Generative Creativity: Adversarial Learning for Bionic Design", Cham, 2019: Springer International Publishing, in *Artificial Neural Networks and Machine Learning – ICANN 2019: Image Processing*, Pages 525-536, 2019.
 18. Chen, L. et al., "An artificial intelligence based data-driven approach for design ideation", *Journal of Visual Communication and Image Representation*, Vol. 61, Pages. 10-22, 2019.
 19. Salehi, H. and Burgueño, R., "Emerging artificial intelligence methods in structural engineering," *Engineering Structures*, Vol. 171, Pages 170-189, 2018.
 20. Alpaydm, E., Dietterich, T., "Ed. *Introduction to Machine Learning*", 3 ed. London: MIT Press, 2014.
 21. Rebal, G., Ravi, A., and Churiwala, S., "An Introduction to Machine Learning", 1 ed. Cham: Springer, 2019.
 22. Houssein, E. H., Emam, M. M., Ali, A. A. and Suganthan, P. N. "Deep and machine learning techniques for medical imaging-based breast cancer: A comprehensive review", *Expert Systems with Applications*, Vol. 167, Page 114161, 2021.
 23. Gal, Y. "Uncertainty in Deep Learning", PhD thesis, Department of Engineering, University of Cambridge, Cambridge, 2016.
 24. Oh, S., Jung, Y., Kim, S., Lee, I., and Kang, N., "Deep generative design: Integration of topology optimization and generative models", *Journal of Mechanical Design*, Vol. 141, Issue 11, 2019.
 25. Singh, R. D., Mittal, A. and Bhatia, R. K., "3D convolutional neural network for object recognition: a review", *Multimedia Tools and Applications*, Vol. 78, Issue 12, Pages 15951-15995, 2019.
 26. Yi, X., Walia, E. and Babyn, P. "Generative adversarial network in medical imaging: A review", *Medical Image Analysis*, Vol. 58, Page 101552, 2019.
 27. Jin, L., Tan, F. and Jiang, S., "Generative Adversarial Network Technologies and Applications in Computer Vision", *Computational Intelligence and Neuroscience*, Vol. 2020, Page 1459107, 2020.
 28. Rahman, R., "Using Generative Adversarial Networks for Content Generation in Games", MSc thesis, Department of Computer Games Technology, Abertay University, Dundee, 2020.
 29. Ray, S. "A Quick Review of Machine Learning Algorithms," in *2019 International Conference on Machine Learning, Big Data, Cloud and Parallel Computing (COMITCon)*, 14-16 Feb. 2019. Pages 35-39,
 30. Brynjolfsson, E. and Mitchell, T., "What can machine learning do? Workforce implications", *Science*, Vol. 358, Issue 6370, Pages 1530, 2017.
 31. Mayda, M. and Börklü, H. "Yeni bir kavramsal tasarım işlem modeli", *TÜBAV Bilim Dergisi*, Vol. 1, Issue 1, Pages 13-25, 2008.
 32. Börklü, H. "Computer-aided conceptual design based on design catalogues", *Politeknik Dergisi*, Vol. 4, Issue 3, Pages. 77-78, 2001.
 33. Koestler, A., "The Act of Creation", Macmillan, Oxford, England, 1964.
 34. Yi, X., Walia, E., and Babyn, P., "Generative adversarial network in medical imaging: A review", *Medical Image Analysis*, Vol. 58, Page 101552, 2019.
 35. Jin, L., Tan F. and Jiang, S., "Generative Adversarial Network Technologies and Applications in Computer Vision", *Computational Intelligence and Neuroscience*, Vol. 2020, Pages 1459107, 2020.
 36. Rahman, R., "Using Generative Adversarial Networks for Content Generation in Games," Thesis, School of Design and Informatics, Abertay University, 2020.
 37. Oh, S., Jung, Y., Kim, S. Lee, I. and Kang, N. "Deep generative design: Integration of topology optimization and generative models," *Journal of Mechanical Design*, Vol. 141, Issue 11, 2019.
 38. Goodfellow, I., Pouget-Abadie, J., Mirza, M. Xu, B., Warde-Farley, D., Ozair, S., Courville, A. and Bengio, Y., "Generative Adversarial Nets," *Advances in Neural Information Processing Systems* 27, Montréal, Canada, Dec. 8–13, Pages 2672–2680, 2014.
 39. Creswell, A., White, T., Dumoulin, V., Arulkumaran, K., Sengupta, B. And Bharath, A. A. "Generative Adversarial Networks: An Overview,"

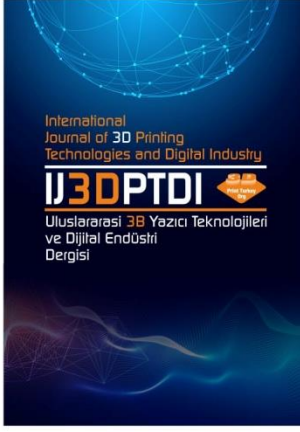
IEEE Signal Processing Magazine, Vol. 35, Issue 1, Pages 53-65, 2018.

40. Fang, W., Zhang, F., Sheng, V. S., and Ding, Y. "A method for improving CNN-based image recognition using DCGAN," Computers, Materials and Continua, Vol. 57, Issue 1, Pages 167-178, 2018.

41. Yüksel, N., Börklü, H. R., Sezer, H. K. and Canyurt, O. E. (2023). Review of artificial

intelligence applications in engineering design perspective. Engineering Applications of Artificial Intelligence, Vol. 118, Pages 105697, 2023.

42. Daly, S. R., Seifert, C. M., Yilmaz, S. and Gonzalez, R., "Comparing Ideation Techniques for Beginning Designers." ASME. Journal of Mechanical Design, Vol. 138, Issue 10, Pages 101108, 2016.




ULUSLARARASI 3B YAZICI TEKNOLOJİLERİ
VE DİJİTAL ENDÜSTRİ DERGİSİ

INTERNATIONAL JOURNAL OF 3D PRINTING
TECHNOLOGIES AND DIGITAL INDUSTRY

ISSN:2602-3350 (Online)

URL: <https://dergipark.org.tr/ij3dptdi>

CYBER ATTACKS FOR DATA BREACH AND POSSIBLE DEFENSE STRATEGIES IN INTERNET OF HEALTHCARE THINGS ECOSYSTEM

Yazarlar (Authors): Ahmet Ali Süzen* 

Bu makaleye şu şekilde atıfta bulunabilirsiniz (To cite to this article): Süzenş A. A.,
“Cyber Attacks For Data Breach and Possible Defense Strategies in Internet of Healthcare
Things Ecosystem” *Int. J. of 3D Printing Tech. Dig. Ind.*, 7(1): 55-63, (2023).

DOI: 10.46519/ij3dptdi.1240743

Araştırma Makale/ Research Article

Erişim Linki: (To link to this article): <https://dergipark.org.tr/en/pub/ij3dptdi/archive>

CYBER ATTACKS FOR DATA BREACH AND POSSIBLE DEFENSE STRATEGIES IN INTERNET OF HEALTHCARE THINGS ECOSYSTEM

Ahmet Ali Süzen^{a*} 

^{a*} Isparta University of Applied Sciences, Faculty of Technology, Department of Computer Engineering, TURKEY

Corresponding Author: ahmetsuzen@isparta.edu.tr

(Received: 23.01.2023; Revised: 02.02.2023; Accepted: 25.04.2023)

ABSTRACT

In this study, the IoT devices used for home patient care have been evaluated for the sources of data leaks and possible security measures that may be experienced in the process from the data owner to data storage stage. In order to identify possible risks and threats, 4 different target scenarios were created. These scenarios include home internet connection resources, data transfer, data storage, and access. 8 different attacks were applied to these possible scenarios where data leakage could occur. In addition, recently, blockchain applications and smart contract transmissions are preferred for data security. Among the attack scenarios, Short Address Attacks and Smart Contract Overflow are attack methodologies used for blockchain security. In particular, denial of service was encountered in all attacks on wireless. Configuration errors, wrong product selection, use of weak passwords, and default configurations in the IOT ecosystem seem to be the main sources of data leaks. As a result, the study includes possible attacker scenarios and possible vulnerabilities have been extracted within the scope of real scenarios. In addition, the measures to be taken against these vulnerabilities were evaluated and recommendations were given to take maximum security measures to prevent data leaks from within the IoT ecosystem.

Keywords: IoT, Healthcare, Cyber Security, Data Leak.

1. INTRODUCTION

Health services can be defined as the whole of services performed by experts to prevent, diagnose and treat diseases, injuries, physical and mental disorders experienced by people [1]. The improvement of health services is one of the most important factors that increase the comfort of human life [2]. The improvement and development of health services day by day are carried out simultaneously with technological developments. The reason for this is based on the need for critical data and instant intervention in healthcare services [3]. Almost all of the developed systems are used to store or process the health information of the patient followed by the internet infrastructure. These developments seem to form the basis of IoT systems in the field of health [4].

The widespread use and rapid growth of the IoT ecosystem in the field of health has enabled the

increase of sensitive data in digital environments today [5]. It is a great threat for sensitive and critical health data to fall into the hands of attackers. Recently, it has been discussed how the developed systems are secure in terms of personal data privacy and data leakage threats [6]. When the devices in the systems used are examined, it is seen that they do not apply sufficient security procedures. The widespread and rapid use of IoT devices reveals security vulnerabilities in these devices and creates question marks in data security, integrity, and confidentiality criteria in health data [7].

In this study, the resilience, risks, and possible importance of IoT devices and data transfer layers used in-home patient care services against possible cyber-attacks were evaluated. First, attack matrices for different layers were developed and attacks were carried out in test

environments. The risks and data leakage sources obtained as a result of these attacks were evaluated and information about possible precautions were given.

2. INTERNET OF HEALTH CARE THINGS ECOSYSTEM

Along with the use and advantages of IoT systems in Industry 4.0, it has also created a vision in the follow-up of people in need of care at home [8,9]. Increasing healthcare costs, rapid response, and instant monitoring make IoT devices preferred in-home patient care. Regular follow-up and monitoring of the person's health information also increases the determination of the experts to diagnose [10]. The increase in the amount of data collected has also paved the way for the spread of artificial intelligence systems. With this, the data has brought with it problems regarding the protection and privacy of this data. Transferring and storing data sources at home to experts via the internet brings security measures to the fore [11].

Recently, blockchain technology has been preferred for the protection of health data due to its security and integrity capabilities. When the literature studies are examined, it is seen that the storage of blockchain-based health data will minimize the possible risks. In this part of the study, studies in the literature that use blockchain technology for data privacy are examined. In their study, Adanur et al. used fog computing and blockchain technology together. A blockchain-based system has been proposed for the confidentiality and transmission of analysis and laboratory results obtained from individuals in the field of health. In this way, it is said that the concerns about the confidentiality and security of the transmitted data are avoided [12]. Rathee et al. proposed a model for the protection of data created with IoT technology in the field of health. The values obtained from the patients, the transfer of these values, the processes of guaranteeing the unchangeability of the drugs in the prescriptions created for treatment were provided with a model they named Healthchain Multimedia. The proposed model has been tested with Falsification Attraction and Wormhole attacks and successful results have been obtained [13]. Dwivedi et al. propose a distributed blockchain structure to eliminate the potential danger of privacy and security after medical data is obtained with IoT technology. Biological

values obtained from the patient through sensors are included in the blockchain system by wrapping them with symmetric encryption methods known as the ARX algorithm to the physician [14]. Griggs et al. proposed a secure system, the infrastructure of which was prepared with IoT technology and supported by smart contracts, which can perform real-time follow-up of patients. All processes of patient records can be easily followed without being manipulated. According to the status of the data received from the wireless body sensors, a notification will be sent to the relevant physician through solid contracts. In this way, correct and early intervention opportunities will be provided for the patient [15]. Srivastava et al. proposed a model that shows how the remote patient monitoring system established with the IoT infrastructure is secured with blockchain technology. The proposed model promises secure data communication over the network. Data is stored on the cloud with the ARX encryption method. Also, a double encryption scheme is used to make the symmetric key more secure over the network, and they use the Concept Diffie-Hellman Key Exchange Technique on the blockchain base, which protects the public key from an intruder [16].

The control of the systems in the house has been provided by electronic systems with the introduction of smart houses into our lives. Especially in the first systems, the controls that started with the command and sound were shaped by joint movements and autonomous systems [17]. Wired and wireless networks established in the house collect data and provide remote control. Together with IoT devices, interconnected devices can process their own data and make autonomous decisions [18]. The increase in systems and the production of data also attract the attention of attackers. Possible configuration errors, use of vulnerable systems or technologies increase data leaks [19]. In this study, it is aimed to identify threats and measures to ensure the security of health records within the IoT ecosystem. In this context, studies carried out for home patient care in order to create the attack matrix were examined and the technologies used were determined. As seen in Table 1, the technologies preferred by the studies related to the production, processing, monitoring, and storage of health data are listed. Thus, the

framework of the attack matrix to be used in our study was formed.

Table 1. Examination of home healthcare practices in terms of the technologies they use.

Study	Study Purpose	Technology
[20]	Early Diagnosis of Heart Attack	MMS and EGPRS
[21]	System of care and emergency medical assistance of chronic lung patients	WIFI and GPRS
[22]	Remote Follow-up of Patients in Coma	GSM and WIFI
[23]	Correct location of faults	Arduino Uno and GPS
[24]	To be able to store the basic health parameters of patients	Raspberry Pi 3, Sensors, BLE Adapter, GSM Module
[25]	Remote Follow-up of Patients in Coma	Arduino Uno, GSM Module, Cloud Storage
[26]	Continuous monitoring of patients	Arduino and WIFI
[27]	Storage of medical data	Zigbee and WBAN
[28]	Storage and monitoring of medical data	Intel Galileo Gen 2, XBEE S2 Sensor
[12]	Secure transmission of medical data	Sensors and Blockchain
[13]	Ensuring the security of medical data and prescriptions	Sensors, IoT, Blockchain
[14]	Keeping medical data encrypted on a distributed blockchain structure	Sensors, IoT, Blockchain
[15]	Real-time secure patient follow-up thanks to smart contracts	IoT, smart contracts, Blockchain
[16]	Developing a secure remote patient monitoring system	IoT, smart contracts, Blockchain

3. CYBER ATTACKS FOR DATA BREACH IN INTERNET OF HEALTHCARE THINGS ECOSYSTEM

IoT networks basically consist of 4 layers: devices, data, connection and users. In particular, the device and data layers face more attacks. In-network short-distance networks (Bluetooth, NFC, WIFI, Zigbee, etc.) are used in the creation of sensitive health records within the IoT ecosystem. After the data is collected in the network, it is transferred to the wide network with different protocols as shown in Table 2. During this process, it may face data leaks and system blockages. In this study, the risks and possible precautions against leaks of patient care data produced within the IoT ecosystem were evaluated. In the tests performed to detect the potential risks of the ecosystem, mock test data were used.

Table 2. Network technologies used in the transmission of health records in the IOT ecosystem

Communication	Standard
WIFI	IEEE 802.11 a/c/b/ d/g/n
WiMAX	IEEE 802.16
WSN	IEEE 802.15.4
LR-WPAN	IEEE 802.15.4 (ZigBee)
Mobile	2G-GSM, CDMA 3G-UMTS, CDMA2000 4G-LTE
LoRa WAN	LoRaWAN R1.0

3.1. Cyber Attacks for Data Breach in Internet of Healthcare Things Ecosystem

A practical attack scenario has been developed, as shown in Figure 1, in order to detect possible vulnerabilities in Call Control or SMS controlled systems where the internet connection in the house is via GPRS. HackRF Dongles are used for this. In the attack scenario, a temporary GSM line was purchased and tests were carried out with the open-source mobile communication called osmocon. The test phone was connected to the computer via USB-TTL and mobile communication was started via osmocon. Basically, it is aimed to capture the information and wireless traffic transmitted by GSM within the IoT ecosystem. The first goal of this attack is to capture the International Mobile Subscriber Identity (IMSI). Used to receive IMSI data, IMSI Catcher acts as a base station and allows the target to connect to itself. The following tools are preferred for attacking IoT networks using GSM-based communication. Application tests were carried out on the Kali operating system.

- Wireshark
- HackRF
- kalibrate
- gr-gsm

Wireshark is an open source software that enables the examination and monitoring of the network data it is connected to from the interface. Network packets can be monitored or recorded instantly with Wireshark. Detailed analysis of the recorded network data can be performed later.

The system created as a result of the hardware and software requirements given above for obtaining GPRS and SMS data is called IMSI-Catcher. It stands midway between the station and the telephone, as shown in Figure 1.

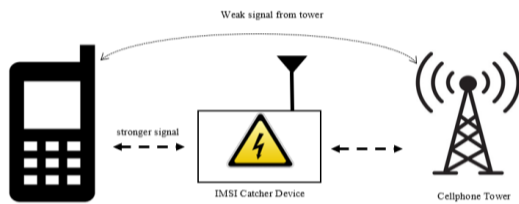


Figure 1. Example attack scenario diagram.

After the applications are installed on the system, first of all, the frequency band ranges should be known in order to monitor the GSM traffic (Turkey: 900 MHz -1800 MHz). When the scenario runs, base stations close to the test environment are detected. Then, GSM traffic was captured with Wireshark. The following filtering is used to see the data of GSMTAP protocol in the Wireshark packet monitor.

```
wireshark -k -f udp -Y gsmtap -i lo
```

The airprobe_rtlsdr_capture tool was used to capture the SMS traffic. The tool is used to capture SMS data in traffic with the following parameter.

```
airprobe_SMS.py -c capture.pcap -s 1000000 -f 949200000 -m SDCCH8 -t 2 -e 1 -k 0x0E,0x10,0xEA,0xF3,0x02,0x99,0xF2,0xC4
```

Here -e 1 specifies the A5/1 algorithm and -k specifies 0x0E,0x10,0xEA,0xF3,0x02,0x99,0xF2,0xC4 Kc. It is the key used to wirelessly encrypt the KC telephone network.

GPRS Tunneling Protocol (GTP) traffic was monitored for possible threats in the transmission of health data via GPRS within the

IOT ecosystem, as seen in Figure 2. There are two different types of traffic in the scenario, GTP Policy Out and GTP Policy In. By examining the GTP traffic, it has been seen that it is possible to access the data of the GPRS flow.

- GTP Policy Out is traffic from client to server
- GTP Policy In is the traffic from the server to the client

```
> Frame 8: 138 bytes on wire (1104 bits), 138 bytes captured (1104 bits)
> Ethernet II, Src: Vmware_da:d1:de (00:0c:29:da:d1:de), Dst: Vmware_e3:c6:4d (00:0c:29:e3:c6:4d)
> Internet Protocol Version 4, Src: 192.168.40.178, Dst: 192.168.40.179
> User Datagram Protocol, Src Port: 2152, Dst Port: 2152
v GPRS Tunneling Protocol
  > Flags: 0x32
  Message Type: T-PDU (0xff)
  Length: 88
  TEID: 0x00000001 (1)
  Sequence number: 0x267c (9852)
  T-PDU Data: 45000054067700004001982ec0a828b2ca0b289e00017e6...
> Internet Protocol Version 4, Src: 192.168.40.178, Dst: 202.11.40.158
> Internet Control Message Protocol
```

Figure 2. Wireshark monitoring of GPRS traffic.

3.2. Attack for Wireless Networks Controlled IOT Ecosystems

The use of wireless networks in smart home systems and IOT ecosystem is carried out with many technologies as shown in Table 1. WIFI offers an average data transfer rate of 1 Mb/s – 6.75 Gb/s and WiMAX offers a data transfer rate between 1 Mb/s – 1 Gb/s. Recently, especially the large number and size of data has brought the widespread use of WIFI and WiMAX to the fore. In the scheme shown in Figure 3, first of all, 8 processes were created on the attack computer and DDOS attacks were made on the detected wireless networks. In the second stage, it has been determined whether it is possible to access the health records and sensitive data in the IOT network with the attack types given below.

- Access Control Attacks
- Confidentiality Attacks
- Integrity Attacks
- Authentication Attacks

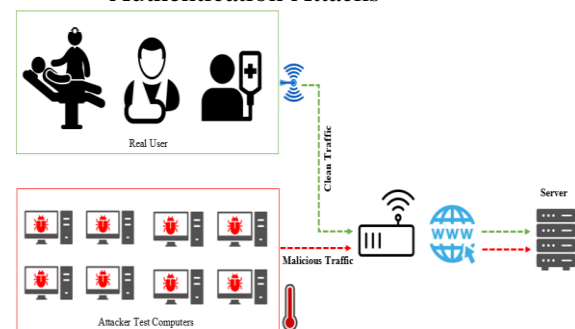


Figure 3. Anomaly diagram for WIFI and WIMAX networks.

First, the attacking computer was put in the USB WIFI adapter monitoring mode, and the WIFI and WIMAX network devices around were listed as shown in Figure 4. For attack targets, wireless network signals within 5 km of average open area were scanned. As a result of the scanning, the ESSIDs of the sample IoT networks were determined.

BSSID	PWR	Beacons	#Data, #s	CH	MB	ENC	CIPHER	AUTH	ESSID
F8:64:8B:8B:05:1E5	-86	2	0	6	278	WPA2	CCMP	PSK	TurkTelekom_270337_2_4GHz
9C:9D:7E:2D:F1:52	-82	3	0	6	138	WPA2	CCMP	PSK	TurkTelekom_TPP494_2_4GHz
2A:8F:23:08:03:01	-70	3	0	11	135	WPA2	CCMP	PSK	<length: 8>
08:32:34:97:77:28	-84	2	0	11	278	WPA2	CCMP	PSK	HZZRREY_2
84:BF:6D:C5:6B:05	-64	5	3	2	138	WPA2	CCMP	PSK	ABEInternet
1C:7F:2C:69:6B:FB	-78	8	0	1	278	WPA2	CCMP	PSK	ARAS_PALACE
5C:63:BF:66:2B:28	-78	19	0	9	138	WPA2	CCMP	PSK	TurkTelekom_T5402
5C:63:BF:66:2B:28	-82	15	0	8	138	WPA2	CCMP	PSK	TurkTelekom_T3567
5C:63:BF:19:1C4:62	-65	7	0	10	138	WPA2	CCMP	PSK	TurkTelekom_T52FE

Figure 4. Monitoring Mode Scanner.

Basically, in the IoT ecosystem with WIFI and WIMAX networks, firstly, the selected user is dropped from the network by sending deauth packets as seen in Figure 5, in order to determine the passwords of the devices belonging to the users. When the active device wants to connect to the network again, its packets are captured and saved as a cap file. Thus, in the registered packets, sensitive data and network password information are searched by performing packet analysis with Wireshark, as in Figure 6.

```
13:34:01 Sending 64 directed DeAuth (code 7), STMAC: [28:16:AD:AB:5E:BE] [ 22/68 ACKs]
13:34:01 Sending 64 directed DeAuth (code 7), STMAC: [28:16:AD:AB:5E:BE] [ 0/50 ACKs]
13:34:02 Sending 64 directed DeAuth (code 7), STMAC: [28:16:AD:AB:5E:BE] [ 0/47 ACKs]
13:34:03 Sending 64 directed DeAuth (code 7), STMAC: [28:16:AD:AB:5E:BE] [37/54 ACKs]
```

Figure 5. Sending deauth packets.

Time	Source	Protocol	Destination	Length	Info
1 0.000000	ZyveICom c5:00:02	802.11	02:64:8B:70:1C:05	1328	[0] Data, Seq=811, Pkts=, Flags=p...F
2 0.002432	ZyveICom c5:00:02	802.11	02:64:8B:70:1C:05	1328	[0] Data, Seq=812, Pkts=, Flags=p...F
3 0.002450	ZyveICom c5:00:02	802.11	02:64:8B:70:1C:05	240	[0] Data, Seq=813, Pkts=, Flags=p...F
4 0.005374	IntelCor 44:7F:CE	[802.11]	ZyveICom c5:00:05 (RA)	20	802.11 Block Ack, Flags=.....
5 0.006750	ZyveICom c5:00:02	802.11	02:64:8B:70:1C:05	1328	[0] Data, Seq=815, Pkts=, Flags=p...F
6 0.008226	ZyveICom c5:00:02	802.11	02:64:8B:70:1C:05	1328	[0] Data, Seq=816, Pkts=, Flags=p...F
7 0.009526	ZyveICom c5:00:02	802.11	02:64:8B:70:1C:05	1328	[0] Data, Seq=817, Pkts=, Flags=p...F
8 0.009414	ZyveICom c5:00:02	802.11	02:64:8B:70:1C:05	1328	[0] Data, Seq=818, Pkts=, Flags=p...F
9 0.009414	ZyveICom c5:00:02	802.11	02:64:8B:70:1C:05	1328	[0] Data, Seq=819, Pkts=, Flags=p...F
10 0.009700	ZyveICom c5:00:02	802.11	02:64:8B:70:1C:05	1328	[0] Data, Seq=820, Pkts=, Flags=p...F
11 0.001182	IntelCor 44:7F:CE	74:48:3e:4d:7f:ce (RA)	10	Clear-to-send, Flags=.....	
12 0.001182	IntelCor 44:7F:CE	74:48:3e:4d:7f:ce (RA)	10	Acknowledgment, Flags=.....	
13 1.004000	ZyveICom c5:00:02	802.11	02:64:8B:70:1C:05	1328	[0] Data, Seq=821, Pkts=, Flags=p...F

Figure 6. Examination of packets with Wireshark.

The network password HASH value obtained after the packet analysis of the target IoT devices should be estimated. As shown in Figure 7, the hash matching process has been completed by uploading the wordlist with the software named aircrack and hashcat.

```
[00:00:21] 138944/9822768 keys tested (6412.37 k/s)
Time left: 25 minutes, 10 seconds 1.41%
Current passphrase: may201986
Master Key : AB AE 0D D6 C1 86 88 D4 A4 05 82 F1 6E C8 75 68
            E9 69 D8 38 B7 C5 F2 75 DE CE 98 55 3D 0B 81 15
Transient Key : 25 29 6F 82 BB^72 72 80 C7 11 CC CA A5 55 1F 2B
              F4 32 C4 DA BA 8C 30 45 93 8D B3 BF AA 26 0B C7
              0B 12 52 EB 00 C2 95 0F 99 A2 1C 92 37 B5 DE A8
              2A 2D 2B 32 34 A6 D8 04 5C 77 FE A4 46 0F 13 9A
EAPOL HMAC : 40 32 32 CE 9A 0F 2A 30 17 BD 38 D4 78 60 C1 CD
```

Figure 7. Brute force attack on IOT networks.

Hashcat is an attack software with GPU and CPU support that enables the detection of open data from the obtained hash data. In decoding the hash data obtained from WIFI and WIMAX networks, a wordlist consisting of seven million data was used by using hashcat GPU support.

An Evil Twin attack was carried out by simultaneously creating a fake wireless network while IoT devices were exposed to the death attack. In the IoT ecosystem, due to the communication network and its protocols between devices, the device automatically connects to the network device that signals closer to it. However, since they both have the same name, the user cannot notice it. Thus, it is aimed to connect IoT devices to the fake network and collect data packets. In addition, a Man in the Middle – MITM attack was carried out on IoT devices whose passwords were detected. With this attack, tests of accessing the data flow of IoT devices, manipulating and blocking the data were carried out.

3.3. Attack For Blockchain-based IOT Ecosystems

Although the blockchain was first mentioned with cryptocurrencies, it has recently been widely used to ensure data security. In particular, ensuring the security and integrity of sensitive data is carried out with blockchain applications. It provides its own security with the mechanisms used in the blockchain structure. However, although it is not possible to provide 100% security, there are possible attacks and risks in the blockchain [29]. Due to its blockchain structure, it can face the following attacks and risks [30].

- 51% Attack
- Long-Range Attack
- P+ Epsilon Attack
- Brute Force Attack
- Distributed Denial-of-Service (DDoS)
- Border Gateway Protocol Hijacking (BGP)

- Balance Attack
- Mining Pool Attacks
- Sybil Attack

The attacks carried out within the scope of the study were carried out in the transfer of the health records shown in Figure 8, which we previously developed, to the expert with the smart contract and their storage in the blockchain [31]. In the case study, data storage is stored in BlockChainDB and Mongoddb. C# programming language interface software has been developed to monitor the collected data.

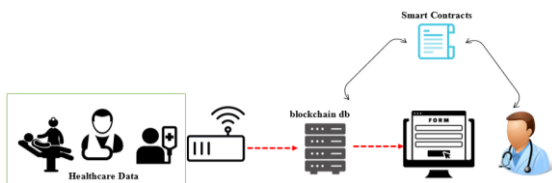


Figure 8. Blockchain-based attack testnet.

First, the Smart Contract Overflow and Underflow method was tested for accessing the data stored in the blockchain. With this method, it occurs in transactions that accept unauthorized health data or value. A smart contract overflow basically occurs when more than the maximum value is supplied. Commonly smart contracts are written in Solidity, which can handle numbers up to 256 bits, where an increment of 1 causes overflow.

As the second attack, a short address attack was made. A Short Address Attack is basically similar to a SQL injection error and occurs when an insufficient data flow is detected. This vulnerability is an input validation error and is mostly exposed by the sender due to weak transaction generation code. Finally, a DDOS attack was applied to test the continuity of communication in all possible scenarios.

3.4. Potential Post-Attack Threat and Risks

The results obtained as a result of attacks on the test environment where devices are controlled by call, sms and GPRS in the IoT ecosystem are given in Table 3. As a result of four different attacks, it was observed that GSM operator headers, call and SMS information were accessed, especially in attacks with IMSI Catcher hardware. In GSM-based systems, it has been determined that there are cases where access to API or database is performed in the target system and session verification is not used. As a result, it is possible to send parameters to IoT devices or to monitor and

copy incoming sensitive data. The attacks on the target system and the results show that the security structures in GSM-based systems are insufficient.

Table 3. Attack evaluation of GSM, SMS and GPRS based IoT systems.

Attack Type	Result
IMSI Catcher	Data Leak - MCC (Mobile Country Code), MNC (Mobile Network Code) and MSIN (Mobile Subscriber Identification Number)
GSMTAP	Data Leak (Call Parameters)
GTP	Data Leak (SMS DATA)
DDOS	Success (service is blocked)

Five different attack modeling has been carried out on WIFI and WIMAX networks, which are more commonly preferred in the communication of IoT devices. Incomplete configuration of IoT devices and edge devices in the data collection and transfer process is one of the most common mistakes. Table 4 shows the attacks on target systems and their results. Although the passwords of the default wireless networks meet the strong password criteria, it is seen that modem, access point (AP), or switch interface configurations are not made. With the MITM attack, access to the data produced by IoT devices is provided. In addition, it has been determined that devices can be dropped from the network with a deauth attack and redirected to fake connections with an Evil Twin attack. In cases where continuous data flow is made and critical health data is monitored instantly, data flow can be interrupted by DDOS attacks. This is expected to result in life-threatening risks.

Table 4. Attack evaluation of WIFI and WIMAX-based IoT systems

Attack Type	Result	Password Detection
Brute Force (aircrack)	-	Fail
Hashcat	-	Yes
MITM	Data Leak	-
Evil Twin	Data Leak	Yes
DDOS	Success (service is blocked)	-

In order to ensure data security, data is stored in the blockchain structure in wired and wireless communication solutions and transferred to experts with smart contracts. Data from within

the IoT ecosystem is mostly transferred to the wide network with web services. For this reason, possible risks in WIFI and WIMAX networks are predicted to be a threat within blockchain-based systems. Three different attacks were applied to the test blockchain network as shown in Table 5. It is seen that the probability of data leakage in blockchain-based systems is very low. However, in these attacks, data access problems are experienced during the transfer of health data to specialists.

Table 5. Attack evaluation of blockchain IoT systems.

Attack Type	Result	Password Detection
Brute Force (aircrack)	-	Fail
Hashcat	-	Yes
MITM	Data Leak	-
Evil Twin	Data Leak	Yes
DDOS	Success (service is blocked)	-

In order to ensure data security, data is stored in the blockchain structure in wired and wireless communication solutions and transferred to experts with smart contracts. Data from within the IoT ecosystem is mostly transferred to the wide network with web services. For this reason, possible risks in WIFI and WIMAX networks are predicted to be a threat within blockchain-based systems. Three different attacks were applied to the test blockchain network as shown in Table 5. It is seen that the probability of data leakage in blockchain-based systems is very low. However, in these attacks, data access problems are experienced during the transfer of health data to specialists.

4. MEASURES TO PROTECT SENSITIVE HEALT RECORDS IN THE IOT ECOSYSTEM

The process of collecting, transferring, and monitoring sensitive health data in the IoT ecosystem needs to be carefully structured. Many of the possible risks and threats appear to be caused by configuration errors. Data leaks and risks have been determined as a result of different attack types and aggressive behavior in test environments. Basically, security requirements must include confidentiality, integrity, source verification, data up-to-date, service integrity, and key management. In the light of the data obtained, the precautions to be taken for the protection and secure

communication of sensitive health records produced within the framework of IoT home patient care services are listed as follows.

- In general, using a Virtual Private Network (VPN) to prevent web traffic from being monitored by attackers helps prevent MITM attacks.
- Data flow of IoT sensors configured in the house is provided by WIFI. Here, the wireless passwords of the modem and AP devices must be at least 10 characters long and a combination of letters-numbers-special characters. In addition, the default configuration of the device interface login screens needs to be adjusted individually.
- Update and security patches of devices used in IoT networks should be checked periodically.
- Firewall should be preferred in order to instantly monitor wired and wireless network traffic and detect possible anomalies.
- IoT devices must be registered to the network with MAC authentication.
- A secure data transfer environment should be created by using strong encryption in Bluetooth, Zigbee, Wi-Fi, GPRS, LoRa, NFC and similar IoT protocols.
- Network capacity and bandwidth should be limited to the lowest value that will be sufficient for the IoT system to operate.
- The daily internet used in the home and the internet networks used by IoT devices should be partitioned.
- IoT protocols such as Message Queue Telemetry Transport (MQTT), Data Distribution Service (DDS), Extensible Messaging and Presence Protocol (XMPP), Advanced Message Queuing Protocol (RestFull HTTP), or Constrained Application Protocol (CoAP) should be preferred.

5. CONCLUSION

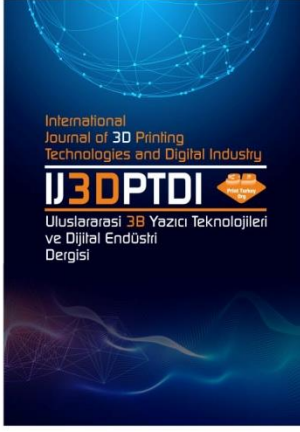
Collecting and processing sensitive health records with IoT devices has become a life abandonment. In this and beyond, low-complexity and high-reliability solutions should be configured for IoT networks. In this study, the current risks, potential threats, and security measures of the IoT ecosystem used in home patient care processes are evaluated. First of all, IoT studies related to patient care were examined and the IoT technologies used were

determined. An attack matrix was created and test attacks were made with the findings obtained. The risks, threats, and possible precautions obtained after the attacks are reported. Today, it is seen that the basis of threats is wrong and incomplete configurations. While designing security mechanisms in the IoT ecosystem, each IoT device layer should be arranged with security requirements in mind. Methods that are resistant to denial of service and eavesdropping attacks should be developed at the physical and media access layers.

REFERENCES

1. Thimbleby, H., "Technology and the future of healthcare", *Journal of public health research*, Vol. 2, Issue 3, Pages 160-167, 2013.
2. Bhavnani, S. P., Narula, J., & Sengupta, P. P., "Mobile technology and the digitization of healthcare", *European heart journal*, Vol. 37, Issue 18, Pages 1428-1438, 2016.
3. Strudwick, G., "Predicting nurses' use of healthcare technology using the technology acceptance model: an integrative review" *CIN: Computers, Informatics, Nursing*, Vol. 33, Issue 5, Pages 189-198, 2015.
4. Farahani, B., Firouzi, F., & Chakrabarty, K., "Healthcare iot", In *Intelligent internet of things*, Pages 515-545, Springer, 2020.
5. Zakaria, H., Bakar, N. A. A., Hassan, N. H., & Yaacob, S., "IoT security risk management model for secured practice in healthcare environment", *Procedia Computer Science*, Vol. 161, Pages 1241-1248, 2019.
6. Chacko, A., & Hayajneh, T., "Security and privacy issues with IoT in healthcare", *EAI Endorsed Transactions on Pervasive Health and Technology*, Vol. 4, Issue 14, Pages 1-7, 2018.
7. Gopalan, S. S., Raza, A., & Almobaideen, W., "IoT Security in Healthcare using AI: A Survey", In *2020 International Conference on Communications, Signal Processing, and their Applications (ICCSPA)*, Pages 1-6, IEEE, 2021.
8. Nausheen, F., & Begum, S. H., "Healthcare IoT: benefits, vulnerabilities and solutions", In *2018 2nd International Conference on Inventive Systems and Control (ICISC)*, Pages 517-522, IEEE, 2018.
9. Gürfidan, R., Ersoy, M., "A new approach with blockchain based for safe communication in IoT ecosystem", *J. of Data, Inf. and Manag.* Vol. 4, Pages 49–56, 2022.
10. Moosavi, S. R., Nigussie, E., Levorato, M., Virtanen, S., & Isoaho, J., "Performance analysis of end-to-end security schemes in healthcare IoT", *Procedia computer science*, Vol. 130, Pages 432-439, 2018.
11. Pradhan, B., Bhattacharyya, S., & Pal, K., "IoT-based applications in healthcare devices", *Journal of healthcare engineering*, Vol. 2021, Pages 1-18, 2021.
12. Adanur, B., Bakir-Güngör, B., & Soran, A., "Blockchain-based fog computing applications in healthcare", In *2020 28th Signal processing and communications applications conference (SIU)*, Pages 1-4, IEEE, 2020.
13. Rathee, G., Sharma, A., Saini, H., Kumar, R., & Iqbal, R., "A hybrid framework for multimedia data processing in IoT-healthcare using blockchain technology", *Multimedia Tools and Applications*, Vol. 79, Issue 15, Pages 9711-9733, 2020.
14. Dwivedi, A. D., Srivastava, G., Dhar, S., & Singh, R., "A decentralized privacy-preserving healthcare blockchain for IoT", *Sensors*, Vol. 19, Issue 2, Pages 326, 2019.
15. Griggs, K. N., Ossipova, O., Kohlios, C. P., Baccarini, A. N., Howson, E. A., & Hayajneh, T., "Healthcare blockchain system using smart contracts for secure automated remote patient monitoring", *Journal of medical systems*, Vol. 42, Issue 7, Pages 1-7, 2018.
16. Srivastava, G., Crichigno, J., & Dhar, S., "A light and secure healthcare blockchain for iot medical devices", In *2019 IEEE Canadian conference of electrical and computer engineering (CCECE)*, Pages 1-5. IEEE, 2019.
17. Jie, Y., Pei, J. Y., Jun, L., Yun, G., & Wei, X., "Smart home system based on IOT technologies", In *2013 International conference on computational and information sciences*, Pages 1789-1791, IEEE, 2013.
18. Alaa, M., Zaidan, A. A., Zaidan, B. B., Talal, M., & Kiah, M. L. M., "A review of smart home applications based on Internet of Things", *Journal of Network and Computer Applications*, Vol. 97, Pages 48-65, 2017.
19. Santoso, F. K., & Vun, N. C., "Securing IoT for smart home system", In *2015 international*

- symposium on consumer electronics (ISCE), Pages 1-2, IEEE, 2015.
20. Fidan, U., Aktürk, T. B., “Application of GPRS Based 12 Derivation EKG Telemonitoring System For 112 Emergency Service”, Engineering Sciences, Vol. 5, Issue 1, Pages 79-87, 2010.
 21. Işık, A. H., “Development of Intelligent Care and Emergency Medical Assistance System for the Follow-up of Chronic Lung Patients with Mobile Communication Technology”. Pages 107. Gazi University, Informatics Institute, Turkey, 2012.
 22. Fatih, S. M., Muneer, A., Mungur, D., & Badawi, A., “Integrated health monitoring system using GSM and IoT”, In 2018 International Conference on Smart Computing and Electronic Enterprise (ICSCEE), Pages 1-7, IEEE, 2018.
 23. Kanani, P., & Padole, M., “Real-time Location Tracker for Critical Health Patient using Arduino, GPS Neo6m and GSM Sim800L in Health Care”, In 2020 4th International Conference on Intelligent Computing and Control Systems (ICICCS), Pages 242-249, IEEE, 2020.
 24. Swaroop, K. N., Chandu, K., Gorrepotu, R., & Deb, S., “A health monitoring system for vital signs using IoT. Internet of Things”, Vol. 5, Pages 116-129, 2019.
 25. Tamilselvi, V., Sribalaji, S., Vigneshwaran, P., Vinu, P., & GeethaRamani, J., “IoT based health monitoring system”, In 2020 6th International conference on advanced computing and communication systems (ICACCS), Pages 386-389, IEEE, 2020.
 26. Yeri, V., & Shubhangi, D. C., “IoT based real time health monitoring”, In 2020 Second International Conference on Inventive Research in Computing Applications (ICIRCA), Pages 980-984, IEEE, 2020.
 27. Akkaş, M. A., Sokullu, R., & Cetin, H. E., “Healthcare and patient monitoring using IoT”, Internet of Things, Vol. 11, Issue 100173, Pages 1-12, 2020.
 28. Kodali, R. K., Swamy, G., & Lakshmi, B., “An implementation of IoT for healthcare”, In 2015 IEEE Recent Advances in Intelligent Computational Systems (RAICS), Pages 411-416, IEEE, 2015.
 29. Huynh, T. T., Nguyen, T. D., & Tan, H., “A survey on security and privacy issues of blockchain technology”, In 2019 international conference on system science and engineering (ICSSE), Pages 362-367, IEEE, 2019.
 30. Sayeed, S., & Marco-Gisbert, H., “Assessing blockchain consensus and security mechanisms against the 51% attack”, Applied Sciences, Vol. 9, Issue 9, Pages 1788, 2019.
 31. Süzen, A.A., & Duman, B., “Protecting the Privacy of IoT-Based Health Records Using Blockchain Technology” In Internet of Medical Things, Pages 35-54, Springer, Cham, 2021.



ULUSLARARASI 3B YAZICI TEKNOLOJİLERİ
VE DİJİTAL ENDÜSTRİ DERGİSİ

INTERNATIONAL JOURNAL OF 3D PRINTING
TECHNOLOGIES AND DIGITAL INDUSTRY

ISSN:2602-3350 (Online)

URL: <https://dergipark.org.tr/ij3dptdi>

3B YAZICILAR İÇİN CAM FİBER KATKILI KOMPOZİT FİLAMENT ÜRETİMİ VE MEKANİK ÖZELLİKLERİ

MANUFACTURING AND MECHANICAL PROPERTIES OF A GLASS FIBER REINFORCED COMPOSITE FILAMENT FOR 3D PRINTERS

Yazarlar (Authors): Suat Altun^{ID*}, Buğra Sekban^{ID}



Bu makaleye şu şekilde atıfta bulunabilirsiniz (To cite to this article): Altun S., Sekban B., “3B Yazıcılar İçin Cam Fiber Katkılı Kompozit Filament Üretimi ve Mekanik Özellikleri” *Int. J. of 3D Printing Tech. Dig. Ind.*, 7(1): 64-77, (2023).

DOI: 10.46519/ij3dptdi.1262980

Araştırma Makale/ Research Article

Erişim Linki: (To link to this article): <https://dergipark.org.tr/en/pub/ij3dptdi/archive>

3B YAZICILAR İÇİN CAM FİBER KATKILI KOMPOZİT FİLAMENT ÜRETİMİ VE MEKANİK ÖZELLİKLERİ

Suat Altun^a , Buğra Sekban^b 

^aKarabük Üniversitesi, Teknoloji Fakültesi, Endüstriyel Tasarım Mühendisliği Bölümü, TÜRKİYE
^bErzurum Şehir Hastanesi, Üniversite Mahallesi, Çat Yolu Caddesi, Erzurum, TÜRKİYE

* Sorumlu Yazar: saltun@karabuk.edu.tr

(Received: 10.03.2023; Revised: 28.03.2023; Accepted: 25.04.2023)

ÖZ

3B yazıcıların hızlı prototipleme ve özel üretim alanlarında kullanımı hızla artmaktadır. En yaygın kullanılan 3B yazıcı teknolojisi olan eriyik biriktirme yönteminde (FDM), polilaktik asit (PLA) malzeme yaygın olarak tercih edilmektedir. 3D yazıcı baskılarının prototip veya model üretiminin ötesinde kullanılabilir parça üretiminde kullanılabilmesi için kullanılan filamentlerin mekanik özelliklerinin de geliştirilmesi gerekli olmuştur. Bu amaçla takviyeli kompozit filamentlerin geliştirilmesi önemlidir. Bu çalışmada ana amaç cam lifi takviyeli kompozit PLA filament üreterek, özellikle eğilme ve darbe direnci daha yüksek, kullanılabilir parçaların 3B yazıcı ile üretilmesine olanak sağlamaktır. Bu amaçla PLA termoplastik malzemeye %5, %10 ve %15 oranlarında cam lifi (CL) katkısı yapılarak çift vidalı ekstrüderde kompozit granül elde edilmiş ve bu granüllerden de 1,75 mm çapında 3B yazıcı filamenti üretilmiştir. Elde edilen kompozit filament kullanılarak 3B yazıcıda yazdırılan parçaların çekme dayanımı (ASTM D638), eğilme dayanımı (ASTM D790) ve darbe direnci (ASTM D6110) değerleri belirlenerek saf PLA'dan üretilen örneklerin değerleriyle karşılaştırılmıştır. 3B yazıcıda parça üretim sürecinde yazdırma parametrelerinin mekanik özelliklere etkisinin belirlenmesi amacıyla da, %10, %50 ve %90 olmak üzere üç farklı doluluk oranı; rectilinear, grid ve honeycomb yazdırma geometrileri ile 190°C ve 210°C yazdırma esnasında ekstrüder sıcaklığı parametreleri kullanılarak deney örnekleri hazırlanmıştır. PLA malzemeye CL katkısı mekanik özellikleri etkilemiş, %5 CLT katkısı ile çekme dayanımında %28, eğilme dayanımında %24 artış; %10 CL katkısı ile de darbe direncinde %8,6 artış elde edilmiştir. CL katkı oranının %15 olması durumunda ise mekanik dirençlerde azalma meydana gelmiştir. Yazdırma parametrelerinden doluluk oranı ile mekanik özellikler arasında doğrusal bir ilişki olduğu ancak yazdırma geometrisi ve sıcaklığının önemli bir etkisinin olmadığı tespit edilmiştir.

Anahtar Kelimeler: 3B Yazıcı, PLA, Cam Lifi, Kompozit Filament.

MANUFACTURING AND MECHANICAL PROPERTIES OF A GLASS FIBER REINFORCED COMPOSITE FILAMENT FOR 3D PRINTERS

ABSTRACT

The use of 3D printers in rapid prototyping and specialty manufacturing areas is increasing rapidly. In the melt deposition method (FDM), which is the most widely used 3D printer technology, polylactic acid (PLA) material is widely preferred. In order for 3D printing to be used in the production of usable parts beyond prototype or model production, it was necessary to improve the mechanical properties of the filaments used. For this purpose, it is important to develop reinforced composite filaments. In this study, the main purpose was to produce glass fiber reinforced PLA composite filament, which has particularly higher bending and impact resistance and to allow producing parts which can be used as a functional part by using a 3D printer. In the study, to produce composite granule, glass fiber powder (GF) were added by 5%, 10% and 15% to a thermoplastic PLA by using a twin-screw extruder. With

these granules, 1,75 mm filament was extruded by using single screw extruder. In order to determine the mechanical properties of the 3D printed specimens, tensile test (ASTM D638), flexural test (ASTMD790) and impact strength (ASTM D6110) test performed. To determine the effect of the printing parameters on the mechanical properties of the printed specimens, three infill geometries (Grid, Rectilinear, Full honeycomb), three infill rate (10%, 50%, 90%) and two nozzle temperatures (190°C and 210°C) were used. Addition of GF to the PLA affected the mechanical properties of the printed parts. Adding 5% GF resulted in a 28% increase in tensile strength and a 24% increase in flexural strength. Adding 10% GF led an 8,6 % increase in Charpy impact strength. It was determined that mechanical properties decrease when the addition ratio of GFP increases to 15%. It was also determined that there was a direct proportion between infill rate and mechanical properties, but neither infill geometry nor nozzle temperature affected the mechanical properties, significantly.

Keywords: 3D Printer, PLA, Glass Fiber, Composite Filament.

1. GİRİŞ

Son yıllarda 3B baskı teknolojisine olan ilgi hızla artmaktadır. 3B baskıda, seçici lazer sinterleme (SLS), eriyik biriktirme yöntemi (FDM) ve benzer çeşitli teknolojiler kullanılmaktadır. Bunlar arasında en yaygın kullanılanı, hem basit çalışma mantığı hem de yatırım maliyeti açısından daha ekonomik olması sebebiyle FDM teknolojisidir [1]. Bu yüzden FDM baskı teknolojisi sürekli olarak gelişmektedir ve sürdürülebilir gelişimi için baskı malzemeleri de son derece önemlidir [2-3].

FDM teknolojisinde genellikle polilaktik asit (PLA), akrilonitril bütadien stiren (ABS) ve polikarbonat (PC) gibi termoplastik materyaller kullanılmaktadır. 3B üretimde elde edilen ürünün kalitesine etki eden faktörler arasında filament kalitesi ve dayanımı da bulunmaktadır. PLA malzemenin dayanımının nispeten düşük olması, yazdırılan parçaların dayanım gerektiren fonksiyonel son ürün olarak kullanım alanlarının sınırlı olmasına neden olmaktadır. Mekanik özellikleri daha iyi olan petrol türevi plastik malzemelerin çevre kirliliğine neden olmasından dolayı, doğal olarak bozunabilen (biobozunur) bir polimer olan PLA'nın sanayide kullanımı çevresel etki açısından da olumlu olacaktır. Bu durum 3B baskı teknolojisinde mekanik özellikleri iyileştirilmiş takviyeli PLA kompozit filamentlerin geliştirilmesine ihtiyaç doğurmaktadır.

Takviyeli kompozit imalatında plastik matrise doğal veya sentetik liflerin veya çeşitli inorganik takviye malzemelerinin katılması yaygın olarak kullanılan bir yöntemdir. Çeşitli boyut ve formlardaki cam lifi (CL) de, bu amaçla yaygın olarak kullanılan bir takviye

malzemesidir. Birçok farklı termoplastik, termoset plastik veya reçineler CL ile güçlendirilerek kompozit malzemeler elde edilmektedir. Bu bağlamda, 3D baskı teknolojisinde kullanılan PLA filamentlerin de CL ile güçlendirilerek PLA filamentin endüstriyel ürünlerde kullanım imkanlarını arttırabilmek mümkün olabilir. Lifli yapısı nedeni ile malzemenin darbe dayanımında çentik etkisini azaltıcı yönde etkileyeceği öngörülmektedir. Ancak lif uzunluklarının fazla olması yazdırma sırasında nozul tıkanması gibi zorluklara neden olabilmektedir. Bu nedenle kısa hatta toz formunda cam lifi kullanılması faydalı olabilir. CL takviyesi ile mekanik özellikleri iyileştirilecek PLA filamentin 3B yazıcılarda kullanımı ile, daha az malzeme ile üretim yapılabilmesi olanağı, daha hafif ürün ve ekonomik üretim yapma imkanı sağlayacaktır.

Literatürde doğal veya sentetik çeşitli lif veya takviye malzemeleri ile güçlendirilmiş kompozit malzemelerin özelliklerine yönelik birçok çalışma bulunmaktadır. Cam lifi (CL) katkısının PLA malzemenin mekanik özellikleri üzerindeki etkisine yönelik de çalışmalar yapılmıştır. Bu kompozitlerin üretiminde çoğunlukla sıcak presleme veya enjeksiyon kalıplama yöntemleri kullanılmıştır. Huda vd. [4] %30 CL katkılı PLA kompozitlerin çekme dayanımında %28, eğme dayanımında %10, darbe dayanımında ise %53 artış tespit etmişlerdir. Lin vd. [5] %30 CL katkısının saf PLA ya oranla çekme dayanımında %84, eğme dayanımında %73 ve darbe dayanımında %200 artış sağlayabildiğini belirtmiştir. Lu vd. [6] de yine %30 CL katkısı ile PLA/HDPE harmanı kompozitinin çekme dayanımında %75 artış, darbe dayanımı ve sünekliğinde ise sırasıyla %57 ve %83 azalış tespit etmişlerdir.

Jaszkiwicz vd. [7] ise %30 CL takviyeli PLA matrisli kompozitlerin çentikli darbe dayanımında %531 gibi oldukça yüksek bir artış elde ettiklerini belirtmişlerdir.

Termoplastik matrisli, takviyeli kompozit termoplastiklerin 3B yazıcı filamentleri olarak kullanımı ve yazdırılan parçaların özelliklerine yönelik akademik çalışmalar sınırlıdır. Bu çalışmalar daha çok ABS matrisli kompozitler üzerine yoğunlaşmıştır. Zhong vd. [8] 3B yazıcılarda kullanılmak üzere ABS matris malzemesine kısa cam fiber takviye elemanlarını ekleyerek ürettikleri filamentin kırılma dayanımının arttığını, bu nedenle 3B yazıcılarda kullanımının sınırlı olduğunu belirtmişlerdir. Ancak kompozite plastikleştirici olarak LLDPE ve uyumlaştırıcı ajan (Hydrogenated Buna-N) katılması ile elde edilen kompozit filamentin çekme dayanımının ABS'ye oranla oldukça yüksek olduğunu ve 3B yazıcılarda kullanılabilirliğini bildirmişlerdir. Shofner vd. [9] ABS matrise %10 karbon nanofiber katarak çekme dayanımında %39, çekme modülünde ise %60 artış sağlamışlardır. Perez vd. [10], ise ağırlıkça %5 oranında hint kenevirli elyafı ekleyerek ürettikleri ABS filament ile yazdırdıkları numunelerin çekme dayanımının saf ABS filamentle yazdırılanlara kıyasla %9 oranında düşük olduğunu belirtmişlerdir. Namıkı vd. [11] PLA ve sürekli karbon fiber kullanarak yazdırdıkları kompozit örneklerin çekme dayanımı ve elastisite değerlerinin, saf PLA ile yazdırılan örneklerle göre daha yüksek olduğunu belirlemişlerdir. Weng vd. [12] %1-5 montmorillonit takviyeli ABS kompozitinin 3B yazıcı ile yazdırılan örneklerinin çekme dayanımı ve modülü değerlerinin enjeksiyon kalıplama yöntemleriyle üretilenlerinkinden %40-45 daha düşük olduğunu belirtmişlerdir. Literatürde CL takviyeli PLA kompozitinin 3B yazıcıda

kullanımına yönelik yalnızca bir çalışmaya ulaşılabilmektedir. Çalışmada %5, 10, 15 ve 20 CL ile takviye edilen PLA kompoziti ile 3B yazıcıda yazdırılan örneklerin ve enjeksiyon kalıplama yöntemi ile elde edilen örneklerin mekanik özellikleri incelenmiştir [13]. Ayrıca PLA ile %10 termoplastik üreten (TPU) harmanlanarak kompozitin tokluğunun artırılması hedeflenmiştir. Enjeksiyon kalıplama ile elde edilen numunelerde %15 CL takviyesi ile PLA'nın çekme dayanımında %32, eğilme dayanımında %21 artış belirlenmiştir. Ancak 3B yazdırılmış örneklerin çekme dayanımında %30 ve eğilme dayanımında %32 azalış olduğu belirtilmiştir.

Bu çalışmada ana amaç, PLA termoplastik malzemeye cam lifleri katılarak mekanik özellikleri daha iyi bir kompozit filament üretmek ve bu filament ile prototip veya modellerden çok, kullanılabilir son ürünlerin 3B yazıcılar ile üretilmesine imkân tanımaktır. Bu amaçla PLA malzemeye %5, %10 ve %15 oranlarında CL katılarak granül halinde kompozit malzeme elde edilmiş ve bu kompozit granüllerden de 3B yazıcı için filament üretilmiştir. Üretilen filament kullanılarak yazdırılan parçaların mekanik özelliklerinin belirlenmesi için ise, doluluk oranı, yazdırma geometrisi ve nozul sıcaklığı gibi yazdırma parametrelerinin farklı seviyeleri kullanılarak parçalar üretilmiş ve optimum yazdırma parametreleri belirlenmiştir.

2. MATERYAL VE YÖNTEM

2.1. Materyal

Çalışmada kullanılan ana matris malzemesi PLA granül halde Kumru Kimya San. ve Tic. Ltd. Şti. (Türkiye) temin edilmiştir. Tedarikçi firma tarafından sağlanan bilgilere göre kullanılan PLA'nın teknik özellikleri Çizelge 1.'de verilmiştir.

Çizelge1. PLA granül teknik özellikleri.

Fiziksel Özellik	Miktar (birim)
Yoğunluk	1.24 g/cm ³
Erime akış indeksi (ISO 1133-A at 210°C/2.16kg)	8 g/10 min
Erime akış indeksi (ISO 1133-A at 190°C/2.16kg)	3 g/10 min
Görünüm	Kristalin beyaz granül
Erime sıcaklığı T _m (DSC)	155 °C
Camsı geçiş sıcaklığı T _g (DSC)	55-60 °C

Takviye elemanı olarak öğütülmüş cam lifi (CL) kullanılmıştır. Fiber Elyaf Kompozit San Tic Ltd Şti firmasından temin edilen cam lifi,

tedarikçi tarafından verilen bilgilere göre, E-camı yapısında, 13 mikron çapında ve 7-300 mikron lif uzunluğuna sahip toz yapısındadır.

2.2. Yöntem

2.2.1. Kompozit malzeme üretimi

3B yazıcıda kullanılacak CL ile güçlendirilmiş filament elde edilmesi için öncelikle kompozit granül elde edilmiş ve bu granüller kullanılarak filament üretimi gerçekleştirilmiştir. Kompozit malzeme ve filament üretimi Anatolia Arge Makine Elektronik Kimya Otomotiv Ltd. Şti. firmasından hizmet alımı yoluyla gerçekleştirilmiştir.

Kompozit malzeme bileşiminde ana matris olarak PLA kullanılmıştır. Takviyeli kompozit üretiminde yüksek oranda takviye kullanımında ana matris oranı da düşmekte ve takviye elemanından beklenen katkı sağlanamamaktadır. Bu nedenle bu çalışmada %5, %10 ve %15 olmak üzere üç farklı oranda CL karışımı ile toplam 4 farklı malzeme elde edilmiştir. Kompozit granül üretiminde termoplastik malzeme PLA çift vidalı ekstrüderin ana besleme haznesinden, katkı olan CL ise belirlenen oranda yan besleme ünitesinden beslenerek istenen homojen karışım elde edilmiştir. Anı zamanda karışımlarda katkı oranını belirtmek için çok düşük oranda (% 0,05) renk pigmenti kullanılmıştır. Hizmet sağlayıcının teknik altyapısına bağlı olarak üretim şartlarına ait bilgiler firma tarafından belirtilmiştir.

Kompozit malzeme, vida boy/çap oranı (L/D) 30, vida dönüş hızı 5 dev/dak, besleme bölgesi

sıcaklığı 20-25 °C, eritme/karıştırma bölgesi sıcaklığı 190-200 °C ve çıkış kalıp sıcaklığı 200 °C işlem parametreleri kullanılarak çift vidalı ekstrüderde üretilmiştir. Elde edilen kompozit kırıcıda kırılarak granül hale getirilmiştir. Granül halde elde edilen kompozit malzeme filament üretimi öncesi 12 saat 80 °C sıcaklıkta vakumlu fırında kurutulmuştur. Rutubetinden arındırılan granüller tek vidalı ekstrüder kullanılarak 1,75 mm çapında filament haline getirilmiştir. Filament üretimi parametreleri ise, L/D=24, besleme bölgesi sıcaklığı 20-25 °C, eritme bölgesi sıcaklığı 200 °C ve çıkış kalıp sıcaklığı 210 °C olarak uygulanmıştır. Elde edilen filamentler makaralara sarılarak 3B yazıcılarda kullanılmak üzere hazır hale getirilmiştir.

2.2.2. Deney Örneklerinin Hazırlanması

Mekanik özelliklerin belirlenmesi için kullanılacak deney örnekleri farklı yazdırma parametreleri kullanılarak Makerbot marka FDM yazıcı ile elde edilmiştir. Çekme testi, eğilme testi ve darbe testi örnekleri ilgili standarda uygun olarak SolidWorks programında modellenmiş ve STL dosya formatında kaydedildikten sonra 3B yazıcının yazılımı ile dilimlenmiş ve yazdırılmıştır. Deney örneklerinin elde edilmesinde kullanılan yazdırma parametreleri Çizelge 2'de verilmiştir.

Çizelge 2. 3B yazıcıda üretilen deney örneklerinin yazdırma parametreleri.

Parametre	Parametre alt seviye
Doluluk oranı	%10
	%50
	%90
Yazdırma geometrisi	Rectilineer
	Grid
	Full Honeycomb
Yazdırma ekstrüder sıcaklığı	190 °C
	210 °C
Yazdırma hızı	45 mm/sn
Katman kalınlığı	0,2 mm

Çalışmanın hedeflerinden birisi malzemenin mekanik özelliklerini iyileştirerek daha az malzeme ile daha hafif parçalar üretilebilmesini sağlamak olduğundan, doldurma oranı olarak %10, %50 ve %90 oranları seçilmiştir. Örneklerin yazdırılmasında kullanılan parametrelerden birisi olan yazdırma geometrisi

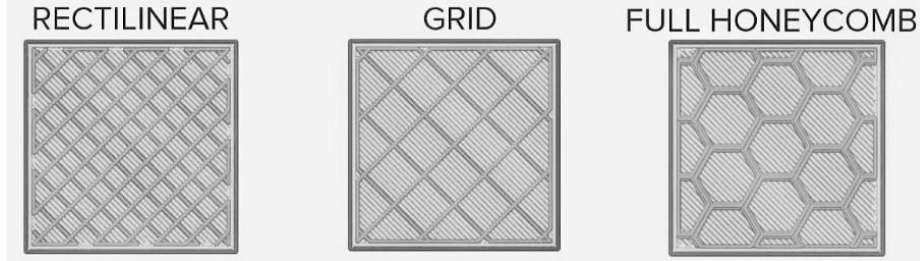
(infill pattern) olarak seçilen 3 farklı geometri şematik olarak Şekil 1'de verilmiştir.

2.2.3. Mekanik testler

CL katkısının ve yazdırma parametrelerinin 3B yazıcılarda üretilecek parçaların mekanik özelliklerini belirlemek amacı ile ilgili standarda göre yazdırılan örneklerin, çekme

dayanımı ASTM D638 (Tip 1) [14], eğilme dayanımı ASTM D790 [15] ve darbe direnci değerleri ASTM D6110 [16] standardına uygun olarak tespit edilmiştir. Çekme ve eğilme testlerinde Zwick/Roel Z50 universal test

makinesi, darbe direnci testlerinde Devotrans DVT CD C model çentik darbe test cihazı kullanılmıştır. Her deney grubu için 5 adet numune kullanılmıştır.



Şekil 1. Yazdırma geometrisi (infill pattern).

2.2.4. Malzeme Karakterizasyonu

CL katkısı ile PLA malzemeden üretilen kompozit malzemede, cam liflerinin matris içerisindeki dağılımı ve arayüz etkileşimine ait değerlendirme taramalı elektron mikroskobu (SEM) (Carl Zeiss Ultra Plus Gemini Fesem) görüntüleri ile değerlendirilmiştir.

2.2.5. Verilerin Değerlendirilmesi

Cam lifi tozu katkılı PLA filament ile, farklı yazdırma parametreleri kullanılarak 3D yazıcıda yazdırılan numunelerin mekanik testlerinden elde edilen veriler, çoklu regresyon analizi ile istatistiksel değerlendirmeye tabi tutulmuştur. Faktör seviyeleri arasındaki farklılıkların tespiti için ise Duncan's çoklu karşılaştırma testi uygulanmıştır.

3. BULGULAR

3.1. Çekme Dayanımı

CL katkılı PLA filament kullanılarak farklı yazdırma parametrelerine göre yazdırılan örneklerin çekme dayanımı değerleri Çizelge 3'te verilmiştir. Elde edilen verilere göre CL katkı oranı ve yazdırma parametreleri örneklerin çekme dayanımı üzerinde etkili olmuştur. En düşük çekme dayanımı değeri 11,07 N/mm² ile saf PLA filamentle, honeycomb yazdırma geometrisi, %10 doluluk oranı ve 190 °C yazdırma sıcaklığında yazdırılmış kontrol örneklerinde tespit edilmiştir. En yüksek çekme dayanımı değeri ise 25,69 N/mm² ile rectilinear geometride, %90 doluluk oranı ve 210 °C yazdırma sıcaklığında saf PLA ile yazdırılan örneklerde ölçülmüştür.

Hem kontrol grubu hem de CL tozu katkılı örneklerin çekme dayanımı arasında doğrusal bir ilişki ve istatistiksel olarak da önemli

($p=0,000$) bir fark bulunmaktadır. Çoğunlukla %5 CL katkılı grupların çekme dayanımının diğerlerine göre daha yüksek olduğu ancak %90 doluluk oranında saf PLA ile yazdırılan örneklerin çekme dayanımı ile aradaki farkın çok az olduğu tespit edilmiştir. Yazdırma geometrisinin çekme dayanımı üzerinde istatistiksel olarak önemli bir etkisi yoktur ($p=0,215>0,05$). Yazdırma sıcaklığının etkisi ise nispeten daha az olmaktadır.

CL katkı oranının çekme dayanımı değerleri üzerindeki etkisini daha anlaşılır şekilde ortaya koyabilmek için doluluk oranından bağımsız olarak değerlendirmek daha uygundur. Doluluk oranı % 10 iken CL katkı oranı % 5 olduğunda en yüksek çekme dayanımı değerleri elde edilmiştir. Yazdırma geometrisinin belirgin bir etkisi görülmezken, yazdırma sıcaklığının artışı ile çekme dayanımının da arttığı belirlenmiştir. Katkı oranı %10'a çıktığında ise sıcaklığın artışı ile çekme dayanımının kontrol grubuna göre daha düşük olduğu belirlenmiştir. Katkı oranı %15 iken çekme dayanımı kontrol grubu ile hemen hemen aynı iken, %5 katkı oranının değerlerine göre daha düşüktür. Yazdırılan örneklerin doluluk oranı %50 iken yine % 5 CL katkılı örneklerin çekme dayanımı diğerlerinden yüksektir. Katkı oranının artışı ile birlikte çekme dayanımı değerleri de azalmaktadır. Özellikle yüksek sıcaklıkta yazdırılan örneklerde bu değer kontrol grubunun da altına düşmektedir. Yazdırma sıcaklıkları arasında ise yüksek sıcaklığın çok az da olsa çekme dayanımını artırdığı söylenebilir. Örneklerin doluluk oranı %90 iken, CL katkı oranının etkisi daha da belirgin olmakta ve çekme dayanımını azaltmaktadır.

Katkı oranı arttıkça genellikle çekme dayanımındaki azalış da artmaktadır.

Yazdırma sıcaklığının ve geometrisinin ise çok belirgin bir etkisi tespit edilememiştir.

Yazdırma doluluk oranına ve CL katkı oranına göre çekme dayanımı değişimi Şekil 2 de verilmiştir. En yüksek çekme dayanımı değerleri %5 CL katkılı filamentle yazdırılan örneklerde tespit edilmiştir.

Çizelge 3. Cam lifli katkılı PLA filamentle yazdırılmış örneklerin çekme dayanımı.

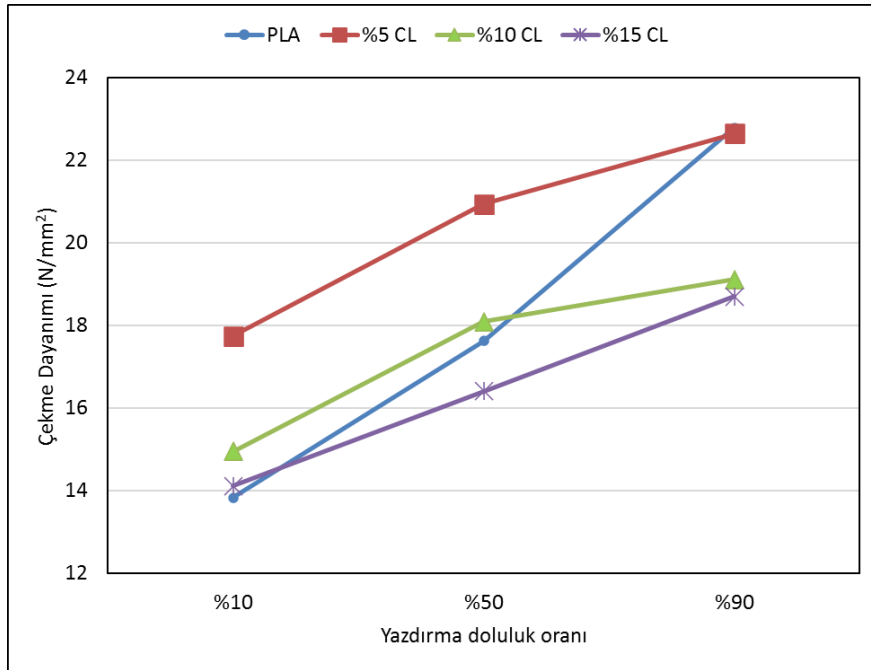
Yazdırma Geometrisi	Yazdırma Sıcaklığı (°C)	Doluluk Oranı (%)	Çekme Dayanımı (N/mm ²)				
			PLA	%5CL	%10CL	%15CL	
Grid	190	10	13,02 (0,42)	17,95 (0,35)	15,45 (0,50)	12,56 (0,46)	
		50	15,12 (1,48)	20,64 (1,06)	18,45 (0,66)	15,28 (0,74)	
		90	22,76 (0,69)	20,38 (0,29)	19,14 (0,64)	20,54 (0,63)	
	210	10	15,72 (0,66)	18,08 (0,22)	14,33 (0,79)	15,50 (0,46)	
		50	18,51 (0,63)	21,07 (0,92)	17,20 (0,65)	17,32 (0,66)	
		90	23,57 (0,29)	23,58 (0,31)	19,99 (0,36)	18,34 (0,77)	
	Honeycomb	190	10	11,07 (0,97)	17,65 (0,59)	15,80 (0,44)	12,98 (0,60)
			50	15,87 (0,66)	21,78 (0,70)	19,11 (0,84)	15,12 (1,18)
			90	19,62 (0,72)	22,47 (0,14)	17,73 (0,15)	19,35 (0,44)
210		10	15,76 (0,54)	17,69 (0,28)	14,59 (0,53)	16,15 (0,45)	
		50	20,56 (0,32)	20,94 (0,72)	17,65 (0,69)	18,36 (0,36)	
		90	23,27 (0,64)	23,55 (0,56)	19,80 (0,36)	18,56 (0,43)	
Rectilinear		190	10	12,33 (0,38)	17,90 (0,98)	15,34 (0,52)	12,50 (0,77)
			50	17,26 (0,33)	20,32 (1,16)	18,30 (1,07)	17,78 (0,61)
			90	21,78 (0,66)	22,69 (0,68)	18,63 (0,76)	18,67 (1,01)
	210	10	15,08 (0,54)	17,20 (0,54)	14,21 (0,70)	15,00 (0,63)	
		50	18,43 (0,50)	20,87 (0,98)	17,86 (0,68)	14,58 (1,90)	
		90	25,69 (1,02)	23,19 (0,72)	19,37 (0,43)	16,75 (0,47)	

PLA:Saf PLA kontrol, %5CL:%5 Cam lifli+%95 PLA, %10CL:%5 Cam lifli+%90 PLA, %15CL:%15 Cam lifli+%85 PLA. Parantez içerisindeki değerler standart sapmayı ifade etmektedir.

Doluluk oranı artıkça kontrol numunesi ile %5 CL katkıli numunelerin deęerleri arasındaki fark azalmakta, %90 doluluk oranında ise neredeyse eşitlenmektedir. %10 ve %15 CL katkıli örneklerin çekme dayanımı sadece %10 doluluk oranında saf PLA'ninkinden yüksek iken, doluluk oranı artıkça saf PLA dan daha düşük deęerler tespit edilmiştir.

Kontrol numunesinin %10, %50 ve %90 doluluk oranlarındaki çekme dayanımına göre deęişim %5 CL katkıli grupta sırasıyla %28, %8 ve %2 artış; %10 CL katkıli grupta %18,78, %2,66 artış, %6,93 azalış ve %15 CL katkıli grupta % 0,61, %16,11 ve %17,92 azalış olarak gerçekleşmiştir. Artan katkı oranının boşluk oranını arttırdığı ve bu nedenle çekme ve eğilme dayanımlarında düşüşe neden olduğu literatürde

de belirtilmiştir [17,18]. Artan katkı oranı ile matrise tutunamayan ve yerinden çıkan fiberlerin oluşturduğu boşlukların gerilme yığılma bölgeleri oluşturabileceği ve dayanımda düşüşe neden olabileceği belirtilmiştir [19]. %10 kısa cam lifi katkıli PLA kompozit ile %100 doluluk oranı ile 3B yazıcıda yazdırılmış örneklerin çekme dayanımında %10,8 azalış tespit edilen çalışmada [13] hem daha uzun hem de lif ile matris arasındaki ara yüzey bağlanmasının daha iyi olduğu silanlanmış cam lifleri kullanıldığından, bu çalışmada elde edilenden daha az düşüş elde edilmiş olabilir. Carneiro vd. [20] ise %30 cam lifi katkıli polipropilenden ürettikleri filamentle % 100 doluluk oranında yazdırdıkları örneklerde %40'a varan bir artış elde etmişlerdir.



Şekil 2. Doluluk oranına göre CL katkı oranının çekme dayanımına etkisi.

3.2. Eğilme Dayanımı

CL katkıli PLA filament ile yazdırılan örneklerin eğilme dayanımları tespit edilmiş ve ortalama ve standart sapma deęerleri Çizelge 4'te verilmiştir.

Eğilme dayanımı sonuçları genel olarak deęerlendirildiğinde en düşük deęer 22,62 N/mm² ile % 15 CL katkıli grupta, grid yazdırma geometrisi, %10 doluluk oranı ve 190 °C yazdırma sıcaklığı kullanılan örneklerde; en yüksek ise 50,87 N/mm² ile kontrol grubu, grid yazdırma geometrisinde %90 doluluk ve 210 °C yazdırma sıcaklığı kullanılan örneklerde tespit

edilmiştir. Genel olarak doluluk oranı ve yazdırma sıcaklığı artışı ile eğilme dayanımının da arttığı görülmektedir. CL katkı oranının artışı ile birçok grupta eğilme dayanımının azaldığı belirlenmiştir. Yapılan varyans analizi sonucuna göre CL katkı oranı, doluluk oranı ve yazdırma sıcaklığı eğilme dayanımı üzerinde etkili iken, yazdırma geometrisinin istatistiksel olarak anlamlı bir etkisinin olmadığı (p=0,064>0,05) tespit edilmiştir. %10 doluluk oranı ile yazdırılan örneklerde % 5 CL katkısı kontrol grubuna göre eğilme dayanımını arttırmış ancak katkı maddesi oranı artıkça eğilme dayanımı düşmüştür. Yazdırma

sıcaklığının belirgin bir etkisi görülmez iken honeycomb yazdırma geometrisinin daha yüksek eğilme dayanımı sağladığı söylenebilir. %50 doluluk oranı ile yazdırılan parçalarda yazdırma parametrelerinin çok belirgin etkisi görülmemekle beraber, %5 cam lifi tozu katkısının az da olsa eğilme dayanımını olumlu

etkilediği söylenebilir. %90 doluluk oranında yazdırılmış örneklerde yalnızca Grid yazdırma geometrisi, 190 °C yazdırma sıcaklığında üretilen grup hariç tüm diğer gruplarda CL katkısı eğilme dayanımı değerini düşürmüştür. Yazdırma geometrisinin ve sıcaklığının ise belirgin bir etkisi görülmemektedir.

Çizelge 4. Cam lifi katkılı PLA filamentle yazdırılmış örneklerin eğilme dayanımı.

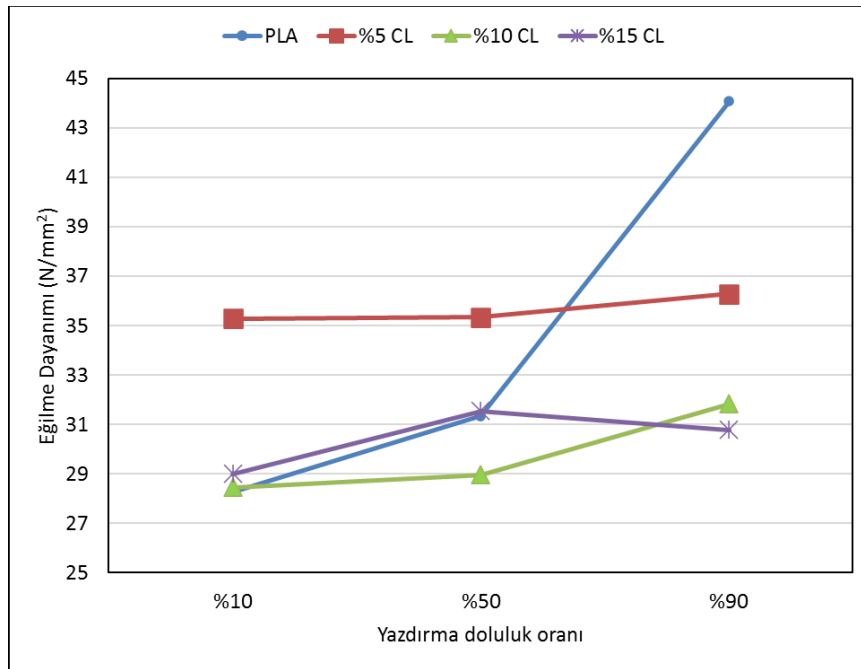
Yazdırma Geometrisi	Yazdırma Sıcaklığı (°C)	Doluluk Oranı (%)	Eğilme Dayanımı (N/mm ²)				
			PLA	%5CL	%10CL	%15CL	
Grid	190	10	31,55 (2,20)	34,74 (2,45)	29,45 (0,59)	22,62 (6,17)	
		50	32,34 (1,03)	48,38 (3,41)	30,36 (0,14)	34,52 (1,83)	
		90	31,37 (2,84)	43,86 (3,38)	34,62 (0,89)	30,62 (1,67)	
		10	30,42 (0,21)	29,76 (2,33)	26,54 (0,76)	28,29 (1,13)	
		210	50	27,38 (2,51)	30,39 (0,17)	29,13 (0,50)	30,80 (1,46)
		90	50,87 (2,35)	33,18 (1,90)	30,19 (0,70)	32,16 (1,20)	
	Honeycomb	190	10	24,29 (1,34)	42,00 (1,37)	34,37 (0,94)	32,42 (2,10)
			50	30,90 (0,31)	31,68 (2,52)	29,04 (1,88)	31,60 (6,00)
			90	47,99 (1,37)	34,50 (0,87)	30,51 (0,14)	30,53 (0,37)
		210	10	29,08 (1,17)	37,22 (7,73)	27,80 (2,11)	27,39 (2,45)
			50	30,71 (0,14)	34,75 (5,06)	30,26 (0,19)	30,80 (0,44)
			90	41,82 (2,51)	38,57 (5,33)	30,41 (0,07)	32,37 (0,46)
Rectilinear	190	10	25,72 (1,17)	38,95 (3,98)	27,58 (0,82)	33,04 (1,28)	
		50	29,79 (0,49)	36,87 (2,46)	30,72 (0,34)	30,77 (0,52)	
		90	46,06 (2,39)	37,77 (5,92)	34,72 (0,39)	27,16 (1,74)	
	210	10	28,61 (1,70)	29,00 (1,84)	24,99 (0,91)	30,23 (0,22)	
		50	36,93 (8,75)	29,96 (0,44)	24,29 (0,51)	30,74 (0,13)	
		90	46,36 (1,27)	29,86 (0,46)	30,54 (0,09)	31,89 (0,95)	

PLA:Saf PLA kontrol, %5CL:%5 Cam lifi+%95 PLA, %10CL:%5 Cam lifi+%90 PLA, %15CL:%15 Cam lifi+%85 PLA. Parantez içerisindeki değerler standart sapmayı ifade etmektedir.

CL katkı oranının etkisini ortaya koymak için yapılan Duncan testi sonucu % 5 oranında katkı yapılmasının eğilme dayanımını istatistiksel olarak anlamlı derecede arttırdığı, ancak %10 ve %15 oranında katkı yapıldığında düşürdüğü belirlenmiştir. %10 ve %15 katkılı grupların eğilme dayanımı arasında istatistiksel olarak önemli bir fark bulunmamaktadır. Literatürde de Nişasta/PLA kompozitinin özelliklerini geliştirmek için CL kullanıldığında %4 oranının en olumlu etkiyi yaptığı, bu oranın üzerine çıkıldığında ise beklenen etkinin sağlanmadığı ve kırılma yüzeylerindeki prüzlülüğün azaldığı belirtilmiştir [21]. Yazdırma doluluk oranı ve CL katkı oranına göre eğilme dayanımındaki değişim Şekil 3'te verilmiştir.

%5 CL katkısı ile %10 ve %50 doluluk oranında yazdırılmış örneklerin eğilme dayanımında sırasıyla %24,75 ve %12,76 artış elde edilirken, %90 doluluk oranında %17,67 azalış meydana gelmiştir. %90 doluluk oranında bu azalış %10 CL katkısında %27,78, %15 CL katkısında ise %30,8'e ulaşmaktadır. Varsavaş [13] %10 kısa cam lifi katkılı PLA kompozit ile %100 doluluk oranı ile 3B yazıcıda yazdırdıkları örneklerin eğilme dayanımında %17,5 azalış tespit etmişlerdir. Kullanılan cam lifinin daha uzun ve silanlanmış oluşu elde edilen sonuçların

farklılığına neden olmuş olabilir. Yazdırma doluluk oranının artışı ile saf PLA polimer katmanları arasında daha iyi bir kaynaşma olduğu ve neredeyse enjeksiyon kalıplama ile elde edilen yapıya yakın bir sonuç elde edildiği, ancak CL katkısının polimer ile yeterince iyi arayüz bağlanması olmamasının mekanik dayanımları azalttığı söylenebilir. Bu açıklamayla uyumlu olarak Varsavaş [13] %100 doluluk oranı ile yazdırılan PLA ile enjeksiyonla üretilen PLA örneklerin hem çekme hem de eğilme dayanımlarının aynı olduğunu belirtmiştir. Chen vd [22] sürekli cam fiber takviyeli PLA ile yaptıkları çalışmada saf PLA ile cam lifleri arasındaki arayüzey bağlanmasının zayıf olduğunu ve bu nedenle de takviyeden beklenen katkının sağlanmadığını ancak % 3 oranında özel bir uyumlaştırıcı olan PLA-g-MAH kullanımında ise eğilme dayanımında %10,4 artış elde edilebildiğini belirtmişlerdir. Yu vd. [23] de, sürekli cam fiber takviyeli PLA kompoziti ile yazdırılan örneklerde, CL katkı oranının artması ile yazdırma katmanları arasındaki asıl bağlanmanın sağlandığı PLA oranının azaldığını ve bu nedenle de parçanın mekanik dayanımında azalma meydana geldiğini belirtmişlerdir.



Şekil 3. Doluluk oranına göre CL katkı oranının eğilme dayanımına etkisi.

3.3. Darbe Direnci

CL katkılı PLA filamentle 3B yazıcıda yazdırılan örneklerin yazdırma parametrelerine

göre darbe direnci değerleri Çizelge 5'te verilmiştir. Darbe direnci testi sonuçlarına göre en yüksek değer 89,47 J/m ile %10 CL katkılı

filamentle, 210 °C yazdırma sıcaklığı, grid yazdırma geometrisinde %50 doluluk oranında yazdırılan parçalarda elde edilmiştir. En düşük darbe direnci ise 77,02 J/m ile kontrol grubu

210 °C yazdırma sıcaklığı, rectilinear yazdırma geometrisinde %10 doluluk oranında yazdırılan parçalarda elde edilmiştir.

Çizelge 5. Cam lifli katkıli PLA filamentle yazdırılmış örneklerin darbe direnci

Yazdırma Geometrisi	Yazdırma Sıcaklığı (°C)	Doluluk Oranı (%)	Darbe Direnci (J/m)				
			PLA	%5CL	%10CL	%15CL	
Grid	190	10	79,76 (5,04)	80,15 (3,06)	87,57 (4,95)	81,07 (5,74)	
		50	77,97 (1,5)	85,04 (1,97)	80,14 (3,04)	82,47 (1,01)	
		90	77,87 (2,75)	84,77 (1,61)	81,37 (2,32)	79,52 (1,27)	
		10	77,56 (5,92)	81,81 (4,86)	87,29 (2,99)	84,95 (0,77)	
		50	78,86 (2,18)	79,56 (2,6)	89,47 (2,44)	83,89 (2,1)	
		90	77,87 (2,58)	81,87 (3,4)	87,34 (1,81)	84,86 (1,97)	
	Honeycomb	190	10	85,85 (3,79)	83,09 (3,97)	89,08 (3,71)	79,66 (1,51)
			50	81,9 (2,95)	82,94 (2,53)	84,59 (2,11)	77,32 (2,73)
			90	77,86 (2,69)	84,55 (1,75)	80,33 (3,63)	77,58 (2,17)
		210	10	78,88 (3,03)	83,18 (2,73)	87,79 (4,32)	80,66 (3,06)
			50	81,35 (3,22)	83,46 (4,2)	86,57 (3)	81,57 (3,3)
			90	82,26 (3,08)	80,81 (5,3)	82,57 (4,71)	79,11 (2,43)
Rectilinear	190	10	80,56 (3,98)	77,75 (3,07)	83,7 (3,85)	77,24 (1,46)	
		50	77,97 (2,23)	80,61 (3,28)	79,63 (1,9)	82,85 (3,33)	
		90	77,34 (3,07)	83,72 (3,5)	82,19 (4,31)	79,31 (0,94)	
	210	10	77,02 (4,72)	81,35 (2,92)	85,34 (1,28)	79,96 (1,82)	
		50	79,23 (4,56)	84,36 (3,6)	87,24 (3,82)	85,3 (3,29)	
		90	79,16 (5,13)	82,62 (3,06)	83,11 (7,02)	81,58 (2,36)	

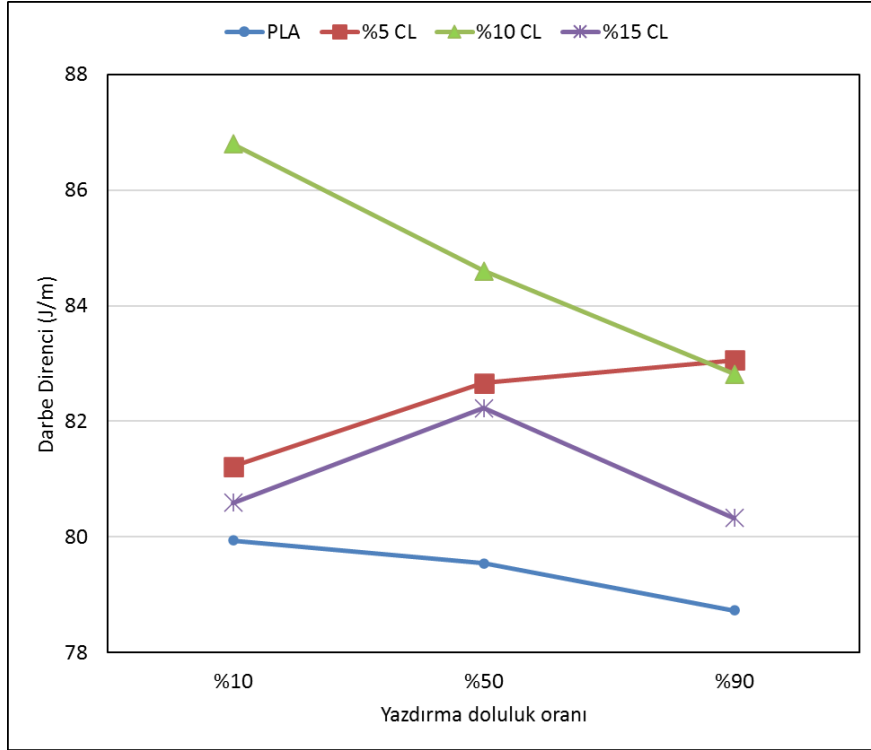
PLA:Saf PLA kontrol, %5CL:%5 Cam lifli+%95 PLA, %10CL:%5 Cam lifli+%90 PLA, %15CL:%15 Cam lifli+%85 PLA. Parantez içerisindeki değerler standart sapmayı ifade etmektedir.

Varyans analizi sonucuna göre CL katkısı PLA örneklerin darbe direncini önemli derecede etkilemekte ve tüm gruplar arasında istatistiksel

olarak anlamlı fark bulunmaktadır. En yüksek darbe direnci değerleri % 10 katkıli örneklerde ölçülmüştür. Daha sonra sırası ile %5 CL

katkılı, %15 CL katkı ve en düşük de kontrol grubunda darbe direnci belirlenmiştir. Yazdırma geometrisi ($p=0,058>0,05$) ve yazdırma sıcaklığı ($p=0,072>0,05$) parçaların darbe direnci üzerinde istatistiksel olarak anlamlı bir fark meydana getirmemiştir. Şekil 4'de yazdırma doluluk oranı ile CL katkısı oranına göre darbe direncinin değişimi görülmektedir. %10 doluluk oranında %10 CL katkı filamentlerle yazdırılan parçalarda darbe direnci artışı % 8,6 iken, %90 doluluk oranında

bu artış %5 ve %10 CL katkı gruplarında %5 seviyesinde olmuştur. Kullanılan katkı malzemesinin toz formunda olması, lif uzunluklarının çok kısa olması nedeni ile darbe direncinde beklenen artış gerçekleşmemiştir. Li vd.[24] %5 uyumlaştırıcı ile %4 CL katkı PLA filamentle yazdırdıkları parçaların darbe dayanımlarlarında %13 artış elde etmişlerdir. Takviyeli kompozitlerde uyumlaştırıcı kullanımının önemi bu sonuçlarla da ortaya konmaktadır.



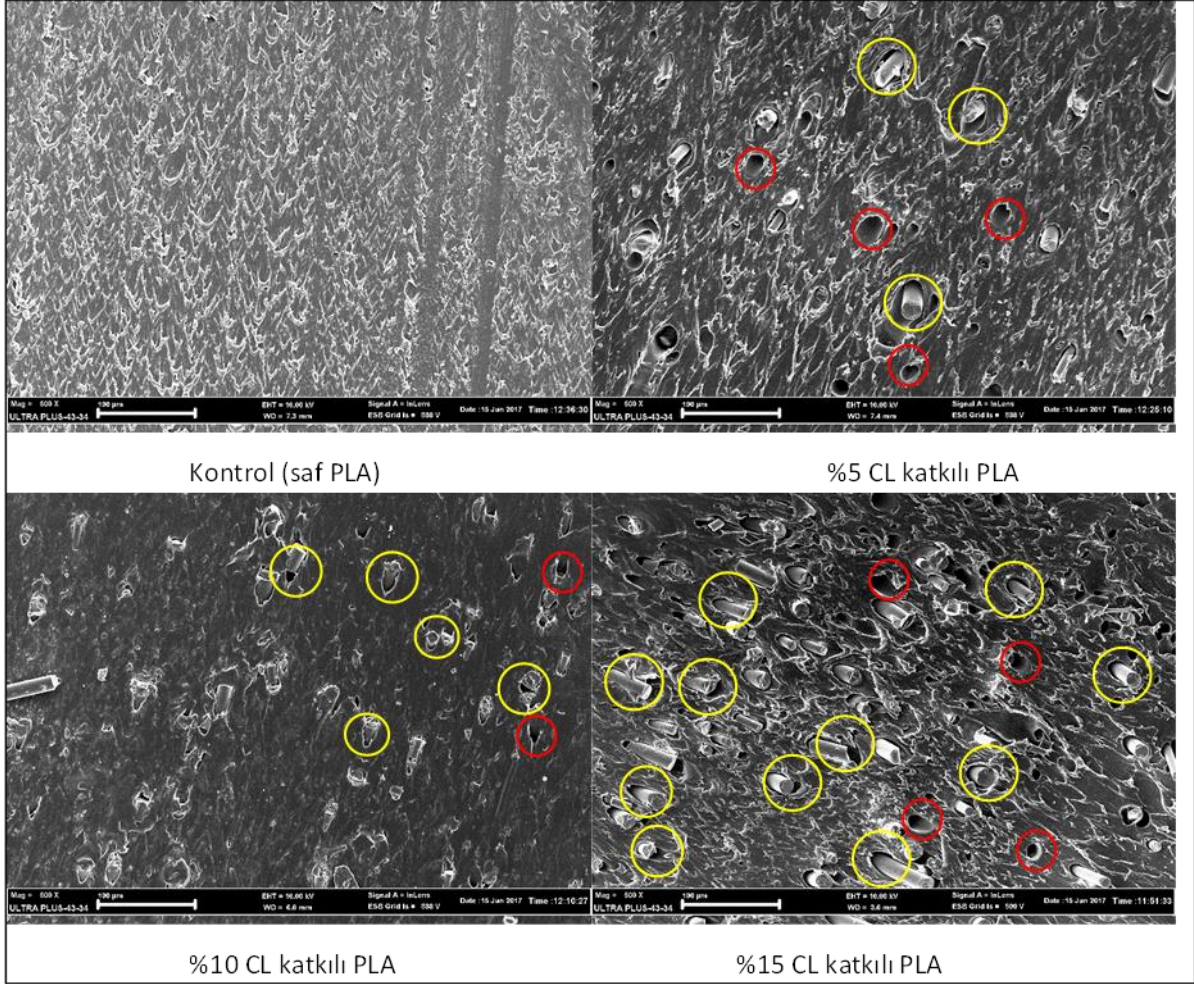
Şekil 4. Doluluk oranına göre CL katkı oranının darbe direncine etkisi.

3.4. Malzeme Karakterizasyonu

CL katkı PLA filament üretimi sürecinde, elde edilen kompozit malzeme içerisinde katkı maddelerinin dağılımı ve bu parçacıklar ile ana matris malzemesi arayüz ilişkisi kırılmış yüzeylerden elde edilen SEM görüntüleri ile incelenmiştir. Şekil 5'te SEM görüntüleri verilmiştir.

SEM görüntülerinde saf PLA kırılma yüzeyinin daha pürüzsüz ve boşluksuz yapıda olduğu görülmektedir. Takviyeli örneklerde CL parçacıklarının her üç örnekte de homojen bir şekilde dağıldığı ve ekstrüzyon yönünde yönlendiği görülmektedir. Lifler ile PLA matris arasındaki arayüz etkileşimi incelendiğinde, aralarında tam bir kaynaşmanın sağlanmadığı

ve yer yer boşluklar oluştuğu görülmektedir. Kırmızı renk ile işaretli yerinden çıkan liflerin oluşturduğu boşluklar ile sarı ile işaretli (tüm boşluklar işaretlenmemiştir) lif ile matris arasındaki boşluklar dikkat çekmektedir. Katkı oranının artışı ile bu oluşan boşlukların da birim alandaki miktarı artmaktadır. Bu nedenle katkı miktarının artışı ile elde edilen mekanik özelliklerdeki değişim paralel olmamaktadır. Katkı oranı % 15'e çıktığında genellikle ölçülen mekanik özelliklerde düşüş meydana gelmiştir. Aynı tespit Rahimizadeh vd. [19] tarafından da yapılmış, yerinden çekilip çıkan fiberlerin oluşturduğu boşlukların matris içerisinde porozite artışına neden olduğu ve artan katkı oranı ile porozitenin de arttığı belirtilmiştir.



Şekil 5. CL katkıli PLA kompozit filamentlerin kırılmış yüzeylerine ait SEM görüntüleri (Büyütme 500X).

4. SONUÇ VE ÖNERİLER

Bu çalışmada 3B yazıcılarda kullanılmak amacı ile cam lifi katkısı ile güçlendirilmiş kompozit PLA filament üretimi hedeflenmiştir. Elde edilen sonuçlar aşağıda sıralanmıştır.

- SEM görüntüleri incelendiğinde cam lifi parçacıklarının PLA matris içinde homojen şekilde dağıldığı ve kompozit hazırlanması ve filament üretim aşamasında başarılı sonuçlar alındığı görülmektedir. Ancak CL ile PLA molekülleri arasında yeteri kadar iyi bir arayüz bağlanmasının olmadığı da belirlenmiştir.
- CL katkısının PLA malzemenin çekme ve eğilme dayanımını istatistiksel olarak anlamlı şekilde etkilediği, %5 oranında CL katkısının çekme ve eğilme dayanımını arttırdığı ancak bu katkı oranı arttıkça, her iki dayanımın da düştüğü tespit edilmiştir.
- CL parçacıkları ile PLA arasında tam bir arayüz bağlanmasının oluşmaması ve katkı oranının artışı ile malzemede boşluklu bir yapının oluştuğu, bu nedenle de çekme dayanımının düştüğü belirlenmiştir. Doluluk oranı arttıkça, yüksek katkı oranının düşürücü etkisi daha da belirginleşmektedir. %5 CL katkısı ile çekme dayanımında elde edilen artış %13 olarak hesaplanmıştır.
- Yazdırma parametrelerinin çekme ve eğilme dayanımı üzerindeki etkisi değerlendirildiğinde, en etkili parametrenin doluluk oranı olduğu belirlenmiştir. Doluluk oranı ile dayanım arasında paralel bir ilişki bulunmaktadır. % 10 doluluk oranı ile %90 doluluk oranı arasında çekme dayanımı %30 luk bir artış göstermiştir. Yazdırma geometrisinin ise dayanım üzerinde önemli bir etkisinin olmadığı belirlenmiştir. Yazdırma sıcaklığının ise çok az da olsa etkili olduğu ve genellikle 210 °C de daha yüksek çekme dayanımı ancak daha düşük

eğilme dayanımı değerleri elde edildiği belirlenmiştir.

5. CL katkısının örneklerin darbe direnci üzerinde arttırıcı bir etkisi olduğu belirlenmiştir. Ancak bu arttırıcı etki, katkı oranı ile doğru orantılı değildir. En yüksek darbe direnci değerleri kontrol grubuna göre %8,6 artış ile %10 CL katkılı grupta elde edilmiştir.
6. Yazdırma parametreleri açısından, yazdırma geometrisi ile sıcaklığının darbe direnci üzerinde önemli bir etkisi bulunmazken, doluluk oranı etkili olmuştur. %10 ile %50 doluluk oranına sahip örneklerin darbe direnci arasında fark bulunmamaktadır. Doluluk oranı artışı ile darbe direnci değerleri düşmektedir.
7. CL katkısı ile PLA filamentin mekanik özelliklerini iyileştirmek üzere yapılan çalışmaların sonucuna göre, %5 CLT katkısı ve 210 °C yazdırma sıcaklığı önerilir. Yazdırma geometrisi ise mekanik özelliklerde etkili değildir. Mekanik özellikler, doldurma oranı ile doğru orantılı olarak arttığından, mukavemet gerektiren parçaların üretiminde %90 doluluk oranının kullanılması uygun olacaktır. Darbe dayanımının önemli olduğu parçaların üretilmesinde %10 CL katkısının ve %90 doluluk oranının tercih edilmesi önerilir.
8. Çalışmadan elde edilen sonuçlara göre CL katkı oranının artışı ile mekanik özelliklerde elde edilen artış paralel olmamaktadır. Bu konuda en önemli faktör katkı elemanı ile polimer arasındaki arayüz etkileşiminin yeterli olup olmamasıdır. Katkı elemanı ile polimerin yalnızca karıştırılması yeterli olmayabilmektedir. Bu nedenle iki farklı karakterdeki malzemenin arakesit kaynaşmasını sağlamak üzere farklı uyumlaştırıcı işlem ya da malzemelerin kullanılması önerilir. Eğer arayüz kaynaşması sağlanabilirse, katkı oranının artışı işe mekanik özelliklerde elde edilecek artış da artacaktır.

TEŞEKKÜR

Bu çalışma Karabük Üniversitesi Bilimsel Araştırma Projeleri Koordinatörlüğü tarafından

KBU-BAP-17/YL-166 numaralı proje kapsamında desteklenmiştir.

KAYNAKLAR

1. Credi, C., Fiorese, A., Tironi, M., Bernasconi, R., Magagnin, L., Levi, M., and Turri, S., “3D Printing of Cantilever-Type Microstructures by Stereolithography of Ferromagnetic Photopolymers”, ACS Applied Materials & Interfaces, Vol. 8, Issue 39, Pages 26332-26342, 2016.
2. Lee, J. S., Hong, J. M., Jung, J. W., Shim, J. H., Oh, J. H., and Cho, D. W., “3D printing of composite tissue with complex shape applied to ear regeneration”, Biofabrication, Vol. 6, Issue 2, 024103, Pages 1-12, 2014.
3. Liu, L., Lin, M., Xu, Z., and Lin, M., “Polylactic acid-based wood-plastic 3D printing composite and its properties,” BioResources, Vol. 14, Issue 4, 8484–8498, 2019.
4. Huda, M. S., Drzal, L. T., Mohanty, A. K., & Misra, M., “Chopped glass and recycled newspaper as reinforcement fibers in injection molded poly(lactic acid) (PLA) composites:A comparative study. Composites Science and Technology, Vol. 66, Issue 11–12, Pages 1813–1824, 2006.
5. Lin, L., Deng, C., Lin, G., & Wang, Y., “Mechanical Properties, Heat Resistance and Flame Retardancy of Glass Fiber-Reinforced PLA-PC Alloys Based on Aluminum Hypophosphite”, Polymer-Plastics Technology and Engineering, Vol. 53, Issue, 6, Pages 613–625, 2014.
6. Lu, X., Tang, L., Wang, L. L., Zhao, J. Q., Li, D. D., Wu, Z. M., & Xiao, P., “Morphology and properties of bio-based poly (lactic acid)/high-density polyethylene blends and their glass fiber reinforced composites”, Polymer Testing, Vol. 54, Pages 90–97, 2016.
7. Jazskiewicz, A., Bledzki, A. K., & Franciszcak, P., “Improving the mechanical performance of PLA composites with natural, man-made cellulose and glass fibers--a comparison to PP counterparts”, Polimery, Vol 58, Issue 6, Pages 435-442, 2013.
8. Zhong, W., Li, F., Zhang, Z., Song, L. and Li, Z., “Short fiber reinforced composites for fused deposition modeling”, Materials Science and Engineering A, Vol. 301, Pages 125–130, 2001.
9. Shofner ML, Lozano K, Rodríguez-Macías FJ, Barrera EV., “Nanofiber-reinforced polymers prepared by fused deposition modeling”, Journal of Applied Polymer Science, Vol. 89, Issue 11, Pages 3081-3090, 2003.

10. Perez, A.R.T., Roberson D.A. and Wicker, R.B., "Fracture Surface Analysis of 3D-Printed Tensile Specimens of Novel ABS-Based Materials", *Journal of Failure Analysis and Prevention*, Vol. 14, Issue 3, Pages 343–353, 2014.
11. Namiki, M., Ueda, M., Todoroki, A., Hirano, Y. ve Matsuzaki, R. "3D Printing of Continuous Fibre Reinforced Plastic", *Proceedings of the Society of the Advancement of Material and Process Engineering*, Seattle, 2-5 June 2014.
12. Weng, Z., Wang, J., Senthil, T., & Wu, L. "Mechanical and thermal properties of ABS/montmorillonite nanocomposites for fused deposition modeling 3D printing", *Materials & Design*, Vol. 102, Pages 276–283, 2016.
13. Varsavaş, S. D. (2017). "Effects of glass fiber content, 3D-printing and weathering on the performance of polylactide", Yüksek Lisans Tezi, [Cam elyaf miktarının, 3D-yazıcı ile şekillendirmenin ve atmosferik yaşlandırmanın polilaktitin performansına etkileri] [Thesis in English], Middle East Technical University, Ankara, 2017.
14. ASTM Standart D638, "Standart test methods for tensile properties of plastics", ASTM International, West Conshohocken, PA, 2010.
15. ASTM Standard D790, "Standard test method for flexural properties of unreinforced and reinforced plastics and electrical insulating materials," ASTM International, West Conshohocken, PA, 2010.
16. ASTM Standart D6110, "Standard Test Method for Determining the Charpy Impact Resistance of Notched Specimens of Plastics", ASTM international, West Conshohocken, PA, 2004.
17. Khan, B.A., Na, H., Chevali, V., Warner, P., Zhu, J., Wang, H., "Glycidyl methacrylate-compatible poly(lactic acid)/hemp hurd biocomposites: Processing, crystallization, and thermo-mechanical response", *J. Mater. Sci. Technology*, Vol. 34, Pages 387–397, 2018.
18. Turner Brian, N., "A review of melt extrusion additive manufacturing processes: II. Materials, dimensional accuracy, and surface roughness", *Rapid Prototyp. J.*, Vol. 21, Pages 250–261, 2015.
19. Rahimizadeh, A., Kalman, J., Henri, R., Fayazbakhsh, K., Lessard, L., "Recycled Glass Fiber Composites from Wind Turbine Waste for 3D Printing Feedstock: Effects of Fiber Content and Interface on Mechanical Performance", *Materials*, Vol.12, Issue 23, Number 3929, Pages 1-12, 2019.
20. Carneiro, O., Silva, A., & Gomes, R., "Fused deposition modeling with polypropylene", *Materials & Design*, Vol.83, Pages 768-776, 2015.
21. Zuo, Y., Wu, Y., Gu, J., Zhang, Y., "Effect of fiber dosage on properties of glass fiber reinforced starch / polylactic acid composites", *Journal of Functional Materials*, Vol. 46, Issue 21, Pages 21148-21152, 2015.
22. Chen, K., Yu, L., Cui, Y., Jia, M., & Pan, K., "Optimization of printing parameters of 3D-printed continuous glass fiber reinforced polylactic acid composites", *Thin-Walled Structures*, Vol. 164, No:107717, Pages 1-9, 2021.
23. Yu, L., Chen, K., Xue, P., Cui, Y., & Jia, M., "Impregnation modeling and preparation optimization of continuous glass fiber reinforced polylactic acid filament for 3D printing", *Polymer Composites*, Vol. 42, Issue 11, Pages 5731-5742, 2021.
24. Li, X., Ni, Z., Bai, S., Lou, B., "Preparation and Mechanical Properties of Fiber Reinforced PLA for 3D Printing Materials", *IOP Conference Series: Materials Science and Engineering*, Volume 322, Issue 2, No:022012, Pages 1-12, 2018.





ULUSLARARASI 3B YAZICI TEKNOLOJİLERİ
VE DİJİTAL ENDÜSTRİ DERGİSİ

INTERNATIONAL JOURNAL OF 3D PRINTING
TECHNOLOGIES AND DIGITAL INDUSTRY

ISSN:2602-3350 (Online)

URL: <https://dergipark.org.tr/ij3dptdi>

AN EVALUATION OF STUDENTS' CYBERSECURITY AWARENESS IN THE MARITIME INDUSTRY

Yazarlar (Authors): İsmail Karaca , Ömer Söner 

Bu makaleye şu şekilde atıfta bulunabilirsiniz (To cite to this article): Karaca İ., Söner Ö., “An Evaluation of Students' Cybersecurity Awareness In The Maritime Industry” *Int. J. of 3D Printing Tech. Dig. Ind.*, 7(1): 78-89, (2023).

DOI: 10.46519/ij3dptdi.1236264

Araştırma Makale/ Research Article

Erişim Linki: (To link to this article): <https://dergipark.org.tr/en/pub/ij3dptdi/archive>

AN EVALUATION OF STUDENTS' CYBERSECURITY AWARENESS IN THE MARITIME INDUSTRY

İsmail Karaca^{a,b} ^{*}, Ömer Söner^b 

^aIstanbul Technical University, Maritime Faculty, Maritime Transportation Management Engineering
Department, Türkiye

^bVan Yüzüncü Yıl. University, Maritime Faculty, Maritime Transportation Management Engineering
Department, Türkiye

* Corresponding Author: ismailkaraca@yyu.edu.tr

(Received: 16.01.2023; Revised: 21.03.2023; Accepted: 25.04.2023)

ABSTRACT

Maritime operations have now become faster, safer, and more secure than before, as technological changes in the maritime industry have increased significantly over the past decade. However, no matter how advanced the technology is, removing the human variable from maritime operations is still impossible. Cybersecurity is one of the primary concepts that both enhance human adaptation to technology and reduce risk within the maritime industry. Training and raising situational awareness of maritime cybersecurity are the most basic of many defences to reduce vulnerabilities resulting from human beings not adopting technological changes. Therefore, this study proposes that maritime students' cybersecurity awareness should be investigated. For this purpose, a questionnaire is used, including 3 attitude scales. This is presented and applied to a sample group including 168 participants representing the population. This evaluation of students' cybersecurity awareness is aimed to provide taking the first steps to raise cybersecurity awareness in the maritime industry. In this study after a comprehensive investigation, quite striking findings have been obtained regarding awareness of maritime students' cyber security, and suggestions are made to increase students' cybersecurity awareness in the maritime industry.

Keywords: Awareness, Cybersecurity, Human Factor, Maritime Students.

1. INTRODUCTION

Despite all that it offers, the effects of the usage of technology cannot be predicted even using new technological methods [1]. According to [2], technology is widely used in many industries due to its advantages such as increased security and easy accessibility. (Matt et al [3]) says that there has been an increase in the number of initiatives to explore new digital technologies and take advantage of their benefits and that these initiatives often involve the transformation of core business operations, products, processes, organizational service structures, and management concepts. As a requirement of the global economy, the concepts of Operational Technology (OT) and Information Technology (IT) are gaining more and more importance [4]. According to [5], there are multi-level effects of using OT and IT in ensuring the sustainability of digitalization.

Undoubtedly, the maritime industry has been and will continue to be affected by digitalization. Even [5] stated that OT and IT have the potential to completely change maritime operations and ship-related activities.

IT and OT are not new concepts for industries, being instead similar concepts to the Internet of Things (IoT) [6]. When IoT is mentioned, it should not be understood that only devices connect to the internet. When objects are equipped with sensors and electronic circuits, they gain abilities to communicate with people and update their status information [7]. In recent years, digitization like IoT has emerged as an important economic driving force that accelerates growth and facilitates job creation because its digital connectivity services have been adopted by consumers, businesses, and governments. In the maritime industry, with

technological developments such as the IoT and digitization, there have been seen transformations that provide huge economic gains, as in the example of Singapore [8]. Digitalization and IoT offer great opportunities for stakeholders of the maritime industry, whenever the right planning is made, and the plan can be implemented with the right tools. The goal, of course, is that ships should be completely unmanned, and autonomous ships may be introduced. The International Maritime Organization (IMO) is the United Nations (UN) specialized agency responsible for the safety and security of shipping and is creating regulations to deal with completely unmanned maritime transportation [9]. According to the most recent IMO regulations, except for fully autonomous degrees, all ships require certain human operators and commands. In short, human beings are an important element of maritime transportation and will continue to be so soon. However, human adaptation to technological developments within the maritime industry leads to vulnerability. This vulnerability may be predicted but cannot be forestalled by taking precautions. Defining and determining maritime cyber vulnerabilities to attacks and threats, as well as defences, should be adopted as an integral part of each maritime operation. There is a problem with people's familiarity with cybersecurity.

Cybersecurity is defined as a computing-based discipline involving the creation, operation, analysis, and testing of secure computer systems [10-11]. Maritime cyber vulnerabilities include those in offices on shore, terminals, the supply chain, and the onboard infrastructure. Maritime cyber-attacks include malware, social engineering, phishing, water holing, port scanning, built-in software weaknesses, third-party contributions, brute force, distributed denial of service (DDoS), spear-phishing, and subverting the supply chain; maritime cyber threats are categorized as targeted, untargeted, intentional, and unintentional. The human factor is separately examined and considered to be a threat [12]. Maritime cyber defences are not exactly specific, but legislation and educations are essential for defences. Therefore, first of all, it is necessary to measure seafarers' awareness of cyber security.

Within (IMO [13]), the IMO developed and adopted some legal policies such as

recommendations for managing cyber risks in the maritime industry, cyber risk management in maritime security management systems, and Resolution MSC. 428 (98), recommendations for cybersecurity on ships. Other authorities like BIMCO, which is an international organization, the US Coast Guard, and the UK government worked to arrange legislation to prevent cyber threats [14–16]. However, technological developments are not only improving maritime transportation but also cybercrime. Cyber threats and attacks are developed swiftly so there are still deficiencies regarding what these threats are and the measures to be taken against them [17]. IMO regulations are basic legislations ensuring ship safety and security internationally and include the International Convention for the Safety of Life at Sea (SOLAS), Standards of Training Certification and Watchkeeping (STCW), MET, the International Safety Management (ISM) Code, and the International Ship and Port Facility Security (ISPS) Code. These all work to deal with the ever-growing threat of cyber security. Comprehensive and detailed legislation, including entirely new regulations, is necessary because technological developments have the potential to change all maritime operations via maritime safety and security.

When maritime legislation regarding technological developments is well-regulated, its contribution is obvious. This contribution lies in it providing shipping, accelerating the cargo handling operations of the ships, and making the commands and manoeuvres of the ships more safe and secure [18]. ECDIS, AIS, communication devices, and similar technological devices speed up maritime operations and ensure less human activity. However, the human factor is not completely removed from operations and, for safe navigation of the ship, continue to be an essential part of maritime operations. This in turn leads humans to be a cause of maritime accidents and incidents [19]. There could be security vulnerabilities that result from the adaptation of humans to advanced technology [20]. Furthermore, according to [21] human and machine intelligence are complementary for solving maritime operations problems. Until completely unmanned maritime operations are achieved, humans will continue to be a key factor in maritime operations. Human errors however have caused new maritime losses [22].

Especially human nonadaptation to technological developments could bring about maritime losses. For instance, cyber incidents can lead to loss of life, loss of control over ships or sensitive data, as well as ship and/or cargo hijacking [23]. Cybersecurity awareness measurement, which is the first step in achieving adaptation, is essential.

Just as the human factor is the key factor for maritime operations, it is also highly important for cybersecurity. The human factor is the weakest link within maritime cybersecurity [12]. What needs to be done to prevent economic and operational losses because of cyber-attacks is clear: to improve education and increase maritime cybersecurity [24]. Together with technological developments in the maritime industry, many issues of Maritime Education and Training (MET) programs need to be addressed and investigated to identify their strengths and limitations [25]. The most important of these issues is maritime cybersecurity. It can be thought that cyber security measures can be achieved in this way, but it is necessary to measure students' cyber security awareness in order to develop METs. Maritime cybersecurity is a basic concept of not only maritime security but also all maritime operations including maritime safety, navigation, loading and discharging operations, and maritime communication because, in these operations, technological devices, networks, and connections are used. There is an awareness of increased technological developments in maritime companies, but it was stated by (Wang et al. [26]) that this should be supported by training. Situational awareness on this topic must urgently be raised because of the dramatic increase in technological developments in the maritime industry. According to (Kimberly et al. [27]), training to raise awareness is the first line of defense against cyber and cyber-physical threats, as well as future threats.

In recent years, maritime science has drawn attention to cybersecurity awareness. In some studies that present cyber security threats and weaknesses that may be encountered in navigation, the lack of cybersecurity awareness has been pointed out [28–30]. Suggestions have been made regarding the cyber security threat to ships, such as the study conducted for ECDIS, which is a technological and mandatory requirement on ships [31]. In recent years, some

unexpected events like the Covid-19 epidemic have accelerated digitalization. This increase has underlined the importance of the concept of cybersecurity for ships, and the concepts of cyber awareness have come to the fore in such studies [32]. There has been also a study that draws attention to the importance of education in cyber awareness [20]. In a further study that included a cyber risk assessment, awareness was likewise highlighted [33]. It is seen that awareness and training are considered two important topics in the cybersecurity management system [34]. Survey studies on seafarers also mention the lack of cyber security awareness among seafarers [17] [35]. It has been found that sharing rules and information does not have a positive effect in terms of cybersecurity awareness in the maritime industry [36]. The common conclusion of all the studies encountered is this: there are deficiencies in ships' cybersecurity awareness [37]. In light of previous studies, it is clear that raising cybersecurity awareness is one of the most important conditions required to ensure more safe and more secure maritime operations, faster and larger volume transportation, and the many benefits of technological developments for the maritime industry are raising cybersecurity awareness.

The next question to be asked is to whom this training should be first targeted. Maritime students are the future of the maritime industry. Existent seafarers' awareness is important but younger students need also to adopt cybersecurity. It is assumed by many that maritime students, being largely digital natives, are more familiar with cyber security; however, this assumption has not been proven. For this reason, in this study maritime students' cybersecurity awareness is investigated. It is, therefore, possible to interpret the issue of education promoting cybersecurity, thanks to maritime students, who are the output of MET. This study uses a comprehensive 5-point Likert-type questionnaire to evaluate students' cybersecurity awareness, applies the aforementioned questionnaire to the sample representing the relevant universe, and evaluates the data formed with the results of the applied questionnaire with the analyses accepted in the literature. The aim is to have evaluated maritime students' cybersecurity awareness, as a first step to raising cybersecurity awareness in maritime

transportation. The target of this study is to take the first step of predicting incidents caused by human error, by evaluating maritime students' cyber security awareness. After that, researchers will more easily be able to ascertain ways to improve maritime cybersecurity awareness.

In this study, firstly, the hypothesis created for the evaluation of maritime students' cybersecurity is explained in section 2 and the method used to evaluate the hypothesis defined previously is explained in section 3. The necessary analysis for assessment of the method is explained in section 4, the findings and results are included in section 5, and discussions of this study are included in section 6. Finally, conclusions are drawn in section 6.

2. HYPOTHESIS

There are many cyber threats in shipping. If they are categorized in the literature, nine categories exist physical access, operating system support, and security patches, operating system configuration, Internet connection establishment, authorized access, awareness, policies and procedures, training, continuous evaluation, and improvement [31]. The crew's lack of awareness of general cyber procedures is considered a threat. It is assumed that the youth growing up at this age are aware of the general cyber security required by all forms of technology. Our first motivation, which is the starting point of this study, is to investigate whether this assumption is true.

H1 Maritime students have been made aware of general cyber security operations.

One of the most important pillars of cybersecurity is the right to protect personal data. For this reason, information security is also considered in cyber security [38]. Before investigating cybersecurity awareness on ships, it is necessary to measure information security awareness, which is essential for maritime cybersecurity awareness. It is thought that students have general knowledge about information security, just as they have general cyber security awareness. Therefore, our second hypothesis in this study is that students are familiar with information security.

H2 Maritime students have taken the necessary precautions against cyber security threats related to information security.

Maritime authorities have intensified their cybersecurity awareness studies over the last 10 years. Therefore, in its "Guidelines on Maritime Cyber Risk Management", the IMO stated that effective cyber risk management would be possible if all seafarers, starting from the highest rank, adopt maritime cyber risk awareness [39]. In this respect, awareness of maritime students who would take part in all levels of the maritime industry is essential. It is vital for seafarers, including maritime students, to be aware of the cyber security hazards and precautions required on board, in terms of cyber security [29]. This is also expected from maritime students.

H3 Maritime students are familiar with cyber threats on ships and the precautions to be taken against these threats.

3. METHOD

In this study, alternative hypotheses explained in section 2 are used. In line with the hypotheses, a questionnaire is created using the items shown in Table 1, and a 5-point Likert scale (from (5) strongly agree to (1) strongly disagree) is used for the questionnaire. Items in the questionnaire are shown in Table 1.

Table 1. Item number and items descriptions.

Number	Item
11	I know the requirements for a strong password.
12	I am aware of the need for a strong password.
13	I would never share my passwords with a friend.
14	I use one strong password for different websites and accounts.
15	I prefer my devices to be updated automatically.
16	I am careful when opening email attachments and links.
17	I only use reliable and reputable sites when surfing the web or downloading content.
18	I take care not to discuss sensitive/critical information in public.
19	I am familiar with appropriate methods for transmitting, storing, labelling, and processing sensitive/critical information.
110	I routinely back up my sensitive/critical data.

- I11 I always make use of encryptions when emailing my sensitive/critical data.
- I12 I know how/when hardware and mobile devices should be encrypted.
- I13 I am aware that posting messages on social sites or posting sensitive data or using third-party storage may violate policies or regulations.
- I14 I know how to protect myself from "social engineering" "phishing" and "cyber-crime".
- I15 I understand that the web address displayed in an email may differ from the link to which it will redirect.
- I16 I know that emails with attachments are the most common method of cyber-attack.
- I17 I know what a DDoS attack is and how it can disrupt or slow down the ship's IT systems or network services.
- I18 I am familiar with the manipulations of seafarers to gain access to the ship's critical systems and networks and to break a ship's security procedures.
- I19 I know the negative effects of seafarers using their own devices on board.

I20 Seafarers are a key factor in cybersecurity vulnerabilities.

Concepts of general cyber security and information security are interchangeable concepts. However, in this study according to hypotheses these concepts are different from each other based on a similar study in literature [40]. The general concept of cyber security specifically addresses what comes with technology, such as passwords, emails, automatic updates, and these risks. In the concept of information security, information security topics such as information, critical/sensitive information, and data are investigated.

Scales for hypothesis, items for scales, and their references given are shown in Table 2 and are taken as a basis. As a result of the hypotheses explained in section 2, the scales and items in Table 2 are determined to test the hypotheses. They are taken from the references listed in Table 2. Items are decided to literature given by references considering the hypotheses. They are accepted scales by literature.

Table 2. Hypothesis, Scale, Item number, References.

Hypothesis Number	Hypothesis	Scale	Item number	References
H1	Maritime students have been aware of general cyber security operations	General Cybersecurity Awareness	I1, I2, I3, I4, I5, I6, I7, I14, I15, I16	[40]
H2	Maritime students have taken the necessary precautions against cyber security threats related to information security	Information Security Awareness	I8, I9, I10, I11, I12, I13	[40]
H3	Maritime students are familiar with cyber threats on ships and the precautions to be taken against these threats	Ship Cybersecurity Awareness	I17, I18, I19, I20	[23]

The participants in this study are students at all levels studying in Turkish Maritime Institutes (Maritime High School, Maritime junior technical college, Maritime faculty, Advanced degree institute for Maritime Studies). Convenience sampling has been used as the sampling method due to easy accessibility, volunteerism, and low cost [41]. The questionnaire is implemented to the participants via the internet [42]. Google Forms is used for administering the questionnaire to the participants and obtaining the data. The link is

shared with the sampling group representing the population. In Turkey, there are totally 22,276 maritime students, 12,165 students are in high school, 10,111 students are in associate degree and bachelor's degree (amount of students in advanced degree are insignificant) [43]. These students are the population for this study. 168 participants constitute the sampling group. The sampling group represents the full population because their categorical distribution, shown in Table 3, is almost the same as that of the sample group. The data is converted to be used in SPSS.

Therefore, this sample group can be used for the population. It doesn't look like men and women are equally spread out in Table 3, but women

constitute a very little bit of currently active seafarers. So, this is an acceptable distribution.

Table 3. Categorical distribution of participants' demographical and educational information.

%	%	%	%
Student of	Age	Class	Sex
27.38	26.19	8.33	88.69
High school	13-17	Preparatory	Male
2.38	60.12	25	11.31
Associate degree	18-23	First-year	Female
69.64	12.5	19.05	
Bachelor's degree	24-30	Second-year	
0.6	1.19	17.26	
Advanced degree	30+	Third-year	
		30.36	
		Fourth-year and more	

To continue, the next step is analysis. In this study, descriptive analysis is used to investigate the hypothesis. However, Analyses regarding the validity and reliability of the data used in the study will be explained in the next section.

4. ANALYSIS

For analysis, IBM SPSS Statistics 20 is used in this study. Cronbach's coefficient alphas are

used for Reliability analysis. The value of the number of components, and Cronbach's Alpha, are given for all scales in Table 4 for reliability analysis. KMO values and Cumulative (%) rotation values are used for the adequacy of the sample and the validity of the descriptive analysis to be made. The cumulative rotation is reasonable and does not suffer from an insufficient number of participants.

Table 4. Results for reliability and validity analysis.

Scale	Number of components	Cronbach's Alpha	KMO value	Cumulative (%) rotation
General Cybersecurity Awareness	10	.925	.911	62.89
Information Security Awareness	6	.914	.888	70.25
Ship Cybersecurity Awareness	4	.852	.723	69.32
Total	20	.957	.932	56.67

Also, for advanced analysis, a Normality test is conducted. Skewness and Kurtosis values were found to be between -1.5 and +1.5 for all items. It is possible to say that the data is normally distributed [44]. Therefore, a parametric test is

convenient, and the data is suitable for descriptive analysis [45].

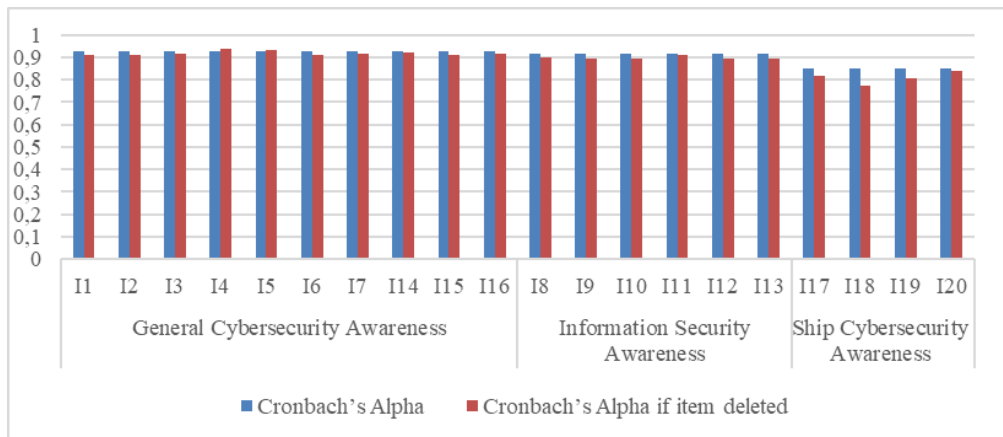


Figure 1. Cronbach's Alpha and Cronbach's Alpha if an item is deleted for items according to scales.

5. FINDING AND RESULTS

Firstly, basic statistics are examined for all items, considering scales.

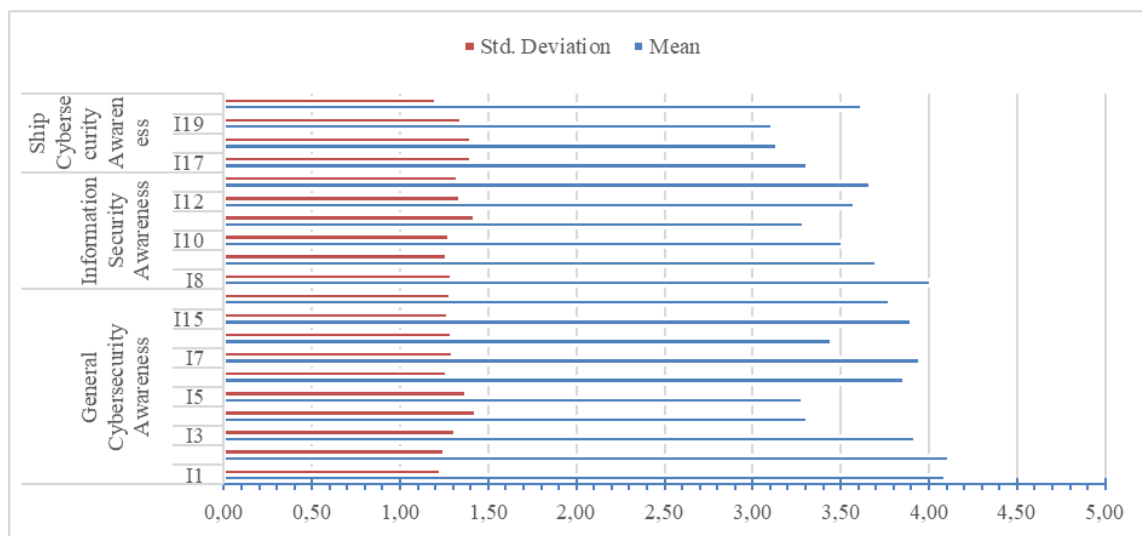


Figure 2. Values of items' basic statistics according to scales.

As a result of the normality test explained in the section Analysis, it was said that our data were normally distributed. It is possible to achieve meaningful results by interpreting values of mean and standard deviations. In Figure 2, all values for all items according to scales are shown. It appears that, although the items have included simple and general cybersecurity measures such as strong passwords and critical information, which are concepts that students are expected to be familiar with, items' mean, and standard deviation values show that maritime students' awareness levels for all scales are not sufficient for the safe usage of technological devices within the industry. There was no significant difference in score between the scales' items' values of mean and standard deviation because maritime students' awareness

levels for all scales are average or below average. To be satisfactory, it must be influenced. Therefore, maritime students' awareness of all scales should raise.

For the scale of ship cybersecurity awareness, items' mean, and standard deviation values show that ship cybersecurity awareness needs to rise because participants' responses to items are unsatisfactory. The deficiency in ship cybersecurity awareness is at the point where it cannot be ignored, and ship cybersecurity awareness is needed urgently. Human beings should adopt technological changes in the maritime industry because students are the primary resource of the future maritime industry. Cybersecurity is one of the basic concepts to ensure human adaptation to

technological development. The future maritime industry will include more complex technology and will need more complex concepts-based cybersecurity. Therefore, situational cybersecurity awareness must improve.

In Figure 2, one of the most remarkable values is I20's values, which are in the scale of ship cybersecurity awareness. I20 is "I know Seafarers are an important factor for ship cyber security." Students responded "agree" to I20. It was stated in the previous chapter that human

beings are a cause of loss from cyber-attacks, whether intentionally or unintentionally. The descriptive statistic of I20 is proof that students' intentions are not bad. It can be deduced from this that attention should be paid to the classification of unintentional cyber threats. This finding will help to determine precautions to raise awareness on this topic. In addition, this statistic explains that there is an awareness among students that they are important to cybersecurity.

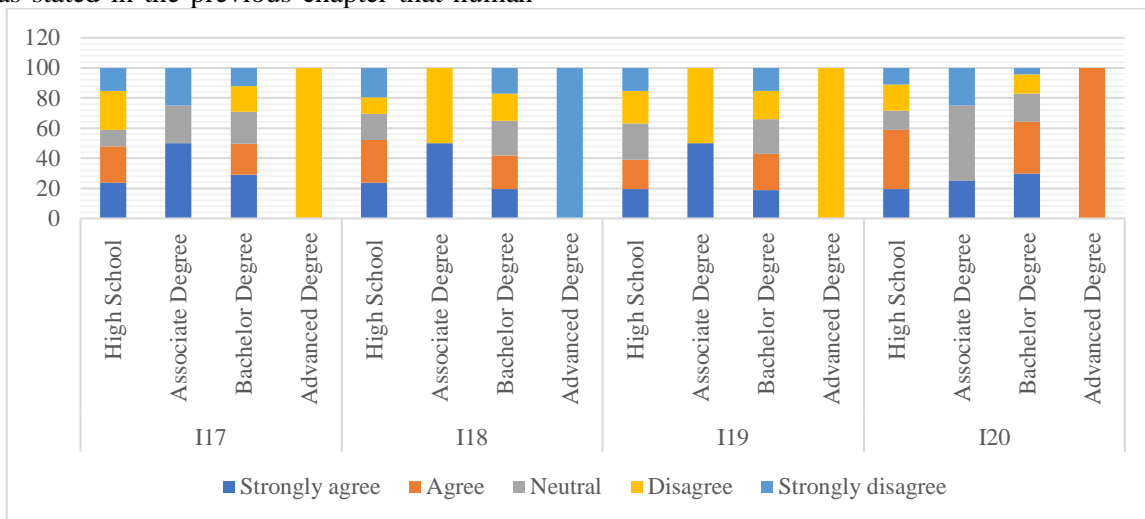


Figure 3. Items' distribution for ship cybersecurity awareness scale according to education level.

Items' distribution for ship cybersecurity awareness scale according to education level is shown in Figure 3. Advanced degree is omitted because the number of students in advanced degree programs is not sufficient to interpret. According to Figure 3, as the level of education increases, awareness increases for I20. This confirms literature and supports the motivation of this study. [26][23]. In general, it is seen

Figure 3 that the response distributions at education levels are similar except for I20. For I17, I18, and I19, response distributions of students in all education are similar. Therefore it is thought that all METs stakeholders are raising cybersecurity awareness similar level. This level is not satisfactory. If MET is thus updated to include maritime cybersecurity, situational awareness is ensured.

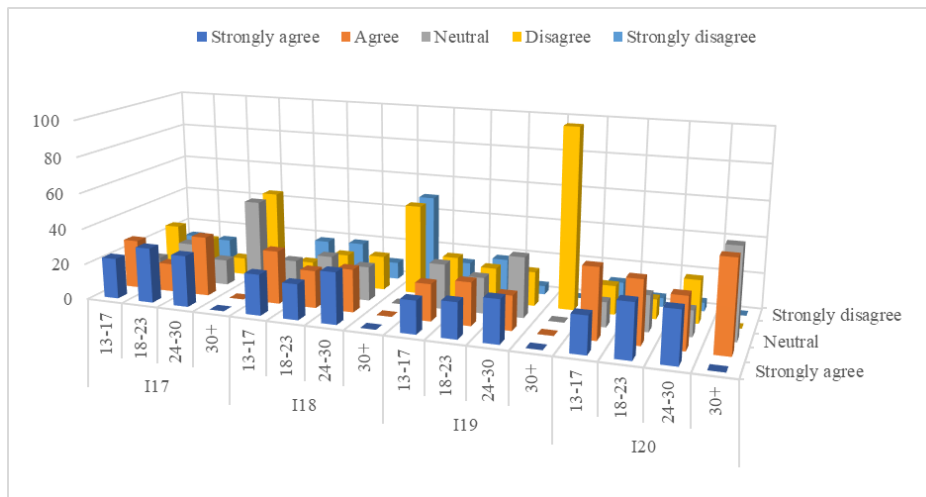


Figure 4. Items' distribution for ship cybersecurity awareness scale according to education level according to age.

Variation of items belonging to the scale of ship cyber security awareness according to age is shown in Figure 4. 30+ is omitted because the number of students aged 30+ is not sufficient to interpret. The rates of responses “Agree” and “Strongly agree” increased with increasing age. It is also possible to say that awareness increases with age. Although the rate of young individuals in technology use is high, it can be considered according to Figure 4 that as age increases, careful usage of technology also increases. It can be interpreted that careful use of technology should be ensured for young people.

Values of Cronbach's Alpha and Cronbach's Alpha if the item is deleted according to scales are shown that Figure 1. This figure shows that all items have relatively high internal consistency.

6. DISCUSSION

The maritime industry will grow and develop with the benefits of technological development like IT and OT, IoT, and digitization. Undoubtedly, safer, more reliable, faster, and more sea transportation is possible with technology. For the latest technology that automatic vehicles are introducing, IMO has even arranged the process for automatic ships [9][19][21]. Although the maritime industry has been convinced of the importance of awareness of cybersecurity, maritime training does not support that and situational awareness for seafarers does not ensure it completely. This is an issue that needs urgent action. The number of cyber threats will grow in the future and

cyber-attacks will also be more challenging [11]. If human adaptation to technology development in the maritime industry is to be ensured, the question of how to deal with the cyber vulnerability that may occur in the future should be discussed [21].

Human beings, one of the most crucial factors causing accidents in maritime transportation and trade, have not adapted to technological developments in the maritime industry. This means that the worker who is the cause of accidents may cause new accidents without being aware of technological developments. A human being can be the cause of cyber incidents and losses both intentionally and unintentionally. Neither METs nor STCW, the most important legal basis of METs, are compliant with cybersecurity [10]. With this study, it was noticed that maritime students do not have sufficient awareness of cybersecurity, and this may jeopardize the safety of the industry in the future. Several steps need to be taken to ensure this. First, STCWs must be regulated; secondly, MET must offer new training about cybersecurity; then the training needs to develop. Otherwise, not ensuring awareness of cybersecurity will cause marine losses. These losses will lead to larger economic losses for the maritime industry and the global economy [17].

The vulnerability caused by not ensuring complete awareness of cybersecurity affects all maritime operations [21]. Trade, loading, discharging, anchoring, navigation, and safety operations are affected by cybersecurity

vulnerabilities. These operations are a part of huge economic activities. These operations are related to not only maritime stakeholders such as the ship and port but also to coastal stakeholders. Cybersecurity attacks in the maritime industry affect coastal units where maritime operations are located and indeed the entire region could be affected. Therefore, cybersecurity awareness in the maritime industry should be enhanced [35]. The importance of increasing this should be discussed as soon as possible.

7. CONCLUSION

Because completely unmanned vehicles do not yet exist in the maritime industry, human beings are not yet remote from maritime operations. Although there are many vulnerabilities resulting from human adaptation to technological developments in the maritime industry, reducing these vulnerabilities is possible by investigating maritime cybersecurity, precautions for maritime cyber threats, and defenses against maritime cyber-attacks. Raising situational awareness and developing training about cyber security will facilitate human adaptation to technological developments in the maritime industry. Therefore, in this study, cybersecurity awareness was investigated, and this investigation was conducted on students engaged in maritime training, the future leaders of the industry. The study presented a first-step investigation to raise maritime students' cybersecurity awareness.

Although it is expected that students' cyber security awareness should be satisfactory since they are digital natives, the cybersecurity awareness of maritime students' needs to be improved swiftly. Students' cybersecurity awareness in the maritime industry is at a lower level than expected. In a period when technology advances and cyber-attacks are intensifying and developing, measures should be taken to close the gap caused by humans or to reduce the risk arising from this gap. Raising awareness and new training in cybersecurity for the maritime industry should be the target. Situational awareness of cybersecurity and maritime training is not sufficient to educate students who will have to deal with cyber-attacks. Technological developments in the maritime industry will supply faster, safer, and more secure maritime operations and these

operations will ensure a larger trade volume for the global economy if situational awareness and training about cybersecurity in the maritime industry are achieved. Otherwise, no matter how much technology improves, the losses caused by cyber security vulnerabilities may be as great as the returns of it.

There is a requirement that studies examine cybersecurity in METs. They could portray the different stances among the younger generations and how this would change the curriculum of MET. Besides, this study is a local study conducted in Turkey, and a future study can be expanded internationally. It covered students' awareness: this can also be expanded. This is also a first step study, and future studies must be done to raise students' cybersecurity awareness.

ACKNOWLEDGES

Authors can refer to companies, businesses, public institutions or projects that contributed to the study in this section.

There is no people/institutions for their support during the research and specify funding institution with grant number.

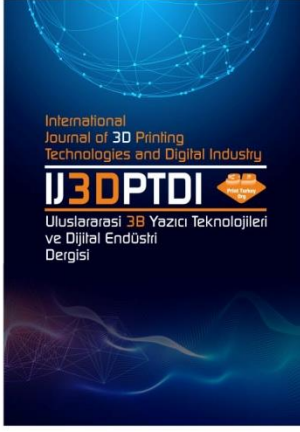
The studies have been approved by the appropriate institutional research ethics committee and have been performed in accordance with the ethical standards as laid down in the 1964 Declaration of Helsinki and its later amendments or comparable ethical standards.

REFERENCES

1. S. O. Hansson, "Coping with the Unpredictable Effects of Future Technologies", *Philosophy & Technology*, Vol. 24, Issue 1, Pages 137-149, 2011
2. S. T. M. Peek, E. J. M. Wouters, J. van Hoof, K. G. Luijkx, H. R. Boeije, and H. J. M. Vrijhoef, "Factors influencing acceptance of technology for aging in place: A systematic review", *Int. J. Med. Inform.*, Vol. 83, Issue 4, Pages 235–248, 2014
3. C. Matt, T. Hess, and A. Benlian, "Digital Transformation Strategies", *Bus. Inf. Syst. Eng.*, Vol. 57, Pages 339-343, 2015
4. C. Chauhan, V. Parida, and A. Dhir, "Technological Forecasting & Social Change Linking circular economy and digitalisation technologies : A systematic literature review of past achievements and future promises", *Technol. Forecast. Soc. Chang.*, Vol. 177, Page 121508, 2022

5. Y. Ichimura, D. Dalaklis, M. Kitada, and A. Christodoulou, "Shipping in the era of digitalization: Mapping the future strategic plans of major maritime commercial actors", *Digit. Bus.*, Vol. 2, Issue 1, Page 100022, 2022
6. I. C. Ehie and M. A. Chilton, "Understanding the influence of IT/OT Convergence on the adoption of Internet of Things (IoT) in manufacturing organizations", *Comput. Ind.*, Vol. 115, Page 103166, 2020
7. F. Wortmann and K. Flüchter, "Internet of Things: Technology and Value Added", *Bus. Inf. Syst. Eng.*, Vol. 57, Issue 3, Pages 221–224, 2015
8. K. Sabbagh, R. Friedrich, B. El-Darwiche, M. Singh, and A. Koster, "Digitization for Economic Growth and Job Creation: Regional and Industry Perspectives", *World Econ. Forum*, Pages 35-42, 2013.
9. IMO, "Outcome of the Regulatory Scoping Exercise for the Use of Maritime Autonomous Surface Ships (MASS)", 2021.
10. K. Cabaj, D. Domingos, Z. Kotulski, and A. Respício, "Cybersecurity education: Evolution of the discipline and analysis of master programs", *Comput. Secur.*, Vol. 75, Pages 24–35, 2018
11. A. M. Shabut, K. T. Lwin, and M. A. Hossain, "Cyber attacks, countermeasures, and protection schemes - A state of the art survey", 10th Int. Conf. Software, Knowledge, Inf. Manag. Appl., Pages. 37–44, 2017
12. S. Lagouvardou, "Maritime Cyber Security: concepts, problems and models," Master thesis, Kongens Lyngby, Copenhagen, 2018
13. IMO, "Maritime Cyber Risk Management In Safety Management Systems", 2017
14. BIMCO, "The Guidelines on Cyber Security Onboard Ships," *Int. Chamber Shipp. Shipp.*, Vol. 4, Pages 1–53, 2021
15. H. Boyes and R. Isbell, *Code of Practice: Cyber Security for Ships*. 2017
16. C. South, "USCG issue Cyber Risk Management Guidelines," 2022
17. S. Karamperidis, C. Kapalidis, and T. Watson, "Maritime Cyber Security_ A Global Challenge Tackled through Distinct Regional Approaches", *J. Mar. Sci. Eng.*, Vol. 9, Pages. 1–17, 2021
18. E. Peynirci, "The rise of emerging technologies : A quantitative-based research on ' maritime single window ' in Turkey", *Res. Transp. Bus. Manag.*, Vol. 1, Issue 1, Page 100770, 2021
19. M. Ramos, I. Utne, and A. Mosley, "On factors affecting autonomous ships operators performance in a Shore Control Center", 14th Probabilistic Safety Assessment and Management, Pages 16-21, Los Angeles, 2018
20. G. Potamos, A. Peratikou, and S. Stavrou, "Towards a maritime cyber range training environment", *IEEE Int. Conf. Cyber Secur. Resilience*, Pages 180–185, 2021
21. Ü. Öztürk, M. Akdağ, and T. Ayabakan, "A review of path planning algorithms in maritime autonomous surface ships: Navigation safety perspective", *Ocean Eng.*, Vol. 251, Pages 111010, 2022
22. A. Galieriková, "The human factor and maritime safety," *Transp. Res. Procedia* 40, 2019
23. I. Mraković and R. Vojinović, "Evaluation of Montenegrin Seafarers' Awareness of Cyber Security" , *Trans. Marit. Sci.*, Vol. 09, Issue 02, Pages 206–216, 2020
24. C. Parka, W. Shib, W. Zhangb, C. Kontovas, and C.-H. Changa*, "Evaluating cybersecurity risks in the maritime industry: a literature review", *The International Association of Maritime Universities (IAMU) Conference*, Pages 79–86, 2019
25. I. Milić-Beran, D. Milošević, and S. Šekularac-Ivošević, "Teacher of the Future in Maritime Education And Training" , *Knowl. Int. J.*, Vol. 46, Issue 1, Pages 119–125, 2021
26. H. Wang, O. L. Osen, G. Li, W. Li, H. N. Dai, and W. Zeng, "Big data and industrial Internet of Things for the maritime industry in Northwestern Norway," *IEEE Reg. 10 Annu. Int. Conf.* Pages 1-5, 2016
27. T. Kimberly, K. Moara-Nkwe, and K. Jones, "The Use of Cyber Ranges in the Maritime Context", *Marit. Technol. Res.*, Vol. 3, Issue 1, Pages 16–30, 2020
28. O. S. Hareide, O. Josok, M. S. Lund, R. Ostnes, and K. Helkala, "Enhancing Navigator Competence by Demonstrating Maritime Cyber Security", *J. Navig.*, Vol. 71, Issue 5, Pages 1025–1039, 2018
29. I. Mraković and R. Vojinović, "Maritime cyber security analysis – How to reduce threats?", *Trans. Marit. Sci.*, Vol. 8, Issue 1, Pages 132–139, 2019

30. B. Svilicic, M. Kristić, S. Žuškin, and D. Brčić, “Paperless ship navigation: cyber security weaknesses”, *J. Transp. Secur.*, Vol. 13, Issue 3–4, Pages 203–214, 2020
31. B. Svilicic, “Assessing ship cyber risks: a framework and case study of ECDIS security” , *WMU Journal of Maritime Affairs*, Vol. 18, Pages 509–520, 2019
32. K. Kuhn, S. Bicakci, and S. A. Shaikh, “COVID-19 digitization in maritime: understanding cyber risks,” *WMU J. Marit. Aff.*, Vol. 20, Issue 2, Pages 193–214, 2021
33. T. Kimberly and K. Jones, “MaCRA: a model-based framework for maritime cyber-risk assessment” , *WMU J. Marit. Aff.*, Vol. 18, Issue 1, Pages 129–163, 2019
34. B. Svilicic, I. Rudan, V. Frančić, and M. Doričić, “Shipboard ECDIS cyber security: Third-party component threats,” *Pomorstvo*, Vol. 33, Issue 2, Pages 176–180, 2019
35. I. Mraković and R. Vojinović, “Evaluation of Montenegrin seafarers’ awareness of cyber security”, *Trans. Marit. Sci.*, Vol. 9, Issue 2, Pages 206–216, 2020
36. P. Bolat and G. Kayışoğlu, “Antecedents and Consequences of Cybersecurity Awareness: A Case Study for Turkish Maritime Sector”, *J. ETA Marit. Sci.*, Vol. 7, Issue 4, Pages 344–360, 2019
37. Lv, Fang-Yuan. "Issues in Maritime Cyber Security Joseph Drenzo III, Nicole K. Drumhiller, Fried S. Roberts (Eds.)(2017)", *Marine Policy*, Volume 117, Pages 568, 2020
38. M. Turhan, “Siber Güvenliğin Sağlanması, Dünya Uygulamaları,” *Bilgi Teknolojileri Ve İletişim Kurumu*, Master Thesis, [Ensuring Cyber Security, World Practices] [Thesis in Turkish], Information technology and communications agency, Ankara, 2010
39. IMO, “ Guidelines On Maritime Cyber Risk Management”, 2017
40. University of Louisville Information Security Office, “Information Security User Awareness Assessment.”, <https://louisville.edu/security/files/user-awareness-questionnaire-pdf> , December 12, 2022
41. V. D. Sousa, J. A. Zauszniewski, and C. M. Musil, “How to Determine Whether a Convenience Sample Represents the Population”, *Applied Nursing Research*, Vol. 17, Issue 2, Pages 130-133 2004
42. İ. Karaca, “Denizcilik Öğrencilerinin Siber Güvenlik Farkındalıklarının Değerlendirilmesi Anketi”, [survey in Turkish], https://docs.google.com/forms/d/e/1FAIpQLSdQUuXyZK2xtUIK1iuGrWmswms_xNEwCMKkptLwLsTLGCvUw/viewform?usp=sf_link, December 12, 2022.
43. Deniz Ticaret Odası, “The Guidelines on Cyber Security Onboard Ships,” *Deniz Ticareti*, Vol. 6, Pages 28, 2022.
44. F. Barbara, Tabachnick; Sanford, “Using Multivariate Statistics (sixth ed.)”. Pearson, Boston, 2013.
45. L. Sthle and S. Wold, “Analysis of variance (ANOVA)”, *Chemom. Intell. Lab. Syst.*, Vol. 6, Issue 4, Pages 259–272, 1989



ULUSLARARASI 3B YAZICI TEKNOLOJİLERİ
VE DİJİTAL ENDÜSTRİ DERGİSİ

INTERNATIONAL JOURNAL OF 3D PRINTING
TECHNOLOGIES AND DIGITAL INDUSTRY

ISSN:2602-3350 (Online)

URL: <https://dergipark.org.tr/ij3dptdi>

CSS ÇATILARININ KULLANIMINDA KARŞILAŞILAN SORUNLAR VE ÇÖZÜM ÖNERİLERİ

USER EXPERIENCE AND ORIGINALITY PROBLEMS IN USING CSS FRAMEWORKS

Yazarlar (Authors): Anar Musayev ^{ID}*, Zülfikar Sayın ^{ID}

Bu makaleye şu şekilde atıfta bulunabilirsiniz (To cite to this article): Musayev A., Sayın Z., "Css Çatılarının Kullanımında Karşılaşılan Sorunlar ve Çözüm Önerileri" *Int. J. of 3D Printing Tech. Dig. Ind.*, 7(1): 90-104, (2023).

DOI: 10.46519/ij3dptdi.1243701

Araştırma Makale/ Research Article

Erişim Linki: (To link to this article): <https://dergipark.org.tr/en/pub/ij3dptdi/archive>

CSS ÇATILARININ KULLANIMINDA KARŞILAŞILAN SORUNLAR VE ÇÖZÜM ÖNERİLERİ

Anar Musayev^a , Zülfikar Sayın^a 

^aHacettepe Üniversitesi, Güzel Sanatlar Fakültesi, Grafik Bölümü, TÜRKİYE

* Sorumlu Yazar: anarmusayev@gmail.com

(Received: 28.01.2023; Revised: 15.03.2023; Accepted: 25.04.2023)

ÖZ

Bu makalede, CSS kod kütüphanelerinin bir sonraki adımı olan CSS çatılarının (Framework) ortaya çıkış, kullanım nedenleri ve web geliştirme süreçlerine olan etkileri incelenmektedir. Web tasarımında CSS çatılarının kullanımı birbirinden ayırmayan web tasarımlarının ortaya çıkmasına neden olmaktadır. Bir grafik tasarım ortamı ve ögesi olarak CSS çatıları hem bir bütün olarak hem de öğelerine ayrılarak irdelenmektedir. Öğeler ayrı ayrı özgünlük ve işlev bağlamında incelenmekle birlikte aynı zamanda grafik tasarım ilkeleri bağlamında da irdelenmektedir. Söz konusu ilkeler bütünlük, farklılık, vurgu, denge, düzen, alan, karşıtlık, tartım (ritim), tamamlayıcılık, devamlılık, oran/orantı vb. olarak belirlenmiştir. CSS çatılarını oluşturan öğeler ve birbirleri ile olan ilişkileri ilgili ilkeler bağlamında incelenmektedir. CSS çatılarının öğelere ayrılıp incelenmesinde özellikle CSS çatı öğelerinin tasarımını etkileyen kullanıcı deneyimi (UX) ile kullanılan teknolojilerin etkileri ve sınırlılıkları göz önünde bulundurulmaktadır. İncelemenin başka bir ölçüt olan işlevsellik açısından değerlendirmeler yapılırken özellikle kullanıcı deneyimi ve teknik özelliklerin etkileri üzerinde durulmaktadır. Yapılan değerlendirmeler sonucunda elde edilen verilerden hareketle web tasarımında nitelikli grafik etkiler elde etmek için CSS çatılarının önemi ortaya konmakta ve bu bağlamda önerilerde bulunmaktadır.

Anahtar Sözcükler: Grafik Tasarım, Web Tasarımı, Arayüz Tasarımı, CSS, HTML, CSS Çatısı, Uygulama Çatısı, Kullanıcı Deneyimi.

USER EXPERIENCE AND ORIGINALITY PROBLEMS IN USING CSS FRAMEWORKS

ABSTRACT

This article examines the emergence of CSS frameworks which is the next step of CSS code libraries, the reason for their usage and the impacts on web development processes. The use of CSS frameworks in web design leads to the emergence of inseparable web designs. As a graphic design environment and element, CSS frameworks are examined both as a whole and by separating them into elements. While elements are individually examined for both genuineness and functionality, they are also examined in the context of graphical design principles. The principles are determined as integrity, explanation, emphasis, balance, order, area, contrast, rhythm, completion, continuity, ratio/proportion. The CSS framework elements and their relationships are examined in the context of the principles. In the analysis of CSS framework elements, the user experience (UX) that affect the design of CSS framework elements and the effects and limitations of the technologies used are especially taken into consideration. While making evaluations in terms of functionality, which is another criterion of the examination, especially the effects of user experience and technical features are emphasized. As a result of the analysis, it reveals the importance of CSS frameworks to obtain desired graphic effects in web design and suggestions are provided in this context.

Keywords: Graphic Design, Web Design, Interface Design, CSS, HTML, CSS Framework, Application Framework, User Experience.

1. GİRİŞ

Web tasarımında CSS çatıları kullanıcı deneyimine olan olumlu etkilerinden dolayı tercih edilirken; söz konusu çatıları kullanarak oluşturulmuş web sitelerinin özgünlük sorunları tartışılarda neden olmuştur. Çağdaş endüstri toplumlarında üretim başarısı; ürünün mümkün olan en kısa sürede, en düşük maliyetle ve kabul edilebilir kalite sınırlarında sunulabilmesi ile doğrudan ilgilidir. Bu ilke bir grafik tasarım ortamı ve ögesi olan web sitesi tasarımı için de geçerlidir. Web sayfalarında etkileşim gereksinimleri, farklı boyut ve aygıtlarda görüntülenebilme ve gereksinim duyulan sayfaların üretim hacminin katlanması gibi nedenlerden dolayı “terzi işi” web sayfalarının yerini CSS çatıları ile hızlandırılmış ve yüksek tutarlılıkta seri üretim web sayfalarına bırakmasına neden olmuştur. Bu durum farklı hedef kitlelere hitap eden ve farklı içeriklere sahip web sitelerinin benzer arayüzlere sahip olmaları gibi bir olumsuz sonuç ortaya çıkarmıştır. Shenoy ve Prabhu’ya göre CSS çatısı veya çerçevesi (Framework), web siteleri ve web uygulamaları geliştirme görevini kolaylaştıran önceden tasarlanmış bir dizi kavram, modül ve standartlaştırılmış ölçütlerin tümüne verilen addır (Shenoy ve Prabhu [1]). Bu çalışmada CSS çatılarının web tasarımına olan etkilerinin yanı sıra bu etkilerin sonuçları da değerlendirilmektedir. Bu çalışmada amaçlanan, konu ile ilgili sorunları belirlemek, nedenlerini açıklamak ve söz konusu sorunların çözümü için öneriler sunmaktır. Tasarım dili odaklı bir CSS çatısı geliştirmek web tasarım sürecine olan bakış açısını değiştirmek açısından önemlidir. Bu çalışma ile CSS çatılarının sadece yazılım sürecini iyileştirmek için değil aynı zamanda özgün ve kullanıcı dostu siteler geliştirmek için de önemini ortaya konması amaçlanmaktadır. CSS Çatısı framework teknolojisine alternatif olabilecek seviyede benzer teknolojiler bulunmadığından bu makalede bir karşılaştırmaya yer verilmemiştir.

2. TANIMLAR ve KAVRAMLAR

Bu çalışmada kullanılan ve açıklanmasına gereksinim duyulan terimler ile kavramlar aşağıdaki gibi tanımlanabilir:

Web Sitesi, ortak bir alan adıyla tanımlanan ve en az bir web sunucusunda yayınlanan web sayfaları ve ilgili içeriklerin tümü için kullanılan bir sözcüktür.

UX (User Experience'in / Kullanıcı Deneyimi), kullanıcıların algı ve davranışlarını etkilemek amacı ile onların belli bir kurum ile olan deneyimlerini etkileyecek öğelerin oluşturulması ve senkronize edilmesidir (Unger ve Chandler,[2]).

CSS, Cascading Style Sheets (Basamaklı Stil Şablonları ya da Basamaklı Biçim Sayfaları, bilinen kısa adıyla CSS), HTML’e ek olarak metin ve format biçimlendirme alanında fazladan olanaklar sunan bir işaretleme dilidir.

Web Sayfası ise internette ulaşılabilen; görüntü, komut dosyaları ve genellikle başka sayfalara bağlantıların yer aldığı hiper metin dosyaları için kullanılmaktadır. (The Free Dictionary, [3]).

UI (User Interface / Kullanıcı Arayüzü), kullanıcıların bir makine, cihaz, bilgisayar programı ya da karmaşık aletlerle etkileşimini sağlayan yöntemlerin bileşkesine verilen ad olarak tanımlanabilirken; İnternet Tarayıcısı için web sayfalarının görüntülediği bilgisayar yazılımıdır, denebilir.

CSS Reset Dosyası (veya reset.css), HTML elementlerinin, tarayıcılara özgü stil kodlarını sıfırlayan kod dosyası olarak tanımlanabilirken; Kod Küçültme, işlevini değiştirmeden tüm gereksiz karakterleri, yorumlanmış programlama dillerinin veya biçimlendirme dillerinin kaynak kodundan kaldırma işlemi için kullanılmaktadır.

Drupal, ücretsiz, açık kaynaklı bir içerik yönetim dizgesi (sistemi) ya da içerik yönetim odaklı bir altyapı yazılımı iken; Duyarlı Web Tasarımı (Responsive Web Design), bir web sitesinin kendisini herhangi bir aygıtta ya da ekran genişliğine uyarlamasını sağlamak için sayfa düzeni (mizanpaj) çalışmalarında uygulanan tekniklerin tümüne verilen ad olarak açıklanabilir (Eva Harb, [4]).

İçerik Yönetim Sistemi: CMS (İng. Content Management System), sayısal (dijital) içeriğin herhangi bir kod yardımı gereksinim duyulmaksızın üretilmesi ve yönetilmesine olanak sağlayan bir çevrimiçi web yazılımıdır. *Animasyonlu GIF*, tek bir dosyada bir dizi görüntü veya çerçeve içeren ve kendi grafik kontrol uzantısı tarafından işlenen, İngilizce

Grafik Değişirme Biçimi anlamına gelen Graphics Interchange Formating (GIF) kısaltması olan kodlanmış bir görüntü türüdür. WYSIWYG, İngilizce'de "What You See Is What You Get" teriminin baş harflerinden oluşan bir bilgisayar terimidir. Türkçesi "Ne Görüyorsan Onu Alırsın" demek olup ekranda görülene çok benzer bir çıktı alınacağı ortamları tanımlamaktadır.

W3C (İng. World Wide web Consortium), üye organizasyonların, tam zamanlı çalışanların ve halkın web standartlarını geliştirmek için birlikte çalıştıkları uluslararası bir topluluktur. Web'in mucidi ve Yöneticisi Tim Berners-Lee ve CEO'su Jefferey Jaff tarafından yönetilmekte olan W3C'nin misyonu, web'in tam potansiyeline ulaşılabilmesidir (W3C, [5]).

3. CSS ÇATILARI

Temel amaçları yazılımcının işini hızlandırmak olan CSS çatıları web sayfaları veya uygulamaları geliştirmek için kullanılabilir araçların ve görsel öğelerin bütünü barındıran bir yazılım çatısı türüdür. Bilgisayar programlamasında, yazılım çatısı, genel işlevsellik sağlayan yazılımın, kullanıcı tarafından yazılan ek kodlarla seçici olarak değiştirilebildiği ve üzerine geliştirme yapılabilen temel kod kaynağıdır. CSS çatılarını incelemeyen önce genel olarak yazılım çatılarının ne olduğunu, özellikle nesne yönelimli kullanım nedenlerini anlamak gerekmektedir. Beck ve Johnson'a göre nesne yönelimli yazılım çatısı en genel tanımıyla, dizge ve alt dizgelerin, sınıflar ve bu sınıfların etkileşimi sayesinde tekrar kullanılabilir kod parçacıklarının bir bütünüdür (Beck ve Johnson, [8]). Yazılım çatıları çalışılan alan ve hedef platformlara göre üç ana öbekte (grupta) toplanabilir: i) mobil platformlar için geliştirilmiş çatılar, ii) veri bilimi ve makine öğrenimi için geliştirilmiş çatılar ve iii) CSS framework'lerin de dahil olduğu web uygulama yazılım çatıları.

CSS kullanımının yaygınlaşması, sadece HTML den oluşan web sitelerinin görsel zenginlik ve kullanıcı deneyimi açısından yetersiz kalması nedeniyle olmuştur. CSS sözcüğü Türkçeye Basamaklı Stil Şablonları ya da Basamaklı Biçim Sayfaları olarak çevrilebilir (İng. "Cascading Style Sheets"). İlk ticari web site olarak bilinen *Global Network Navigator* (GNN) web sitesini tasarlayan

Jennifer Niederst, buradaki "cascading" kavramını yukarıdan aşağıya birbirinin üzerine yazarak (bu aynı doküman için veya farklı dosyalar tarafından yapılabilir) oluşturulan ters hiyerarşiyi açıklamak için kullanıldığını belirtmektedir (Niederst, [6]).

CSS framework'lerin temelinde tasarım örüntüleri (İng. design patterns) ve kod kütüphaneleri (kod kitaplıkları) vardır. Bir kitaplık kullanmanın avantajı, kullanılmak istenen özelliğin veya çalıştırılmak istenen algoritmanın kütüphane kullanıcısı tarafından tekrar kodlanması gereksinimini ortadan kaldırmasıdır. Bunun yerine kütüphanenin yapısal tarafı için talimatlara uyularak sonuç elde edilebilmektedir (Meiert, [7]).

Günümüzde yaygın olarak kullanılan CSS Çatılarının birçoğu büyük web siteleri tarafından iç gereksinimler için geliştirilmiş ve daha sonra açık kaynak olarak internette paylaşılan projelerdir. Başlangıçta Twitter Baseline olarak adlandırılan Bootstrap birçok geliştirici için ilk kapsamlı CSS çatısı olmuştur. Mark Otto ve Jacob Thornton tarafından Twitter'da dahili araçlar arasında tutarlılığı teşvik etmek için bir çerçeve oluşturmak amacı ile geliştirilmeye başlanmıştır. Bootstrap'tan önce, kullanıcı arayüzü geliştirme için kullanılan çeşitli kütüphaneler, tutarsızlıklara ve yüksek bakım yüküne neden olmuştur. Tüm bu çalışmalar tek çatı altında toplanarak ilk olarak "Twitter Blueprint" daha sonra da 2011 Ağustos ayında Bootstrap olarak yayınlanmıştır (Otto, [9]).

CSS çatılarının ortaya çıkma nedeni olan büyük web projeleri birden çok ekip tarafından geliştirilen, bazen yüzlerce yazılımcı ve tasarımcının bir arada çalıştığı sürekli güncellenen ve gelişen kapsamlı projelerdir. Bir ekip tarafından oluşturulan bir modülün başka bir ekip tarafından kolaylıkla kullanılabilmesi ve hatta geliştirilebilmesi veya değiştirilebilmesi gerekmektedir. Günümüzde yaygın olarak kullanılan framework'lerin çoğu büyük web projeleri tarafından geliştirildikten sonra açık kaynak kod olarak paylaşılmışlardır. Twitter'ın Bootstrap ve Facebook'un React frameworkü en bilinen site, proje eş örneklerdendir (Çizelge 1). CSS Framework kullanımı yaygınlaştıkça, yazılımcı ve tasarımcılardan oluşan geniş camialar oluşmuştur. Bu da yazılım çatılarının test ve geliştirilmelerine katkı sağlamıştır. Herkese

açık olarak yayınlanan CSS çerçevelerin, onu kullanan, test eden ve geliştiren birçok geliştiricisi bulunmaktadır. Geniş topluluk tarafından geliştirilen ve test edilen kod hem güncel kalmakta hem de daha az hata içermektedir.

Çizelge 1. Farklı CSS çatılarının webde kullanım oranları. (bir web sitesinde birden çok CSS çatısı kullanılabilir). (Web Technology Surveys, [21]).

Bootstrap	% 78.9
Animate	% 39.3
Foundation	% 2.3
UIkit	% 0.7
Skeleton	% 0.6
Tailwind	% 0.5
Materialize	% 0.5
Material Design Lite	% 0.3
Semantic UI	% 0.3
Bulma	% 0.2
MetroUI	% 0.1

Geniş web tasarımcı kitleleri tarafından düzenli olarak framework'lerin kullanılması, iyileştirmek için bir yol bulunduğu veya karşılaşılan sorunlara çözüm üretildiğinde, geri bildirimlerle framework'lerin tasarımlara etkileri özyinelemeli hale gelmektedir (Bradley , [10]).

4. CSS ÇATISI KULLANIMININ AVANTAJLARI

CSS Çatısı kullanmanın en büyük avantajı geliştirme hızını ve üretkenliği artırmasıdır. Herhangi bir tasarıma (projeye) başlamadan önce üzerine geliştirme yapılabilecek temelin hazır olması çalışmaya başlama yolunda kolaylıklar sağlamaktadır. CSS çatısı kullanılmadan geliştirilen web sitelerinde projenin başlangıç süreci uzamakta ve farklı çözünürlüklerde tutarlılık sorunları ortaya çıkmaktadır. Özellikle, kullanılan tarayıcı çeşitliliğinin artması nedeniyle, oluşturulması gereken ilk proje dosyası artık reset.css olmaktadır . Farklı tarayıcılarda girdi alanları (İngilizce; input fields), açılır liste menüleri (İngilizce; drop-down), ipuçları, etiketler, tablolar, sıralı ve sırasız listeler farklı yorumlandığından CSS çatılarının sağladığı sıfırlama özellikleri reset.css dosyası gereksinimini de karşılayabilmektedir. CSS çatılarında uyarı pencereleri, bildirim iletileri, butonlar ve birçok tekrar kullanımına gereksinim duyulan tasarım öğelerinin hazır

bulunması nedeniyle doğrudan ve hızlı bir biçimde web sitesinin tasarımına başlanması kolaylaşmaktadır. Çok özel durumlar dışında web tasarımında ve genel olarak yazılım geliştirmede uygulama çatısı kullanmanın daha avantajlı olduğu söylenebilir. Standartlaşmış kod temelini oluşturulması hem bireysel hem de kurumsal kullanımda, CSS çatı kullanımının tercih edilmesinin en önemli nedenlerinden biridir. Özellikle geçmişe dönük bakım, destek çalışmalarında ve yeni özellikler ile modüllerin eklenmesinde CSS Çatısı kullanımı zamandan ve emekten tasarruf sağlayabilmektedir. Takım olarak çalışmayı kolaylaştırması, yazılım şirketlerinin CSS yazılım çatılarını tercih etmelerinin en önemli nedenlerinden biridir. CSS'e organize yaklaşım sağlaması ve şirket içi eğitim maliyetlerini düşürmesi başka bir nedendir. Yukarıdaki açıklamalar bağlamında denebilir ki; yazılım çatısı kullanmak hem takım olarak hem de bireysel kullanımda doğru tasarım alışkanlıkları geliştirilmesi açısından çokça önemli ve gereklidir.

Çizelge 2. meyerweb.com web sitesinden alınmış örnek CSS Reset Dosyası. (CSS Tools: Reset CSS. [22])

```
html, body, div, span, applet, object, iframe,
h1, h2, h3, h4, h5, h6, p, blockquote, pre,
a, abbr, acronym, address, big, cite, code,
del, dfn, em, img, ins, kbd, q, s, samp,
small, strike, strong, sub, sup, tt, var,
b, u, i, center,
dl, dt, dd, ol, ul, li,
fieldset, form, label, legend,
table, caption, tbody, tfoot, thead, tr, th, td,
article, aside, canvas, details, embed,
figure, figcaption, footer, header, hgroup,
menu, nav, output, ruby, section, summary,
time, mark, audio, video {
    margin: 0;
    padding: 0;
    border: 0;
    font-size: 100%;
    font: inherit;
    vertical-align: baseline;
}
article, aside, details, figcaption, figure,
footer, header, hgroup, menu, nav, section {
    display: block;
}
body {
    line-height: 1;
}
ol, ul {
```

```

        list-style: none;
    }
    blockquote, q {
        quotes: none;
    }
    blockquote:before, blockquote:after,
    q:before, q:after {
        content: "";
        content: none;
    }
    table {
        border-collapse: collapse;
        border-spacing: 0;
    }

```

5. CSS ÇATISI KULLANIMININ DEZAVANTAJLARI

Grafik tasarım açısından CSS Çatısı kullanımının istenmeyen en önemli sonuçlarından biri ortaya çıkan web sitelerinin özgünlükten yoksun olmasıdır denebilir. Bunun nedeni CSS çatısının, geliştirildiği platformun tasarım dilini taşıyor olmasıdır. Büyük web tasarımları için geliştirilen CSS çatılarındaki söz konusu tasarımların kurumsal izlerini silmek için teknik sınırlılıkların bilincinde olan tasarımcılar tarafından yapılan düzenlemeler ve bu düzenlemelerin koda uygulanması ile bu sorun aşılabilmektedir. Bu düzenlemelerin uygulama maliyeti yüksektir. Web tasarımında CSS çatısı kullanmanın getirisinin ötesine geçmesinden dolayı bu tarz özgünleştirme çalışmalarının çoğu CSS çatısının kullanımını sınırlamaktadır. Buna ek olarak belli bir tasarımın gereksinimleri için geliştirilmiş CSS çatıları kod yapısı ve modül içeriği bakımından tam olarak genel kullanıma uygun olmayabilmektedir. Buna karşın herhangi bir çatı kullanmadan yapılan geliştirmeler özgünlüğü kısıtlaya bilecek teknik sınırlılıklardan azat olmaktadır.

CSS çatılarının web tasarımına olan etkileri konusunda farklı bakış açıları söz konusudur. Bu etkiler kimilerine göre olumlu, kimilerine göre ise çeşitli olumsuzluklar bağlamında değerlendirilebilmektedir. CSS Çatılarında uygulanan grafik tasarımlarda karşılaşılan özgünlük sorunları grafik tasarımcılar açısından bir kayıp olarak görülürken, birçok geliştirici ise bu durumun kullanıcı deneyimine olumlu yansımalarını düşünmektedir.

CSS çatılarının yaygın olarak kullanılmasının en büyük etkisi duyarlı web tasarımlarının yaygınlaşması olmuştur. Özbahçe'ye göre Türkçe'ye "duyarlı" olarak çevrilen bu kavram, henüz evrensel kullanımı olan "responsive" kadar yaygınlaşmamıştır (Çelik Özbahçe, [11]). Bootstrap gibi CSS çatıları sayesinde birçok web tasarımcı farklı platformlarda çalışabilen akışkan ve hatasız web sitesi tasarlayabilme olanağına kavuşmuştur denebilir. CSS çatısının parçalarını kullanarak hızlı bir şekilde web sitesi oluşturma olanakları web sitelerinde özgünlük sorunlarına yol açabilmektedir. Öyle ki, bu bağlamda tüm sitelerin birbirinin benzeri haline geldiği eleştirisi sıklıkla ortaya atılmaktadır. CSS çatıları hazır birçok görsel modülü sunarken, bu modüllerin kullanımını zorunlu da kılmamaktadır. Tasarlanan web siteleri için özgün bir kurumsal kimlik oluşturmak yerine doğrudan CSS çatılarının sunduğu öğeleri kullanmak, tasarımcıların sıklıkla tercih ettiği özgünlükten yoksun uygulamalardır. İşe yeni başlayan duyarlı web tasarımcıların veya web sitesi tasarlayan duyarlı yazılım uzmanlarının CSS çatısı kullanması; zaman zaman özgün olmayan web sitelerinin ortaya çıkması sonucunu doğurmakta ise de hem görsel hem de işlevsel anlamda çok da kötü olmayan web sitelerinin tasarlanmasına da yol açabilmiştir. Denebilir ki; CSS çatılarının kullanımı bir kartopu etkisi yaratarak hem CSS çatılarını hem de web tasarım ilkelerini değiştirebilmektedir.

Web sitelerinin kullanılan aygıtlara göre kendini şekillendirebilmeleri genel olarak sayfalardaki arayüz yapılarının sağladığı esneklikler ile sağlanabilmektedir. Çünkü, aygıtlara özellikli davranış gösterme eylemleri, web sitelerini oluşturan sayfalardaki arayüz yapılarının kendilerini aygıtlara uydurması olanağı ile de gerçekleştirilebilmektedir.

Web siteleri, genellikle belirli aygıtların görüntülük (ekran) boyutlarına göre geliştirilebilmektedir. Çünkü tasarımcılar, hangi boyutta uygulama geliştireceklerine, hedef kitlelerinin yoğun olarak kullandığı aygıt ya da dünya genelinde en yoğun olarak kullanılan aygıt boyutuna göre karar vermektedirler. Aygıt boyutuna göre uygulama geliştirme sürecinde birden fazla görüntülük boyutundan söz edildiği zaman ise, işler biraz daha karmaşıklaşabilmektedir. EWT (Esnek Web Tasarımı) tanımı ortaya çıkmadan önce

tasarlanan web siteleri, ziyaretçilere, çoğunlukla masaüstü bilgisayar ortamında hizmet verirken, zamanın popüler görüntülük boyutuna göre tasarlanmışlardır. Ancak, zamanla İnternet erişim özelliği bulunan farklı aygıtların da insan yaşamına girmesi bu durumunun değiştirilmesin neden olabilmektedir. Bu nedendir ki, farklı aygıtların kullanım oranlarının artması ve özellikle de mobil aygıtların oldukça yoğun bir şekilde kullanımı, EWT'nin gitgide daha fazla önem kazanmaya başlamasına neden olmuştur (Budak ve Gezer, [12]). CSS çatılarının kullanımı duyarlı web sitelerinin tasarlanmasını hem yaygınlaştırmış hem de kolaylaştırmıştır. Esnek tasarımların akışkan yapılarının yetersiz kaldığı durumlarda, yani geniş yelpazede çeşitlenen boyutlara sahip mobil aygıtlar için CSS3 Medya sorguları (İngilizce; Media Queries) kullanılması gerekmektedir.

Medya sorguları, belirli bir tür görünüm için bir öğeye birden fazla CSS atanmasına olanak tanıyan bir sorgu türüdür. Bu sorgular, görüntülük tipine ve çözünürlüğüne göre stilleri yeniden yapılandırarak genişlik, yükseklik, yön ve hatta çözünürlük gibi özellikleri değiştirmeyi kolaylaştırabilmektedir (Turan ve Şahin, [13]). Dolayısıyla, akışkan tasarım ve mobil uyumluluk sorunları CSS çatılarında çözümünü bulmuş sorunlardan olmuştur.

Yazılım kütüphaneleri ve CSS çatılarının eskiden beri en çok dile getirilen bir sorunu da gereğinden fazla kod barındırmaları olmuştur. Bazen kod kütüphanesinin sadece %5'ne gereksinim duyulmasına karşın, bu kütüphanenin tüm uygulamaya dahil edilmesi gerekebilmektedir. Ama bu sorun, günümüzde bilgisayar ve telefonların işlem ve görüntü işleme güçlerinin artması ve internet hızlarının kod temelli dosyaları yüklerken yeterli seviyede olmasından dolayı -özel durumlar hariç- ciddi bir dezavantaj olarak görülmemektedir. Ayrıca CSS çatısı kodları genellikle kod küçültme (İngilizce; minification) işlemi yapılarak dağıtılmaktadır.

6. YAYGIN KULLANILAN CSS ÇATILARININ KARŞILAŞTIRILMASI

CSS çatılarının geliştirilme nedenleri, kullanım amaçları, hedef kitleleri ve ortaya çıkma öyküleri farklı olduğundan birçok CSS çatısının birbirleri ile kategorik karşılaştırılması pek doğru olmayabilmektedir. Geliştirici ve

tasarımcılar framework tercih ederken önceliklerini belirleyip onlara en uygun CSS çatısı ile devam etmeyi seçmektedirler. Bu kararlar bireysel veya kurumsal olmalarından bağımsız olarak gerçekleştirilecek tasarımın kapsamına göre belirlenmektedir. Eğer kullanılan teknoloji güncel ise genellikle en yaygın olan uygulama çatısını seçmek bazı durumlarda özgünlükten ödün vermek anlamına da gelebilmektedir. CSS çatısının yaygın olarak kullanılıyor olması ve özgün web siteleri oluşturabilmeye uygun olması istenen en temel özelliklerdir. Bu iki ekten birbirini sınırladığından dolayı, bu kısır döngü genellikle gelişen teknoloji ile çözülmektedir.

CSS çatısı kullanmada iki temel yaklaşım söz konusudur. Bunlardan birincisi CSS çatısını temel alıp onun mevcut sınıflarının üzerine özelleştirilmiş sınıflar yazarak ilerlemektir. Söz konusu yaklaşım genellikle daha geleneksel CSS çatılarının kullanıcıları için geçerlidir ve sonuçta ortaya çıkan siteler büyük farklılıklar gösterebilmektedirler. Diğer bir yaklaşım ise CSS çatılarındaki sınıfları tasarım genelinde eksiksiz kullanmaktır. Bazı durumlarda söz konusu ön tanımlı çatı sınıfları yetersiz kalabilmektedir. Böylesi durumda ise kullanıcı topluluklarının veya üçüncü tarafların sağladığı eklentiler kullanılmaktadır.

Tüm CSS çatıları sundukları özellikleri farklı şekillerde sınıflandırmaktadırlar. Bunun nedeni bazen CSS çatısının tarihsel gelişimi bazen de çatıyı geliştirenlerin anlamsal (semantik) bakış açısıdır. Bazı CSS çatısı belgelerinde listelenen sınıflandırmalar aşağıdaki gibi sıralanabilir.

Aeon: Sadece ızgara sisteminden oluşmaktadır.

Bootstrap: Yerleşim, İçerik, Formlar, Bileşenler, Yardımcılar, Araçlar.

Bulma: Sütunlar, Elemanlar, Bileşenler, Formlar, Yerleşim, Yardımcılar.

Materialize CSS: Bileşenler, JavaScript Öğeleri, Forumlar, Mobil, Temalar.

Milligram: Tipografi, Blok Alıntılar, Butonlar, Listeler, Formlar, Tablolar, Izgara, Kod, Araçlar.

Pure CSS: Izgara, Formlar, Tuşlar, Tablolar, Menüler, Araçlar, Özelleştirme.

Semantic UI: Elemanlar, Koleksiyonlar, Görüntüleme, Modüller, Davranışlar.

Tailwind CSS: Özelleştirme Araçları, Temel Stillere, Yerleşim, Flexbox ve Izgara, Boşluk, Ölçülendirme, Tipografi, Fonlar, Çerçeveler,

Efektler, Filtreler, Tablolar, Geçiş ve Animasyonlar, Dönüşümler, Etkileşimler, SVG, Erişilebilirlik, Eklentiler.

UIKit: Bileşenler.

YAML: Normalleştirme Bileşenleri, Düzen, Izgara Sistemi, Sütün Yapısı, Form Elemanları, Yüzen Öğeler, Erişilebilirlik.

ZURB Foundation: Araçlar, Tipografi, Kontroller, Navigasyon, Konteynerler, Media, Eklentiler, Kütüphaneler.

Bu listeden de anlaşılacağı gibi, CSS çatılarının web tasarımına yaklaşımları arasında birçok ortak ve ayrışan nokta bulunmaktadır. Bu durum CSS çatılarının işlev ve özgünlük bakımından farklı ve birbirlerinin eşdeğeri olmadıklarını göstermektedir.

CSS Çatılarının gelişimi Izgara sistemlerine ihtiyaç duyulması ile başlamaktadır. Tüm CSS çatılarının temellerini ızgara sistemleri oluşturmaktadır. 960 Grid Sistem, yaygın olarak kullanılmaya başlanan ilk ızgara sistemidir (960 Grid System, 2021). Söz konusu sistemin ilk yayınlandığı dönemde ekran çözünürlükleri günümüzdeki gibi çok yüksek değerlerde olmadığından maksimum genişliği 960 piksel olarak sabitlenmiştir. Bu değer belirlenmesindeki başka bir etken de 960'ın , 3, 4, 5, 6, 8, 10, 12, 15, 16, 20, 24, 30, 32, 40, 48, 60, 64, 80, 96, 120 , 160, 192, 240, 320 ve 480 ile bölünebilmesidir. Daha sonra geliştirilen birçok CSS çatısında da benzer bir yol izlenmiştir.

Özellikle hem üçe hem de ikiye bölünebildiği için 12'lik sistem 2000'lerin ortalarında yaygın olarak kullanılan Drupal gibi içerik yönetim sistemlerinde de kullanılmıştır. Bootstrap'ın 12'lik ızgara sisteminin temelinde de benzer bir mantık vardır (Şekil 1). Bu ızgara sistemlerinin kullanımı CSS çatılarının günümüz web sitelerinin plan ve yerleşimini önemli derecede etkilemiştir. Birçok web sitesinin benzer oranlara sahip olmasının temel nedeni Bootstrap ızgara sistemidir. Bu şekilde sayfaların bölünmesi tasarımın bütünlüğüne, ritmine ve öğelerin birbirileri olan oran ilişkilerini olumlu olarak etkilemektedir.

.col-md-8	.col-6.col-md-4	
.col-6.col-md-4	.col-6.col-md-4	.col-6.col-md-4
.col-6	.col-6	

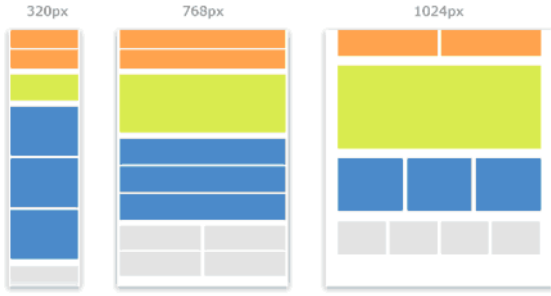
Şekil 1. Bootstrap 5'in farklı genişliklerdeki kolonlarına örnek

(<https://getbootstrap.com/docs/5.0/layout>).

7. CSS ÇATILARININ ÖĞELERİ BAĞLAMINDA İNCELENMESİ

7.1. Platformlar arası uyum

Platformlar arası uyum sorunu CSS Çatılarının çözüm getirdiği sorunların başında gelmektedir. Duyarlı tasarım sadece ana ızgaranın ölçülendirilmesinde değil, buton, menü, görsel gibi diğer tüm öğelerin tasarımında da belirleyici olmuştur. İçerik kolonlara yerleştirilirken içeriğin türüne göre farklı boyutlandırmalar gerekebilmektedir. Örneğin bir metin yerleştirilirken satırların çoğalıp metnin boyunu uzatması sebebiyle metin kesme işlemini ön yüzde yapmak gerekebilmektedir. Görseller boyutlanırken en boy oranını koruyarak boyutlandırmak önemlidir. Önceleri, tasarımların uyum sağlaması gereken aygıt boyutları bu kadar fazla değilken, her boyut için özelleştirilmiş tasarımlar yapılmış ve yazılımlar uyarlanmıştı. CSS medya sorguları böylesi sorunların çözümü için geliştirilmiştir. CSS sorguları tek başına yeterli olmayacağından, ölçü birimi olarak piksel ve punto yerine yüzde kullanılmaktadır. Bu tasarım yaklaşımı duyarlı web tasarımı (İng. Responsive Web Design) olarak adlandırılmaktadır. Duyarlı bir web sitesinde içeriklerin yer aldığı paneller belirlenmiş alanı tam kaplayacak şekilde yerleştirilmektedirler. Eğer içeriği göstermek için yatayda yeterli alan bulunmazsa sağda bulunan öğe soldakinin altına geçerek yine yataydaki genişliği doldurmaktadır (Şekil 2). Bu yerleşim tarzı da sadece mobil cihazlarda değil genel olarak web tasarımında kullanıcı deneyimini büyük ölçüde olumlu etkileyen dikey akışın önemini artırmıştır.



Şekil 2. Farklı çözünürlüklerde web sayfasını oluşturan blokların yerleşiminden görüntüler.

7.2. Dikey Akış

İnsanlar günlük yaşamlarında genellikle yatay düzlemde hareket ettiğinden, ufka baktıklarında gözlerini sağdan sola ya da soldan sağa hareket ettirmektedirler. Dolayısıyla ilk web sayfaları da yatay monitörlere uygun olarak yatay tasarlanmıştır. Mobil aygıtların gelişimi ile bu durum değişmiştir, tek parmak hareketi ile tüm içeriği dikey gezmek zorunluluğu ortaya çıkmıştır. İlk başta mobil aygıtlar için seçenekli tasarımlar geliştirilirken özellikle CSS çatılarının yerleşimi ile standartlaştırma çabalarından dolayı bütünlüklü çözümler ortaya çıkmıştır. Bunun sonucunda *dikey akış* web sitelerinin genelinde yaygınlaşmıştır.

Dikey akışın CSS çatılarında temel yönelim olmasının nedeni sadece mobil aygıtlarla uyumluluğu yakalamak değildir. Konuya psikolojik açıdan bakıldığında da öğelerin görsel olarak nasıl algılandığıyla ilgili en ünlü kuramlardan biri, aslen 19. yüzyılın sonlarında Almanya'da ortaya çıkan psikolojik bir kavram olan Gestalt ilkesidir. "Gestalt'ın Kapanış Yasası" gereği yatay tasarımlarda kapalı bir blok içerisinde içeriğin devamı olmadığı var sayılır ve daha fazla bilgi aranmaz. Sonuç olarak sayfanın geri kalanı gözden kaçırılabilir (Margalit, [14]). Çok geniş ekranlarda CSS çatılarının ızgara sistemleri kullanılarak kullanıcılara içeriğin bitmediği mesajı verilmektedir. Gözün sürekli kesilmiş görselleri tamamlama dürtüsü ile sayfa kullanıcı tarafından kaydırılmaya devam edilmektedir. Böylece yatayda yan yana duran içerikler bile dikey akışta bir devamlılık sağlayabilmektedir. Dikey akışı sağlamak için dikdörtgen kutular ve yatay kurallar, içeriğin sona erdiğinin görsel bir göstergesini ekler ve aksi takdirde sonraki içerik öğesini görüntüleyebilecek dikey pikselleri kullanır. Bu öğeleri ortadan kaldırmak ve sayfanın dikey boyutunu daraltmak, ziyaretçinin daha fazla kaydırma

olasılığını arttırmaktadır. Web sayfalarının dikey bir akış içerisinde yer alması, ritim, devamlılık ve denge bağlamında incelendiğinde grafik tasarım açısından olumlu sonuçlar doğurmakla beraber tasarımın özgün ve etkileyici görünmesini sağlayan zıtlık ve vurgu ilkelerinden ödün verilebilmektedir.

7.3. Konteynırlar

CSS çatılarının web tasarımında kullanımının yaygınlaşmasına önyak olan başka bir kavram "konteynır"dır. Konteynır kullanılmadığı zaman sayfadaki metin içeriklerinin gazete sayfalarında olduğu gibi görsel içeriklerin etrafını sarması ve boşlukları doldurması genel kabul gören tasarım yaklaşımıdır. CSS çatı kullanımı metin içeriklerinin ayrı bir blok içinde görsellere denk değerlendirilmesini sağlamıştır. Konteynır terimi bazı CSS çatıları tarafından içeriğin bulunduğu tüm öğeler için kullanılırken, diğerleri tarafından sadece içerik ve öğeleri kapsayan en dış çerçeveler için kullanılmaktadır. Dış çerçeveler yeniden boyutlanabilir ana öğeler oldukları için, sitelerin ekran boyutlarına göre yerleşime ve içindeki öğelerin kendi aralarındaki düzenine etki etmektedir. Konteynırların konumları ve görevleri kullanıcılar tarafından iyi bilinmekte bu da sayfaların kullanılabilirliğini artırmaktadır. Kanvası bölerek oluşturulan konteynırların yanı sıra, bir diğer konteynır türü de 'sticky on scroll' konteynırlardır. Bu konteynırlar, sayfanın üstünde, altında veya kenarında bulunan ve referans noktaları sayfanın kendisi olan "kanvas"ın bölünmesiyle oluşan aksine, tarayıcı kenarında bulunan yapışkan konteynırlardır. Özellikle mobil aygıtların yaygınlaşması ile aktif olarak web tasarımında kullanılmaya başlanmış ve CSS çatılarının önemli parçalarından biri haline gelmişlerdir. Bu tür konteynırlara örnek olarak mobil sayfalardaki ana menü konteynırları veya sayfanın bir kenarında bulunan iletişim butonları verilebilir (Şekil 3). Bu ve benzeri standartlaşmalar birbirine benzeyen ama kullanıcıyı hiç zorlamayan web şablonlarının oluşmasına neden olmuştur. Bu düzende bütünlük, denge, tartım (ritim) ve alan kullanımı gibi grafik tasarım ilkelerine uyum sağlanırken, farklılık ve vurgu gibi tasarımın ayırt ediciliğini artıran grafik tasarım ilkelerinden ödün verilmektedir.



Şekil 3. Rollrein.de sitesinin mobil görünümünde sağ altta yer alan telefon simgesi.

7.3. Tipografi

CSS çatıları ve CMS'ler dinamik metin içeriklerinin web sitelerine eklenme yöntemlerini de etkilemiştir. Dinamik sitelerde içerik veri tabanından iki yöntemle gelmektedir. Bunlardan birincisi WYSIWYG aracı kullanılarak yapılan girdilerin gösterilmesidir. Son kullanıcılar tarafından özellikle diğer tasarım kurallarını ezecek şekilde oluşturulan içeriklerin CSS çatıları tarafından formatlanması çok zordur. Genel görünüm için yönetim paneli kullanıcısı tarafından yapılan bazı düzenlemelerin sayfayı şekillendirmesine izin verilmekle beraber özellikle mobil görünüm için birçok tasarım düzenlemelerinin geçersiz kılınması gerekmektedir.

İkinci bir yöntem ise web tasarımı açısından daha sağlıklı olan, içeriklerin veri tabanına saf metin olarak kaydedilmesi ve gösterilirken tümüyle CSS çatılarına ait sınıflar tarafından şekillendirilmesidir. Böylece son kullanıcılar, ellerindeki yönetim paneli araçları ile genel tasarımın bütünlüğünü bozmamış olurlar. Kullanıcıların sınırlandırılması aynı zamanda içeriğe yoğunlaşmalarına yardımcı olduğundan, daha etkin bir yönetim deneyimi sağlamasına katkıda bulunmaktadır. CSS çatısı kullanımı böylece web sitelerinin bütünlüğüne de olumlu katkı sağlamış olmaktadır.

Metin temelli içeriklerin gösterilmesinde Tüm CSS çatıları var olan HTML etiketlerini aktif olarak düzenlemektedirler. Bunlar <h1>, <h2>, <h3>, <h4>, <h5>, <h6> gibi hiyerarşik başlık etiketleri, <p>, <mark>, , <s>, <ins>, <u>, <small>, ve gibi temel düzenleme etiketleri ve , , gibi özel listeleme etiketleridir. Bu etiketler genellikle temel hiyerarşi ve karakter korunarak minimum düzeyde şekillendirilir, zira bu tür ana öğeler sitenin tasarımını temelden etkilediğinden tasarımcı tarafından düzenlenmeye bırakılmadıklarıdır. Tema veya web sitesi tasarımcısı tarafından özelleştirilmeden bırakılan temel etiketler sitelerin özgünlüklerini kaybetmelerinde en önemli etkidir. Temel HTML etiketlerin yanı sıra yardımcı sınıflar da birçok CSS çatısı tarafından kullanılmaktadır. Metin hizalama, özel paragrafların ayrıştırılması, temel listelerin yanı sıra özelleştirilmiş listelerin oluşturulması ve alternatif başlık hiyerarşilerinin belirlenmesi için de yardımcı sınıflar kullanılmaktadır. CSS çatılarının HTML içeriğindeki tipografik öğelerin hiyerarşik yapısıyla uyumlu çözümler sunduğundan dolayı web tipografisinde bütünlüğü, dengeyi, zıtlığı ve vurguyu hem CSS çatısı öğeleri kullanarak hem de çatı üzerine ekleme yaparak sağlamak mümkündür.

7.4. Tablolar

Yine temel HTML öğelerinden olan tablolar, web tasarım tarihinde çok önemli bir yere sahiptir. İnternetteki içeriğin sadece metinlerden oluştuğu dönemde, içeriğin dikey ve yatay yerleşimini HTML tabloları sağlamışlardır. Modern web tasarımında satır ve sütunların oluşturulmasında HTML tablolar kullanılmaktadır. Tablonun ilk sütunu ve ilk satırı diğerlerinden ayrıştırılarak ve satırları tek ve çift olarak renklendirerek temel görünüm sağlanmaktadır. Tabloların yapısı neredeyse tüm CSS çatılarında aynıdır. Farklılıklar genellikle isimlendirme ve renklendirmeler ile sınırlıdır. JavaScript kullanılarak listeleme ve filtreleme özellikleri de eklenmektedir. Tabloların mobil aygıtlarda görünümü en sık karşılaşılan sorunlardan biridir. Bu yerleşim sorunlarının iki temel çözümü vardır. Birincisi aslında sorunu görmezden gelerek, tabloyu yatayda sürüklenerek şekilde yerleştirmektir. Bu çözüm mobil sitelerdeki dikey akışı bozduğundan daha az tercih edilmektedir. Ayrıca tabloların bu şekilde yerleştirilmesi denge, oran/orantı ve alan gibi grafik ilkeleriyle

ters düşmektedir. Diğer bir çözüm tabloyu mobil görünüm için yeniden tasarlamaktır. Sütunları kaldırıp içerikleri kartlar olarak satıra yerleştirerek ya da bazı içerikleri kapatıp açarak yatay bir tabloyu dikey ekrana yerleştirmek mümkündür (Şekil 4).

Kullanıcı No	İsim	Soyad	Yaş
0000001	Anar	Musayev	40
0000002	Ayşe	Kaya	37
0000003	Mehmet	Yılmaz	55
0000004	Fatma	Öztürk	28
0000005	Ahmet	Kara	95

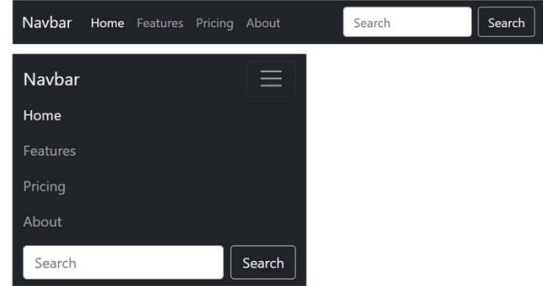
Şekil 4. Farklı ekranlarda tablo görünümü örneği.

CSS çatılarının bileşen listeleri büyük farklılıklar göstermektedir. Bazı CSS çatıları internette kullanılacak tüm modülleri kapsarken diğerleri oldukça sınırlı ana bileşen havuzuna sahiptir. Kullanılan çatının geliştirilecek olan web sayfasının kurumsal kimliği üzerindeki etkisini azaltmak için bileşenlerin tasarım kodlarının küresel dosyalara yazılması önemlidir. Yazı karakteri/boyutu ve renk paleti gibi özelliklerin tek bir yerden yönetilebilir olması CSS çatılarının kullanım kolaylığını artırmakla beraber, düzenlenmesi ek iş yükü getirmeyeceğinden tasarlanan web sitesinin özgünlüğünün korunmasını da kolaylaştırmaktadır.

7.5. Menü ve Bağlantılar

CSS çatı bileşenlerinde hiyerarşik olarak en başta menüler gelmektedir. Menülerin yerleşimi -katı kurallara bağlı olmasa da- web sitelerinde genellikle sol veya en üstedir. Bunun nedeni ekranın alt bölümünün işletim sistemlerinin, yönetim çubukları tarafından sahiplenilmiş olmasıdır. Yatay konumlama ise sayfa dilinin alfabetinin yazım yönü ile

alakalıdır; başka bir deyişle menüler genellikle ekranın sol tarafında yer almaktadır. Mobil tasarımda bu yerleşim ergonomik sebeplerden dolayı tümüyle değişmiştir. İşletim sistemi bildirim ekranları tepededir ve kapalıdır. Bu durum butonların bir kısmının sayfanın altında ve yatayda çok yer tutan menü bağlantılarının da hamburger ikonu olarak da bilinen ve üç yatay çizgiden oluşan tek bir simgenin altında gruplanmasına neden olmaktadır. Bu tercihte yazı yönünden ziyade insanın alet kullanmasında önemli rolü olan başparmak etkili olmuştur. Bazı CSS çatıları, geliştiricilere bağlantıların yanı sıra arama alanları ve özel bazı butonlar yerleştirme olanağı da sunmaktadır. Her durumda mobil görünüm için yeniden yerleşim yapılmaktadır (Şekil 5). Bu şekilde menülerin CSS çatıları tarafından standartlaştırılması farklılık, vurgu, alan, zıtlık (karşıtlık), ritim (devamlılık) gibi grafik tasarım ilkeleri bağlamında değerlendirildiklerinde sonucun olumlu olduğu pek söylenememektedir. Ama kullanıcı deneyimi açısından bu yapının vazgeçilmez olduğu kabul edilmektedir.



Şekil 5 . Bootstrap Navbar, bilgisayar ve mobil aygıtta görünümü (Bootstrap, 2018).

Metin ve büyük görsellerin yanı sıra web tasarımında simgelerin özel bir yeri vardır. Birçok simge takımı farklı CSS çatısı ile uyumlu çalışmaktadır. Bunlardan en yaygın olarak kullanılanı Font Awesome'dur. İlk versiyonlarında adından da anlaşılacağı gibi simgeleri font karakteri olarak kullanıma sunan Font Awesome en güncel versiyonunda SVG dosya formatının tüm olanaklarından yararlanmaya olanak tanımaktadır. Sonuç olarak, ister CSS çatıları için tasarlanmış olsun, ister bağımsız proje olarak geliştirilmiş olsun, genellikle simgeler çapraz olarak kullanılabilir durumdadır. Tasarımdaki özgünlüğün korunması adına simgelerin tasarıma özel olarak hazırlanması doğru seçenek olarak görülmektedir.

7.6. Uyarı ve Mesaj Pencereleri

Uyarı ve mesaj pencereleri kullanıcıları bilgilendirmek için kullanılan genellikle metinden ve bazen de bilgilendirici simgelerden oluşan öğelerdir. Söz konusu öğeler genellikle yapılan bir işlem sonucu veya işlem öncesi uyarı ve bilgilendirilme amacı ile yerleştirilmektedir. Bazı özel durumlarda üzerlerinde küçük butonlar da yer alabilmektedir. CSS çatılarının büyük bir bölümünde bulunan bu uyarılar; bilgi (İng. info), dikkat (İng. alert), başarı (ing. success), temel (İng. primary), uyarı (İng. warning), tehlike (İng. danger) gibi anahtar sözcükler ile adlandırılarak kullanım amaçlarına uygun renklerle eşleştirilip sınıflandırılmaktadır. Semantic UI örneğinde olduğu gibi sadece renklerin İngilizcedeki isimleri de kullanılabilir. Bu tür uyarı pencereleri gereksinim duyulan alana yerleştirilmek için <div> etiketleri içerisinde oluşturulmaktadır.

Web 2.0 ile yaygınlaşan etkileşimli web sitelerinin kullanıcıdan girdi almasının en önemli yollarından biri web formlardır. <input>, <textarea>, <select> <option>, <checkbox>, <radio>, <file> form etiketleri ile oluşturulan form elemanları <label> etiketi ile isimlendirilmektedir. Kullanıcıyı yönlendirmek için en basit şekliyle girdi alanlarının üzerine yazılan <label> etiketleri bazen aynı satırda bazen de yüzen etiket olarak tasarlanabilmektedir. Girdi alanları sade metin temelli girdiler dışında aralık, tarih, zaman ve renk gibi seçiciler için özelleştirilmiş tasarımlarla gelmektedir. Form alanları doldurulurken birçok kullanıcının yetersiz yönlendirilmesi kullanıcı deneyimini negatif etkilemektedir. Boş bırakılamaz alanlar için uyarılar, girilen içeriğin türünün uygunluğu gibi ön denetimlerin yapılması gerekmektedir. CSS çatılarında JavaScript ile yazılmış doğrulama araçlarının tespitlerini uyarı olarak kullanıcıya iletmek amaçlı renklendirme ve uyarı/bilgilendirme metinleri kullanılmaktadır.

7.7. Tuşlar veya Butonlar

Tuşlar veya butonlar web sitelerinde hem sayfalar arası yönlendirmeyi hem de zamanlanmış görevler hariç, yürütmeyi sağlayan önemli öğelerdir. CSS Çatılarında farklı görevleri üstlenen ve hem görünüm hem de işlevsellik bakımından farklılık gösteren tuş birim ve grupları bulunmaktadır. Tuşlar genellikle üzerine gelince (hover) renk veya

form değiştiren içerisinde metin ve/veya simge barındırabilen <input>, <a>, <button> etiketleridir. Gelişmiş CSS Çatılarında değişimler canlandırmalar (animasyon), hareketlendirmeler ile gerçekleştirilmektedir. CSS çatılarında semantik veya kurumsal renkler doğrultusunda renklendirme olanakları sunulmaktadır.

7.8 Etiketler

Farklı CSS çatıları tarafından İngilizce “tag”, “label”, “ribbon”, “badge” veya “tooltip” olarak adlandırılan, içeriğe ikincil bir açıklama olarak eklenen çeşitli etiket türleri vardır. Küçük bir görsel ile desteklenen etiket, kullanıcı listeleme ekranında veya herhangi bir listede renklendirmenin de yardımıyla öğeleri ayırtmaya yardımcı olabilmektedir.

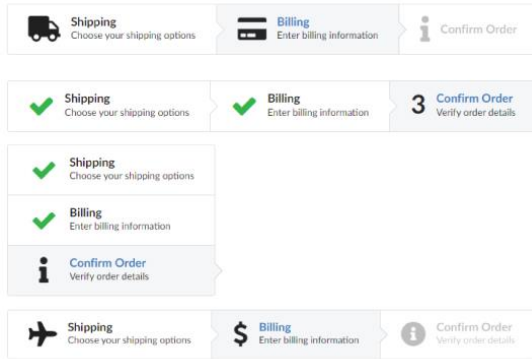
CSS çatıları tarafından animasyonlu GIF veya daha modern bir yaklaşım olan CSS canlandırmaları kullanılarak oluşturulan hareketli ilerleme veya önyükleme göstergeleri (İng. Preloader, Loader, Progress Bar, Spinners) farklı çatılar tarafından farklı isimlendirilmektedir. Özellikle AJAX kullanılarak içerik oluşturulurken, simge ve yüklenme çubukları söz konusu içeriğin yükleniyor olduğu bilgisini vermek için kullanıcı deneyimi göz önünde bulundurularak tasarlanmıştır.

7.9. Sayfalama ve Yönlendirme Bileşenleri

Web tasarımlarında kullanıcıyı yönlendirmede kullanılan bir başka önemli uygulama da sayfalama bileşenleridir. Genellikle tablolarda sayfalara numara koymak için kullanılan sayfa numaralandırmalarında önemli görevler üstlenen CSS çatılarında kartlardan oluşan haber başlıkları gibi içerikler de sayfalanamaktadır. Bir genel geçer olarak, sırasız liste etiketleri içerisine yerleştirilen (,) numaralı sayfa ve yönlendirme bağlantılarından da oluşan CSS çatılarının neredeyse tümünde benzer yapı ve görünümler söz konusudur.

Grafiksel kontrol ögesi olan Breadcrumbs (Türkçe: Ekmek Kırıntısı), bir sayfanın ara yüzünde kolay gezinmeyi sağlayan bir çeşit gezinti menüsüdür. Bu nitelime Hansel ve Gretel masalında iki kardeşin eve dönüş yolunu hatırlamak için yerlere serptiği ekmek kırıntılarında faydalanmalarına bir göndermedir (Levene, [15]). Breadcrumb'lar

Sayfalama aracında olduğu gibi neredeyse tüm CSS çatılarında benzer yapı ve tasarıma sahiptir. Ya “/” ya da “>” simgesi ile ileri sayfa hiyerarşisi gösterilmektedir. Örneğin *Anasayfa / Hakkımızda / Vizyonumuz* vb. Burada en sağda yer alan ve genellikle diğerlerinden yazı karakteri ağırlığı veya renk bakımından farklı olan öge aktif sayfanın adıdır. Genellikle <a> etiketleri içerisine yerleştirilen bağlantılar aktiftir. Modern interaktif sitelerde kullanımı yaygınlaşan başka bir sayfalama ögesi de adımlardır. Adımlar aşamalı işlemlerin sayfanmasında kullanılmaktadır. CSS Çatılarının birçoğu bu alanda yeterli olmadığından genellikle framework dışı çözümler aranmaktadır. Başarılı örneklerden biri Semantic Framework’ü tarafından sağlanan Step bileşenidir. Sırasız liste etiketleri içerisine yerleştirilen (,) bileşenleri duyarlı tasarım (İng. responsive) özelliğindedir (Şekil 6).



Şekil 6. *Semantic UI adımlar bileşeni (Semantic UI Steps, [16]).*

Yukarıda söz edilen bileşenler (uyarılar/mesajlar, form bileşenleri, tuş/tuş grupları, etiketler/rozetler, sayfalama bileşenleri) CSS çatılarının çoğu tarafından büyük ölçüde sağlanmaktadır. Bu bileşenlerin kullanılması kullanıcı deneyimini olumsuz etkilese de doğru tasarlanmış özgün bileşenlerle değiştirilmeleri web tasarımlarını daha özgün ve bütünlük, farklılık, vurgu, karşıtlık, ritim, devamlılık ve oran/orantı gibi grafik tasarım ilkeleri ile de uyumluluk göstermektedir.

7.10. Açılır Pencere

Uyarı, yönlendirme, vurgulama ve sayfalama gibi bileşenlerin yanı sıra birçok CSS çatısı seçenekli içerik gösterimi için açılır pencereler, genişleyen ve kayan öğeler ve kartlar gibi bileşenler sunmaktadır. Aktif sayfayı terk etmeden kullanıcıya daha fazla bilgi vermenin yaygın bir yolu farklı açılır pencereler

kullanmaktır. Web tasarımının gelişimi sürecinin ilk yıllarında tarayıcılar tarafından sağlanan açılır uyarı pencereleri kullanılmıştır. Genellikle otomatik açılan ve reklam gibi istenmeyen içerikler içeren bu pencereler pop-up olarak adlandırılmıştır ve kısa sürede yine tarayıcı ile antivirüs yazılımları tarafından engellenmeye başlanmıştır. Bu dönemde modal pencerelerin kullanımı yaygınlaşmıştır. Bootstrap tarafından yaygınlaştırılan bu biçim birçok diğer CSS çatısı tarafından da benimsenmiştir. Modallar genellikle tüm içeriği kapatacak şekilde açılan bir fonla gelmektedir ve modal içeriği sayfanın odak noktasına yerleşmektedir. Daha küçük (mütevazi) açılır pencerelere gereksinim duyulduğunda ise Bootstrap kullanıcılara Toast olarak adlandırılan sayfanın farklı köşelerinde açılan, gerektiğinde saydam (transparan) olabilen seçenekli bir bileşeni sunmaktadır. Benzer bileşenler diğer CSS çatıları tarafından Rail, FeatureDiscovery gibi isimlerle farklı ve özgün olarak tasarlanmıştır. Semantic UI tarafından tasarlanan Railer sadece pencerenin değil aynı zamanda sayfayı oluşturan konteynerlerin içinde veya dışında konumlanabilmektedir.

7.11. Diğer Bileşenler

Üste ve yana açılan pencereler dışında buldukları yerde genişleyen bileşenler, akordeon ya da İngilizce ‘collapse’ pencere olarak adlandırılmaktadırlar. Akordeon, etiketler veya küçük resimler gibi dikey olarak yığılmış öğeler listesi içeren bir grafik kontrol ögesidir. Her öğe, o öğeyle ilişkili içeriği ortaya çıkarmak için "genişletilebilir" veya "daraltılabilir" özelliğindedir. Akordeonlar *Sıkça Sorulan Sorular* gibi içeriklerin gösteriminde özellikle tercih edilmektedir. Arayüz tasarımında, sekmeli belge arabirimi (İngilizce; tabbed document interface, kısaca TDI) veya sekme olarak da adlandırılan bu bileşenler aslında kâğıt dosyalara veya kart dizinlerine eklenen geleneksel kart sekmelerinden esinlenerek tasarlanmışlardır. Tablar veya Sekmeler, belge kümeleri arasında geçiş yapmak için bir gezinme aracı olarak kullanılarak birden çok belgenin veya panelin tek bir pencerede yer almasına izin veren grafiksel kontrol öğelerindedir.

Açılan öğelerin yanı sıra carouseller gibi kayan öğeler de birçok CSS çatısı tarafından sunulmaktadır. “Carouseller web tasarımında

genellikle iki şekilde kullanılır. Bunlardan birincisi sayfada gezinti anında kullanıcılara sadece tek bir görüntünün sunulduğu düzendir. Genellikle ileri geri ve sayfalama tuşları ile geçişler yönlendirilmektedir. Çok fazla mesaj, hiç mesaj anlamına geldiğinden, özenle tasarlanmış Carouseller, afiş körlüğünün kurbanı olur ve içeriği çoğu kullanıcının dikkatinden kaçırır” (What is a carousel in web design, [17]). Bu nedenle web sitelerinin ana sayfalarında değişken fon görüntüsü olarak resmi olarak kullanılırlar. Carousellerin ikinci kullanımı başka bir web tasarım bileşeni olan kartların sergilenmesi amaçlıdır. Bu seçenek özellikle sayfada çok fazla bilgi yer aldığı, söz konusu bilgiyi daha kompakt bir şekilde gruplamaya yardımcı olmaktadır. Atlı karınca içerisine resimler eklemek, otomatik düzeni etkinleştirmek, devre dışı bırakmak, ayarlayabilmek ve tasarımı özelleştirmek mümkündür. İdeal olarak, her kart, kullanıcının soldan ve sağdan göz atabileceği farklı bir öge içerir. UIKit (Slider) ve Bootstrap (Carousel) en CSS çatılarında sunulan en kapsamlı atlı karınca bileşenleridir.

Bazı CSS çatıları tarafından geleneksel web bileşenlerine ek olarak “Paralax” veya “İraklık açısı” gibi modern web bileşenleri de sunulmaktadır. “Paralaks terimi ilk olarak, derinlik yanılması yaratmak amacıyla farklı hareket hızlarındaki fon görüntüsü kullanan, iki boyutlu ve yandan kaydırmalı video oyunlarının görsel etkisinden / efektinden gelmektedir. Bu etki, genellikle oyunun arka planının daha uzakta görünmesi için ön plana göre daha yavaş hareket ettirilmesiyle sağlanmaktadır” (Brown, [18]). Bir paralaks web sitesi, arka planda yerinde tutulan sabit görüntüler içermektedir ve kullanıcı, görüntünün farklı bölümlerini görmek için sayfayı aşağı kaydırabilmektedir. Görselin farklı bölümlerinin yanı sıra görsel üzerine yerleştirilmiş içerik üstünde de sayfa kaydırıldıkça değişiklikler olabilmektedir. UIkit tarafından sunulan bir Paralaks örneğinde sayfa aşağı kaydırıldıkça görselin renk tonu değişmekte ve üzerindeki yazılı metin aşamalı olarak kaybolmaktadır. Bu gibi farklı uygulamalar web sayfaları farklılık ve ritim bakımından ayrışmasını sağlamaktadır.

HTML 5 ve CSS 3 sayesinde CSS çatılarına eklenen canlandırmalar ve geçiş etkileri en son özellikler olarak sıralanabilir. Sözde sınıf olan

‘hover’ yıllardır ilkel canlandırmalar oluşturmak için kullanılmıştır. 2009 yılının mart ayında W3C tarafından resmen duyurulmasıyla sadece CSS kullanılarak sınırlı da olsa HTML etiketleri içerisine yerleştirilen görsel ve metinler bu sınıf kullanılarak hareketlendirilmeye başlanmıştır. İlk versiyonu 2012 yılında yayımlanan “CSS ANIMATIONS LEVEL 1” projesi W3C tarafından yönetilmektedir (World Wide Web Consortium (W3C), [19]). Günümüzde tarayıcı desteği büyük ölçüde sağlanmış olmakla beraber, bazı sorunların tümüyle çözülmemiş olmasından dolayı CSS çatılarında CSS canlandırma kullanımı hala gelişim aşamasındadır. TailwindCSS canlandırmalar, UIkit ise geçişler adı ile söz konusu özellikleri kullanıcılara sunmaktadır. Bunun yanı sıra Bootstrap gibi yaygın kullanılan birçok CSS çatısının da JavaScript tabanlı animasyon bileşenleri mevcuttur.

Paralaks ve canlandırma / hareketlendirme kullanımı vurgu, zıtlık ve denge gibi grafik tasarım ilkeleri bağlamında değerlendirildiğinde tasarıma çokça olumlu etkiler katmaktadır. Çünkü, web ortamlarının görünür olmasını sağlayan temel öğeler olarak grafik tasarım yapıtları ve uygulamaları ile karşılaşmaktadır. “*Grafik tasarım yapıtlarının* da gücü, niteliği, etkisi vd. özelliklerinin bilimsel irdelenmesi ancak kendine özgü tasarım ilkeleriyle gerçekleştirilebilmektedir” (Sayın [20]). Dolayısıyla Paralaks daha çok teknik bir özellik olmasından kaynaklı olarak web sayfalarının özgünlüklerine negatif bir etki göstermemekte, hatta tam tersi yaratıcı grafik tasarım çözümleri için olanaklar sunmaktadır.

CSS çatıları tarafından sunulan bir başka özellik de temalardır. Temalar geleneksel CSS çatılarının kapsamının dışında olmakla beraber, çatının görünen yüzü olduğundan genellikle temanın örnek uygulamaları hazırlanmaktadır. CSS Çatısını temel alacak bir projenin renk paleti, yazı tipi ölçeği, yazı tipleri, kesme noktaları ve köşe yarıçap değerleri tema dosyalarında tanımlanmaktadır. Özelleştirilmiş temaların kullanımı web tasarımında özgünlükten yoksun kalınmasının temel nedenlerindedir. Çatı kullanıcıları ürün veya kurumsal kimliğe en yakın temayı tercih edecekleri için temanın kullanıldığı her yerde aynı butonlar ve uyarı metinleri ile karşılaşabilmektedir. CSS çatıları genellikle

açık kaynaklı ve ücretsizdirler. Ama CSS çatılarında kullanılmak üzere üçüncü taraflarca hazırlanan şablonlar templatemonster.com gibi sitelerde satışa sunulmaktadır. CSS çatılarına bütünleşmiş temaların da daha küçük ölçekli bir pazarı mevcuttur. MaterializeCSS gibi bazı CSS çatıları, temaları ayrı bir ücret karşılığı resmi sitelerinde sunmaktadır. Temaların hem kullanıcı deneyimi hem sürdürülebilirlik hem de grafik tasarım ilkeleri açısından profesyonel anlamda kullanımından kaçınılmaktadır.

8. SONUÇ

CSS Çatılarında uygulanan grafik tasarımlarda karşılaşılan özgünlük sorunları grafik tasarımcılar açısından bir kayıp olarak görülmekte iken, birçok geliştirici ise bu durumun kullanıcı deneyimine olumlu yansıdığını düşünmektedir. Web tasarımında CSS çatısı kullanımı büyük ölçüde kullanıcı deneyimini olumlu etkilemektedir. Yazılım maliyetlerini düşürmesinin yanı sıra bazı projelerde kullanıcı deneyimi açısından tercih edilmektedir. Web sitesi tasarımlarında özgünlüğe olan olumsuz etkileri en aza indirmek teknik ve tasarım çözümleri ile olanaklıdır. Bu makalede söz konusu çözümler üzerinde durulmuş var olan çözümler incelenmiş ve yeni öneriler sunulmuştur. Bu makalede uzman yazılım ve tasarımcılar tarafından CSS çatısının sunduğu bileşenlere yapılan modifikasyonlar ile özgünlük ve kullanılabilirlik dengesini sağlamanın önemi anlaşılmıştır. CSS çatılarının sadece kullanıcı deneyimi ve teknik açılarından avantajlı olduğunu söylemek yanlış olur. Çünkü bütünlük, oran/orantı, denge ve ritim gibi grafik tasarım ilkeleri bağlamında web tasarımına olumlu etkileri söz konusudur. Grafik tasarım eğitimi veren yükseköğretim kurumlarındaki ilgili bölümlerde web yazılımları ile ilgili bir dersin ya da derslerin okutulması, söz konusu CSS çatılarından yararlanan grafik tasarımcıların özgünlük ve estetik açısından çok daha nitelikli yapıtlar ortaya koymasına için önemli katkılar yapacaktır.

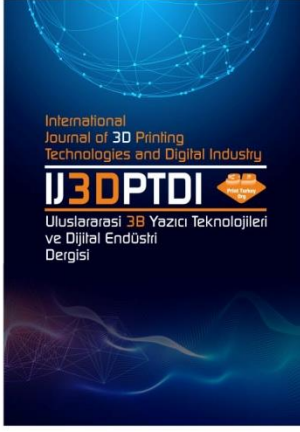
KAYNAKLAR

1. Shenoy, A., & Prabhu, A. "CSS Framework Alternatives: Explore Five Lightweight Alternatives to Bootstrap and Foundation with Project Examples", 25-26, Apress, Mumbai, 2018.
2. Unger, R., & Chandler, C. "A Project Guide to UX Design: For User Experience

Designers in the Field or in The Making (Second Edition)", New Riders, Berkeley, CA. 35-36, 2012.

3. "The Free Dictionary" www.thefreedictionary.com <https://www.thefreedictionary.com/web+page> Ağustos 20, 2021.
4. Eva Harb, Paul Kapellari, Steven Luong, Norbert Spot, "Responsive Web Design", iaweb, ws201, 18-17, Eylül 10, 2021.
5. "W3C, Consortium", <https://www.w3.org/Consortium/>, Eylül 13, 2021.
6. Niederst, J. "Web Design In A Nurshell", O'Reilly, Sebastopol. CA, 2021.
7. Meiert, J. O., "The Little Book of HTML/CSS Frameworks", O'Reilly, Sebastopol, CA, 2015.
8. Beck K., Johnson R., "Patterns generate architectures. 8th European Conference, ECOOP '94 July 4-8, Proceedings", 139-149. Bologna, 1994.
9. Otto, M., "Building Twitter Bootstrap", <https://alistapart.com/article/building-twitter-bootstrap/>, Ocak 17, 2021.
10. Bradley, "The Pros And Cons Of CSS Frameworks", <https://vanseodesign.com/css/css-frameworks-pros-cons/>, Mayıs 14, 2021.
11. Çelik Özbahçe, G., "Responsive Css Frameworkleri İle Yapılan Web Sayfalarında Ortaya Çıkan Özgünlük Problemi Ve Örnek Bir Responsive Web Sayfası Çalışması", Gazi Üniversitesi, Ankara, 2019.
12. Turan, O. B., & Şahin, K., "Responsive Web Design And Comparative Analysis Of Development Frameworks", The Turkish Online Journal of Design, Art and Communication, Ocak s., 14-16, TOJDAC, 2017.
13. Budak, V. O., Gezer, M., "Farklı Ekran Çözünürlükleri İçin Esnek Web Arayüz Yapıları Tasarlanması", Ejoboc (Electronic Journal of Vocational Colleges), 10-24, 2016.
14. Margalit, L., "Is Your New Website Layout Killing Your Engagement?" Neuroscience Marketing: <https://www.neurosciencemarketing.com/blog/articles/horizontal-website-layouts.htm>, Temmuz 11, 2021.

15. Levene, M., "An Introduction to Search Engines and Web Navigation." Wiley, London, 2010.
16. "Semantic UI Steps." semantic-ui.com: <https://semantic-ui.com/elements/step.html>, Eylül 07, 2021.
17. "What is a carousel in web design." <https://elevationballoonacademy.com/xxkvm/what-is-a-carousel-in-web-design>, Temmuz 11, 2021.
18. Brown, J., "What Is Parallax Web Design? Definitions, Tips & Considerations", <https://www.unleashed-technologies.com/blog/what-parallax-web-design-definitions-tips-considerations>, Eylül 10, 2021.
19. "World Wide Web Consortium CSS ANIMATIONS", <https://www.w3.org/standards/history/css-animations-1>, Temmuz 11, 2021
20. Sayın, Z., "Grafik Tasarımda Etki. 2. Baskı." Pegem Akademi, Ankara.
21. "Web Technology Surveys", https://w3techs.com/technologies/overview/css_framework, Mayıs 04, 2023.
22. "CSS Tools: Reset CSS", tarihinde <https://meyerweb.com/eric/tools/css/reset>, Mayıs 04, 2023.



ULUSLARARASI 3B YAZICI TEKNOLOJİLERİ
VE DİJİTAL ENDÜSTRİ DERGİSİ

INTERNATIONAL JOURNAL OF 3D PRINTING
TECHNOLOGIES AND DIGITAL INDUSTRY

ISSN:2602-3350 (Online)

URL: <https://dergipark.org.tr/ij3dptdi>

THE EFFECT OF NOZZLE DIAMETER AND LAYER THICKNESS ON MECHANICAL BEHAVIOR OF 3D PRINTED PLA LATTICE STRUCTURES UNDER QUASI-STATIC LOADING

Yazarlar (Authors): Emre Demirci^{ID*}, Safa Şenaysoy^{ID}, Salih Emre Tuğcu^{ID}




Bu makaleye şu şekilde atıfta bulunabilirsiniz (To cite to this article): Demirci E., Şenaysoy S., Tuğcu S. E., “The Effect of Nozzle Diameter and Layer Thickness on Mechanical Behavior of 3D Printed PLA Lattice Structures Under Quasi-Static Loading” *Int. J. of 3D Printing Tech. Dig. Ind.*, 7(1): 105-113, (2023).

DOI: 10.46519/ij3dptdi.1256993

Araştırma Makale/ Research Article

Erişim Linki: (To link to this article): <https://dergipark.org.tr/en/pub/ij3dptdi/archive>

THE EFFECT OF NOZZLE DIAMETER AND LAYER THICKNESS ON MECHANICAL BEHAVIOR OF 3D PRINTED PLA LATTICE STRUCTURES UNDER QUASI-STATIC LOADING

Emre Demirci^a ^{*}, Safa Şenaysoy^a , Salih Emre Tuğcu^a 

^aBursa Technical University, Faculty of Engineering and Natural Sciences, Department of Mechanical Engineering, TURKIYE

* Corresponding Author: emre.demirci@btu.edu.tr

(Received: 27.02.2023; Revised: 30.03.2023; Accepted: 25.04.2023)

ABSTRACT

Lattice structures are widely preferred because they have good properties such as lightness, high energy absorption capacity, and strength. Moreover, these lattice structures can be produced by utilizing a 3D printer. Therefore, this study aimed to explore the effect of the mechanical behavior of the different printing parameters on the lattice structures. Firstly, FBCC and FBCCZ lattice structures were printed with various printing parameters such as nozzle diameter of 0.25 mm-0.4 mm and layer thickness of 0.1 mm-0.15 mm. Then, quasi-static compression tests were performed to determine the mechanical behavior of lattice structures. Force-displacement behavior, equivalent elastic modulus, and energy absorption capabilities of lattice structures printed with different parameters were calculated from the results of the quasi-static compression test. According to the results, it was observed that the mechanical behavior was significantly affected when the nozzle diameter and layer thickness were changed. It was determined that the strength and energy absorption of the structures printed with a nozzle diameter of 0.25 mm and a layer thickness of 0.15 mm were decreased. In addition, it was observed that the influence of the printing parameters on the mechanical performance can be different according to the lattice type and lattice rod diameter. The combination of small nozzle diameter and high layer thickness caused a decrease in mechanical strength in both lattice types. Moreover, the highest specific energy absorption value was obtained in the samples printed with a 0.4 mm nozzle diameter and a 0.15 mm layer thickness.

Keywords: Lattice Structure, Printing Parameters, Mechanical Behavior, 3D Printing, PLA.

1. INTRODUCTION

Industrial revolutions undoubtedly have a great impact on our lives. When these revolutions are examined, it is observed that knowledge is constantly developing and changing. With each development, a higher quality, faster, lower cost, more functional, safer, and more accurate industrialization is aimed. 3D printing technology, which comes to the fore when the cornerstones of the sector are examined and has become the focus of attention of a wide segment, is an important technological development that will shape the current and future manufacturing process. The additive manufacturing method is universally used in various fields from defense to the aerospace industry, from the automotive to the biomedical sector [1-4]. Thanks to the developments in the field of additive manufacturing, complex

structures can be produced with different methods for the desired material. Some of these methods can produce 3D structures in layers by melting powder or filament materials, solidifying liquid materials, or injecting the material [5,6].

Additive manufacturing employs a variety of techniques, and among them, Fused Deposition Modeling (FDM) is one of the most widely utilized and popular processes. With the FDM process, the thermoplastic filament material is melted and combined layer by layer with a moving nozzle to obtain the desired geometry [7,8]. In addition, different types of polymeric materials such as Polylactic acid (PLA), Polypropylene (PP), Acrylonitrile butadiene styrene (ABS), Polycarbonate (PC), and composites can be used in this method and thus

structures can be produced according to different strength and thermal requirements [9]. In addition, the mechanical behavior of FDM-printed structures is influenced by a variety of manufacturing factors. The literature predominantly focuses on investigating the influence of manufacturing parameters on the mechanical characteristics of tensile test specimens printed via FDM [10-12]. Many studies show that various parameters such as layer thickness [13,14], building direction [15,16], infill densities [17-19], nozzle diameter [20], and printing speed [20,21] have notable effects on the mechanical features of FDM printed structures.

One of the most significant gains of additive manufacturing to production technologies is the ability to easily print structures that cannot be produced by traditional production methods. In this sense, lattice structures are prominent examples of situations where strength and lightness are desired together. Many different lattice structures have drawn the attention of researchers for various reasons. Lattice structures can be optimized for specific applications using generative design software, allowing for greater material efficiency and reduced weight without sacrificing mechanical performance [22, 23]. This makes them ideal for a range of industries, including aerospace, automotive, and medical, where weight reduction is critical for improved performance and efficiency. In addition, lattice structures provide a high level of design flexibility and customization, enabling the production of intricate geometries that would be challenging or unfeasible with conventional manufacturing techniques. Gürkan and Sağbaşı [24] investigated Ti6Al4V star, octahedral, and dodecahedron lattice structures for biomedical applications. In other studies, a 25% weight reduction was observed in the engine hood by using pyramidal lattice structures and 19% in gears thanks to honeycomb lattice structures [25,26]. Nasrullah et al. [27] studied the crashworthiness of eleven different types of lattice structures. Poyraz et al. [28] numerically investigated the elastic and physical properties of simple cubic, face-centered cubic, and body-centered lattice structures. Tang et al. [29] examined how the mechanical properties of PLA lattice structures are impacted by changes in both printing speed and printing temperature.

In this paper, equivalent young's modulus and energy absorption characteristics of face-and-body-centered cubic (FBCC) and FBCC with Z-strut (FBCCZ) lattice structures with different production and structural parameters were investigated.

2. MATERIALS AND METHODS

2.1. Lattice Design

For lattice structure design, cubic structure, one of the most widely used types in the research studies, was considered. FBCC and FBCCZ unit cells, which were determined to have superior mechanical properties among cubic-based structures in the literature review, were selected for the lattice structure design [30, 31]. The authors selected two distinct cell types to ascertain whether the impact of diverse parameters on mechanical properties remains constant, irrespective of the unit cell type utilized. The computer-aided design (CAD) models of the unit cell and lattice structures that were employed in this research were presented in Figure 1.

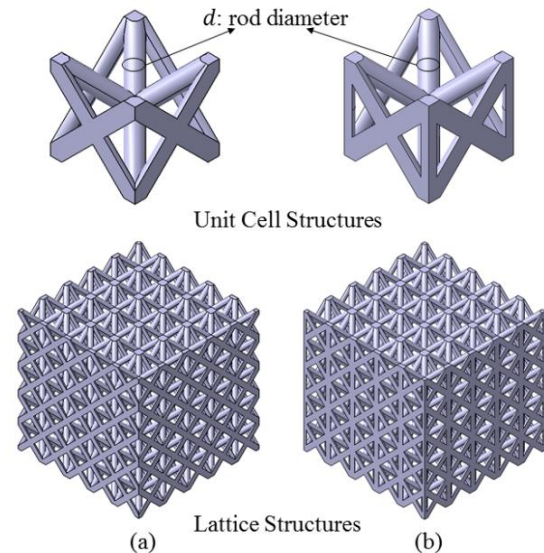


Figure 1. CAD model of the unit cell and lattice structures; (a) FBCC, (b) FBCCZ.

The unit cells were designed as 8x8x8 mm, as in many studies in the literature [32,33]. As the number of repetitions of the unit cell increases, the lattice structures better satisfy the periodic boundary conditions. On the other hand, the high number of repetitions of the unit cell leads to long printing time. Thus, the lattice structures were composed of 5x5x5 cells. The rod (strut) diameters of unit cells were determined as 0.75 mm and 0.1 mm as structural parameters. In this

way, a total of 4 different lattice structures, 2 FBCC, and 2 FBCCZ, were designed.

2.2. 3D Printing with FDM

The designed lattice structure CAD files were converted to STL format for manufacturing with FDM. The Ultimaker 3 Extended 3D printer was used for the additive manufacturing of lattice samples as shown in Figure 2. Ultimaker PLA filament with a diameter of 2.85 mm was utilized as the material. The mechanical properties of the PLA material for flat printing orientation were given in Table 1.

Table 1. Properties of the PLA material.

Property	Value	Unit
Young's modulus	3250	MPa
Yield stress (tensile)	52.5	MPa
Breaking stress (tensile)	45.5	MPa
Maximum elongation	7.8	%
Flexural modulus	3019	MPa



Figure 2. Manufacturing of lattice specimen with the 3D printer.

In order to print the lattice samples on the 3D printer, adjustment of the printing parameters and the G-code transformation of the STL data were performed with Cura software. All lattice samples, except for variations in nozzle diameter and layer thickness, were printed using constant printing parameters as listed in Table 2.

Table 2. Printing parameters.

Parameter	Value
Nozzle diameter	0.25 mm - 0.4 mm
Printing speed	30 mm/s
Build plate temperature	60 °C
Nozzle temperature	200 °C
Infill density	100 %
Filament diameter	2.85 mm
Layer thickness	0.1 mm – 0.15 mm

This study's goal was to find out how variations in nozzle diameter and layer thickness, as production parameters, impact the mechanical performance of lattice structures. Accordingly, two nozzle diameters, 0.4 mm, and 0.25 mm were selected utilizing diverse print cells that are compatible with the 3D printer. Also, as another production parameter, layer thicknesses were determined as 0.1 mm and 0.15 mm. Layer thicknesses were chosen considering the limitations of nozzle diameters for production. Table 3 lists the notation describing the combination of production and design parameters used in this research. A and B indicate the rod diameter as 0.75 mm and 1 mm, X and Y indicate the nozzle diameter as 0.4 mm and 0.25 mm, and 1 and 2 indicate layer thickness as 0.1 mm and 0.15 mm.

Table 3. Specimen combinations notation.

Specimen ID	Rod dia. (mm)	Nozzle dia. (mm)	Layer thickness (mm)
FBCC_AX1	0.75	0.4	0.1
FBCC_BX1	1.0	0.4	0.1
FBCC_AY1	0.75	0.25	0.1
FBCC_BY1	1.0	0.25	0.1
FBCC_AX2	0.75	0.4	0.15
FBCC_BX2	1.0	0.4	0.15
FBCC_AY2	0.75	0.25	0.15
FBCC_BY2	1.0	0.25	0.15
FBCCZ_AX1	0.75	0.4	0.1
FBCCZ_BX1	1.0	0.4	0.1
FBCCZ_AY1	0.75	0.25	0.1
FBCCZ_BY1	1.0	0.25	0.1
FBCCZ_AX2	0.75	0.4	0.15
FBCCZ_BX2	1.0	0.4	0.15
FBCCZ_AY2	0.75	0.25	0.15
FBCCZ_BY2	1.0	0.25	0.15

Variable parameters, such as nozzle diameter and layer thickness, were observed to affect the appearance of printed samples in a non-macroscopic manner. Hence, the pictures of FBCC_BX1 and FBCCZ_BX1 were given in Figure 3 as examples of printed samples.

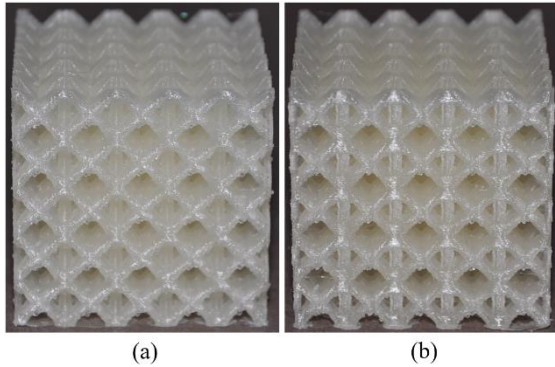


Figure 3. Example pictures of printed lattice structures: a) FBCC_BX1, b) FBCCZ_BX1.

2.3. Experimental Setup

The Shimadzu AG-X universal testing machine with a 250 kN load cell was used for the compression test of the lattice specimens. Experimental tests were carried out at room temperature. Compression speed was applied as 1 mm/min to provide quasi-static condition. As seen in Figure 4, the lattice specimen was placed on the fixed base table and subjected to compression load with the movable fixture. During the test, data were collected with TRAPEZIUM X software, and force-stroke values were obtained.

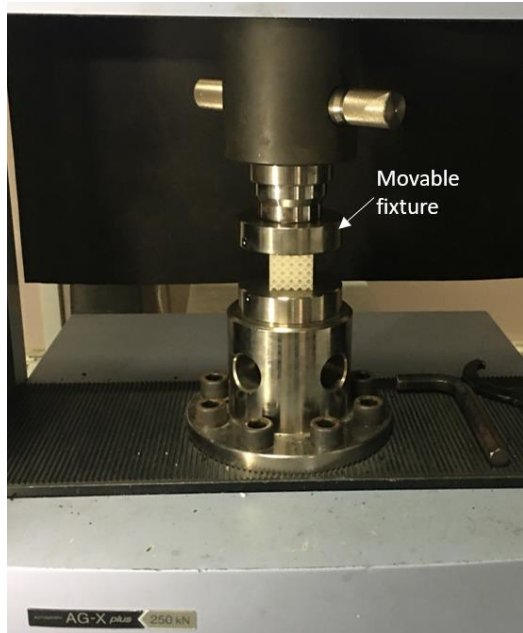


Figure 4. Compression test setup.

3. RESULTS AND DISCUSSION

3.1. Force-Displacement Behavior

In order to observe how production and structural parameters affect the crushing behavior of lattice structures, force-displacement curves of all samples were plotted in the same graph. As a result of the material's accumulation due to deformation during the test, the reaction forces increased significantly towards the end of the test, but this increase was not caused by the characteristics of the lattice structure. Therefore, all the graphs were plotted for 20 mm deformation. Figure 5 illustrates the force-displacement behavior of all FBCC samples.

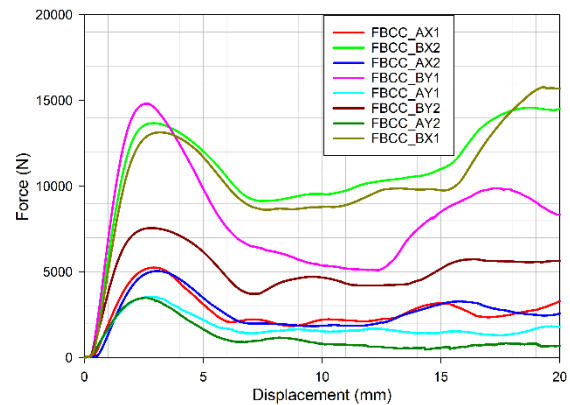


Figure 5. Force-displacement curves of FBCC samples.

It was seen that all FBCC samples show a linear behavior in reaction force increase to the first peak. It was observed that the first peak forces of the samples with a rod diameter of 1 mm were higher as expected. Samples FBCC_BX1 and FBCC_BX2 with layer thickness of 0.1 and 0.15 mm printed with a 0.4 mm nozzle exhibited similar behavior. However, it was observed that the curve characteristics of the FBCC_BY1 and FBCC_BY2 samples printed with a 0.25 nozzle were very different. The compressive strength of the 1 mm rod diameter FBCC_BY2 sample, which includes the combination of small nozzle diameter and high layer thickness, was considerably lower than the other 1 mm rod diameter samples. On the other hand, examining the results of the samples with a rod diameter of 0.75 mm, it was found that the compressive strength of the samples printed with a 0.4 mm nozzle was higher than that of those printed with a 0.25 mm nozzle. In addition, it was observed that the effect of the layer thickness was not much for the 0.4 mm nozzle, whereas the low

layer thickness value increased the strength in the samples printed with the 0.25 mm nozzle.

It was investigated whether parameter changes in the FBCCZ lattice structure gave similar results. Figure 6 illustrates the force-displacement behavior of all FBCCZ samples.

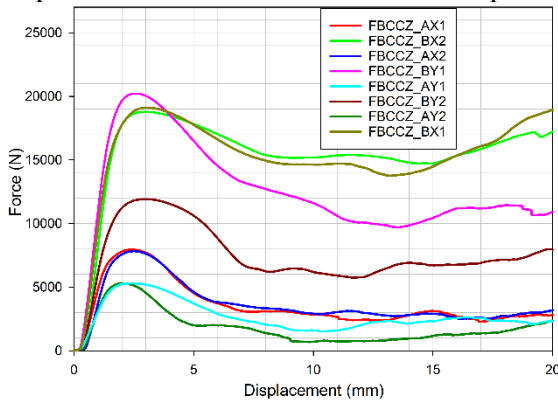


Figure 6. Force-displacement curves of FBCCZ samples.

When the graph is examined, it was seen that all FBCCZ samples have higher compressive strength compared to FBCC samples printed with the same parameters, thanks to the Z strut structures. Among the FBCCZ samples with a rod diameter of 1 mm, the strength of the sample printed with a nozzle with a diameter of 0.25 mm and a layer thickness of 0.15 mm is significantly lower than the others. Similar to the findings for the FBCC structures, it was observed that the structures printed with a 0.4 mm nozzle exhibited greater strength, particularly for the 0.75 mm rod diameter samples.

3.2. Equivalent Elastic Modulus

Elastic modulus is defined as resistance against deformation in the linear-elastic region and is one of the essential material properties. The equivalent elastic modulus approach is widespread to characterize the mechanical behavior of lattice structures. The lattice structure is considered as a continuous medium when calculating the equivalent elastic modulus. The equivalent elastic modulus was determined by using linear regions of force-displacement curves in Figures 5 and 6. Results of equivalent elastic modulus were given in Figure 7.

Figure 7 shows that FBCCZ lattice structures have higher equivalent elastic modulus than FBCC lattice structures since FBCCZ lattice

structures contain additional vertical struts in the compression test direction. As the bar diameter changes from 0.75 mm to 1.00 mm, the porosity ratio decreases, and the equivalent elastic modulus increases for both FBCC and FBCCZ structures. Therefore, lattice structures with a rod diameter of 1.0 mm exhibit more robust mechanical behavior. In lattice structures with a rod diameter of 0.75 mm, as the nozzle diameter decreases, the equivalent elastic modulus decreases for each lattice structure and layer thickness.

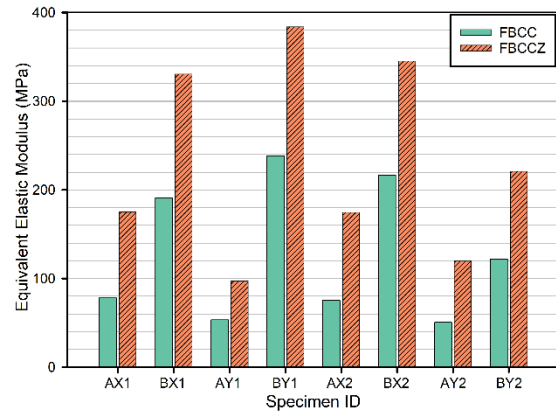


Figure 7. Equivalent elastic modulus of FBCC and FBCCZ samples.

It was determined that the model with the highest equivalent elastic modulus among all samples was the FBCCZ_BY1 model with a value of 383.79 MPa. Furthermore, among the FBCC lattice samples, the BY1 model reached the highest equivalent elastic modulus value. The lowest equivalent elastic modulus was obtained as 50.57 MPa for the FBCC_AY2 model. On the other hand, for the FBCCZ lattice type, the lowest value was obtained in the AY1 model. In the circumstances, lattice samples printed with 0.75 mm rod diameter and 0.25 mm nozzle diameter appear to be the worst combination for the equivalent elastic modulus. In combinations where the rod and nozzle diameters were kept constant and the layer thickness changed, no significant changes were observed between the results of the AX1-AX2, BX1-BX2, and AY1-AY2 models. On the contrary, increasing the layer thickness to 0.15 mm at 0.1 mm in the samples in which the lattice structures with a rod diameter of 1 mm were printed with a 0.25 mm nozzle resulted in a decrease of more than 50% in the equivalent elastic modulus.

3.3. Energy Absorption Characteristics

Determining a lattice structure's capacity to absorb energy is one of the important indicators used throughout the mechanical evaluation of that structure. The total energy absorption (E_T) is defined as the area under the force-displacement graph and is expressed as shown in Equation (1).

$$E_T = \int_0^{\delta} F(x)dx \quad (1)$$

where δ is the total displacement during the compression test and F is the crushing force. In cases where the weight of a structure is also

important, the total energy absorption index may not be an adequate comparison or evaluation parameter [34-35]. The specific energy absorption (SEA) value, which additionally considers the structure's mass, can be applied in this circumstance. SEA can be calculated by the formulation in Equation (2).

$$SEA = E_T/m \quad (2)$$

In this formula, the mass of the structure is denoted by m . The total energy absorption and SEA values obtained as a result of the test applied to all samples were given in Figure 8.

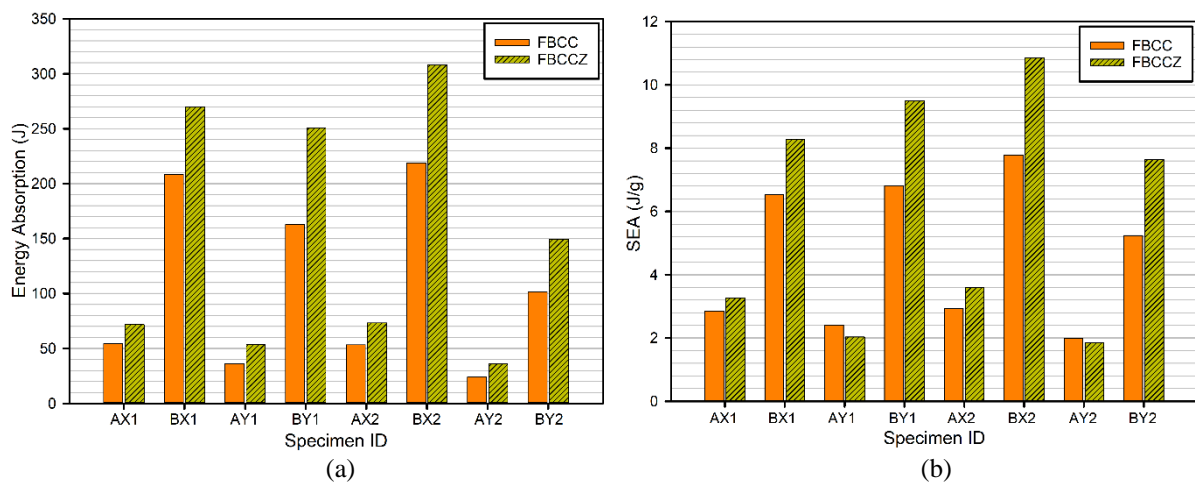


Figure 8. Comparison of lattice samples: a) total energy absorption values, b) specific energy absorption values.

When Figure 8a is examined, it is seen that the Z-supported structures absorb more energy. The structures that absorb the most and the least energy were FBCCZ_BX2 and FBCC_AY2 with the values of 380.18 J and 23.97 J, respectively. It is also an expected result that structures with a 1 mm rod diameter absorb more energy than structures with a 0.75 mm rod diameter. Among the structures with a rod diameter of 1 mm, the combination that absorbed the most energy was the BX2 samples produced with a layer thickness of 0.15 mm and a nozzle diameter of 0.4 mm for both lattice types. When the results of 0.75 mm rod diameter structures are examined, the layer thickness did not have a significant effect on energy absorption in the samples printed with 0.4 mm nozzle diameter, while the lower layer thickness gave better results in the samples printed with 0.25 mm nozzle diameter. Considering the nozzle diameter as the only variable, samples printed with a 0.4 mm nozzle absorbed more energy than samples printed

with a 0.25 mm nozzle for both FBCC and FBCCZ lattice structures.

In the production of thermoplastic materials with additive manufacturing, the mass of the lattice structure is affected by the production parameters [36]. It was necessary to take into account the change in the mass of the structures caused by the layer thickness and nozzle diameter variables. Therefore, in addition to total energy absorption, SEA values were calculated and shown in Figure 8b. Similar to the total energy absorption graph, the highest SEA value was obtained in the FBCCZ_BX2 as 10.85 J/g. Although it was observed that the FBCCZ structures absorb more energy in general, it was determined that the FBCC structure reaches a higher SEA value in the AY1 and AY2 models with the combination of 0.75 mm rod diameter and 0.25 mm nozzle diameter. This was due to the lighter mass of the samples printed with the 0.25 mm nozzle compared to the 0.4 mm nozzle. On the other side, it was found that increasing the layer thickness led to

the creation of lighter PLA structures, resulting in higher SEA values. While the structure with the worst performance in total energy absorption was FBCC_AY2, when the SEA values were considered, the lowest value belongs to the FBCCZ_AY2 structure with 1.85 J/g.

4. CONCLUSIONS

In this research, the mechanical performances of FBCC and FBCCZ lattice structures printed with different parameters using FDM under the quasi-static compression test were investigated. Two different layer thicknesses and two different nozzles were considered as printing parameters, and the effects of these parameters on structures with 0.75 mm and 1 mm rod diameters were evaluated. The experimental study's results were condensed and presented in the following manner:

- The Z structure added to the FBCC structure increased the initial reaction force under loading by an average of 48% in samples with a 0.75 mm rod diameter and by an average of 44% in samples with a bar diameter of 1 mm.
- Among the lattice structures with a rod diameter of 1 mm, the structures with the lowest strength were the samples printed with a nozzle diameter of 0.25 mm and a layer thickness of 0.15 mm. The initial reaction force of the samples printed with this combination decreased by about 83% and 62% for FBCC and FBCCZ, respectively, compared to the other samples.
- When the effect of production parameters on the equivalent elastic modulus was examined, it was observed that the effects changed according to the rod diameter of the lattice structures.
- Regardless of the lattice type and rod diameter, the best results in total energy absorption were obtained with the combination of 0.4 mm nozzle diameter and 0.15 mm layer thickness. When only the nozzle diameters were compared, the structures printed with 0.4 mm nozzle in all sample types absorbed more energy.
- It was determined that the combinations of 0.15 mm layer thickness - 0.4 mm nozzle diameter and 0.1 mm layer thickness - 0.25 mm nozzle diameter were more effective in terms of energy absorption.
- The effect of printing parameters was more notable on SEA. While the total energy absorbed by FBCC and FBCCZ structures with 1 mm rod diameter was approximately 4.1 times higher than for 0.75 mm diameter structures, this rate decreased to 2.6 for FBCC structures and 3.4 for FBCCZ structures in SEA.
- The combination of small nozzle diameter and high layer thickness caused a decrease in mechanical strength in both lattice types.
- It was determined that the effect of the nozzle diameter on the mechanical properties is more significant compared to the other parameters.
- Although there are different research studies examining the printing parameters, this study showed that the effect of the parameters may have different results depending on the lattice type and porosity ratio.

ACKNOWLEDGES

This study was supported by the Bursa Technical University Scientific Research Project Units (Project No: 211N003).

REFERENCES

1. Vilardell, A.M., Takezawa, A., Du Plessis, A., Takata, N., Krakhmalev, P., Kobashi, M., Yadroitsev, I., "Topology optimization and characterization of Ti6Al4V ELI cellular lattice structures by laser powder bed fusion for biomedical applications", *Materials Science and Engineering: A*, Vol. 766, 138330, 2019.
2. Özel, Ş., Zeren, M., Alp, Ç.N., "Application Of Layered Manufacturing Technology With 3d Printers In Automotive Industry", *International Journal of 3D Printing Technologies and Digital Industry*, Vol. 4, Issue 1, Pages 18-31, 2020.
3. Özsoy, K., Duman, B., Gültekin, D.İ., "Metal part production with additive manufacturing for aerospace and defense industry", *International Journal of Technological Sciences*, Vol.11, Issue 3, Pages 201-210, 2019.
4. Aslan, B., Yıldız, A.R., "Optimum design of automobile components using lattice structures for additive manufacturing", *Materials Testing*, Vol. 62, Issue 6, Pages 633-639, 2020.
5. Bhushan, B., Caspers, M., "An overview of additive manufacturing (3D printing) for microfabrication", *Microsystem Technologies*, Vol. 23, Issue 4, Pages 1117-1124, 2017.

6. Ngo, T. D., Kashani, A., Imbalzano, G., Nguyen, K. T., Hui, D., “Additive manufacturing (3D printing): A review of materials, methods, applications and challenges”, *Composites Part B: Engineering*, Vol. 143, Pages 172-196, 2018.
7. Mohamed, O. A., Masood, S. H., Bhowmik, J. L., “Optimization of fused deposition modeling process parameters: a review of current research and future prospects”, *Advances in Manufacturing*, Vol. 3, Issue 1, Pages 42-53, 2015.
8. Başçı, Ü.G., Yamanoglu, R., “Yeni Nesil Üretim Teknolojisi : FDM ile Eklemeli İmalat”, *International Journal of 3D Printing Technologies and Digital Industry*, Vol. 5, Issue 2, Pages 339-352, 2021.
9. Dezaki, M. L., Ariffin, M. K. A. M., Hatami, S., “An overview of fused deposition modelling (FDM): Research, development and process optimization”, *Rapid Prototyping Journal*, Vol. 27, Issue 3, Pages 562-582, 2021.
10. Tuğcu, S. E., Şenaysoy, S., Demirci, E., “Effect of Build Orientation and Layer Thickness on Tensile Properties of FDM Printed PLA and PA Materials”, 1st International Materials Engineering and Advanced Manufacturing Technologies Congress, Pages 105-110, İstanbul, 2022.
11. Altan, M., Eryildiz, M., Gumus, B., Kahraman, Y., “Effects of process parameters on the quality of PLA products fabricated by fused deposition modeling (FDM): surface roughness and tensile strength”, *Materials Testing*, Vol. 60, Issue 5, Pages 471-477, 2018.
12. Hsueh, M. H., Lai, C. J., Chung, C. F., Wang, S. H., Huang, W. C., Pan, C. Y., ... & Hsieh, C. H., “Effect of Printing Parameters on the Tensile Properties of 3D-Printed Polylactic Acid (PLA) Based on Fused Deposition Modeling”, *Polymers*, Vol. 13, Issue 14, 2387, 2021.
13. Kamaal, M., Anas, M., Rastogi, H., Bhardwaj, N., Rahaman, A., “Effect of FDM process parameters on mechanical properties of 3D-printed carbon fibre-PLA composite”, *Progress in Additive Manufacturing*, Vol. 6, Issue 1, Pages 63-69, 2021.
14. Samykano, M., Selvamani, S. K., Kadirgama, K., Ngui, W. K., Kanagaraj, G., Sudhakar, K., “Mechanical property of FDM printed ABS: influence of printing parameters”, *The International Journal of Advanced Manufacturing Technology*, Vol. 102, Issue 9, Pages 2779-2796, 2019.
15. Camargo, J. C., Machado, Á. R., Almeida, E. C., Silva, E. F. M. S., “Mechanical properties of PLA-graphene filament for FDM 3D printing”, *The International Journal of Advanced Manufacturing Technology*, Vol. 103, Issue 5, Pages 2423-2443, 2019.
16. Popescu, D., Zapciu, A., Amza, C., Baciuc, F., Marinescu, R., “FDM process parameters influence over the mechanical properties of polymer specimens: A review”, *Polymer Testing*, Vol. 69, Pages 157-166, 2018.
17. Fernandez-Vicente, M., Calle, W., Ferrandiz, S., Conejero, A., “Effect of infill parameters on tensile mechanical behavior in desktop 3D printing”, *3D printing and additive manufacturing*, Vol. 3, Issue 3, Pages 183-192, 2016.
18. Dobos, J., Hanon, M. M., Oldal, I., “Effect of infill density and pattern on the specific load capacity of FDM 3D-printed PLA multi-layer sandwich”, *Journal of Polymer Engineering*, Vol. 42, Issue 2, Pages 118-128, 2021.
19. Eryildiz, M., “The effects of infill patterns on the mechanical properties of 3D printed PLA parts fabricated by FDM”, *Ukrainian Journal of Mechanical Engineering and Materials Science*, Vol. 7, Pages 1-8, 2021.
20. Solomon, I. J., Sevel, P., Gunasekaran, J., “A review on the various processing parameters in FDM”, *Materials Today: Proceedings*, Vol. 37, Pages 509-514, 2021.
21. Algarni, M., Ghazali, S., “Comparative study of the sensitivity of PLA, ABS, PEEK, and PETG’s mechanical properties to FDM printing process parameters”, *Crystals*, Vol. 11, Issue 8, 995, 2021.
22. Pan, C., Han, Y., Lu, J., “Design and optimization of lattice structures: A review”, *Applied Sciences*, Vol. 10, Issue 18, 6374, 2020.
23. Baykasoğlu, A., Baykasoğlu, C., Cetin, E., Multi-objective crashworthiness optimization of lattice structure filled thin-walled tubes”, *Thin-Walled Structures*, Vol. 149, 106630, 2020.
24. Sağbaş, B., Gürkan, D., “Additively manufactured Ti6Al4V lattice structures for biomedical applications”, *International Journal of 3D Printing Technologies and Digital Industry*, Vol. 5, Issue 2, Pages 155-163, 2021.
25. Yin, S., Chen, H., Wu, Y., Li, Y., Xu, J., “Introducing composite lattice core sandwich structure as an alternative proposal for engine hood”, *Composite Structures*, Vol. 201, Pages 131-140, 2018.
26. Kulangara, A. J., Rao, C. S. P., Bose, P. S. C. “Generation and optimization of lattice structure on

a spur gear”, *Materials Today: Proceedings*, Vol. 5, Issue 2, Pages 5068-5073, 2018.

27. Nasrullah, A. I. H., Santosa, S. P., Dirgantara, T., “Design and optimization of crashworthy components based on lattice structure configuration”, *Structures*, Vol. 26, Pages 969-981, 2020.

28. Poyraz, Ö., Bilici, B. E., Gedik, Ş. C. “Numerical Investigations and Benchmarking of The Physical and Elastic Properties of 316L Cubic Lattice Structures Fabricated by Selective Laser Melting” *International Journal of 3D Printing Technologies and Digital Industry*, Vol. 6, Issue 1, Pages 13-22, 2022.

29. Tang, C., Liu, J., Yang, Y., Liu, Y., Jiang, S., Hao, W., “Effect of process parameters on mechanical properties of 3D printed PLA lattice structures”, *Composites Part C: Open Access*, Vol. 3, 100076, 2020.

30. Seharing, A., Azman, A. H., Abdullah, S., “A review on integration of lightweight gradient lattice structures in additive manufacturing parts”, *Advances in Mechanical Engineering*, Vol. 12, Issue 6, 1687814020916951, 2020.

31. Zhang, X. Z., Leary, M., Tang, H. P., Song, T., Qian, M., “Selective electron beam manufactured Ti-6Al-4V lattice structures for orthopedic implant applications: Current status and outstanding challenges” *Current Opinion in Solid State and*

Materials Science, Vol. 22, Issue 3, Pages 75-99, 2018.

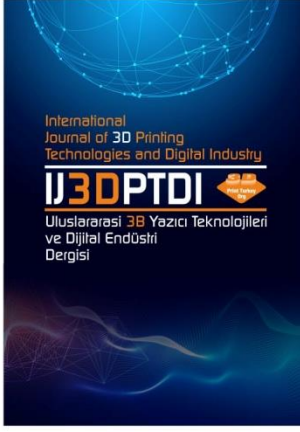
32. Cao, X., Xiao, D., Li, Y., Wen, W., Zhao, T., Chen, Z., Fang, D., “Dynamic compressive behavior of a modified additively manufactured rhombic dodecahedron 316L stainless steel lattice structure”, *Thin-Walled Structures*, Vol. 148, 106586, 2020.

33. Mancini, E., Utzeri, M., Sasso, M., “Investigation on Homogeneous Modeling of Gyroid Lattice Structures: Numerical Study in Static and Dynamic Conditions” *Key Engineering Materials*, Vol. 926, Pages 2119-2126, 2022

34. Yildirim, A., Demirci, E., Karagöz, S., Özcan, Ş., Yildiz, A.R., “Experimental and numerical investigation of crashworthiness performance for optimal automobile structures using response surface methodology and oppositional based learning differential evolution algorithm”, *Materials Testing*, Vol. 65, Issue 3, Pages 346-363, 2023.

35. Albak, E. İ., “Optimization for multi-cell thin-walled tubes under quasi-static three-point bending”, *Journal of the Brazilian Society of Mechanical Sciences and Engineering*, Vol. 44, Issue 5, 207, 2022.

36. Butt, J., Bhaskar, R., Mohaghegh, V., “Analysing the effects of layer heights and line widths on FFF-printed thermoplastics”, *The International Journal of Advanced Manufacturing Technology*, Vol. 121, Issue 11-12, Pages 7383-7411, 2022.



ULUSLARARASI 3B YAZICI TEKNOLOJİLERİ
VE DİJİTAL ENDÜSTRİ DERGİSİ

INTERNATIONAL JOURNAL OF 3D PRINTING
TECHNOLOGIES AND DIGITAL INDUSTRY

ISSN:2602-3350 (Online)

URL: <https://dergipark.org.tr/ij3dptdi>

A COMPARATIVE STUDY ON PRECISION METROLOGY SYSTEMS FOR ADDITIVE MANUFACTURING

Yazarlar (Authors): Binnur Sagbas^{ID}, Ozgur Poyraz^{ID*}, Numan Durakbasa^{ID}




Bu makaleye şu şekilde atıfta bulunabilirsiniz (To cite to this article): Sagbas B., Poyraz O., Durakbasa N., "A Comparative Study on Precision Metrology Systems For Additive Manufacturing" *Int. J. of 3D Printing Tech. Dig. Ind.*, 7(1): 114-123, (2023).

DOI: 10.46519/ij3dptdi.1206753

Araştırma Makale/ Research Article

Erişim Linki: (To link to this article): <https://dergipark.org.tr/en/pub/ij3dptdi/archive>

A COMPARATIVE STUDY ON PRECISION METROLOGY SYSTEMS FOR ADDITIVE MANUFACTURING

Binnur Sagbas^a, Ozgur Poyraz^b*, Numan Durakbasa^c

^aDepartment of Mechanical Engineering, Yildiz Technical University, Istanbul, Turkiye

^bDepartment of Mechanical Engineering, Eskisehir Technical University, Eskisehir, Turkiye

^cResearch Group for Production Metrology and Adaptronic Systems, Institute for Production Engineering and Laser Technology, TU Wien, Vienna, Austria

* Corresponding Author: ozgurpoyraz@eskisehir.edu.tr

(Received: 22.11.2022; Revised: 09.03.2023; Accepted: 26.04.2023)

ABSTRACT

This paper presents a comparative study on precision metrology systems such as Coordinate Measuring Machine (CMM), 3-Dimensional Scanning (3DS) and Computed Tomography (CT) for polymer additive manufacturing. A special test sample was designed and manufactured by Fused Deposition Modeling (FDM) and Selective Laser Sintering (SLS) AM systems. The manufactured parts were then measured by three different precision metrology systems and the results were compared in terms of different measurement and AM methods. Uncertainty analyses were conducted based on the results of CMM measurements. The benchmark highlighted the difference between part characteristics manufactured by FDM and SLS, where FDM part represented higher surface roughness and more deviation to the nominal design. Furthermore, expanded uncertainties computed for the FDM manufactured part were almost three times of the uncertainties computed for the SLS manufactured part. It was also demonstrated that one of the major contributors to the expanded uncertainty occurred because of rougher surface of FDM manufactured part. Similar tendency of part to nominal deviations were observable in all metrology systems including CMM, CT and 3DS. Findings of the study revealed the need of standardized measurement for inspection and control of AM parts.

Keywords: 3-Dimensional Scanning (3DS), Coordinate Measuring Machine (CMM), Computed Tomography (CT), Additive Manufacturing (AM), Fused Deposition Modeling (FDM), Selective Laser Sintering (SLS).

1. INTRODUCTION

Additive manufacturing, also known as “3-dimensional (3D) printing” or “rapid prototyping”, is a group of emerging process technologies. AM enables its users to produce high-value, lightweight, complex, and individually customized components without significant increase in production costs [1]. In contrast to conventional manufacturing techniques, AM accomplishes its success through joining materials to make objects from 3D model data usually layer upon layer [2]. In this way, the need for using cutters for traditional machining or molds/dies for injection/deformation processes is eliminated. On top of aforementioned design advantages, AM working principle provides flexibility in production volumes, reduces design-to-

production lead times and allows the application of different materials even for a single component. AM, which is categorized into seven major classes can be applied for various material families such as polymers, metals, ceramics and their composites [2], [3].

Among the so-called material families, polymer materials are being developed since the first introduction of the AM technology, and for the current state-of-the-art both thermosetting and thermoplastic polymers are available to process [4]. Furthermore, many of the AM classes have the ability to process polymers including photopolymerization, powder bed fusion, material extrusion, material jetting and binder jetting. On the other hand, powder bed fusion and material extrusion-based AM technologies

are reported to provide good strength, and thus they are utilized for functional parts production in addition to prototype manufacturing [4], [5]. However, there are still challenges to be overcome in miscellaneous research areas including product design, process parameter optimization, material characterization and component verification.

Component verification is of critical importance to the end users and industry in terms of functional part production. It practices all the issues related with the design specifications covering material, physical and geometrical properties. However, there are many gaps on the inspection and quality assurance of complex AM components in terms of geometrical and dimensional properties [6], [7]. Studies are being conducted to fill these gaps and researchers evaluate AM components by means of different measurement techniques including Coordinate Measuring Machine (CMM), 3D Scanners (3DS) and Computed Tomography (CT) [8]-[12]. Minetola et al. adopted ISO 286 standard and conducted CMM measurements for verification and benchmarking of low cost Fused Deposition Modeling (FDM) machines based on a reference part [9]. Authors of the study highlighted the importance of inspection and came up with the results showing that the accuracy of FDM process is influenced by filament and nozzle diameter. In another study conducted on metrology of FDM parts, Sagbas and Durakbasa characterized specially designed test artifacts by optical systems instead of CMM and accentuate the faster inspection opportunity with optical systems [6]. Gillaugh et al. captured the geometrical characteristics of a turbo engine stream vane component by optical systems using structured light [10]. Poyraz et al. presented a specially designed and additively manufactured test artifact for surface roughness characterization, and benchmarked tactile systems with the optical ones to show the differences on curved surfaces [7]. Furthermore, Liou et al. employed optical vision systems during AM process and alter process parameters according to the received information from the optical system [11]. Stavroulakis and Leach reviewed optical form metrology for industrial-grade metal additive manufactured parts and emphasized the research needs on new metrology tools, procedures, tolerancing rules and characterization methods for to cope with the

complexity of AM parts [12]. Additional works on CT systems were also presented to capture the geometrical characteristics of internal surfaces or porosities of AM produced parts [13], [14]. In depth assessment on application of CT measurement for high quality metal additive manufacturing was studied by Du Plessis and lattice structures were included on top of geometrical features [15]. CT and CMM was also applied to benchmark stereolithography and Selective Laser Sintering (SLS) by Shah et al. [16]. Finally, CT and CMM was applied for the verification of high-speed sintering AM produced parts by Gomez et al. considering the uncertainty values [17].

Although research have been done about the subject, there is still lack of standards, scientific or industrial procedures for identification of optimum measurement system for novel AM processes to consider the characteristic of AM technology, specifications of measurement systems, available accuracy, risk of uncertainties and the ease of inspection activities [8], [12].

This paper presents a comprehensive study on the metrology for functional polymer AM components. In this respect, a special test part was designed and manufactured by FDM and SLS additive manufacturing systems to provide a benchmark for different part characteristics considering low and high-cost polymer AM processes. The manufactured test parts were then measured by CMM, 3DS and CT precision metrology systems, and the results were compared in terms of different measurement and AM methods. Uncertainty analysis per JCGM 100:2008 were conducted based on the results of repeated CMM measurements [13]. To the authors' knowledge, there is no study comparing FDM and SLS AM methods by three precision measurement systems in terms of dimensional accuracy. With these aspects, this study, which provides novel and important contributions to scientific knowledge, presents the comparison of two different polymer additive manufacturing methods with three different measurement systems.

2. MATERIALS AND METHOD

2.1. Test part design

The use of benchmark and test parts have found a widespread application area among AM research, and they have been used for various

purposes including machine selection, AM process comparison, parameter optimization and production strategy evaluation [18]. The developed artifacts were able to assess minimum feature size, repeatability, surface quality, dimensional and geometrical accuracy of the processes [19], [20]. In this study, the test part used for the comparisons was designed to meet a set of criteria in terms of manufacturing and metrology (see Fig. 1). In this regard, the outer dimensions of the parts were kept as minimum as possible to fit into the build volume for most of the FDM and SLS systems available in the market, to spend less material and to be

manufacturable in a relatively short cycle time. In addition to that, metrological evaluation was considered during design as the main aim of the study. For this reason, it was designed as stiff as possible to avoid warping effects and thinner sections were excluded from the part. Moreover, test part was designed with a constant cross section perpendicular to the build direction, and by this way the need for support structures was eliminated and the risk for stair stepping effect was reduced. Lastly, diversified metrological benchmark capability was provided adding different features such as holes, radii, planes and angular faces.

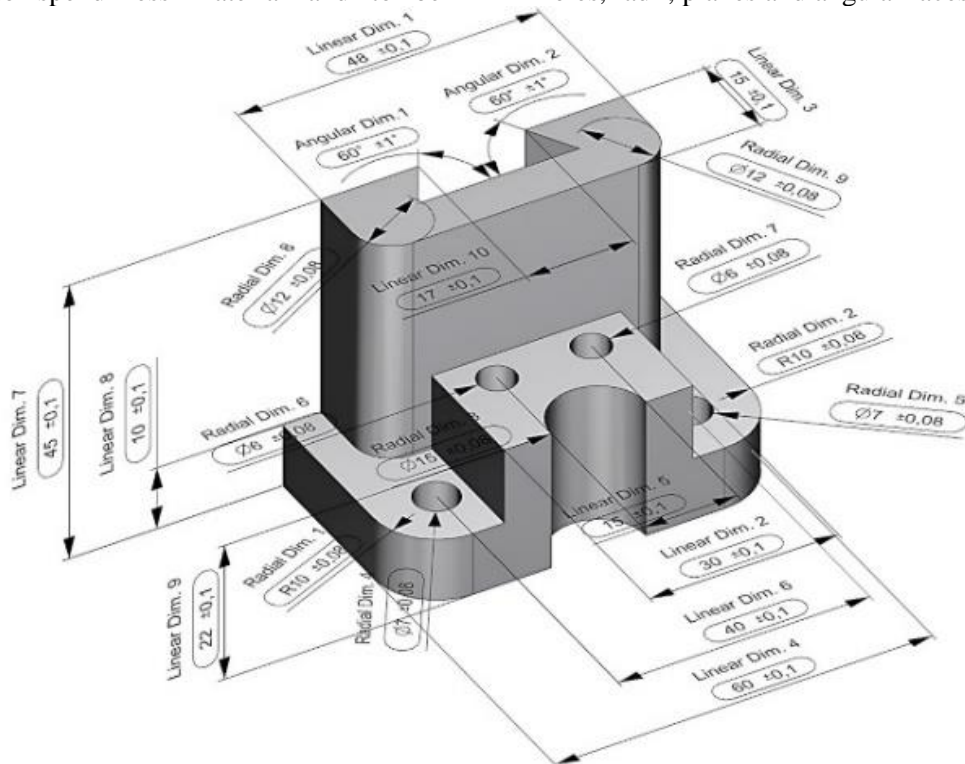


Figure 1. Test artifact with the dimensions.

2.2. Manufacturing of test artefacts

Thanks to the developments in AM technology and similar to the other material families available for AM, functional part productions of polymer materials are continuously increasing their application areas. In accordance with the purpose of functional part production, a sufficient level of strength is required and several AM techniques are reported to ensure good strength [3]. Among these, FDM and SLS are highlighted as low and high cost AM technologies considering the machine investment and material prices [4]. These two techniques were selected for the current study to benchmark two polymer AM technologies

compatible for functional part production and representatives for diverse budget ranges.

FDM, also known as “fused filament fabrication”, is an extrusion-based AM technology and it feeds polymer materials in filament form by means of an extruder. The fed filament materials are melted by a heating element and extruded through a nozzle. The movable extrusion system follows part cross section in the layer plane axes and the build platform is indexed one layer down (Fig. 2a). This cycle is repeated until the part reaches its full height. On the other hand, SLS is a powder bed fusion based AM technology, and it feeds polymer materials in powder form by means of

a re-coater. Part cross-section is scanned by a laser directed by mirrors. After the scanning of the part cross-section is completed, build platform moves one layer down and this cycle is repeated until the part reaches its full height (Fig. 2b). In the scope of this study, Mfact 3D printer was used as FDM and EOS P110 as SLS systems. As the part materials, typical grades for each system were selected. Acrylonitrile butadiene styrene (ABS) was applied in FDM and polyamide (PA) was applied in SLS.

The optimum process parameters recommended by the suppliers were selected for manufacturing of the sample parts. These parameters were presented consecutively in Table 1 and Table 2.

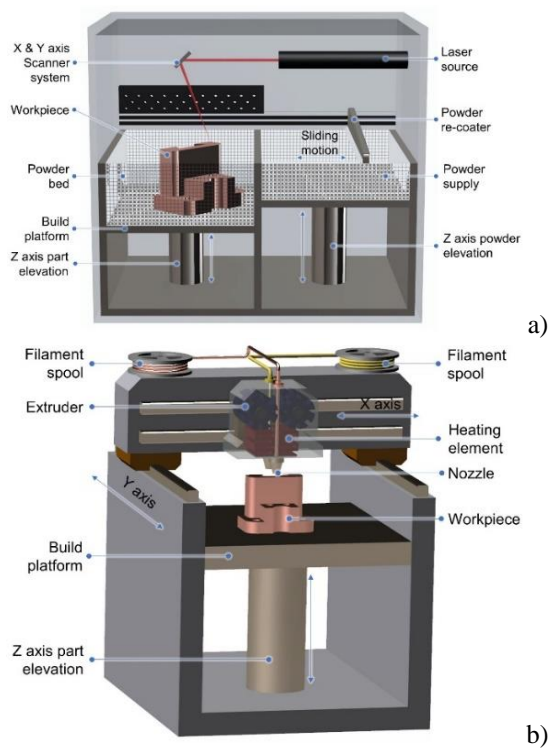


Figure 2. Working principles of a) FDM and b) SLS technologies.

Table 1. FDM process parameters.

Parameter	Unit	Value
Layer thickness	mm	0.2
Printer speed	mm/min	3000
Extruder temperature	°C	205
Shells	Number	3
Infill percentage	%	35

Table 2. SLS process parameters.

Parameter	Unit	Value
Layer thickness	mm	0.1
Scanning speed	mm/s	2500
Hatch distance	mm	0.25
Laser power	W	30

2.3. CMM Measurements and uncertainty analysis

CMM measurements in this study were carried out at the Interchangeable Manufacturing and Industrial Metrology Laboratory of the Institute for Production Engineering and Laser Technology of Vienna University of Technology. The reference temperature range of the relevant laboratory was kept at $20^{\circ}\text{C}\pm 0.1^{\circ}\text{C}$ and relative humidity was $45\%\pm 5$. In addition to these, vibration isolation was maintained and maximum ground amplitudes at frequencies greater than 5 Hz was $0.05\ \mu\text{m}$. The CMM was Aberlink Axiom Too equipped with a probe having 3 mm diameter and the parts were fixed on top of the CMM table with the help of a vise. A sample view of the CMM set-up consisting of the vise and the SLS part is given in Fig. 3 and the CMM specifications are provided in Table 3. All the geometrical features of the test sample were five times measured under the same conditions.



Figure 3. CMM set-up consisting of the vise and the part.

Table 3. CMM specifications.

Characteristic	Unit	Value
Volumetric accuracy*	µm	(2.1+0.4L/100)
Scale resolution	µm	0.1
Optimum temperature range	°C	18-22
Max velocity vector	mm/s	866
Max acceleration vector	mm/s ²	1200

* Maximum Permissible Error MPE_{CMM} according to ISO 10360-2. 2009 within the thermal limits defined for optimum temperature range.

Since the tactile coordinate metrology is commonly used a reference method, uncertainty analyses were conducted following to CMM measurements. According to related standards and guides [22], uncertainty can be estimated using two type of evaluations.

Type A evaluations estimates the uncertainty by the statistical analysis of series of observations, and in this study, repeated measurements were considered to estimate the Type A uncertainty of the CMM. First of all, average value for a series of n measurements were calculated using Eq. (1), where x is measurand and \bar{x} is average value of measurements.

$$\bar{x} = \frac{\sum_{i=1}^n x_i}{n} \quad (1)$$

Subsequently, standard deviation was studied using Equation (2) and is expressed with S_x .

$$S_x = \sqrt{\frac{\sum_{i=1}^n (x_i - \bar{x})^2}{(n-1)}} \quad (2)$$

Finally, Type A uncertainty based on repeatability of measurements, u_p , was estimated using Equation (3).

$$u_p = S_x / \sqrt{n} \quad (3)$$

In contrast to Type A evaluations, Type B evaluations estimates the uncertainty by non-statistical methods considering other issues such as measuring system, measured workpiece, environmental conditions and past experiences. Among these issues, uncertainty contributions of measuring system can be added to the combined uncertainty budget as calibration uncertainty, u_i , and can be expressed using Equation (4). MPE_{CMM} is the maximum permissible error of the CMM

system and was defined in the specifications given in Table 3.

$$u_i = 0.5 MPE_{CMM} \quad (4)$$

Uncertainty contributions of measured workpiece and the effect of environmental conditions can be considered together as u_w and expressed using Equation (5), where u_T is the uncertainty of the work piece, caused by temperature variations and u_R is uncertainty of the workpiece caused by surface roughness.

$$u_w = \sqrt{u_T^2 + u_R^2} \quad (5)$$

However, this study neglects the effect of temperature variations since the temperature was under tight control ($20^\circ\text{C} \pm 0.1^\circ\text{C}$) at the laboratory where measurements were carried out. On the other hand, surface roughness was especially considered to reveal the differences between two processes in terms of metrological evaluation. For this reason, surface roughness was measured with a 5 µm diameter probe and 8 mm cut-off length, and average values $R_{z.mean} = 96.63 \mu\text{m}$ and $R_{z.mean} = 48.5 \mu\text{m}$ were obtained for FDM and SLS manufactured artifacts respectively. u_R uncertainty was calculated using the $R_{z.mean}$ values and Equation (6). $\sqrt{3}$ was considered following to the observations and likelihood of a rectangular distribution.

$$u_R = (R_{z.mean}/2) / \sqrt{3} \quad (6)$$

Estimated Type A and Type B values were integrated into a single uncertainty, u_{CMM} , magnitude by combining those using Equation (7).

$$u_{CMM} = \sqrt{u_p^2 + u_i^2 + u_w^2} \quad (7)$$

Finally, expanded uncertainty was calculated by multiplying the combined uncertainty with $k = 2$ as coverage factor for a confidence level of 95% (Equation (8)).

$$U_{CMM} = k u_{CMM} \quad (8)$$

2.4. CT Measurements

CT scan measurements were performed in the same laboratory with the CMM measurements

and Werth Tomo Scope Technology XS was used as the measurement system. The measurement system consisted of X-ray source tube, detector and a rotating table between source tube and detector. The resolution of the system was $0.1 \mu\text{m}$ and maximum permissible error MPE_{CT} was defined with $MPE_{CT} = 7.5 + L/50$ where L is the measuring length in mm comparable to ISO 10360. To construct 3D model of the measured workpiece, images were taken at different angular positions by fixing the part on the table and rotating the table between source tube and detector. Taken images were combined using the necessary algorithms provided by WinWerth® software. A sample view of CT set-up consisting of the table and the SLS part is given in Fig. 4 and CT scan parameters are provided in Table 4.



Figure 4. CT set-up consisting of the table and the part.

Table 4. CT scan parameters.

Parameter	PA2200
Voltage (kV)	146
Current (μA)	408
Filter material	Copper
Filter thickness (mm)	0.2
Voxel size (μm)	34.07

2.5. 3DS Measurements

As the last measurement system, Solutionix Rexcan 3D optical scanner was used. The system had twin camera with phase shifting optical triangulation. Laser light was projected on to the measured workpiece and by means of a beam deflecting mirror, the workpiece was scanned. Triangulation angle defines the resolution of the system and 0.003 mm was used in this study. Before the scanner was calibrated to minimize the errors, the workpiece was spray coated and target points were placed on necessary regions. ezScan and Geomegic Control-X were used as scan and evaluation software. A sample view of 3DS set-up

consisting of the table and the SLS part is given in Fig. 5.

3. RESULTS AND DISCUSSIONS

Results were evaluated for the identified tolerance ranges based on the average value of selected FDM and SLS system manufacturer specifications, following to repeated CMM measurements of 14 different geometrical features (Table 5).

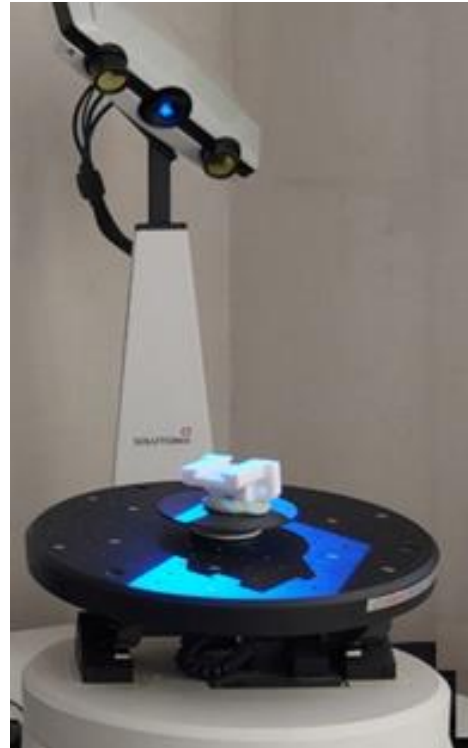


Figure 5. 3DS set-up consisting of the table and the part.

Table 5. CMM measurement results.

Dimension	Ref. Value	Tol.	FDM	SLS
			(ABS) Actual	(PA) Actual
Angular Dim.1 ($^{\circ}$)	60	1	60.471	61.850
Angular Dim.2 ($^{\circ}$)	60	1	60.696	61.540
Linear Dim.5 (mm)	15	0.1	14.963	14.986
Linear Dim.6 (mm)	40	0.1	39.870	39.893
Linear Dim.7 (mm)	45	0.1	44.884	44.891
Linear Dim.8 (mm)	10	0.1	9.883	9.880
Linear Dim.10 (mm)	17	0.1	17.002	17.071
Radial Dim.1 (mm)	10	0.1	9.733	9.701
Radial Dim.2 (mm)	10	0.1	9.698	9.698
Radial Dim.3 (mm)	15	0.1	15.325	15.356
Radial Dim.4 (mm)	7	0.1	6.874	6.978
Radial Dim.5 (mm)	7	0.1	6.841	6.928
Radial Dim.6 (mm)	6	0.1	5.829	5.948
Radial Dim.7 (mm)	6	0.1	5.826	5.942

Considering the nominal value and tolerance ranges of the workpiece, both the FDM and SLS systems showed similar performance in terms of linear dimensions. On the other hand, SLS manufactured workpiece showed better performance for the curved features which were represented with the radial dimensions. For this trend, the only outlier were the angular features. The reason for this was interpreted as the lack of sufficient flat surface of FDM manufactured parts after excluding the unintended radii in the corner of the angular faces.

Uncertainty analyses were conducted for 5 selected features following to initial benchmark. Selected 5 features represent different properties like linear length, inner/outer radial dimensions and center to center distances. As can be seen from the Table 5 and Table 6, the difference between FDM and SLS manufactured parts is more pronounced in uncertainty values comparing to measurement values.

It is obvious that all the uncertainty values are elevated in FDM parts. Detailed interpretation of Table 6 reveals the major contributors to the combined uncertainty are Type A uncertainty (u_p) based on the repeatability of measurements and Type B uncertainty based on surface roughness (u_w).

Table 6. Uncertainty budgeting and benchmark for the CMM measurements in μm .

Part	Feature	u_p	u_i	u_w	u_{CMM}	U_{CMM}
FDMed part	Hole (Radial Dim.3)	30.1	2.31	13.9	33.3	66.5
	Hole to hole distance (Linear Dim.5)	1.0	2.31	13.8	14.2	28.4
	Radius (Radial Dim.1)	33.9	2.29	14.0	36.7	73.4
	Plane to plane distance (Linear Dim.7)	0.8	2.43	13.7	14.1	28.2
SLSed part	Hole (Radial Dim.3)	2.0	2.31	7.0	7.6	15.3
	Hole to hole distance (Linear Dim.5)	0.3	2.31	7.1	7.4	14.8
	Radius (Radial Dim.1)	8.8	2.29	6.9	11.5	22.9
	Plane to plane distance (Linear Dim.7)	0.4	2.43	6.8	7.2	14.4

The results of the interpretations are comparable with previous studies. Santons et al. designed, characterized and estimated a benchmark artefact using high-speed sintering additive manufacturing and estimated uncertainty values based on CMM measurements [23]. They have presented $80 \mu\text{m}$ uncertainty for a 10 mm cylinder diameter with $75 \mu\text{m} R_{z,mean}$ which is a close value to the current study achieved for the Radial Dim. 3b (cylindrical hole) having 15 mm diameter [23]. Related study has also emphasized the dependence of CMM uncertainty on the surface roughness of high-speed sintering AM parts [22]. Additional to this, Zanini et al. characterized a lattice structure part of Ti6Al4V manufactured by laser powder bed fusion AM process and estimated uncertainty values based on CMM and CT measurements [24]. They reported a CT uncertainty of $45 \mu\text{m}$ by using substitution method and including the contribution of surface roughness [24]. Moreover, they highlighted the need for further investigations on multiple measurement approach whether it gives sufficient weight to the effect of surface roughness [24]. A study conducted by Minetoal et al., benchmarked three different polymer AM methods and highlighted that SLS part's dimensional accuracy is better than FFF part [25]. The authors of the study have associated the findings with the smaller layer thickness providing a better definition and higher dimensional accuracy of the part dimensions of part dimensions in line with this studies benchmark between SLS and FDM [25]. In this regard, it can be stated that increased surface roughness of FDM manufactured part leads to errors and uncertainties during tactile measurement techniques such as CMM. Fig. 6 shows a benchmark of all manufacturing and measurement systems.

In Fig. 6, horizontal axis shows the dimensional magnitude of measured feature in mm where the vertical axis shows absolute value of deviation from nominals. Table 7 shows the measurement results with CT and 3DS. The results obtained by non-tactile measurement systems of CT and 3DS were also benchmarked in the scope of this study. As can be observed from Table 7 and Fig. 6, similar tendency of higher deviations in FDM manufactured parts can be observed for non-tactile measurement systems. The reason for that could be the rough nature of the FDM manufactured part but also evaluation and

reporting errors occur as a result of intermediate steps carried out in non-tactile measurement such as fitting.

It is clear from Table 5 and Table 7 that measurement results of the parts taken by three different systems varied from each other for

some of the dimensional features. These variations, which have different values for angular, linear and radial dimensions, were recorded at the highest rate in measuring angular dimensions while they were lowest in linear dimension measurements.

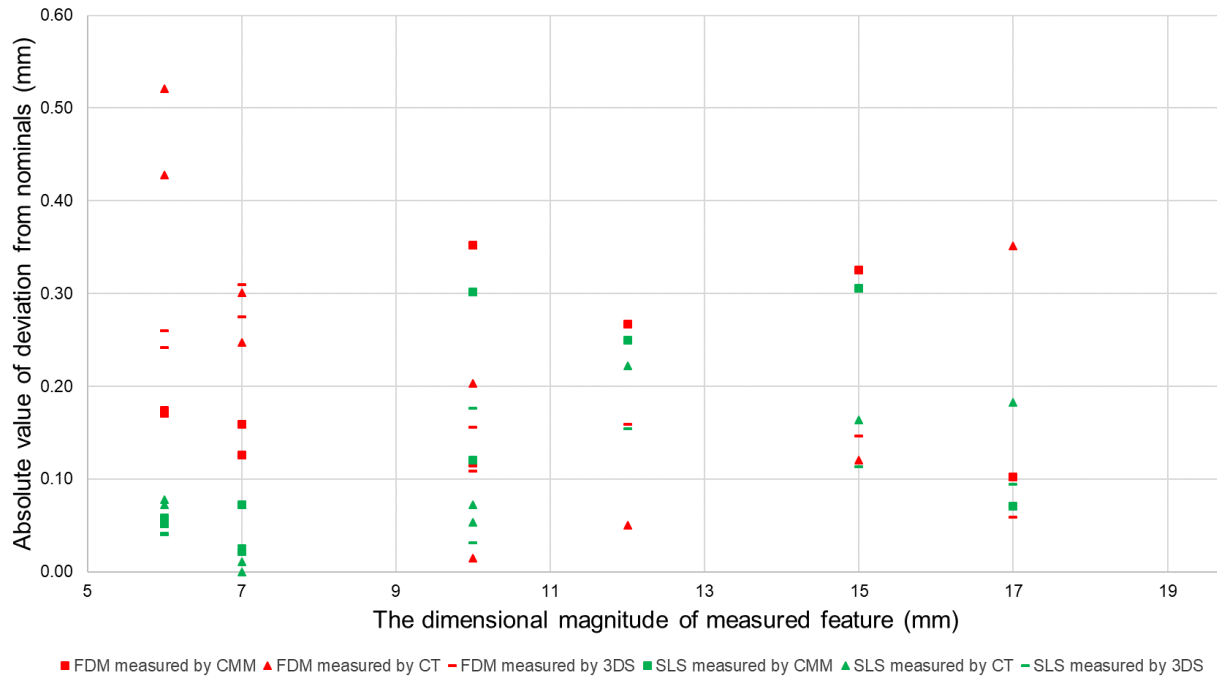


Figure 6. Benchmarking of manufacturing and measurement systems.

Table 7. CT and 3DS measurement results in mm.

Dimension	3DS		X-Ray CT	
	FDM	SLS	FDM	SLS
Angular Dim.1 (°)	60.09	61.123	60.465	61.223
Angular Dim.2 (°)	60.14	61.405	59.574	60.484
Linear Dim.5 (mm)	14.97	15.001	15.013	14.988
Linear Dim.6 (mm)	39.89	39.947	39.867	39.920
Linear Dim.7 (mm)	44.86	44.919	44.816	44.878
Linear Dim.8 (mm)	9.84	9.969	9.797	9.928
Linear Dim.10 (mm)	16.941	17.094	16.649	17.383
Radial Dim.1 (mm)	9.841	9.846	10.051	9.778
Radial Dim.2 (mm)	9.892	9.823	10.015	9.947
Radial Dim.3 (mm)	14.854	15.313	14.880	15.364
Radial Dim.4 (mm)	6.725	6.972	6.699	7.011
Radial Dim.5 (mm)	6.690	6.981	6.753	7.000
Radial Dim.6 (mm)	5.758	5.960	5.572	5.928
Radial Dim.7 (mm)	5.740	5.958	5.479	5.922

Variations between radial dimensions were also different for each measurement system. For instance, deviation of the FDM part angular dimension 2 from its nominal value recorded as

0.140 mm by optical scan while it was recorded as -0.426 mm and -0.695 mm for XCT and CMM respectively. Similarly, for SLS part angular dimension 2, the deviation was recorded as 1.205 mm, 0.484 mm and 1.815 mm for optical scan, XCT and CMM respectively. These deviations may arise by different measurement procedures, algorithms and measurement parameters such as probe diameter for CMM [26], voxel size, voltage, current, filter materials and its thickness for XCT. [14] Collecting the measured point data from insides, diameter of the holes and inclined geometries is more difficult than simple linear geometries. Therefore, measurement errors and deviations can be seen at a higher rate in these regions. Also, the variability is more pronounced in FDM parts. This may be as a result of relatively higher surface texture irregularities and roughness.

Although, providing generation of 3D complex geometries, AM techniques also bring some challenges at the point of metrological

evaluation of parts with these geometries. For dealing with these challenges measurement procedures have to be developed for AM parts manufactured with different materials by different AM methods.

The focus of this study was comparison of three most widely used precision metrology system in terms of dimensional inspection of polymer AM parts. Further analyses are needed by different measurement system parameters on different AM parts to develop measurement procedures and standards.

4. CONCLUSIONS

This study presented a benchmark for two polymer additive manufacturing technologies and their metrological evaluation using three different measurement systems of CMM, CT and 3DS using a special test artifact. As can be seen through the items listed below, the study revealed the superiorities and shortcomings of dimensional measurement systems relative to each other in products fabricated by polymer additive manufacturing. It can be concluded that;

- The benchmark highlighted the difference between part characteristics manufactured by FDM and SLS, where FDM part represented higher surface roughness and more deviation to the nominal design.
- Expanded uncertainties computed for the FDM manufactured part were almost three times of the uncertainties computed for the SLS manufactured part. It was also demonstrated that one of the major contributors to the expanded uncertainty occurred because of rougher surface of FDM manufactured part.
- In general consideration, similar tendency of part to nominal deviations were observable in all metrology systems including CMM, CT and 3DS. However, values of these deviations were in different ranges which revealed the need of standardized measurement and evaluation procedures for inspection and control of AM parts.
- Further comparative studies with different measurement system parameters, on different AM methods and materials would be valuable to development of required inspection procedures.

ACKNOWLEDGES

CMM and CT measurements were carried out at the Laboratory of Industrial Metrology and Adaptronic Systems, TU Wien (Vienna University of Technology), Austria. 3DS measurements were taken at Mayis Tasarim-Turkey. The authors would like to thank for all the supports.

REFERENCES

1. Razavi, S. M. J., Bordonaro, G. G., Ferro, P., Torgersen, J., Berto, F., "Porosity effect on tensile behavior of Ti-6Al-4V specimens produced by laser engineered net shaping technology", Proceedings of the Institution of Mechanical Engineers, Part C: Journal of Mechanical Engineering Science, Vol. 235, Issue 10, Pages 1930-1937, 2018.
2. ISO/ASTM52900-15., "Standard Terminology for Additive Manufacturing – General Principles – Terminology", ASTM International, West Conshohocken, PA, 2015.
3. Gibson, I., Rosen, D. W., Stucker, B., Khorasani, M., Rosen, D., Stucker, B., Khorasani, M., "Additive manufacturing technologies", Springer, Vol. 17. Cham, Switzerland, 2021.
4. Wang, X., Jiang, M., Zhou, Z., Gou, J., Hui, D., "3D printing of polymer matrix composites: A review and prospective", Composites Part B: Engineering, Vol. 110, Pages 442-458, 2017.
5. Singh, R., Garg, H. K., "Fused deposition modeling—a state of art review and future applications", Reference Module in Materials Science and Materials Engineering, Pages 1-20, 2016.
6. Sagbas, B., Boyacı, T. H., Durakbasa, N. M., "Precision metrology for additive manufacturing", In The International Symposium for Production Research, Springer, Cham, Pages 324-332, 2019.
7. Poyraz, Ö., Solakoğlu, E. U., Ören, S., Tüzemen, C., Akbulut, G., "Surface texture and form characterization for powder bed additive manufacturing", Journal of the Faculty of Engineering and Architecture of Gazi University, Vol. 34, Issue 3, Pages 1653-1664, 2019.
8. Leach, R. K., Bourell, D., Carmignato, S., Donmez, A., Senin, N., Dewulf, W., "Geometrical metrology for metal additive manufacturing", CIRP annals, Vol. 68, Issue 2, Pages 677-700, 2019.
9. Minetola, P., Iuliano, L., Marchiandi, G., "Benchmarking of FDM machines through part

quality using IT grades”, *Procedia CIRP*, Vol. 41, Pages 1027-1032, 2019.

10. Gillaugh, D., Copenhaver, W. W., Janczewski, T., Holycross, C., Sanders, D., Nessler, C., “Aeromechanical Evaluation of an FDM Printed Thermoplastic StreamVane (TM)”, In 53rd AIAA/SAE/ASEE Joint Propulsion Conference, Pages 4600, 2017.

11. Wang, Z., Liu, R., Sparks, T., Liu, H., Liou, F., “Stereo vision-based hybrid manufacturing process for precision metal parts”, *Precision Engineering*, Vol. 42, Pages 1-5, 2015.

12. Stavroulakis, P. I., Leach, R. K., “Invited review article: review of post-process optical form metrology for industrial-grade metal additive manufactured parts”, *Review of Scientific Instruments*, Vol. 87, Issue 4, 041101, 2016.

13. Thompson, A., Körner, L., Senin, N., Lawes, S., Maskery, I., Leach, R. K., “Measurement of internal surfaces of additively manufactured parts by X-ray computed tomography”, *Conf. Industrial Computed Tomography*, Leuven, Belgium, 2017.

14. Sagbas, B., Durakbasa, M. N., “Industrial computed tomography for nondestructive inspection of additive manufactured parts”, In *Proceedings of the International Symposium for Production Research 2019*, Pages 481-490, Springer, Cham, 2019.

15. Du Plessis, A., “X-ray tomography for the advancement of laser powder bed fusion additive manufacturing”, *Journal of Microscopy*, Vol. 285, Issue 3, Pages 121-130, 2022.

16. Shah, P., Racasan, R., Bills, P., “Comparison of different additive manufacturing methods using computed tomography”, *Case studies in nondestructive testing and evaluation*, Vol. 6, Pages 69-78, 2016.

17. Villarraga-Gómez, H., Lee, C., Smith, S. T., “Dimensional metrology with X-ray CT: A comparison with CMM measurements on internal features and compliant structures”, *Precision Engineering*, Vol. 51, Pages 291-307, 2018

18. Thompson, M. K., Moroni, G., Vaneker, T., Fadel, G., Campbell, R. I., Gibson, I., Martina, F., “Design for Additive Manufacturing: Trends,

opportunities, considerations, and constraints”, *CIRP annals*, Vol. 65, Issue 2, 737-760, 2016

19. Rebaioli, L., Fassi, I., “A review on benchmark artifacts for evaluating the geometrical performance of additive manufacturing processes”, *The International Journal of Advanced Manufacturing Technology*, Vol. 93, Issue 5, Pages 2571-2598, 2017.

20. Carmignato, S., De Chiffre, L., Bosse, H., Leach, R. K., Balsamo, A., Estler, W. T., “Dimensional artefacts to achieve metrological traceability in advanced manufacturing”, *CIRP annals*, Vol. 69, Issue 2, Pages 693-716, 2020.

21. ISO 10360-2, “Acceptance and Reverification Tests for Coordinate Measuring Machines (CMM)—Part 2: CMMs Used for Measuring Linear Dimensions”, International Organization for Standardization, Geneva, Switzerland, 2009.

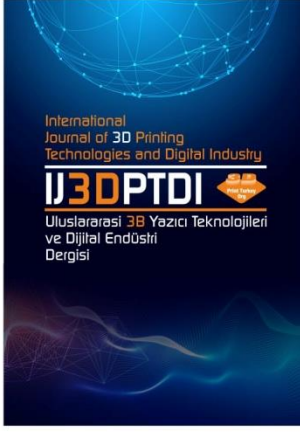
22. ISO/IEC Guide 98-3, “Uncertainty of measurement — Part 3: guide to the expression of uncertainty in measurement”, International Organization for Standardization, Geneva, Switzerland, 2008.

23. Santos, V. M. R., Thompson, A., Sims-Waterhouse, D., Maskery, I., Woolliams, P., Leach, R., “Design and characterization of an additive manufacturing benchmarking artefact following a design-for-metrology approach”, *Additive Manufacturing*, Vol. 32, Pages 100964, 2020.

24. Zanini, F., Sorgato, M., Savio, E., Carmignato, S., “Uncertainty of CT dimensional measurements performed on metal additively manufactured lattice structures”, In *10th Conference on Industrial Computed Tomography*, Wels, Austria, 2020.

25. Minetola, P., Calignano, F., Galati, M., “Comparing geometric tolerance capabilities of additive manufacturing systems for polymers”, *Additive Manufacturing*, Vol. 32, Pages 101103, 2020.

26. Drbul, M., Czán, A., Šajgalík, M., Piešová, M., Stępień, K., Influence of normal vectors on the accuracy of product's geometrical specification. *Procedia engineering*, Vol. 192, Pages 119-123, 2017.



ULUSLARARASI 3B YAZICI TEKNOLOJİLERİ
VE DİJİTAL ENDÜSTRİ DERGİSİ

INTERNATIONAL JOURNAL OF 3D PRINTING
TECHNOLOGIES AND DIGITAL INDUSTRY

ISSN:2602-3350 (Online)

URL: <https://dergipark.org.tr/ij3dptdi>

PRODUCTION OF WASTE JUTE DOPED PLA (POLYLACTIC ACID) FILAMENT FOR FFF: EFFECT OF PULVERIZATION

Yazarlar (Authors): Havva Nur Özdemir^{ID}, Ayberk Sözen^{ID}, Murat Demir^{ID}, Alperen Doğru^{ID*}, Yasemin Seki^{ID}

Bu makaleye şu şekilde atıfta bulunabilirsiniz (To cite to this article): Özdemir H. N., Sözen A., Demir M., Doğru A., Seki Y., "Production of Waste Jute Doped PLA (Polylactic Acid) Filament For Fff: Effect Of Pulverization" *Int. J. of 3D Printing Tech. Dig. Ind.*, 7(1): 124-128, (2023).

DOI: 10.46519/ij3dptdi.1213659

Araştırma Makale/ Research Article

Erişim Linki: (To link to this article): <https://dergipark.org.tr/en/pub/ij3dptdi/archive>

PRODUCTION OF WASTE JUTE DOPED PLA (POLYLACTIC ACID) FILAMENT FOR FFF: EFFECT OF PULVERIZATION

Havva Nur Özdemir^a, Ayberk Sözen^b, Murat Demir^c, Alperen Doğru^{d*}, Yasemin Seki^c

^a Dokuz Eylül University, Department of Chemistry, TURKEY

^b Dokuz Eylül University, Institute of Marine Sciences and Technology, TURKEY

^c Dokuz Eylül University, Engineering Faculty, Textile Engineering Department, TURKEY

^d Ege University, Aviation HVS, Aircraft Technology, TURKEY

* Corresponding Author: alperen.dogru@ege.edu.tr

(Received: 02.12.2022; Revised: 03.03.2023; Accepted: 26.04.2023)

ABSTRACT

In recent years, there has been an outbreak of research on natural fiber-reinforced materials to reduce non-recycled material effects and produce environmentally friendly products. In parallel with the increasing popularity of additive manufacturing, the development of new natural fiber-reinforced materials in this field has also increased to improve pure material characteristics and reduce raw materials usage. This study presents the manufacturing process of 5% waste jute-reinforced PLA filaments and the characteristics of 3D printed parts. For the production of jute-reinforced filaments, polylactic acid (PLA) granules were pulverized to increase the material surface for better bonding between materials in the composite matrix structure. The effectiveness of pulverizing PLA granules was exposed by comparing it with the production of the same composite matrix with PLA granules. Both matrices were formed into filaments to produce 3D parts in Fused Filament Fabrication technology. Thermo-gravimetric analysis (TGA) and differential scanning calorimetry (DSC) will be presented in filament form. Besides, the mechanical properties of 3D parts will also be presented. Within the scope of the study, it is aimed to reveal the material size effect for producing natural fiber-reinforced filaments for additive manufacturing.

Keywords: PLA, Jute, Additive Manufacturing, FFF, Pulverization.

1. INTRODUCTION

3-Dimensional (3D) printing has gained a lot of attention and popularity with the help of producing complex geometries without special tools in good accuracy, and ease of production for prototyping. Various technologies have been presented for 3D printing. Fused Filament Fabrication (FFF) is probably the most popular used 3D printing technology [1]. In the working principle of FFF printers, filament-form material is fed through a heated nozzle, and designed parts are produced by the deposition of molten polymers on the printing bed. There has been increasing attention to research on producing different types of polymers and/or particle-doped filaments via FFF printers.

Recently additives from natural sources have been utilized for sustainable and ecologically friendly filament manufacturing [2]. Ease of availability and low cost also make these

materials indispensable for doped polymeric materials for any application. The type and number of doped materials, the aspect ratio esp. for fibers, and the interface between the polymer and the reinforced materials are highly effective parameters on the final performance of produced bio-composite filament [3]. The main drawback of bio composite filament manufacturing is to achieve homogeneous filler dispersion. The effect of wood amount on tensile properties of PLA was studied [4]. It is determined there is an optimum particle content for the improvement of the tensile properties of PLA. In another paper, it is stated lower wood particle size can ease the fabrication of wood-reinforced PLA filament [5]. The particles particularly cellulosic materials can also be treated with different physical/chemical methods to improve particle distribution along

the filament and also facilitate 3D printing [6-9].

The properties of the polymer can play an acting role in particle-doped filament manufacturing. The polymer can be modified by grafting and/or can be pulverized to enhance particle/polymer interface and particle distribution [10,11]. Pulverization of the polymer granules may enhance the homogeneity of the ground particle/polymer mixture prior to the extrusion processes. This study presents the manufacturing process of 5% waste jute-reinforced PLA filaments with FFF and the characteristics of 3D printed parts. For the production of jute-reinforced filaments, jute fibers were ground and polylactic acid (PLA) granules were pulverized with the aim of increasing the material surface for better bonding between materials in the composite matrix structure. Then, thermal degradation behavior is investigated by a thermogravimetric analyzer (TGA), and the mechanical properties were determined by means of maximum tensile strength, elasticity modulus, and breaking at elongation. The uniformity and distribution of jute particles in PLA filament were observed via fluorescence microscopy. In order to realize the effect of pulverization and dopping of jute, pristine PLA as in the granule form was tested as a control sample.

2. MATERIALS AND METHODS

2.1. Materials

PLA was used as matrix material in this research. This PLA was the product of FKUR Kunststoff company, and its label is Bio-Flex F7510. The density of the used PLA is 1.25 gr/m³, the melting temperature is 155 °C and

the melt flow rate is 2-4 g/10min. This material is efficiently processed with the FFF method and 100% recyclable raw material. PLA can be destroyed in the same way as petro-based plastics. However, it has the nature of biodegradability, which is an environmental advantage. PLA materials converted into different forms were modified with 5% jute by weight. No pre-treatment was applied to the reinforced jute fibers which were doped to increase the mechanical properties. Jute wastes were obtained from the carpet factory.

2.2. Preparation of PLA matrix

In order to pulverize PLA, polymer sizes were reduced by grinding in a mechanical shredder

using liquid nitrogen and the surface area was increased. Liquid nitrogen has been found to contribute greatly to this grinding process. The particle size has been reduced from 5 mm to an average of 400 μm.

2.3. Preparation of Re-Jute

Jute fibers are produced from natural hemp by grinding in the Retsch SM 100 device. The ground hemp fibers were passed through a 500 μm sieve. Jute fibers have an average density of 0.86 g/cm³, a diameter of 10–400 μ and a length of 100–1200μ. No surface treatment has been applied to jute fibers.



Figure 1. Grinded jute fibers.

2.4. Compounding

The jute addition to the powder and graded PLA matrices was carried out with a mechanical mixer. The weight ratio was determined with digital precision balance (Accuracy: 0.001) branded Weightlab Instruments WI 3031. Recycled Jute additives and PLA matrices were mechanically mixed with Thermo Digital's vortex mixer. Two different compounds were prepared in powder and granule form.



Figure 2. Jute and powder PLA mix, before entering the mixer.

2.5. Filament Production

Filament production was carried out with Arya Flux brand single screw extruder by using 5% re-jute added powder PLA and 5% re-jute added graded PLA compounds by weight. In order to produce samples with the FFF method, filaments with a diameter of 1.75 mm(-/+0.15mm) were produced.

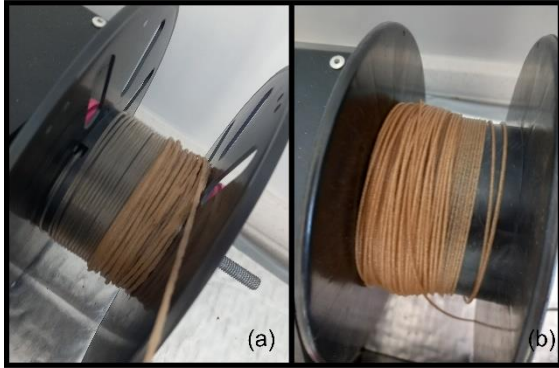


Figure 3. (a) Pellet PLA + jute, (b) Powder PLA + jute Fiber

2.6. Production of Samples

The effect of an 5% re-jute additive to two different PLA forms on the mechanical properties and thermal properties was investigated.

Tensile test specimens were produced in accordance with ASTM D-638 standard by using the FFF method using filaments having two different PLA forms. Due to the long production times in the FFF method, type-5 sample sizes, the sizes of which are specified in figure 2, were preferred.

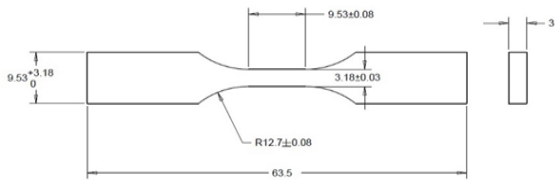


Figure 4. D638 ASTM standard type V tensile test sample.

The drawings of the test specimens were created with the AutoCAD Fusion 365 named CAD program. Using the drawing files in STL format, the gcode file required for production with FFF methods was created with the CAM program named CURA. Production parameters are given in table 1. Standard production parameters of PLA material were used.

Table 1. FFF Production Parameters.

Parameters	Value
Nozzle diameter	400micron
Infill Density	100%
Printing Temperature	200°C
Build Plate Temperature	70°C
Material Flow	100%
Print Speed	15 mm/s
Cooling Fan Speed	50%
Support	None
Build Plate Adhesion	None

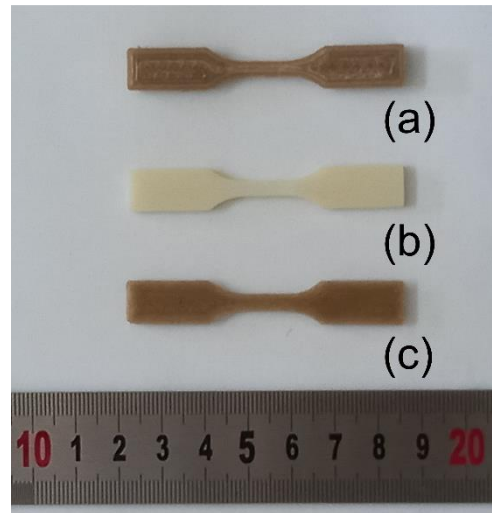


Figure 5. D638 tensile test specimen, (a) Pellet PLA + jute, (b) PLA, (c) Powder PLA + jute Fiber,

2.7. Experimental Testing

2.7.1 Tensile Tests

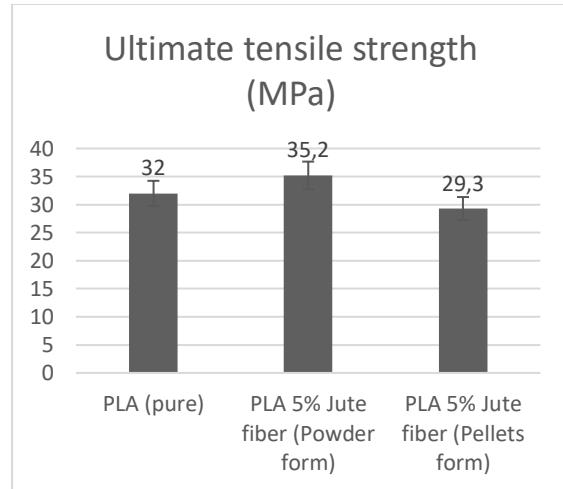


Figure 6. Tensile test results.

Tensile tests were performed according to the related standard (D638 ASTM). 5 samples were used for each configuration. Instron 1114 testing machine was used with its data acquisition system at a constant crosshead speed

of 0.5 mm/min. Pulverized PLA compound clearly, gives better results than Pure PLA and pellets PLA + jute as seen in figure 6.

2.7.2 Thermal Analysis

Thermogravimetric analysis (TGA) is used to investigate thermal resistance. The results show that pulverized PLA approximately 5% degraded due to liquid nitrogen application during grinding as seen in figure 7 and 8.

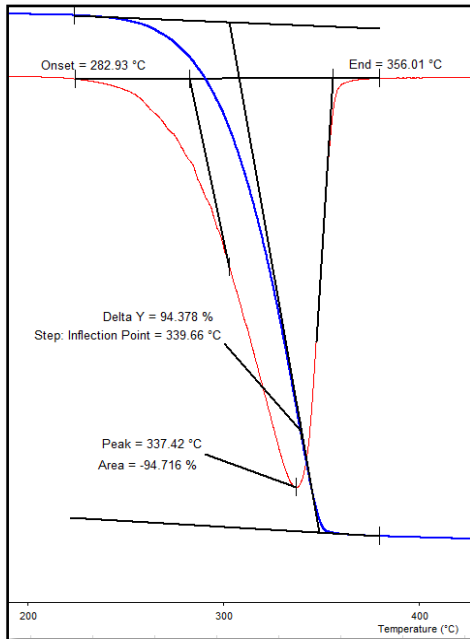


Figure 7. TGA analysis for Powder PLA + jute.

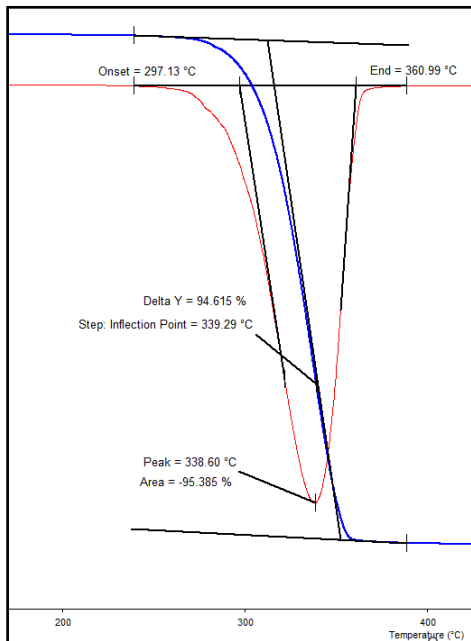


Figure 8. TGA analysis for Pellet PLA + jute.

3. CONCLUSIONS

This study shows that if a natural fiber supported compound is to be made, same fiber and matrix sizes for single screw extrusion will increase the homogeneity of the mixture and the interfacial bonding, which is clearly seen in the tensile tests. The compound made with powder PLA gave better results mechanically, but it is anticipated that such a mixture will be made with twin screw extruder for future studies will give better results. If access to twin screw extrusion is not available, pulverizing the granule can be seen as an alternative and successful method.

REFERENCES

1. Dip, T. M.; Emu, A. S.; Nafiz, M. N. H.; Kundu, P.; Rakhi, H. R.; Sayam, A.; Akhtarujman, Md.; Shoaib, M.; Ahmed, M. S.; Ushno, S. T. et al., "3D printing technology for textiles and fashion." *Textile Progress*, Vol. 52, Issue 4, Pages 167-260, 2020
2. Royan, N. R., Leong, J. S., Chan, W. N., Tan, J. R., & Shamsuddin, Z. S. B. "Current state and challenges of natural fibre-reinforced polymer composites as feeder in fdm-based 3D printing." *Polymers*, Vol. 13, Issue 14, 2289, 2021.
3. Deb, D., Jafferson, J.M., "Natural fibers reinforced FDM 3D printing filaments." *Materials Today:Proceedings*. Vol. 46, Issue 2, Pages 1308-1318, 2021.
4. Kariz, M., Sernek, M., Obucina, M., Kuzman, M.K., "Effect of wood content in FDM filament on properties of 3D printed parts." *Materials Today:Communications*. Vol. 14, Pages 135-140, 2018.
5. Petchwatta, N., Channuan, W., Naknaen, P., Narupai, B., "3D Printing Filaments Prepared from Modified Poly(Lactic Acid)/ Teak Wood Flour Composites: An Investigation on the Particle Size Effects and Silane Coupling Agent Compatibilisation." *Journal of Physical Science*. Vol.30, Issue 2, Pages 169-188, 2019.
6. Figueira, D., Holmen, S., Melboss, J.K., Moldes, D., Echtermeyer, A.T., Chinga-Carrasco, G., "Enzymatic-Assisted Modification of Thermomechanical Pulp Fibers To Improve the Interfacial Adhesion with Poly(lactic acid) for 3D Printing." *ACS Sustainable Chem. Eng.*, Vol. 5, Issue 10, Pages 9338-9346, 2017.

7. Le Duigou, A., Barbe, A., Guillou, E., Castro, M., "3D printing of continuous flax fibre reinforced biocomposites for structural applications." *Materials & Design*, Vol. 180, 107884. 2019.
8. Gama, N., Magina, S., Ferreira, A., Barros-Timmons, A., "Chemically modified bamboo fiber/ABS composites for high-quality additive manufacturing." *Polymer Journal*. Vol. 53, Pages 1459-1467., 2021.
9. Long, Y., Zhang, Z., Fu, K., Li, Y., "Efficient plant fibre yarn pre-treatment for 3D printed continuous flax fibre/poly(lactic) acid composites." *Composites Part B:Engineering*. Vol. 227, 109389, 2021.
10. Lacerda, P.S.S., Gama, N., Freire, C.S.R., Silvestre, A.J.D., Barros-Timmons, A., "Grafting Poly(Methyl Methacrylate) (PMMA) from Cork via Atom Transfer Radical Polymerization (ATRP) towards Higher Quality of Three-Dimensional (3D) Printed PMMA/Cork-g-PMMA" *Materials*. Vol. 12, Issue 9, 1867, 2020.



ULUSLARARASI 3B YAZICI TEKNOLOJİLERİ
VE DİJİTAL ENDÜSTRİ DERGİSİ

INTERNATIONAL JOURNAL OF 3D PRINTING
TECHNOLOGIES AND DIGITAL INDUSTRY

ISSN:2602-3350 (Online)

URL: <https://dergipark.org.tr/ij3dptdi>

INVESTIGATION OF ENERGY GENERATION FROM INCREASED WIND VELOCITY WITH BUILDING GEOMETRIES USING COMPUTATIONAL FLUID DYNAMICS AND WEIBULL FUNCTION

Yazarlar (Authors): Mehmet Bakırcı^{id}, Noor Adil Mohammed^{id}*

Bu makaleye şu şekilde atıfta bulunabilirsiniz (To cite to this article): Bakırcı M., Mohammed N. A., "Investigation of Energy Generation From Increased Wind Velocity With Building Geometries Using Computational Fluid Dynamics and Weibull Function" *Int. J. of 3D Printing Tech. Dig. Ind.*, 7(1): 129-141, (2023).

DOI: 10.46519/ij3dptdi.1171463

Araştırma Makale/ Research Article

Erişim Linki: (To link to this article): <https://dergipark.org.tr/en/pub/ij3dptdi/archive>

INVESTIGATION OF ENERGY GENERATION FROM INCREASED WIND VELOCITY WITH BUILDING GEOMETRIES USING COMPUTATIONAL FLUID DYNAMICS AND WEIBULL FUNCTION

Mehmet Bakırcı^a, Noor Adil Mohammed^a

^aKarabük University, Faculty of Engineering, Mechanical Engineering Department, TURKEY

* Corresponding Author: nuram9559@gmail.com

(Received: 06.09.2022; Revised: 05.12.2022; Accepted: 26.04.2023)

ABSTRACT

Recently, humans have resorted to the use of renewable energies for the purpose of reducing global warming problems that affect the safety of the environment. Wind energy has started to occur in the first place among renewable energy types. However, it is difficult to obtain wind energy in areas where the wind speed is relatively low, so this study dealt with how to increase the production of wind energy in areas where the wind speed is relatively low by designing buildings that increase the wind speed by using of the phenomenon of venturi. How wide the high velocity values take place, how homogenous the distribution of the velocity is, and the turbulence values were calculated by CFD for four cases. It has been determined which of the four cases in which the wind turbine selected can operate most efficiently. One-year wind speed data measured at 10 m above the ground were taken from the Karabük Ovacık meteorological station. Annual energy calculations were made using the power characteristics of the selected wind turbine and Weibull graphs. It has been concluded that the amount of energy that can be obtained with the proposed building geometry layout in the mentioned region can be increased by 4 times.

Keywords: Wind Turbine, Buildings, Windspeed, Venturi Effect, Weibull, CFD.

1. INTRODUCTION

The rapid development of technology, science, and industries, as well as the occurrence of significant improvements in the standard of living, have greatly increased human needs in the areas of planning and living[1]. The need for energy has also increased to keep pace with the developments that have occurred recently, leading people to consume fossil energy greatly, but there are significant negatives such as environmental pollution caused by carbon dioxide released into the atmosphere, and high costs. After the occurrence of oil crisis in 1973, oil costs also increased. Therefore, people were forced to find inexpensive and environmentally friendly energy, so they started relying on a new energy source, which has been called renewable energy [2]. The use of renewable energy has spread widely in the world, as special complexes have been established to invest this energy[3]. This energy come from the sun, wind, and soil. Wind energy is one of the types of renewable energy that does not emit gases

that cause global warming[4]. It is extracted from the kinetic energy of the wind by means of wind turbines to produce electrical energy, as it is considered abundant and renewable energy [5]. The wind turbines are installed especially in regions where annual wind power distribution is sufficient. It is important to choose turbines compatible with annual statistical data of wind speed[6]. While vertical axis wind turbines are selected in regions where the wind speed changes frequently, horizontal axis wind turbines are selected to take advantage of the increasing wind speed as it rises from the ground [7]. For local electricity needs, turbines that are small and have a battery system for energy storage can be used. However, in areas with high wind speed throughout the year, commercial large wind turbines connected to the grid are used [8]. Wind turbines cannot be used in residential areas due to buildings and other obstacles that negatively affect wind speed. In addition, there are negative effects such as noise [9]. However, due to the increase

in wind speed with height, special designs have been applied in very high buildings, and applications have been made by placing turbines in the buildings and meeting some of the building's electricity needs [10]. In addition, successful results have been achieved in obtaining energy from the wind placing turbines while adding special designs to the roofs of buildings that are not very high [11]. There are also studies to obtain energy from vertical air movement on building facades by placing specially designed wind turbines on the side surfaces of the buildings [12]. There are experimental and CFD studies in the literature investigating and analysing how the wind moves around buildings [13]. In some of these studies, how the comfort of life inside the building is affected by the air movement outside the building was examined, while in another part, how the wind affects the building statics, especially in high-rise buildings was investigated [14–16].

Many studies examining the increase in velocity of the air by narrowing the distance between buildings with Computational Fluid Dynamics (CFD) are encountered in the literature. This is also called the venturi effect [15–18].

The focus of this study has been on benefiting from the wind energy in areas where the wind velocity is relatively low, not enough to operate wind turbines. It can be done by suitable placement of buildings in order to get the venturi effect. The buildings have been placed in a semi-parallel manner, and an attempt was made to narrow some areas of the buildings in order to increase the velocity of the wind flow. Four different cases were obtained by symmetrical placement of four different placement of building geometries in this study. They were analysed by CFD. After comparing the results of CFD study for the four cases of the buildings, the most suitable case has been chosen, and the power at which the wind turbines start to operate was checked. Finally, graphs were presented about Weibull distribution and the annual energy production. The main objective of this study is to fill in the existing literature gap on how to benefit from wind energy even in areas where the wind speed is low.

1.1. Theoretical Background

1.1.1 Mass Conservation

The conservation of fluid mass principle states that the product of density, velocity and cross-sectional area of the fluid passing through a certain cross-section will remain constant. This creates the possibility of increasing the low wind speed by placing the two building geometries in a way that narrows the cross-sectional area [19].

According to the law of conservation of mass, the mass flow of a fluid (air) for steady flow is

$$\sum_{in} m = \sum_{out} m \quad (1)$$

Where $m_1 = m_2$ When m_2 Indicates mass flow rate of fluid (air) (kg/sec).

$$m_1 = Q_1 \rho_1 \quad (2)$$

Q_1 Is the volume flow rate (m^3/sec)

Whereas $Q_1 = V_1 A_1$, V is the velocity of air (m/sec). A is the cross-section area (m^2)

So $m_1 = \rho_1 V_1 A_1$.

$$\rho_1 V_1 A_1 = \rho_2 V_2 A_2 \quad (3)$$

So $V_1 A_1 = V_2 A_2$ because the fluid (air) is incompressible in this case.

From here, it was reached that the smaller the area, the velocity increases, that is, the proportionality between the fluid velocity and the cross-sectional area is reversed. Accordingly, the design of the buildings has been chosen and the area where the air velocity reaches the highest possible was determined for the purpose of operating the wind turbines.

1.1.2. Weibull Distribution

In a given location, the wind speed does not remain constant throughout the year. So how much energy is obtained from the wind blowing in this place during a year is related to how the wind speed changes throughout the year. This evaluation is mostly done with the Weibull distribution [20].

The Weibull probability graph is obtained through the use of Equation (4) by taking the hourly average speed values in the measurements made during the year (in order to

obtain more reliable results, or a few years) in the region where the turbine will be installed[21].

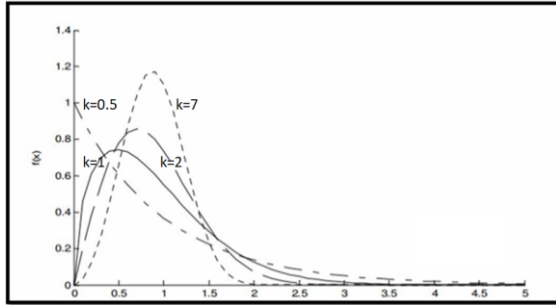


Figure 1. Graphs by parameters of the Weibull distribution[22].

For $v_i < v < v_{i+1}$

$$p(v_i < v < v_{i+1}) = \exp\left(-\left[\frac{v_i}{A}\right]^k\right) - \exp\left(-\left[\frac{v_{i+1}}{A}\right]^k\right) \tag{4}$$

Where A and k are found for a given site on the Equation(4) [23].

In this function k and A values are measurements of how wind velocity is distributed in a year. Every placement has its own k and A values. Weibull graphs shows the relation between probability and velocity values, for different k values, shown in the figure 1 [22]. A wind turbine should be chosen according to the Weibull distribution.

In this study, k and A values were calculated as 1.2 and 7 respectively by using the wind data values at the meteorology station for Karabük-Ovacık in 2021.

1.1.3. Efficiency of wind turbine

The amount of energy to be obtained in a year from a wind turbine installed in a certain location depends on the Weibull values at that location, and also on the efficiency and power curve of the wind turbine. The overall efficiency of the turbine depends on rotor aerodynamic efficiency, mechanical efficiency and electrical efficiency. These efficiencies are shown mathematically in the equations[23].

From Betz’s equations about the maximum power available in the wind [24]. Power is defined as Equation. (5).

$$P_{max} = \frac{16}{27} \frac{1}{2} \rho \cdot v_1^3 \cdot A \tag{5}$$

Where $C_p = C_{p,Betz} = 16/27$ was used .

In Equation (5) A is the swept area of the rotor, and in the following we define this area as

$A = (\pi/4) \cdot D^2$ (It has been neglected that some part of the hub area is not producing any power).

The rotor efficiency is defined as.

$$\eta_{max} = \frac{P_{rotor}}{P_{max}} \tag{6}$$

Where P_{rotor} is the power in the rotor shaft.

The rotor efficiency can be calculated on the basis of a Blade Element Momentum (BEM) Theory. The efficiency of the rotor is derived from the product of three efficiencies. As shown in Equation (7).

$$\eta_{rotor} = \eta_{wake} \cdot \eta_{tip} \cdot \eta_{profile} \tag{7}$$

Where “wake” indicates the loss because of rotation of the wake, “tip” represents the tip loss and “profile” represents the profile losses. The wake loss can be calculated on the basis of Schmitz’ theory [23].

Figure 2. indicates the components of a wind turbine.

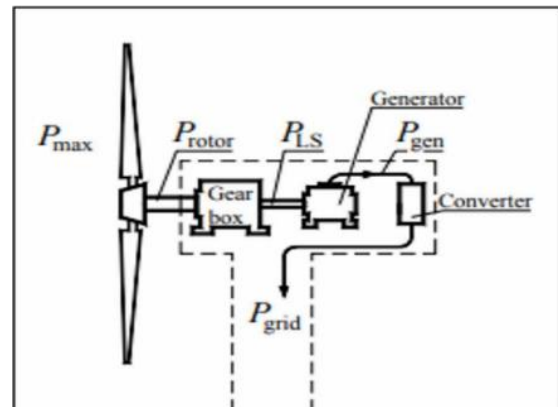


Figure 2. Main components in wind turbine[22].

The total efficiency of such a turbine can be defined as Equation (8).

$$\eta_{total} = \frac{P_{grid}}{P_{max}} = \eta_{rotor} \cdot \eta_{gearbox} \cdot \eta_{gen} \cdot \eta_{conv} \tag{8}$$

Where

$$\eta_{rotor} = \frac{P_{rotor}}{P_{max}}$$

$$\eta_{gearbox} = \frac{P_{HS}}{P_{rotor}}$$

$$\eta_{gen} = \frac{P_{gen}}{P_{HS}}$$

$$\eta_{conv} = \frac{P_{grid}}{P_{gen}}$$

Where the indices stand for “LS” = low speed (shaft); “gen” = generator; “conv” = frequency converter and “grid” = grid net. So typical values for the efficiencies are – at nominal power Gearbox:0.95-0.98, Generator: 0.95-0.97, Converter: 0,96-0,98 at part load, the lower values can be expected[22].

In this study, maximum efficiency (η_{max}) of the wind turbine chosen is 0.4.

The turbine power curve shows at which wind speed the turbine starts to operate (cut in), after which wind speed it is stopped (cut out), and in which wind speed range it produces maximum (nominal) power. This characteristic is a result of turbine efficiency values and design parameters [23].

In this study, cut in velocity, cut out velocity, nominal velocity of the selected wind turbine are 3 m/s, 26 m/s, 11 m/s respectively.

1.1.4. Annual Energy Calculation

The energy that the turbine can produce in a year depends on the wind speed statistics of the region where the turbine is located and the power graph of the turbine. The total amount of energy that can be obtained annually is calculated by the Equation (9)[23].

If the power for the turbine at a given wind speed is $P(v_m)$, the annual production can be calculated as:

$$E_{ann} = \sum\{8766h. p(v_i < v < v_{i+1}). P(v_m)\} \quad (9)$$

Where v_m is the mean value of v_i and v_{i+1} i.e.

$$v_m = (v_i + v_{i+1})/2$$

1.1.5. Wind homogeneity and turbine efficiency

Frequent changes in the magnitude and/or direction of the wind speed over time cause the turbine rotor to be under the influence of inhomogeneous wind. This situation negatively affects the energy to be obtained from the turbine. Therefore, the homogeneity of the wind should be taken into account in the place where the turbine will be installed[25].

1.2. Computational Fluid Dynamics (CFD)

Computational Fluid Dynamics is based on the numerical solution of partial differential equations expressing the conservation of mass, momentum and energy of fluids in a large number of cells created in the defined flow area. Boundary conditions of the defined flow area are defined[26].

In this study, inlet boundary velocity, output boundary pressure, solid surfaces ‘wall’, and flow field boundaries ‘symmetry’ are defined, and conservation equations are solved in the cells (mesh) created, and velocity in each cell, static pressure values as well as turbulence kinetics are determined. Energy equations are not solved in this study. Because energy equations are solved in analyses involving heat and temperature and/or compressible fluid analysis.

In CFD calculations, there are three basic calculation methods: Reynolds-Averaged Navier-Stokes (RANS), Large Eddy Simulation (LES) and Detached Eddy Simulation (DES). RANS equations are the most widely used CFD approach for practical engineering applications. They solve for time-averaged flow properties and are typically used for steady-state simulations. However, this approach is not suitable for predicting unsteady or transient flow phenomena, where large fluctuations in the turbulent flow field can have a significant impact on the results. The choice of CFD approach depends on the specific application and the level of accuracy required. RANS is the most widely used and computationally efficient CFD approach for practical engineering applications, while LES and DES are more suitable for predicting unsteady or transient flow phenomena and complex flow regions [27]. The easiest and most widely used RANS was used in this study.

The most common turbulence models used in RANS simulations are the Spalart-Allmaras, k-omega, and k-epsilon models. The Spalart-Allmaras model is a one-equation model that solves for a single variable to represent the turbulent viscosity, and it is particularly useful for attached boundary layers and external flows. The k-omega model is a two-equation model that solves for both the turbulent kinetic energy (k) and the specific dissipation rate (omega), and it is particularly useful for flows with strong vortices and shear layers. The k-epsilon model is also a two-equation model that solves for the turbulent kinetic energy (k) and the rate of dissipation of turbulence kinetic energy (epsilon), and it is particularly useful for flows with complex turbulence structures.

There are also many sub-varieties of these models, which include modifications and enhancements to improve their accuracy or to account for specific flow characteristics. For example, the RNG k-epsilon model is a modification of the standard k-epsilon model that includes additional terms to improve its performance in swirling flows. The SST k-omega model is a hybrid model that combines aspects of both the k-epsilon and k-omega models to improve its accuracy in a wide range of flow regimes [28]. In present CFD simulations, the SST k-omega model was used.

2. METHOD

2.1. Numerical Calculations

From the literature[29], four different two-dimensional (top view) building geometries were taken, and four different cases were obtained by bringing together two symmetrical buildings as shown in the figure 3.

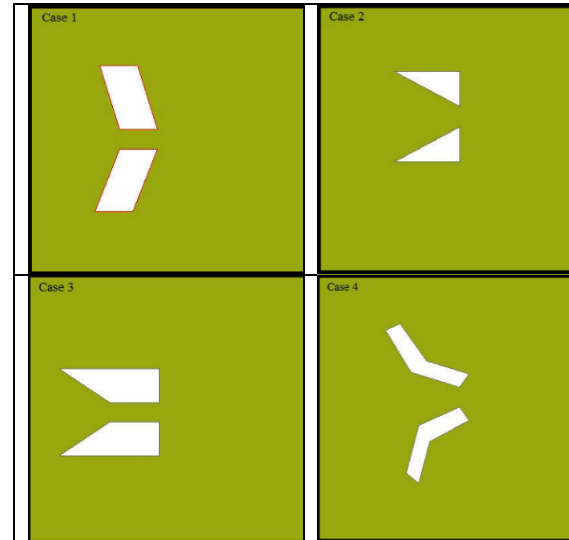
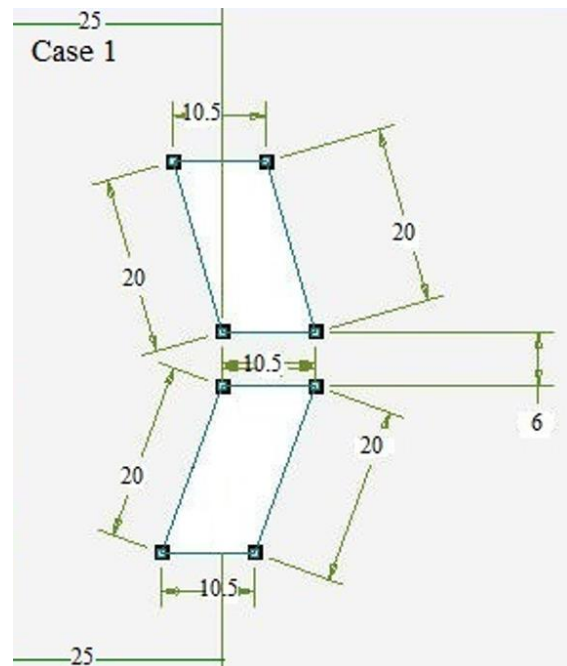


Figure 3. The geometry of the four cases of the buildings [25].

For these four cases, flow fields were created as shown in the figure. On the left edges of these flow areas, the wind entering edge, the wind entry velocity is defined. Since this study is for regions with low wind speed, the velocity values taken are 2, 4, 6 m/s.

The dimensions of four different cases are shown in the figure 4.



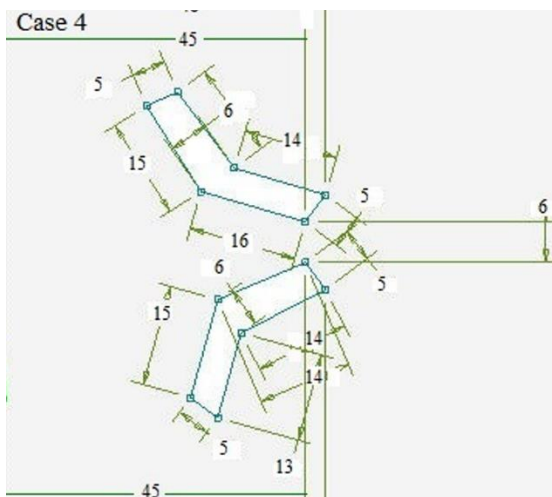
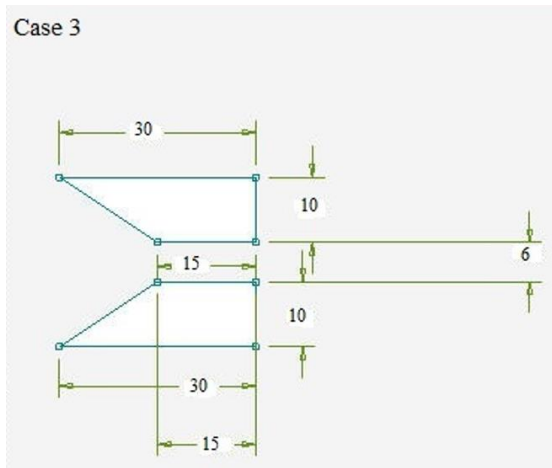
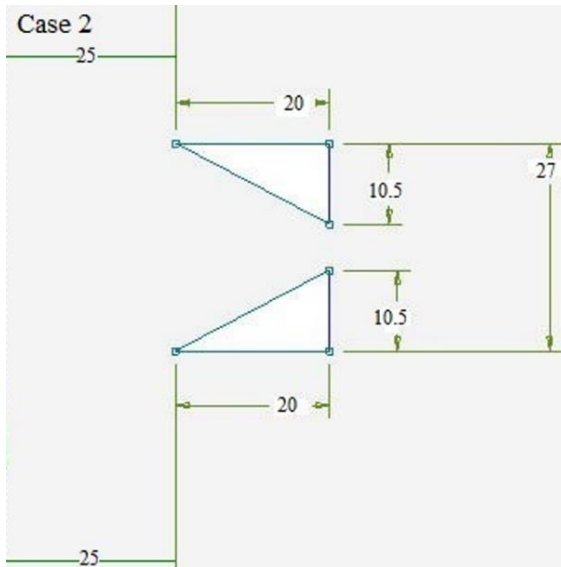


Figure 4. The geometry of the four cases of the buildings that were studied with their parameters.

The fluid domain used in this CFD simulation is shown in Figure 5. The left edges of the flow field are named as ‘inlets’. For ‘inlet’, the wind is defined as perpendicular to the left edge with the speed value. The building geometries are

defined as ‘wall’, the upper and lower edges of the flow area are defined as ‘symmetry’ and the right edges are defined as ‘outlets’. Zero effective pressure value is taken for the outlet.

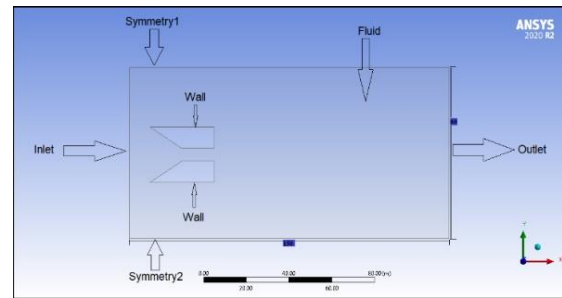


Figure 5. Named sections of the geometry.

2.2. Mesh quality and independence

There are different methods to see the accuracy of the results obtained from the computational fluid dynamics analysis. The most important of these are validation, comparison of calculation results with theoretical formulas, comparison with test results for the same geometries and under the same conditions. However, verification, on the other hand, is one of the most important ones to show whether the computational fluid dynamics results are consistent within themselves or not, to show that the quality of the cells created in the flow field is good enough and to show that the results obtained do not change when the number of cells is increased[31]. Figure 6 indicates the mesh structure in Case3.

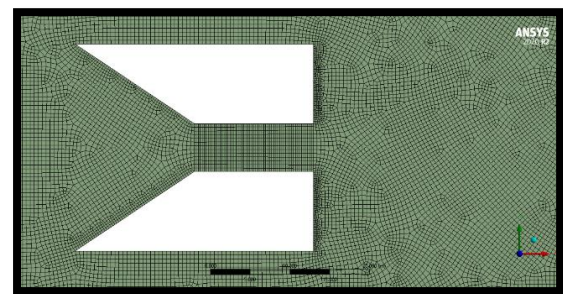


Figure 6. Mesh structure.

When the mesh number was increased from 2000 to 7000, it was seen that the results (output velocity values) changed very little and after 7000 cells the results did not change at all (Figure 7). Apart from this, in order to have high mesh quality in CFD simulations, it is recommended to have skewness values below 0.5 and orthogonality values above 0.7 [31]. In the CFD study conducted here, it was ensured that the mesh quality was high enough.

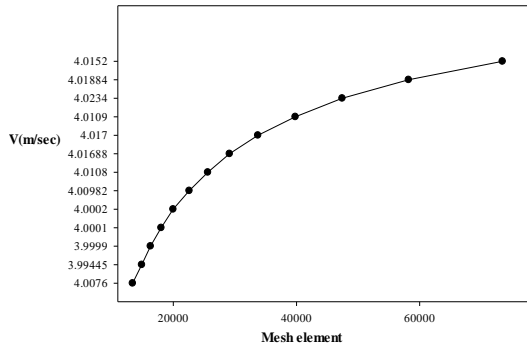


Figure 7. Mesh independence test.

2.3. Setup

The following physical conditions and numerical solution criteria are taken into account in the computational fluid dynamics solution:

- 1.The solution was taken as steady.
- 2.Energy was turned off.
3. Viscous Model is k- ω (SST). It was chosen because it achieves better and more accurate results when the mesh is very fine near the wall [32].
- 4.Boundary conditions:
 - At inlet velocity is (2,4,6 m/sec)
 - In this study, walls are designed as no-slip
 - Neglected direction of velocity
- 5.Solution method is coupled
- 6.Number of iterations is 500.

3. RESULTS AND DISCUSSIONS

The maximum wind speed values that can be obtained between and around the building geometries were calculated using the same inlet speeds in four different situations (Table 1).

Table 1. Maximum velocity flow for four cases to the buildings.

Inlet Velocity (m/sec)	Case1	Case2	Case3	Case4
2	6.64	4.04	5.18	5.91
4	13.3	8.07	9.77	12.2
6	20	12.7	15.3	18.3

While the largest maximum speed values for all input speeds were obtained in Case1, the smallest maximum speed values were obtained in Case2. But this does not necessarily mean that Case1 is the best one.

The case of wind turbine placement cannot be evaluated based on this result alone. Because the general distribution and homogeneity of the wind speed to which the turbine rotor is exposed, as well as the turbulence situation should also be taken into account.

For the Case1, we can see how the velocity value changes around the building geometry from the contour graph given in figure 8.

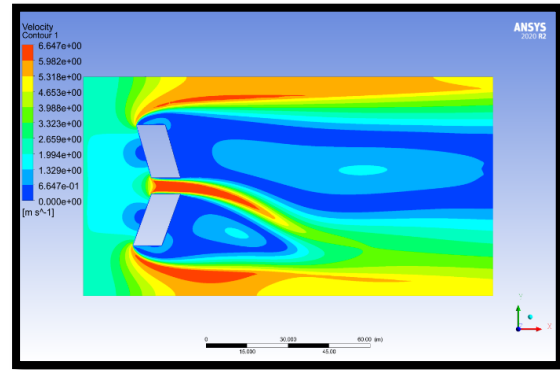


Figure 8. Velocity contour in Case1.

In Case1, when looking at the streamlines, vortices formed around the building geometries can be noticed. As shown in Figure 9.

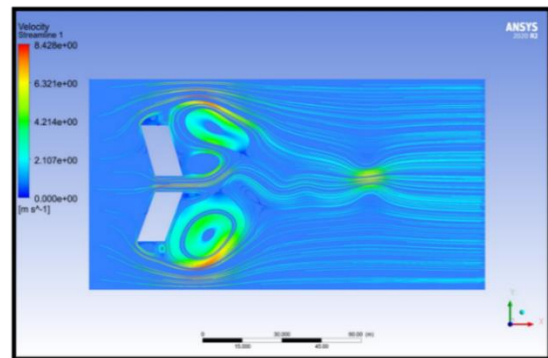


Figure 9. Streamline contour for velocity Case1.

It can be concluded that, in Case1, the velocity distribution does not have enough homogeneity and stable velocity although it has the largest maximum velocity value.

Therefore, how wide the highest speed values are spread, how the distribution of high-speed values is in the section where the turbine can be placed between two buildings, what the turbulence values are will affect the efficiency of the turbine to be used. All these properties of the flow around the building geometries were investigated in CFD study. When all of this

criterion was analysed for four different cases, Case 3 was found to be the best.

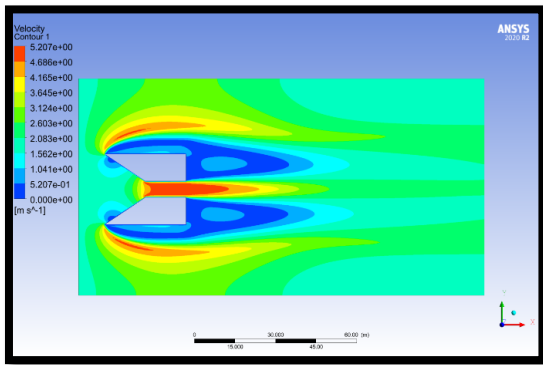


Figure 10. Velocity contour in Case3.

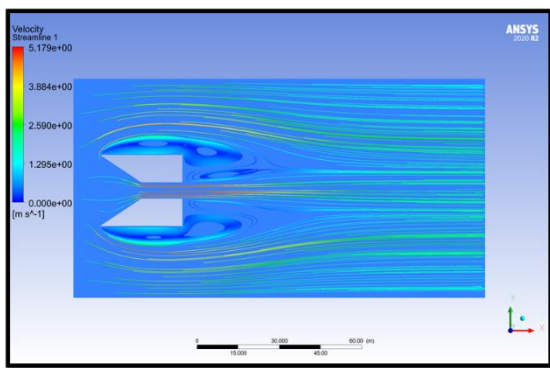


Figure 11. Streamline of Velocity contour for Case3.

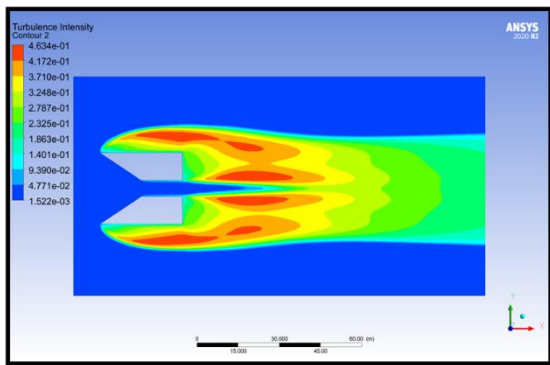


Figure 12. Turbulence intensity contour for Case3.

How the velocity values for the Case3 change around the two buildings can be seen from the velocity contour shown in figure 10 and the velocity streamlines shown in figure 11. Also, considering the turbulent kinetic energy distribution contour shown in Figure 12, the low values between the two buildings and the homogeneous velocity distribution give a clue that the Case3 may be suitable for turbine installation. Therefore, Case3 should be examined more closely.

The velocity distributions and turbulent kinetic energy changes between and around the buildings for four different cases were examined and it was concluded that the most favourable situation would be obtained in the Case3 with homogeneous velocity distribution of high velocity values.

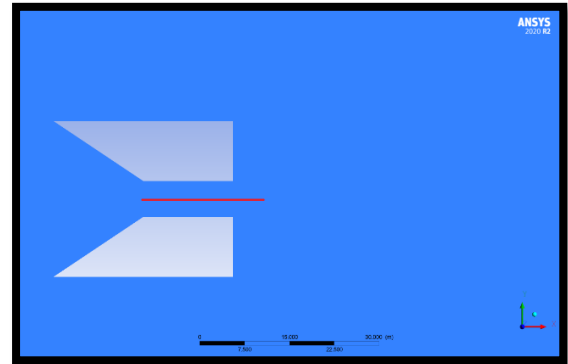


Figure 13. Pressure line.

The static pressure change on this line is shown in figure 13. It is seen that the pressure first decreases rapidly along the line and then does not change much. As shown in figure 14.

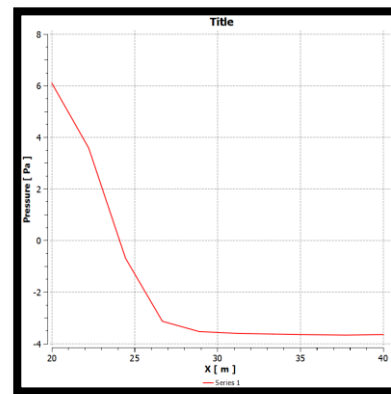


Figure 14. Pressure graphic between two buildings on the pressure line.

In order to specify the placement of the wind turbine in between the two buildings in Case3, pressure, velocity and turbulence conditions were examined in 6 different positions taken on the line drawn in the middle between the two buildings and the best position where the turbine could be placed was determined. Those positions are shown in the figure 15.

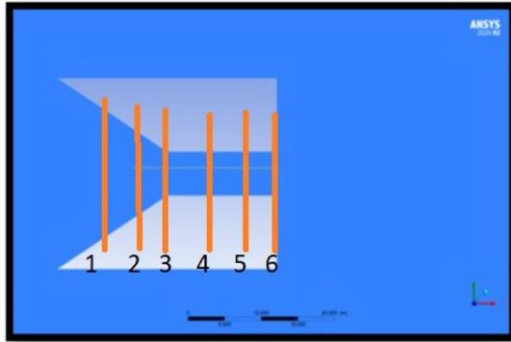


Figure 15. Lines for the possible positions of the wind turbine.

Figure 16 refers to the wind speed graphic at the six positions identified in Figure 15.

It was found that the wind speed increases gradually at the 4th, 5th and 6th position, especially in the side that is in the middle of the two buildings and achieves the highest value at the line 6. As shown in the graphics, the wind speed starts to increase at one of the buildings until it reaches an area in the middle of the two buildings, where it will see a state of stability in the wind speed, but then it gradually decreases when it reaches the edge of another building. The wind speed has been studied in the six sites in order to discover that the high wind speed is maintained for long distances between the two buildings for the purpose of selecting the appropriate wind turbines.

Figure 17 shows the graphic of wind turbulence between the two buildings at position 6 that were previously divided. Whereas it is necessary to study wind turbulence and its amount, because wind turbulence has a great impact on the work of wind turbines, as wind turbulence causes vibrations and fatigue in the turbine blades, which leads to reducing efficiency and increasing wear in the turbines. It was noticed that the wind turbulence graphic is opposite to the wind speed graphic. The turbulence begins with its highest value at the edge of the one of building. It gradually decreases in the central region between the two buildings, and then gradually increases until it reaches the edge of another building. The two graphics have been studied in detail for the purpose of determining the appropriate area for placing the wind turbine, as well as determining the type of turbine suitable for this study and its dimensions. Table 2 indicates the value of velocity and turbulence at position 6 that were previously divided.

Table 2. Velocity value and Turbulence intensity in each line.

Line	Velocity (m/sec)	Turbulence intensity
1	1.80641	0.006
2	4.02142	0.016
3	4.2449	0.028
4	4.25129	0.027
5	4.25726	0.028
6	4.43688	0.109

The distribution of velocity values and turbulence intensity values obtained as a result of computational fluid dynamics analysis at these 6 different locations are compared with graphs (Figures 16 and 17). It can be said that the position where the highest velocity is obtained, the velocity distribution is most homogeneous, and the lowest turbulent intensity value is obtained is line 2.

Since the distance at the selected location between the two buildings where the turbine can be placed is slightly more than 6 m, the turbine rotor diameter can be chosen as 5 m. The selected horizontal axis wind turbine has a start speed (cut in) of 3 m/s, stop speed (cut out) of 26 m/s, nominal speed of 11 m/s. Its rated power is 1.22 kWatt. The power curve of this turbine is shown in figure 18.

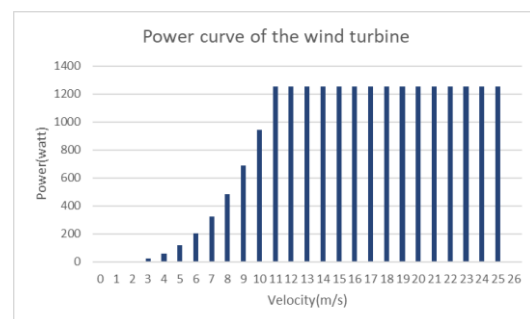


Figure 18. Annual power of wind turbine.

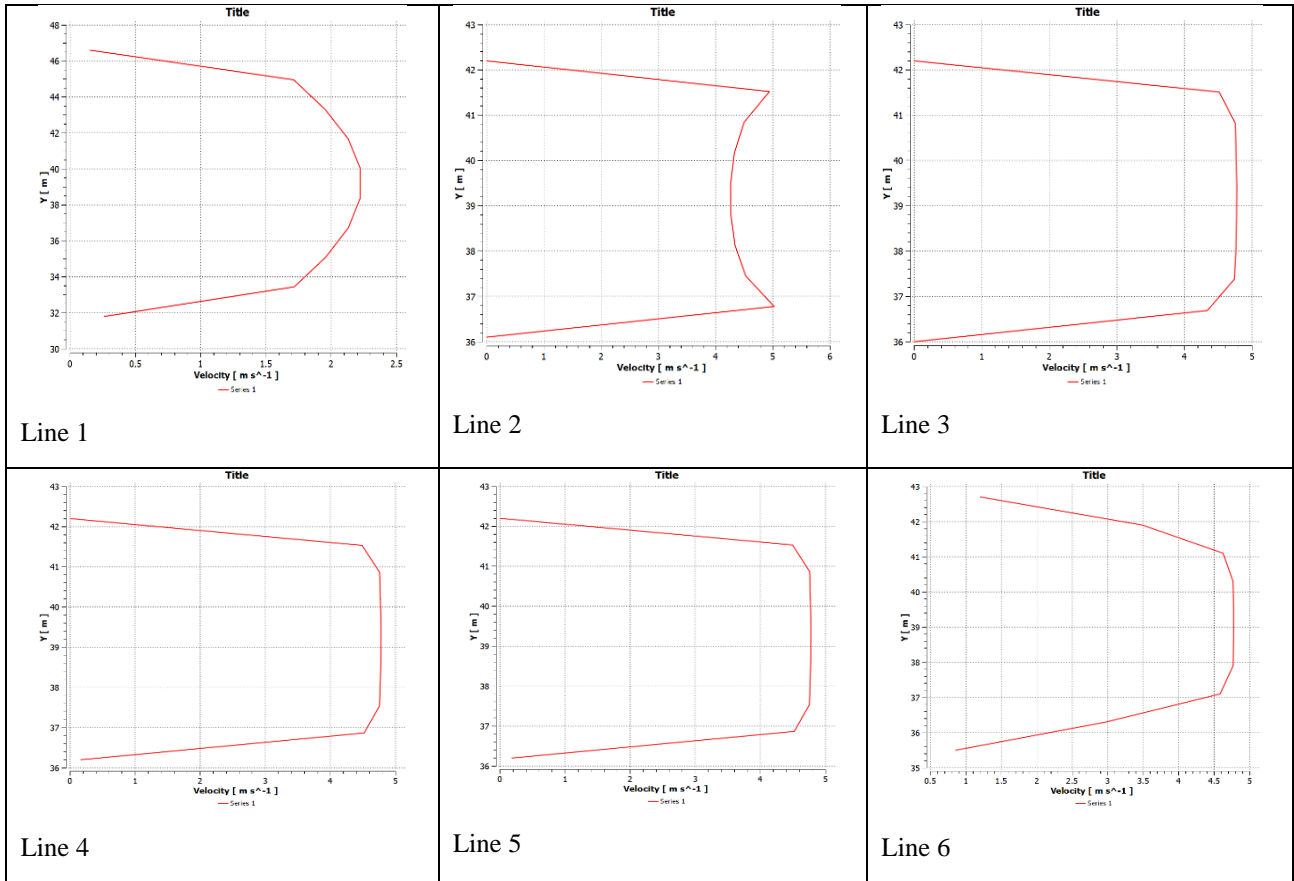


Figure 16. Diagrams of the velocity flow between two buildings in each of the lines (1,2,3,4,5,6) respectively.

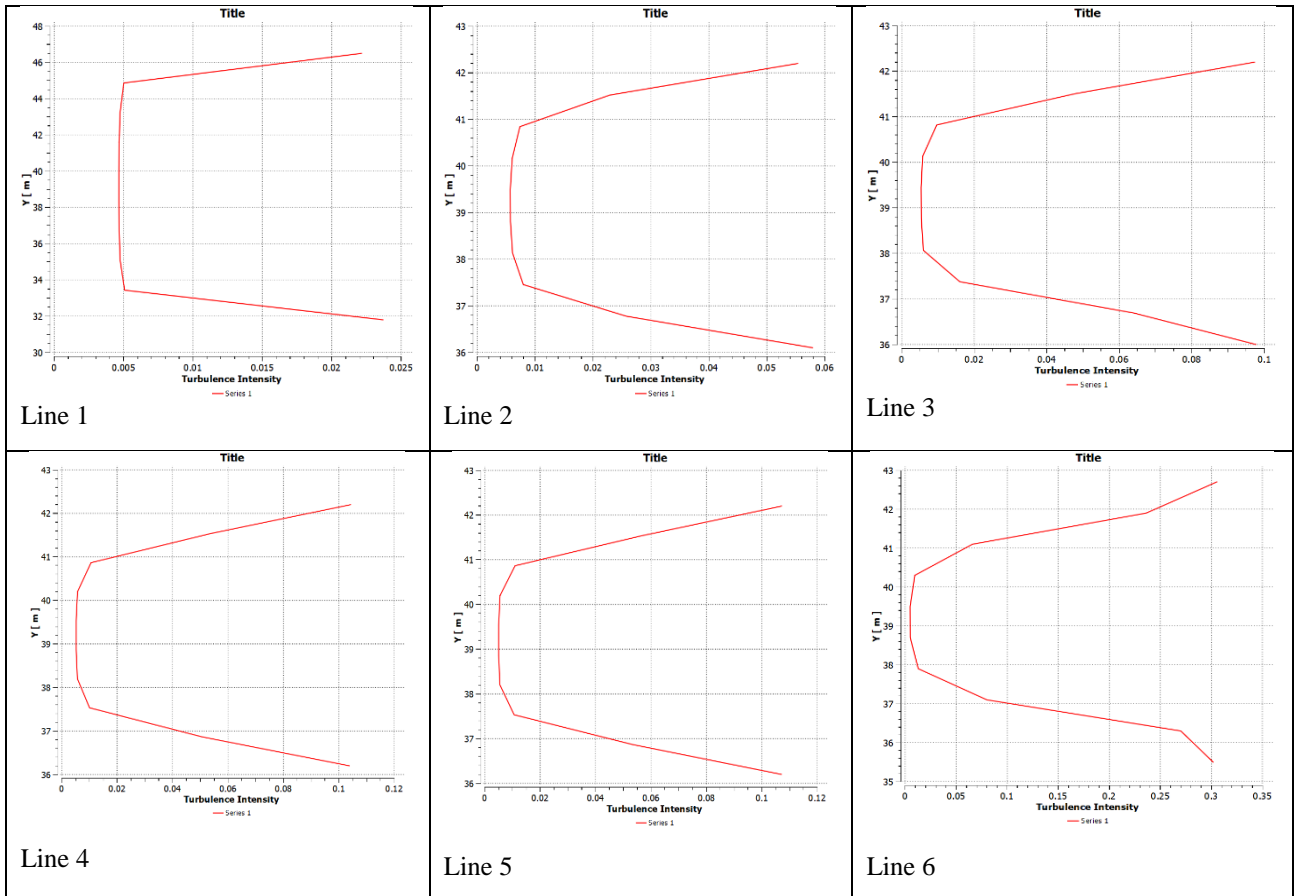


Figure 17. Diagrams of the turbulence intensity between two buildings in each of the lines ((1,2,3,4,5,6) respectively.

As a suitable example for the low wind speeds mentioned in this study, energy calculations were made using one-year wind speed data obtained from the meteorology station located in the Ovacık region of Karabük province. New speed values were obtained by interpolation, considering the wind speeds of this region and the results of the Case2 analysed with computational fluid dynamics. The Weibull distributions of the velocity values of the region at a height of 10 m and the two building placements in Case3 were obtained and compared as shown in Figure 19.

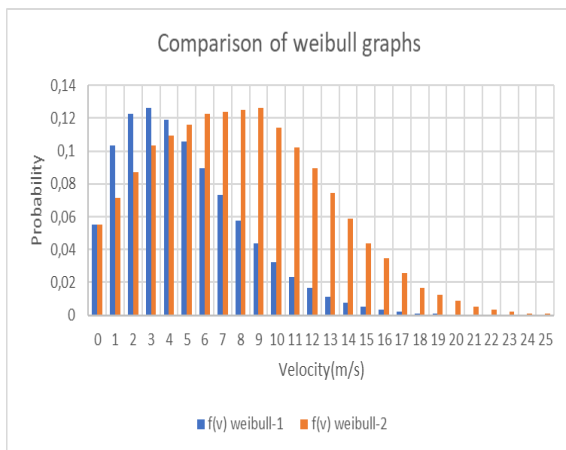


Figure 19. A windspeed probability density function.

It is seen that the velocity values between 1 m/s and 19 m/s in the region reached values between 1 m/s and 29 m/s with the placement of the two buildings as in Case3 (Figure 19). More importantly, it can be seen from the graphs given in Figure 19 that the Weibull probability values increase for the turbine's operating range of 3 m/s and 24 m/s speed values (especially for the speed range between 3 m/s and 19 m/s).

When the annual energy calculation is made for Case2, the amount of energy (energy-1) obtained by the wind turbine (shown in blue) at different wind speeds in the region without the venturi effect and the amount of energy (energy-2) obtained by the same wind turbine (shown in green) according to the new speed values obtained by placing two buildings are compared. Graphics are given in Figure 20.

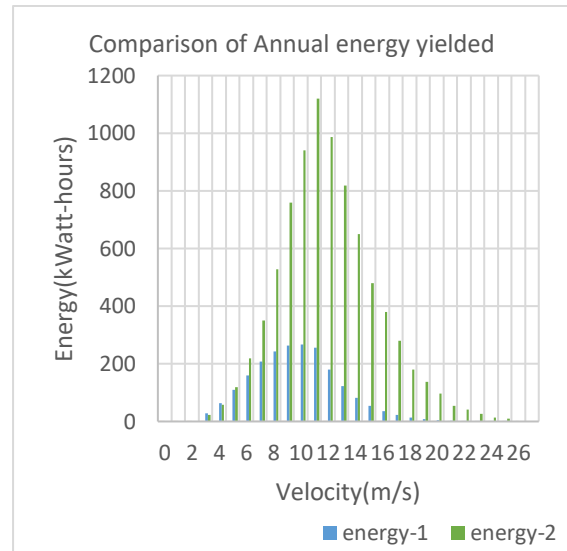


Figure 20. Annual power production.

4. CONCLUSION

In this study, a solution has been proposed to meet some of the electricity needs of the buildings in regions where the wind speed is not sufficient to operate the wind turbine efficiently and where a new settlement can be established. The creation of a venturi effect by placing two symmetrical buildings in the direction of the wind was analysed by computational fluid dynamics. Four different situations were created with four different building geometries, and the wind speeds of 2, 4, 6 m/s in each of them were calculated by CFD, up to which speeds could be increased by the venturi effect. The homogeneity of the wind and the turbulence situation were also analysed to determine the state where the turbine can operate most efficiently. Since there is a 6 m gap between the two buildings, a 5 m diameter horizontal axis wind turbine installed on a 10 m high tower was chosen.

One-year wind speed data measured in the meteorological station area in the Ovacık region of Karabük province and Weibull statistical graphics for the new speed values obtained as a result of CFD analyses were used to calculate the amount of energy that can be obtained in this region for a year, and the results were compared.

While the amount of energy that can be obtained in a year with a wind turbine with a diameter of 5 m and used in this chosen location is 2126.58 kWh, this amount increases to 8272.58 kWh with the effect of venturi resulting from the proper placement of the buildings. It

has been observed that the amount of energy that can be obtained with the proposed building layout in the mentioned region can be increased by approximately 4 times.

In this study, the change of wind direction was not taken into account. The heights of the buildings were not taken into account in the CFD study. However, the speed of the wind increases as it rises from the ground.

If the wind direction values are taken into account in the data taken from the meteorology in a region taken as an example, more accurate results will be achieved. Taking into account the roughness coefficient values of the region will cause the study results to be more reliable.

Considering the heights of the buildings, more accurate results will be achieved if both the variation of wind speed with height and how the vertical surfaces of the buildings affect the air flows are taken into account.

REFERENCES

1. IEA, "Key World Energy Statistics 2021 Statistics Report" IEA Publ., Pages 1–82, 2021.
2. Euclid A. Rose "OPEC's Dominance of the Global Oil Market: The Rise of the World's Dependency on Oil", *The Middle East Journal*, Vol. 58, Issue 3, Pages 424-443, 2004.
3. B. Bulut, "Remaining Useful Life Prediction in Wind Farms", *International Journal of 3D Printing, Technology and Digital Industry* Vol. 5, Issue 2, Pages 145–154, Aug. 2021.
4. S. Gorjian, "An Introduction to the Renewable Energy Resources", *Renewable Energy Technologies* Vol. 4, Pages 41-42, June. 2017.
5. IRENA, International Renewable Energy Agency, "Global renewable outlook - energy transformation 2050", 2020.
6. Department of Energy, "Wind Market Reports: 2021 Edition", <https://www.energy.gov/eere/wind/wind-market-reports-2021-edition>, 2021.
7. A. Iqbal, V. Chitturi, and K. V. L. Narayana, "A Novel Vertical Axis Wind Turbine for Energy Harvesting on the Highways", 2019 *Innov. Power Adv. Comput. Technol. i-PACT* 2019.
8. G. Boroumandjazi, R. Saidur, B. Rismanchi, and S. Mekhilef, "A review on the relation between the energy and exergy efficiency analysis and the technical characteristic of the renewable energy systems", *Renewable and Sustainable Energy Reviews*, Vol. 16, Issue 5, Pages 3131–3135, Jun. 2012.
9. C. M. Hsieh and C. K. Fu, "Evaluation of Locations for Small Wind Turbines in Coastal Urban Areas Based on a Wind Energy Potential Map", *Environmental Modeling and Assessment*, Vol. 18, Issue 5, Pages 593–604, 2013.
10. K. C. S. Kwok and G. Hu, "Wind energy system for buildings in an urban environment", *Journal of Wind Engineering and Industrial Aerodynamics*, Vol. 234, Issue(-), Pages 105349, Mar. 2023.
11. H. Zhu, B. Yang, Q. Zhang, L. Pan, and S. Sun, "Wind engineering for high-rise buildings: A review", *Wind and Structures. An International Journal*, Vol. 32, Issue 3, Pages 249–265, 2021.
12. T. Stathopoulos et al., "Urban wind energy: Some views on potential and challenges", *J. Wind Engineering Industrial Aerodynamics*, Vol. 179, Pages 146–157, Aug. 2018.
13. R. Djedjig, E. Bozonnet, and R. Belarbi, "Experimental study of the urban microclimate mitigation potential of green roofs and green walls in street Canyons", *International Journal of Low-Carbon Technologies*, Vol. 10, Issue 1, Pages. 34–44, 2015.
14. A. Aflaki, N. Mahyuddin, G. Manteghi, and M. Baharum, "Building Height Effects on Indoor Air Temperature and Velocity in High Rise Residential Buildings in Tropical Climate", *OIDA International Journal of Sustainable Development*, Vol. 07, Issue 07, Pages 39–48, 2014.
15. D. R. Bhola, "CFD analysis of flow through venturi of carburetor", *IJRMET* Vol. 4, Issue 2, Spl-2 May - October 2014.
16. B. Li, Z. Luo, M. Sandberg, and J. Liu, "Revisiting the 'Venturi effect' in passage ventilation between two non-parallel buildings", *Building and Environment*, Vol. 94, Issue November, Pages 714–722, 2015.
17. System Analysis Blog Cadence, "Explaining Venturi Effect Wind Flow Analysis in Structural Design", <https://resources.systemanalysis.cadence.com/blog/msa2022-explaining-the-venturi-effect-and-wind-flow-analysis-in-structural-design>, 2022.
18. A. Whiston "Urban Street Canyons", Harvard Graduate School of Design,

- http://web.mit.edu/nature/archive/student_projects/2009/jcalamia/Frame/05_canyonwind.html 1986.
19. R. S. Subramanian, "Engineering Bernoulli Equation", Department of Chemical and Biomolecular Engineering. Clarkson University., Pages. 1–19, 2014.
<https://web2.clarkson.edu/projects/subramanian/ch330/notes/Engineering%20Bernoulli%20Equation.pdf>
 20. F. Oral, I. S. Ekmekçi, and N. Onat, "Weibull distribution for determination of wind analysis and energy production", World Journal of Engineering, Vol. 12, Issue 3, Pages 215–220, 2015.
 21. S. Heier "Wind Energy Conversion Systems", Grid Integr. Wind Energy, Pages 31–117, Apr. 2014.
 22. E. Dick, "Wind Turbines", Fluid Mechanics and Its Applications, Vol. 130, Issue June, Pages 371–396, 2022.
 23. N. Jenkins and A. Vaudin, "Wind Power Plants", Wiley Encyclopedia of Electrical and Electronics Engineering, Germany, 1999.
 24. E. Barlas, W. J. Zhu, W. Z. Shen, and S. J. Andersen, "Wind Turbine Noise Propagation Modelling: An Unsteady Approach", Journal of Physics Conference Series, Vol. 753, Issue 2, 2016.
 25. R. Gasch and J. Tvele, "Wind power plants: Fundamentals, design, construction and operation, second edition", Pages 1–548, Springer Science and Business Media, Berlin, 2012.
 26. T. J. Chung, "Computational Fluid Dynamics", second edition, Vol. 9780521769., Cambridge University Press, Cambridge, 2010.
 27. M. Moshinsky, "Computational Methods for Fluid Dynamics", Vol. 13, Issue 1. 1959.
 28. F. R. Menter, "Two-equation eddy-viscosity turbulence models for engineering applications", AIAA J., Vol. 32, Issue 8, Pages 1598–1605, 1994.
 29. Z. T. Ai, C. M. Mak, and J. L. Niu, "Numerical investigation of wind-induced airflow and interunit dispersion characteristics in multistory residential buildings", Indoor Air, Vol. 23, Issue 5, Pages 417–429, Oct. 2013.
 30. A. Chabas et al., "Long term exposure of self-cleaning and reference glass in an urban environment: A comparative assessment", Build. Environ., Vol. 79, Pages 57–65, Sep. 2014.
 31. A. Samadi and H. Arvanaghi, "CFD simulation of flow over contracted compound arched rectangular sharp crested weirs", Iran Univ. Sci. Technol., Vol. 4, Issue 4, Pages 549–560, 2014.
 32. H. Yu and J. The, "Validation and optimization of SST k- ω turbulence model for pollutant dispersion within a building array", Atmospheric Environment, Vol. 145, Pages 225–238, Nov. 2016.